

Evolution of the Antagonistic Tumor Necrosis Factor Receptor One-Specific Antibody ATROSAB

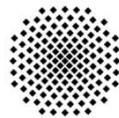
Von der Fakultät Energie-, Verfahrens- und Biotechnik der
Universität Stuttgart zur Erlangung der Würde eines Doktors der
Naturwissenschaften (Dr. rer. nat.) genehmigte Abhandlung

Vorgelegt von
Fabian Richter
aus Filderstadt

Hauptberichter: Prof. Dr. Roland Kontermann
Mitberichter: Prof. Dr. Peter Scheurich

Tag der mündlichen Prüfung: 03. Juni 2015

Institut für Zellbiologie und Immunologie



**Universität
Stuttgart**

2015

Declaration

I hereby declare that I performed and wrote this thesis independent from further help or other materials than stated.

Erklärung

Hiermit erkläre ich, dass die vorgelegte Dissertation von mir persönlich und ohne Zuhilfenahme anderer Unterstützung oder Materialien als den angegebenen durchgeführt und geschrieben wurde.

Fabian Richter

Stuttgart den 17. Juli 2015

Table of Contents

Table of Contents	5
Abbreviations	9
Zusammenfassung.....	11
Abstract	13
1. Introduction.....	15
1.1. Historical Background.....	15
1.2. The Biology and Pathophysiology of TNF	16
1.3. TNF and TNF-Receptors - Expression and Interaction.....	17
1.4. TNFR1 Mediated Intracellular Signaling.....	18
1.5. Tumor Necrosis Factor and its Cognate Receptors as Therapeutic Targets	21
1.6. Preliminary Work and Study Content	22
2. Materials.....	24
2.1. General declarations	24
2.2. Special Material	24
2.3. Kits	24
2.4. Online tools	25
2.5. Buffers and Solutions	25
2.6. Proteins.....	25
2.7. Media.....	26
2.8. Tissue Culture	26
2.9. Bacteria and Phages	27
2.10. Eukaryotic Cells.....	27
2.11. Mice	27
2.12. Plasmids.....	27
2.13. Primer (acquired from Sigma-Aldrich, Munich, Germany)	28
3. Methods	30
3.1. Preparation of chemically competent <i>E. coli</i> TG1	30
3.2. Cloning procedures.....	30
3.3. Cloning Strategies.....	32
3.3.1. Cloning of huTNFR1-Fc Receptor mutations.....	32
3.3.2. Cloning of moTNFR1-Fc.....	32
3.3.3. Cloning of scFvIZI06.1-Fc.....	33
3.3.4. Cloning of IgG-FabL	33
3.3.5. Cloning of FabATROSAB	33
3.3.6. Cloning of 2scFv-HSA	34
3.3.7. Cloning of scFvT12B	34
3.3.8. Cloning of scFvFRK13.1 to scFvFRK13.8.....	34
3.3.9. Cloning of Acceptor Vectors	35
3.3.10. Cloning of IgG13.7, Fab13.7, Fab13.7L, Fab13.7CH3.....	36
3.4. Second Humanization of H398.....	36
3.4.1. Homology modelling.....	37
3.5. Protein Expression.....	37
3.5.1. Expression of Antibody Fragments in the Periplasm of <i>E. coli</i> TG1.....	37

3.5.2.	Expression of Antibodies and Fusion Proteins in Stably Transfected HEK293T Cells.....	37
3.5.3.	Transient Expression of Antibodies and Fusion Proteins in HEK239T Cells.....	38
3.6.	Protein purification	38
3.6.1.	Immobilized Metal Affinity Chromatography (IMAC).....	38
3.6.2.	Antibody and Protein A Affinity Chromatography.....	39
3.6.3.	Preparative Size Exclusion Chromatography	39
3.7.	Protein Characterization	39
3.7.1.	Poly-Acryamide Gel Electrophoresis (SDS-PAGE)	39
3.7.2.	Size Exclusion Chromatography (SEC).....	39
3.7.3.	Thermal Stability by Dynamic Light Scattering	40
3.8.	Enzyme-Linked Immunosorbent Assay (ELISA)	40
3.9.	Flow Cytometry	41
3.10.	Affinity Measurements using the Quartz Christal Microbalance.....	42
3.11.	Competition of ¹²⁵ I-labeled TNF	42
3.12.	Interleukin Release Assay	43
3.13.	Kym-1 Cytotoxicity Assay	43
3.14.	Complement-dependent Cytolysis (CDC).....	44
3.15.	Antibody-Dependent Cellular Cytotoxicity (ADCC)	44
3.16.	IκBα Immunoblot.....	45
3.17.	Pharmacokinetics	45
3.18.	Phage Display	46
3.18.1.	Cloning of Acceptor Vector pHENIS_scFvIG11-fsSTOP	46
3.18.2.	Generation of Selection Library EP03	46
3.18.3.	Preparation of Electrocompetent <i>E. coli</i> TG1	46
3.18.4.	Electroporation of <i>E. coli</i> TG1	47
3.18.5.	Preparation of helper Phages	47
3.18.6.	Phage Rescue and Precipitation	47
3.18.7.	Immunotube Selection.....	48
3.18.8.	Biotinylation of Receptor-Fc Fusion Proteins	48
3.18.9.	Equilibrium Selection on Magnetic Dynabeads.....	49
3.18.10.	Polyclonal Phage ELISA	49
3.18.11.	Screening of Phage Display Selections.....	49
3.18.12.	Off-Rate Screening of Phage Containing Bacteria Culture Supernatants....	50
3.18.13.	Calculation of ATROSAB-TNFR1 Complexes on the Cell Surface	50
4.	Results	52
4.1.	Receptor Binding and <i>in vitro</i> Bioactivity of ATROSAB	52
4.1.1.	ATROSAB Lacks Fc-Mediated Effector Functions.....	52
4.1.2.	ATROSAB Shows Target Mediated Clearance From the Blood.....	54
4.1.3.	Binding of ATROSAB to Human TNF Receptor 1.....	55
4.1.4.	Inhibition of TNF Binding, Signaling and TNFR1-Mediated Interleukin Release	56
4.1.5.	Comparison of ATROSAB with the Agonistic Antibody Htr-9	58
4.1.6.	Crosslinking of ATROSAB by an Anti-human IgG Antibody.....	61
4.1.7.	Epitope Mapping of ATROSAB and Htr-9.....	64
4.1.8.	Structural Aspects of the TNF-TNFR1 Complex	66
4.2.	Alternative Antibody Formats	69
4.2.1.	Purification and Expression of ATROSAB Derivatives	70

4.2.2.	Receptor Selectivity of Antibody Fusion Proteins with ATROSAB Variable Domains	71
4.2.3.	Characterization of TNFR1 Binding by Alternative Antibody Formats	73
4.2.4.	Activity of ATROSAB Derivatives on Interleukin-8 Release from HT1080 Cells	75
4.3.	Superior Bioactivity of H398.....	77
4.3.1.	Serum Stability, pH-value and Incubation Time in the Bioactivity of ATROSAB and H398.....	78
4.3.2.	Binding of ATROSAB and H398 to huTNFR1 at Low Receptor Density.....	81
4.4.	Affinity Maturation of ATROSAB	82
4.4.1.	Selection of the Affinity Matured Clone scFvT12B.....	83
4.4.2.	Characterization of scFvT12B.....	87
4.5.	Repeated Humanization of H398	89
4.5.1.	<i>In Silico</i> Evaluation of Humanized VH and VL Sequences	90
4.5.2.	Expression and Characterization of scFvFRK13	92
4.5.3.	Structural Analysis of Homology Modeled scFvFRK13 Variants.....	94
4.6.	Conversion of scFvFRK13.7 into the IgG and Fab-Format.....	96
4.6.1.	Binding of FRK13.7 Antibodies to Human TNFR1	97
4.6.2.	<i>In vitro</i> Bioactivity of scFvFRK13.7 Derived Proteins	99
4.7.	Half-life Extension of Fab13.7	103
5.	Discussion.....	106
5.1.	Reduced Induction of ADCC/CDC and Target Mediated Clearance	106
5.2.	High and Low Affinity Interaction of ATROSAB to TNFR1 Inhibits Binding of TNF.....	108
5.3.	Intra- and Extracellular Effects of TNFR1 Inhibition.....	109
5.4.	Agonism and Antagonism at the Site of TNFR1	111
5.5.	Alternative Antibody Formats and Avidity	112
5.6.	Affinity Maturation and Framework Exchange	113
5.7.	IgG13.7 and Fab13.7.....	115
5.8.	Implications on the Model of TNFR1 Activation	116
5.9.	Outlook and Conclusions.....	120
6.	References.....	122
7.	Sequences.....	135
7.1.	Legend	135
7.2.	Human TNFR1-Fc mutants.....	135
7.3.	moTNFR2-Fc	137
7.4.	scFvIZI06.1-Fc	138
7.5.	IgG-FabL Light Chain	138
7.6.	gG-FabL Heavy Chain	139
7.7.	FabATR Light Chain.....	141
7.8.	FabATR Heavy Chain.....	142
7.9.	2scFv-HSA	143
7.10.	scFvIG11.....	145
7.11.	scFvIG11-fsSTOP	146
7.12.	scFvT12B	147
7.13.	scFvFRK13.1	148
7.14.	scFvFRK13.2	149
7.15.	scFvFRK13.7	150

7.16.	pAB1-L1-EMP1-CLk-Li1	151
7.17.	pAB1-L1-EMP1-hg1e3-Li1.....	151
7.18.	pAB1-L1-EMP1-CH1only	152
7.19.	pAB1-L1-EMP1-2CLk.....	153
7.20.	pAB1-L1-EMP1-2CH1	154
7.21.	pAB1-L1-EMP1-CLk-CH3	155
7.22.	pAB1-L1-EMP1-CH1-CH3	156
7.23.	Light Chain Variable Domain of IgG13.7, Fab13.7, Fab13.7L and Fab13.7CH3...	157
7.24.	Heavy Chain Variable Domain of IgG13.7, Fab13.7, Fab13.7L and Fab13.7CH3	157
8.	Acknowledgements	159
9.	Curriculum Vitae - Fabian Richter	160

Abbreviations

α hulG	anti-human IgG antibody	EAE	experimental autoimmune
[A]	ATROSAB concentration		encephalomyelitis
ADA	anti-drug antibody	EC ₅₀	half maximal effective
ADCC	antibody dependent cellular		concentration
	cytotoxicity	ecd	extracellular domain
ADCP	antibody dependent cellular	EDTA	ethylenediaminetetraacetate
	phagocytosis	EGFR	epidermal growth factor
amp	ampicillin		receptor
AP-1	activator protein-1	ELISA	enzyme-linked
APS	ammonium persulfate		immunosorbent assay
AR	ATROSAB monovalently bound	EMP1	EPO mimetic peptide
	to TNFR1	Fab	fragment antigen binding
AR ₂	ATROSAB bivalently bound to	FabL	Fab "long" with two CH1 and
	TNFR1		two CLk
ATF-2	activating transcription	Fc	fragment crystallizable
	factor 2	FcRn	neonatal Fc receptor
ATR	ATROSAB	FCS	fetal calf serum
AUC	area under the curve	FcγR	Fc gamma receptor
BLAST	Basic local alignment search	FPLC	fast performance liquid
	tool		chromatography
Bmax	calculated maximal binding	FR	framework region
	in QCM measurements	Fv	fragment variable
BSA	bovine serum albumin	GS	glutamin synthetase
CD	cluster of differentiation	hdc	high density chip
CDC	complement dependent	hg1e3	mutated human IgG1 Fc part
	cytotoxicity		(no ADCC/ADCP/CDC)
CDR (H/L)	complementarity determining	HPLC	high performance liquid
	region (heavy /light chain)		chromatography
CH	constant domain of the heavy	HRP	horse reddish peroxidase
	chain	HSA	human serum albumin
CIA	collagen induced arthritis	hu	human
clAP	cellular inhibitor of apoptosis	IC ₅₀	half maximal inhibitory
CLk	constant domain of the light		concentration
	chain (kappa gene)	icd	intracellular domain
CNS	central nervous system	IgG	immunoglobulin gamma
cpm	counts per minute	IKK	inhibitor of NF-κB kinase
CRD	cysteine rich domain	IL	interleukin
Da	dalton (g/mol)	IMAC	immobilized metal ion
DNA	deoxyribonuclein acid		affinity chromatography
DR5	death receptor 5	IPTG	isopropyl-β-D-
DTT	dithiotreitol		thiogalactopyranoside
E:T	effector to target cell ratio		

izi	Institute of Cell Biology and Immunology	PLAD	pre-ligand binding assembly domain
I κ -B α	inhibitor of NF- κ B alpha	QCM	quartz crystal microbalance
JNK	c-Jun N-terminal kinase	[R]	TNFR1 concentration
K _D	dissociation constant	R1antTNF	antagonistic TNFR1-specific TNF mutein
k _{off}	dissociation rate constant	RA	rheumatoid arthritis
k _{on}	association rate constant	RIP1	receptor-interacting serine/threonine protein kinase
L1	Ig κ leader with AgeI restriction site	RT	room temperature
LB	lysogeny broth	scFv	single chain Fv
ldc	low density chip	SD	standard deviation
Li	linker	SDS	sodium dodecyl sulfate
LMV	ligation mix volume	SEC	size exclusion chromatography
LPS	lipopolysaccharides	shRNA	short hairpin RNA
LT α	lymphotoxin alpha	SOB	super optimal broth
mAb	monoclonal antibody	SOC	SOB medium and 20 mM glucose
MAPK	mitogen-activated protein kinase	STD	standard
MCP-1	monocyte chemoattractant protein-1	sTNF	soluble TNF
mo	mouse/murine	T _{1/2}	half-life
MPBS	skim milk on PBS basis	TAB	TAK1 binding protein
MS	multiple sclerosis	TACE	TNF α converting enzyme
mTNF	membrane bound TNF	TAE	tris-acetate-EDTA buffer
MTX	methotrexate	TAK1	transforming growth factor- β -activated kinase 1
NEMO	NF- κ B essential modifier	TEA	triethylamine
NF- κ B	nuclear factor κ B	TMB	tetramethylbenzidine
NIK	NF- κ B inducing kinase	TNF	tumor necrosis factor
NK cells	natural killer cells	TNFR	TNF receptor
OD	optical densits	TNFRSF1A	TNFR1
PAGE	polyacrylamide gelelectrophoresis	TRADD	TNFR-associated death domain
PBS	phosphate buffered saline	TRAF	TNFR-associated factor
PBST	PBS with tween20	TY	trypton-yeast medium
PCR	polymerase chain reaction	VH	variable domain of the heavy chain
PEG	polyethylene glycol	VL	variable domain of the light chain
PEGylated	PEG-modified		
PIGS	prediction of Immunoglobulin structure		
plkB α	phosphorylated I κ B α		

Zusammenfassung

Das pleiotrope Zytokin Tumor Nekrose Faktor (TNF) ist an vielzähligen biologischen Prozessen beteiligt und seine deregulierte Expression beeinflusst etliche, zumeist autoimmune oder entzündliche Erkrankungen. Folglich konnten TNF neutralisierende Therapeutika mit großem Erfolg gegen Krankheiten wie beispielsweise Rheumatoide Arthritis oder Morbus Crohn eingesetzt werden, wobei die damit einhergehende Blockade beider TNF Rezeptoren (TNFR1 und TNFR2) zu schwerwiegenden Nebenwirkungen geführt hat. Insbesondere TNFR1 wurde kürzlich den schädigenden TNF-Wirkungen zugeordnet, weshalb seine selektive Blockade eine vielversprechende therapeutische Strategie darstellt. In dieser Studie werden weitergehende Daten der *in vitro* Charakterisierung des antagonistischen TNFR1-spezifischen Antikörpers ATROSAB und die Entwicklung eines vielversprechenden Moleküls für die selektive therapeutische Inhibierung von TNFR1 präsentiert.

ATROSAB zeigte aufgrund der eingefügten Mutationen keine oder nur minimale Fc-vermittelten Effektorfunktionen. In einer früheren Studie wurde gezeigt, dass diese Mutationen keinen Einfluss auf die Serum-Halbwertszeit von ATROSAB im Blut von Wildtyp-Mäusen haben. Das pharmakokinetische Profil von ATROSAB in transgenen Mäusen, welche die extrazelluläre Domäne des human TNFR1 exprimieren, legt jedoch eine Rezeptorbedingte Beseitigung aus dem Blutkreislauf nahe. ATROSAB interagierte mit TNFR1 über eine hochaffine, bivalente Bindung (0,2 nM) und eine monovalente Bindung mit moderater Affinität (73 nM). Dies führte in Interleukin-Freisetzung Experimenten zu IC_{50} -Werten im nanomolaren Bereich. Eine Hemmung der TNFR1-vermittelten intrazellulären Signaltransduktion durch ATORSAB konnte anhand der inhibierten Phosphorylierung von I κ -B α gezeigt werden. Die zuvor für ATROSAB beobachtete marginale TNFR1-Aktivierung wurde mit dem stark antagonistischen, murinen Antikörper Htr-9 verglichen, wodurch der antagonistische Charakter von ATROSAB bestätigt werden konnte. Im Gegensatz dazu zeigte ATROSAB in Gegenwart eines anti-IgG1 Antikörpers eine klare Aktivierung von TFNR1. Darüber hinaus wurden die Aminosäuren P23, R68 und H69 im TNFR1-Molekül als ATROSAB-Bindestelle identifiziert. Im Folgenden wurde die Auswirkung einer Veränderung des Molekülformats auf die TNFR1-Bindung und -Aktivierung anhand von alternativen

Antikörperformaten und Antikörper-Fusionsproteinen mit einer bzw. zwei der TNFR1-Bindungsdomänen von ATROSAB untersucht. Im Vergleich mit den übrigen, stark Rezeptor-aktivierenden, bivalenten Molekülen zeigte ausschließlich ATROSAB keine nennenswerte stimulierende Wirkung, wodurch der einzigartige Antagonismus von ATROSAB ein weiteres Mal hervor gehoben werden konnte.

Die verminderte TNFR1-hemmende Wirkung von ATROSAB, im Vergleich zu seinem murinen Vorgänger H398, konnte einer erhöhten Dissoziierungskonstante zugeordnet und diese Beobachtung anschließend in einer Affinitäts- bzw. Dissoziierungs-Reifung mittels Phage Display auf Basis des scFv-Formates angewendet werden. Der zusätzliche Austausch der Framework-Regionen der leichten Kette (scFvFRK13.7) resultierte zudem in einer erhöhten Thermostabilität. Das korrespondierende Fab13.7 zeigte eine verbesserte TNFR1-Bindung und im Vergleich mit dem bivalenten ATROSAB eine effizientere Hemmung der TNF-vermittelten TNFR1-Aktivierung. Darüber hinaus zeigte Fab13.7 keinerlei aktivierende Wirkung auf TNFR1, im Gegensatz zum entsprechenden, bivalenten IgG13.7, das eine starke TNFR1-Antwort hervorrief. Schlussendlich wurden die in den Experimenten gewonnenen Einsichten in die TNFR1-Biologie auf das Erstellen eines mechanistischen Modells der TNFR1 Aktivierung angewandt, welches eine veränderte relative Orientierung der beiden interagierenden Rezeptor-Moleküle bzw. eine Konformations-Änderung der Rezeptor-Struktur zwischen aktivem und inaktivem Zustand vorschlägt. Dies steht im Widerspruch zu vorherigen Hypothesen, welche der TNFR1-Aktivierung eine Liganden-Induzierte Trimerisierung des Rezeptors zugrunde legten.

Abstract

The pleiotropic cytokine tumor necrosis factor (TNF) is involved in numerous processes of human physiology and its dysregulated expression affects multiple, mainly inflammatory or autoimmune diseases. Thus, TNF-neutralizing therapeutics are highly successful in the treatment of e.g. rheumatoid arthritis or Crohn's disease. However, the resulting blockade of both TNF receptors (TNFR1 and TNFR2) led to diverse, sometimes serious side effects. Recently, the detrimental effects of chronic TNF activity were attributed to TNFR1 and hence, its selective blockade represents a promising therapeutic strategy. This thesis presents further data on the *in vitro* characterization of the antagonistic TNFR1-specific antibody ATROSAB and the development of a novel promising therapeutic candidate for selective TNFR1 inhibition.

ATROSAB revealed greatly reduced or lacking induction of Fc-mediated effector functions, due to mutations introduced into the Fc part. According to a previous study, these mutations did not affect the pharmacokinetic profile of ATROSAB in wild type mice. However, reduced terminal serum half-life in transgenic mice, expressing the extracellular domain of human TNFR1, suggested a target-mediated clearance from the circulation. Moreover, ATROSAB bound with a high bivalent (0.2 nM) and a moderate monovalent affinity (73 nM) to TNFR1, resulting in inhibition of TNFR1 binding and activation by TNF with IC_{50} values in the nanomolar range. ATROSAB also inhibited phosphorylation of I κ -B α , indicating suppression of TNFR1-mediated intracellular signal transduction. The marginal TNFR1 stimulation observed for ATROSAB was compared with the highly agonistic murine antibody Htr-9, supporting the overall antagonistic character of ATROSAB. However, in the presence of an anti-IgG1 antibody, ATROSAB clearly induced interleukin release from HT1080 cells. Moreover, a mutagenesis study showed that the epitope of ATROSAB on TNFR1 comprises residues P23, R68 and H69 of the receptor. In the following, the effect of the molecular format on TNFR1 binding and activation was assessed by the production and characterization of alternative mono- or bivalent antibody formats. Exclusively ATROSAB revealed hardly any stimulatory effect and thereby substantiated its unique antagonistic potential, when compared with the remaining bivalent molecules, clearly activating TNFR1.

Furthermore, the decreased inhibitory potential of ATROSAB, compared with its parental mouse antibody H398, could be attributed to an increased dissociation rate constant. Using the scFv format, affinity/off-rate maturation was subsequently performed by phage display. In addition, exchange of the light chain framework regions by alternative germline sequences (scFvFRK13.7) resulted in better TNFR1 binding and higher thermal stability. The corresponding Fab13.7 exhibited improved monovalent TNFR1 binding and, compared with ATROSAB, superior inhibition of TNF-mediated TNFR1 activation. Moreover, Fab13.7 did not reveal any detectable activating effect on TNFR1, even in the presence of anti-Fab serum antibodies, while the related IgG13.7 induced a strong TNFR1 response. Finally, the gained insights into TNFR1 biology were implemented into a mechanistic model of TNFR1 activation, suggesting a change in the conformation or orientation of interacting TNFR1 molecules between inactive and active state, which is in contradiction to former hypotheses postulating TNFR1-activation by ligand-induced receptor trimerization.

1. Introduction

Onset and progression of diverse autoimmune and inflammatory diseases were found to be affected by the pleiotropic cytokine TNF. Interestingly, TNF seemed to be also involved in the resolution of inflammation and in cellular regeneration. These contradictory observations could be attributed to two different cell surface receptors, TNFR1 and TNFR2, responsible for the detrimental and regenerative effects of TNF, respectively. Therefore, in addition to TNF-neutralization, which is successfully applied in the clinic, the selective inhibition of TNFR1 represents a promising therapeutic strategy, holding the potential to overcome severe side-effects, observed for anti-TNF treatment.

1.1. Historical Background

The bioactivity of TNF was already observed in the late 19th century, when sarcoma patients recovered after bacterial infection (Bruns 1868). During the following decades, research on the treatment of cancer with bacterial cultures or extracts thereof (Coley 1891) narrowed down the reported tumoricidal effect to be induced by a serum factor released from immune cells in response to bacterial lipopolysaccharides (LPS; Gratia and Linz 1931, Shear and Turner 1943, Algire et al. 1952, O'Malley et al. 1962, Carswell et al. 1975). The isolation of this cytokine and the determination of its amino acid composition and genetic sequence allowed for the recombinant production of human TNF and its use in a mouse model of induced sarcoma, resulting in tumor cell necrosis (Pennica et al. 1984, Aggarwal et al. 1985). However, treatment of non-human primates with TNF resulted in systemic inflammation and septic shock, which could be prevented by the application of anti-TNF antibodies in advance to the TNF injections (Tracey et al. 1987). Similarly, in a human dose escalation study, TNF administration provoked signs of inflammation in a dose-dependent manner, accompanied by influenza-like symptoms and hypotension (Feinberg et al. 1988). These severe side effects of systemic TNF application could be avoided in certain cases by separated perfusion of the tumor-affected extremity upon blockade of the patient's circulation and connection of the limb's main vessels to an extracorporeal circuit. This method, called isolated limb perfusion, enables the treatment of e.g. advanced soft tissue

sarcoma and different malignancies of the skin by very high local TNF concentrations, resulting in response rates of around 75 % (Eggermont et al. 2003).

1.2. The Biology and Pathophysiology of TNF

Efficient killing of tumor cells by TNF was found to be rather independent of direct TNF-mediated cytotoxicity and, interestingly, to require the presence of reactive cytotoxic T-cells (Hock et al. 1993). This functional involvement of TNF in the immune system was observed on multiple levels (reviewed by Locksley 2001). For example, TNF is a potent activator of the innate immune system, e.g. in terms of acute inflammation in response to LPS treatment or by activating macrophages during microbial infection (Havell 1989, Pfeffer et al. 1993, Rothe et al. 1993, Dumitru et al. 2000). TNF was further reported to be dispensable for the formation of granuloma in response to mycobacterial challenge, however, to be important for their maintenance, which ensures containment of the pathogens (Zganiacz et al. 2004). In addition, the morphogenesis of secondary lymphoid organs like the formation of B-cell follicles, dendritic cell networks and germinal centers is impaired in TNF knock-out mice (Pasparakis et al. 1996, Fu and Chaplin 1999). Especially membrane-bound TNF was shown to activate immune cells like dendritic cells, natural killer cells and T-cells in a co-stimulatory way (Marino et al. 1997, Clark et al. 2005, Xu et al. 2007). However, chronic exposure to endogenous levels of TNF or repeated TNF injections limit the reactivity of the immune system by e.g. modulation of T-cell receptor signaling or activation of regulatory T-cells (Cope et al. 1997, Aspalter et al. 2005, Chen et al. 2007).

Independent from the immune system, chronic TNF expression has been linked to detrimental effects like *de novo* carcinogenesis in the skin (Moore et al. 1999). Furthermore, TNF overexpression in the central nervous system (CNS) of mice induced a 100 % penetrating demyelinating disease (Probert et al. 1995). Moreover, dysregulation of TNF can lead to the development of autoimmune or inflammatory disorders like systemic lupus erythematosus (SLE; Jacob et al. 1991) or type II diabetes (Hotamisligil et al. 1994, Emanuelli et al. 2001). Especially in the case of rheumatoid arthritis (RA), TNF rapidly induces cytokine expression, resulting in promoted vascularization, influx of immune cells and bone destruction by the recruitment and activation of osteoclasts (Feldmann 2002, Romas et al. 2002, Müssener et al. 1997, Kontermann et al. 2009a).

1.3. TNF and TNF-Receptors - Expression and Interaction

Tumor necrosis factor is expressed by macrophages, natural killer (NK) cells, B- and T-cells, but also by some non-immune cells, e.g. fibroblasts. TNF is a type II transmembrane protein (mTNF), characterized by the intracellular location of the N-terminus, connected to the extracellular C-terminal domain by a single-pass transmembrane α -helix (Kriegler et al. 1988). The functional unit of TNF is represented by a homotrimer (Tang et al. 1996), which can be cleaved at membrane proximal residues by the metalloprotease TACE (TNF α converting enzyme), leading to its shedding in the form of a soluble trimeric cytokine (sTNF; Black et al. 1997).

Two different cell surface receptors have been identified to interact with TNF, designated TNF receptor 1 (TNFR1) and TNFR2 (Brockhaus et al. 1990, Loetscher et al. 1990a, Loetscher et al. 1990b). Both receptors are type I transmembrane proteins (extracellular N-terminus and intracellular C-terminus), composed of 4 cysteine-rich domains (CRD) in the extracellular portion, each containing 6 cysteine residues, which form intramolecular disulfide bonds and thus stabilize the conserved CRD structure. The intracellular domain is responsible for signal transduction, as shown for C-terminally truncated TNFR1, revealing a lack of cytotoxicity induction (Brakebusch et al. 1992). TNFR1 is expressed constitutively on a broad variety of cells, while TNFR2 expression occurs in a stimulus-dependent manner and is restricted to immune cells (e.g. thymocytes, T-cells, monocytes), endothelial cells, neuronal cells (neurons, oligodendrocytes, astrocytes) and mesenchymal stem cells (reviewed by Cabal-Hierro and Lazo 2012). The induction of TNFR1 and TNFR2 signaling is regulated by a multifaceted network of agonistic and antagonistic molecules, collectively determining which intracellular pathway is induced to mediate a certain cellular response. Interestingly, while the membrane-bound form of TNF stimulates TNFR1 and TNFR2, the soluble form accomplishes sustained activation only in the case of TNFR1 (Fig. 1-01; Grell et al. 1995). In contrast, both TNF receptors interact equally strong with lymphotoxin α (LT α), another soluble member of the cytokine family of TNF-related proteins (TNF superfamily; Medvedev et al. 1996, Hehlhans and Männel 2002). Moreover, progranulin binding to TNFR1 and TNFR2 was recently shown to exhibit an antagonistic effect, which is, however, controversially discussed in the recent literature (Tang et al. 2011, Chen et al. 2013, Etemadi et al. 2013). Finally, constitutive shedding of both TNF receptors after proteolytic cleavage and hence,

inhibition of sTNF and mTNF, was reported to contribute to the modulation of a threshold for TNFR activation (Himmler et al.1990, Pinckard et al. 1997, Xanthoulea et al. 2004).

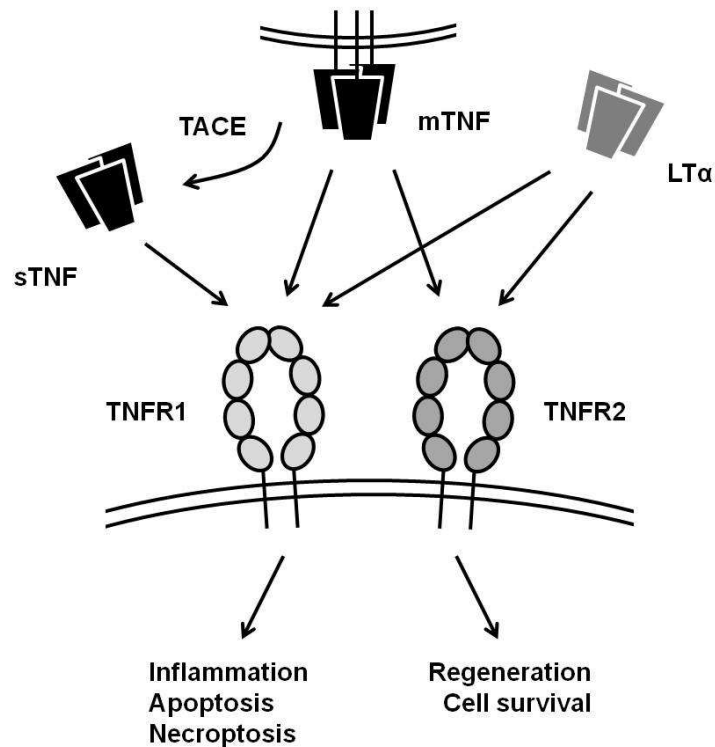


Figure 1-01. TNF-TNFR interaction. The soluble form of TNF, cleaved from its transmembrane domain by TACE, mainly stimulates TNFR1, while mTNF and LTα equally stimulate both receptors. TNFR1 induces inflammatory gene expression, apoptosis and necroptosis. TNFR2 activation leads to regeneration and cell survival.

1.4. TNFR1 Mediated Intracellular Signaling

Stimulation of TNFR1 by TNF and LTα primarily results in the expression of pro-inflammatory genes (Picarella et al. 1992, Sacca et al. 1998, Calmon-Hamaty et al. 2011). The underlying mechanisms of TNF-induced signal transduction are extensively reviewed in the literature and shortly described below (e.g. Wajant et al. 2003, Bianchi and Meier 2009, Wilson et al. 2009, Razani et al. 2011, Verhelst et al. 2011, Walczak 2011, Cabal-Hierro and Lazo 2012, Workman and Habelhah 2013). Following ligand binding, the rearrangement of the intracellular TNFR1 domains results in the recruitment of TRADD (TNFR-associated death domain) as platform for the interaction of further signaling components. TRAF2 (TNFR-

associated factor) and RIP1 (Receptor-interacting serine/threonine protein kinase) both bind to TRADD and, in addition, interact with each other. TRAF2 then recruits cIAP1 (cellular inhibitor of apoptosis) and cIAP2, while RIP1 interacts with the TAK complex, composed of TAK1 (transforming growth factor- β -activated kinase 1), TAB1 (TAK1 binding protein) and TAB2, and the IKK complex (inhibitor of NF- κ B [nuclear factor κ B] kinase complex), containing IKK α , IKK β and NEMO/IKK γ (NF- κ B essential modifier). The TAK1 complex is responsible for the phosphorylation-mediated activation of IKK α , which subsequently phosphorylates I κ B α (inhibitor of NF- κ B α), leading to the proteasomal degradation of I κ B α . Non-phosphorylated I κ B α sequesters NF- κ B (p50/RelA) in the cytosol upon masking of its nuclear localization sequence and hence, its depletion allows for nuclear translocation of NF- κ B, where it regulates the expression of various genes. Polyubiquitylation events are involved in many of the occurring interactions of TNFR1 signaling, contributing to the stabilization of the receptor-induced signaling complex.

Alternatively, NF- κ B subunit p100 can be activated in a TRAF2, TRAF3 and NIK (NF- κ B inducing kinase)-dependent manner, exhibiting gene regulatory activities in complex with other NF- κ B subunits like RelB or p50. Moreover, the TNF-dependent induction of MAPK (mitogen-activated protein kinase) pathways results in gene expression in response to the transcription factors AP-1 (activator protein) or ATF-2 (activating transcription factor 2), mediated by p38 and JNK (c-Jun N-terminal kinase). In contrast to the inflammation-mediating induction of gene expression via NF- κ B, under certain circumstances like e.g. internalization of the receptor and simultaneous inhibition of NF- κ B activation, TNFR1 also promotes the execution of apoptotic and necroptotic cell death (Fig. 1-02).

Finally, TNFR2 also recruits TRAF2, inducing similar signaling pathways as described above and, in addition, TNFR2 triggers phosphorylation-mediated degradation of TRAF2. Thus, TNF receptor stimulation activates a complex intracellular signaling network with possible cross-talk on multiple levels, resulting in highly cell type-dependent and tissue-specific cellular responses.

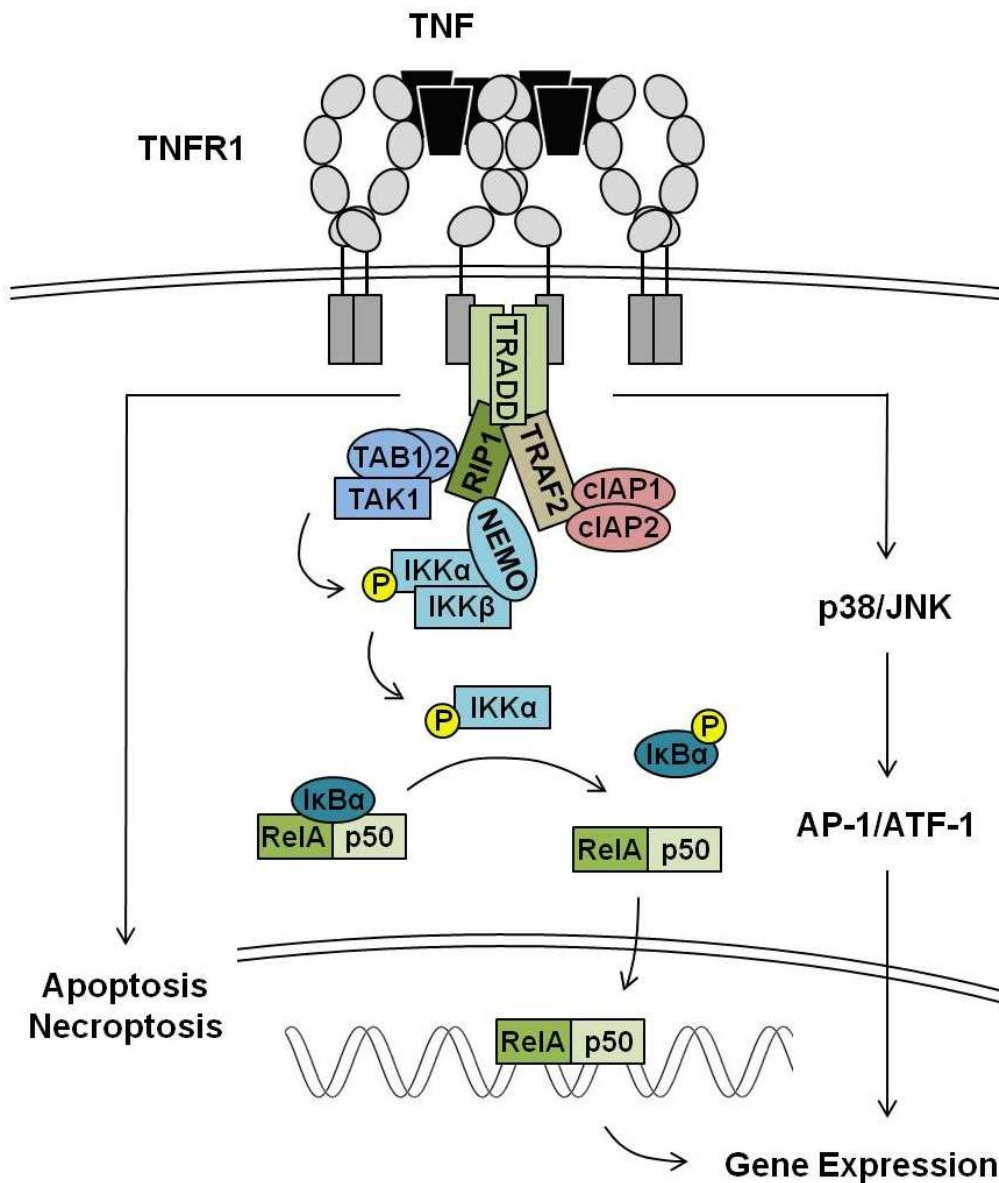


Figure 1-02. TNFR1 signal transduction. TNF-mediated activation of TNFR1 results in a series of intracellular events, eventually inducing gene expression or cell death. TRADD, binding to the intracellular death domain of TNFR1, recruits TRAF2 and RIP1, which serve as binding platform for the TAK1 complex (TAK1, TAB1 and TAB2), the IKK complex (IKK α , IKK β and NEMO), cIAP1 and cIAP2. TAK1 activates IKK α by phosphorylation. Active IKK α subsequently phosphorylates I κ B α and thus initiates I κ B α degradation. This leads to the liberation of the NF- κ B dimer RelA/p50, allowing for its nuclear translocation and the induction of gene expression. Moreover, gene expression can be induced by TNFR1-mediated stimulation of MAPK pathways via p38 or JNK and the transcription factors AP-1 and ATF-2. Under conditions of receptor internalization and NF- κ B inhibition, TNFR1 activation can also induce apoptotic or necroptotic cell death.

1.5. Tumor Necrosis Factor and its Cognate Receptors as Therapeutic Targets

Inflammatory and autoimmune diseases such as RA were formerly treated with non-steroid anti-inflammatory drugs like ibuprofen or paracetamol, followed by disease-modifying anti-rheumatic drugs, e.g. methotrexate (MTX), leflunomid and cyclosporine (reviewed by Hwang and Moreland 2014). The use of antibody-mediated TNF blockade in combination with MTX showed superior efficacy, especially when initiated at early time-points after diagnosis (van der Heijde et al. 2010). In 2014, nine antibodies or antibody fusion proteins were in the clinic, approved either by the American Food and Drug Administration or the European Medicines Agency, for the treatment of rheumatoid arthritis as single therapeutic or in combination with MTX. Five of them are directed against TNF (Table 1-01; Kotsovilis and Andreakos 2014, www.FDA.gov, www.EMA.eu).

Table 1-01: Approved biologics for treatment of inflammatory diseases

Generic Name	Commercial Name	Format
Infliximab	Remicade®	chimeric anti-TNF mAb
Adalimumab	Humira®	hu anti-TNF mAb
Etanercept	Enbrel®	TNFR2-Fc fusion protein
Golimumab	Simponi®	hu anti-TNF mAb
Certolizumab pegol	Cimzia®	PEGylated Fab fragment
Rituximab	Rituxan®/MabThera®	chimeric anti-CD20 mAb
Tocilizumab	Actemra®	humanized anti IL-6 mAb
Anakinra	Kineret®	recombinant hu IL-1R α
Abatacept	Orenica®	CTLA-4-Fc fusion protein

Anti-TNF therapy is successfully applied in the treatment of inflammatory diseases, however, a large number of severe side effects has been reported (reviewed by Desai and Furst 2006). Among these adverse events, the increased susceptibility to new infections or the reactivation of persistent infections, especially in the case of tuberculosis, but also for listeria, salmonella and several viruses, was widely reported in the literature (Gardam et al. 2003, Wallis 2008, Rosenblum and Amital 2011). Moreover, blockade of TNF was associated with the development of several malignancies like melanoma or lymphoma, however, due to the overall low number of reported cases, these observations were controversially discussed (Bongartz et al. 2006, Calzascia et al. 2007, Diak et al. 2010, Zidi et al. 2011). Interestingly,

anti-TNF therapy resulted in certain cases in the onset or worsening of inflammatory and autoimmune diseases like SLE, psoriasis, type I diabetes, cutaneous vasculitis or interstitial lung disease (Shakoor et al. 2002, de Gannes et al. 2007, Ramos-Casals et al. 2007, Tack et al. 2009). In particular, a clinical phase II study on the efficacy of the TNFR1 antibody-Fc fusion protein lenercept in multiple sclerosis (MS) attracted considerable attention due to exacerbation of MS symptoms and earlier occurrence of relapses in treated patients, compared with the control group (Lenercept MS Study Group 1999).

Accumulating knowledge on the distinct roles of TNFR1 and TNFR2 in the pathology of TNF-affected diseases connected TNFR1 with e.g. the progressive phase in experimental autoimmune encephalomyelitis (EAE) and TNFR2 with rather beneficial effects like cellular regeneration, suggesting selective inhibition of TNFR1 to be a promising treatment strategy (Arnett et al. 2001, Kassiotis and Kollias 2001, reviewed by van Hauwermeiren 2011). For example, the antagonistic TNFR1-specific TNF mutein R1antTNF and its polyethylene glycol-modified (PEGylated) derivative revealed therapeutic efficacy in mouse models of inflammatory diseases like CIA, EAE, acute hepatitis and hyperplasia (Shibata et al. 2008a, Shibata et al. 2008b, Nomura et al. 2011, Kitagaki et al. 2012). In addition, a single heavy chain variable domain antibody, specifically binding to TNFR1 (GSK1995057; Holland et al. 2013), a triple V_HH Nanobody, comprising two binding sites for TNFR1 and a third one for albumin (Steeland et al. 2014), as well as two different soluble pre-ligand binding assembly domains (PLAD), intended to disrupt TNFR1 cluster formation (Deng et al. 2005, Cao et al. 2011), are currently under investigation. Finally, shRNA (short hairpin RNA) or antisense oligonucleotide-based drugs, interfering with the expression of TNFR1 or molecules involved in TNFR1 signal transduction, were tested successfully e.g. in CIA and radiation-induced TNF-mediated liver toxicity (Huang et al. 2006, Arntz et al. 2010, van Hauwermeiren 2011).

1.6. Preliminary Work and Study Content

Thoma and coworkers isolated in 1990 the TNFR1-specific antibody H398 from mice, immunized with affinity-purified receptor material from HL-60 cells. H398 was subsequently reported to specifically block TNFR1-mediated NF- κ B activation in Jurkat cells (Kruppa et al. 1992). Furthermore, the recombinant expression of a single-chain variable fragment (scFv) of H398 with retained biologic activity and its humanization were published (Moosmayer et al. 1995, Kontermann et al. 2008). The humanized version of scFvH398, scFvIZI06.1, was

recently converted into an antagonistic TNFR1-specific antibody (ATROSAB), revealing bivalent high affinity binding to its target and potent inhibition of TNF-mediated interleukin-release and cytotoxicity (Zettlitz et al. 2010a). In addition, an scFvZI06.1-HSA (human serum albumin) fusion protein also revealed inhibition of TNF-induced release of interleukin-8 (IL-8) and IL-6, however to a lower extent, when compared with ATROSAB (Berger et al. 2013). The terminal serum half-life of scFvZI06.1-HSA was also clearly reduced in comparison with ATROSAB, but increased, compared with the scFv. During preparation of this dissertation, ATROSAB was tested for safety and tolerability in a clinical phase I trial.

The aim of the present study was to further characterize ATROSAB in terms of receptor binding and *in vitro* bioactivity, to verify alternative molecular formats and to develop molecules with improved TNFR1 binding and inhibition. Lack of Fc-mediated effector functions, due to a mutated heavy chain, used for the generation of ATROSAB, was confirmed (Zettlitz et al. 2010a). In addition, the *in vivo* circulation time in transgenic mice, expressing the extracellular domain of human TNFR1 was determined and the residues on TNFR1, responsible for ATROSAB binding were localized. Moreover, TNFR1 binding, activation and inhibition of TNF and LT α -mediated TNFR1 activation were extensively studied for ATROSAB and Htr-9, a murine agonistic TNFR1-specific antibody. In addition, several different antibody formats (Fab, scFv-HSA, Diabody, scFv-Fc, 2scFv-HSA and IgG-FabL), containing one or two ATROSAB binding sites, were expressed and characterized *in vitro*. Furthermore, binding affinity of ATROSAB and its thermal stability were improved on the basis of scFv antibodies, using phage display and repeated humanization. Finally, the obtained scFv fragment (scFvFRK13.7) was converted into the IgG, Fab, FabL and FabCH3 formats, followed by the analysis of receptor binding kinetics, the investigation of agonistic or antagonistic potential and the determination of their pharmacokinetic profile.

2. Materials

2.1. General declarations

Plastic ware for all laboratory use was acquired from Greiner bio-one (Frickenhausen, Germany). Chemicals were bought from Roth (Karlsruhe, Germany) while enzymes (cloning and PCR) and supplemental reagents were purchased from ThermoFisher (Munich, Germany). Any different source of consumables is clearly stated in the Material or Methods section.

2.2. Special Material

Bradford Reagent	500-0006, BIO-RAD, Munich, Germany
Calcein	Invitrogen, Germany
Centrifugation tubes (MIDI 11136 *g)	60.540.500, Sarstedt, Nuembrecht, Germany
Dynabeads® M-280 Streptavidin	112.05D, Life Technologies, Carlsbad, CA, USA
Glycogen	R0551, Thermo Fisher, Waltham, MA, USA
HiTrap KappaSelect I ¹²⁵	17-5458-12, GE Healthcare, Chalfont St Giles, GB
iodo-BEADS	I-RB-31, Hartmann Analytic, Braunschweig, Germany
Ni-NTA Agarose	28666, Thermo scientific, Munich, Germany
PD-10 Column Sephadex™ G-25 M	64-17-5, Macherey-Nagel, Dueren, Germany
Poly-Prep® Chromatography Columns	17-0851-01, GE Healthcare, Chalfont St Giles, GB
Pre-cast gels, 4–15%, 10 well Mini-PROTEAN® TGX™ Gel	731-1550, BIO-RAD, Munich, Germany
pUC DNA	456-1084, BIO-RAD, Munich, Germany
Reaction tubes	200231-42, StrataGen, Kirkland, WA, USA
REDTaq® ReadyMix™	Eppendorf, Hamburg, Germany
Sulfo-NHS-SS-Biotin	R2523-100RXN, Sigma-Aldrich, Taufkirchen, Germany
TOYOPEARL® AF-rProtein A-650F	21328, Pierce, Rockford, USA
	22805, Tosoh, Stuttgart, Germany

2.3. Kits

GeneMorph II Random Mutagenesis Kit	200550, Agilent Technologies, Santa Clara, CA, USA
IL-6 Kit	31670069, ImmunoTools, Friesoythe, Germany
IL-8 Kit	31670089, ImmunoTools, Friesoythe, Germany
NucleoBond® Xtra Midi	740410.100, Macherey-Nagel, Dueren, Germany

NucleoSpin®	
Gel and PCR Clean-up	740609.250, Macherey-Nagel, Dueren, Germany
NucleoSpin® Plasmid	740588.250, Macherey-Nagel, Dueren, Germany

2.4. Online tools

IgBLAST	http://www.ncbi.nlm.nih.gov/igblast/
Z-score	http://www.bioinf.org.uk/abs/shab/
Cothia canonicals	http://www.bioinf.org.uk/abs/chothia.html
NCBI-BLAST	http://blast.be-md.ncbi.nlm.nih.gov/Blast.cgi
PIGS	http://www.biocomputing.it/pigs
YASARA	http://www.yasara.org/minimizationserver.htm

2.5. Buffers and Solutions

ATROSAB formulation buffer	25 mM histidine, 102 mM NaCl, 26 mM trehalose, 0.04% Tween 20, pH 6.2
Crystal violet	0.5 % crystal violet, 20 % methanol in H ₂ O
IMAC buffer, (5x)	250 mM Na-phosphate (37.38 g Na ₂ HPO ₄ · 2H ₂ O + 6.24 g NaH ₂ PO ₄ · 2H ₂ O), 1.25 M NaCl, pH 7.5, ad 1 L H ₂ O
PBA	2 % FCS, 0.2% NaN ₃ in sterile PBS
PBS (1x)	2.67 mM KCl, 1.47 mM KH ₂ PO ₄ , 137.93 mM NaCl, 8.06 mM Na ₂ HPO ₄ · 7H ₂ O, pH 7.5
PEG-NaCl	200 g Polyethylenglycol 6000, 2.5 M NaCl, ad 1 L H ₂ O
Periplasmatic preparation buffer, PPB	30 mM Tris-HCl pH 8.0, 1 mM EDTA, 20 % sucrose in H ₂ O
PFA	PBS, 1 % BSA, 0.1 % NaN ₃
Reagent Diluent	0.1 % BSA, 0.05 % Tween 20, 20 mM TRIS, 150 mM NaCl, pH7.5
SDS loading (5x)	non-reducing: 30 % (v/v) glycerol, 3 % (w/v) SDS, 2 µg/ml bromophenol blue in 62.5 mM Tris-HCl, pH 6.8 reducing: add 5 % (v/v) β-mercaptoethanol
SDS running (10x)	1.92 M glycine, 0.25 M Tris, 1 % SDS, pH 8.3
Solubi Shu lysis buffer	150 mM NaCl, 1 mM EDTA, 20 mM Tris, 1% Triton-X-100, pH 7.6
TAE buffer (50x)	2 M Tris, 0.95 M glacial acetic acid, 50 mM EDTA in H ₂ O, pH 8
TMB substrate	100 µl TMB (100 mg/ml stock in DMSO) 2 µl 30 % H ₂ O ₂ 10 ml Na- acetate buffer, pH 6 (100mM)

2.6. Proteins

Anti-C1q HRP (Sheep polyclonal)	ab46191, Abcam , Cambridge, UK
Anti-His-HRP (HIS-6 His-Probe-HRP)	sc-8036, Santa Cruz Biotechnology, Santa Cruz, CA, USA
Anti-HSA (Rabbit)	A0433, Sigma-Aldrich, Taufkirchen, Germany
Anti-human Fab (Goat, polyclonal)	2085-01, SuthernBiotech, Birmingham, AL, USA
Anti-human IgG	

(Fab specific) Anti-human IgG	A 0293 Sigma-Aldrich, Taufkirchen, Germany
(Fc specific) Anti-human IgG (heavy chain)	A 0170, Sigma-Aldrich, Taufkirchen, Germany
Anti-Ik β	BM476, ACRIS antibodies, Herford, Germany
Anti-M13	551819, BD Pharmigen, Heidelberg, Germany
Monoclonal HRP-Conjugate	27942101, GE Healthcare, Chalfont St Giles, GB
Anti-murine IgG (Fc specific)	A 2554, Sigma-Aldrich, Taufkirchen, Germany
Anti-plk β	9246, Cell Signaling Technology, Cambridge, UK
Anti-Rabbit-HRP	A0545, Sigma-Aldrich, Taufkirchen, Germany
Anti-TNF α -HRP	ab24473, Abcam, Cambridge, UK
Anti-Tubulin	MS-581-P, ThermoFisher, Munich, Germany
C1q	204876, Merck Millipore, Darmstadt, Germany
Db-IZI06.1	In house production (Institute of Cell Biology and Immunology, University of Stuttgart, Germany, cloned by Dr. Kirstin Zettlitz)
FcgRIA	10256-H08H, Sino Biological, Beijing, China
FcgRIIB	10259-H08H, Sino Biological, Beijing, China
FcgRIIIA	10389-H08H, Sino Biological, Beijing, China
H398	HM2020SP-b, Hycult biotech, Plymouth Meeting, PA
Htr-9	In house production (Institute of Cell Biology and Immunology, University of Stuttgart, Germany)
Human IgG	I4506, Sigma-Aldrich, Taufkirchen, Germany
huTNFR1-Fc	Celonic, Juelich, Germany
huTNFR2-Fc	Celonic, Juelich, Germany
LT	Prof. Dr. Peter Scheurich
moTNFR1-Fc	Dr. Kirstin Zettlitz
MR2-1	HM2007, Hycult biotech, Plymouth Meeting, PA
Rituximab	Celonic, Juelich, Germany
scFv-HSA	Dr. Verena Berger, Celonic, Juelich, Germany
TNF	Prof. Dr. Peter Scheurich
Trastuzumab	Hans-Heinrich Heidtmann, St. Joseph-Hospital, Bremerhaven

2.7. Media

2xTY medium	1.6 % peptone, 1 % yeast extract, 0.5 % NaCl in H ₂ O
2xTYamp, glc Plates	2xTY medium and 1.5 % agar, 100 μ g/ml ampicillin, 1 % glucose
LB	1 % peptone, 0.5 % yeast extract, 0.5 % NaCl (low salt = 5 g/L) in H ₂ O
LB _{amp} agar plates	LB medium, 1.5 % (w/v) agar, 100 μ g/ml ampicillin, 1 % glucose
M9 stock (10x)	0.5 M Na ₂ HPO ₄ , 0.22 M KH ₂ PO ₄ , 5 % NaCl, 10 % NH ₄ Cl, pH 7.2
Minimal plates	1.5 % agar, 0.2 % glucose, 1 mM MgSO ₄ , 2 μ g/ml vitamine B1, M9
SOB	0.5 % (w/v) yeast extract, 2 % (w/v) peptone, 10 mM NaCl, 2.5 mM KCl, 10 mM MgSO ₄ , 10 mM MgCl ₂
SOC	SOB medium and 20 mM glucose (catabolite repression by glucose)

2.8. Tissue Culture

RPMI 1640 (1X)	21875-034, Life Technologies, Carlsbad, CA, USA
Opti-MEM [®]	31985-047, Life Technologies, Carlsbad, CA, USA
FCS	GIBCO Invitrogen, Karlsruhe, Germany
Lipofectamine [™] 2000	11668-019, Invitrogen, Karlsruhe, Germany

Trypsin/EDTA, 10 x	GIBCO Invitrogen, Karlsruhe, Germany
Penicillin/Streptomycin 100 x	104 U/ml / 104 µg/ml, GIBCO Invitrogen, Karlsruhe, Germany
Zeocin™	Invitrogen, Karlsruhe, Germany
human Serum	Blood Donation Center SRK Basel

2.9. Bacteria and Phages

<i>E. coli</i> HB2151	Carter et al. 1985, StrataGen, Kirkland, WA, USA
<i>E. coli</i> TG1	Genotype: supE thi-1 Δ(lac-proAB) Δ(mcrB-hsdSM)5 (rK-mK-) [F' traD36 proAB lacIqZΔM15], StrataGen, Kirkland, WA, USA
VSC M13 helper phages	StrataGen, Kirkland, WA, USA

2.10. Eukaryotic Cells

DOHH-2	human B-cell lymphoma cell line, DSMZ, ACC-47
HEK293T	Human embryonic kidney, DSMZ, ACC-635
HeLa	Human cervix carcinoma, DSMZ, ACC 57
HT1080	Human fibrosarcoma, ECACC85111505
Kym-1	Human rhabdomyosarcoma from neck tumor, JCRB0627), supplied by M. Sekiguchi, University of Tokyo, Japan
MEF	Immortalized mouse embryonic fibroblasts from TNFR1/TNFR2 double knock-out mice, stably transfected with human TNFR1-Fas or TNFR2-Fas, Krippner-Heidenreich et al. 2002

2.11. Mice

C57BL/6J wt	Janvier Labs, Saint Berthevin Cedex, France
C57BL/6J- huTNFRSF1A _{ecd} ^{tm1UEG} /IZI	Transgenic C57BL/6J mice, bearing the gene of the extracellular domain of human TNFR-1 instead of the respective mouse gene. Transmembrane domain and intracellular domain are from genetic mouse background. Institute of Cell Biology and Immunology, University of Stuttgart, Germany

2.12. Plasmids

pAB1	Vector for prokaryotic protein expression in <i>E. coli</i> TG1 (Kontermann et al. 1997)
pEE14.4	GS-encoding expression vector, GS-System™pEE Expression Vectors, Lonza Biologics, Berkshire, UK
pEE6.4	Accessory vector, GS-System™pEE Expression Vectors, Lonza Biologics, Berkshire, UK
pSecTagA	Eukaryotic expression, Invitrogen, Karlsruhe, Germany
pSecTagA-L1-His	pSecTagA, containing a restriction site for AgeI in the Igk Leader and a HIS-Tag C-terminal of the MCS

pCV072	Shuttle vector, Celonic, Juelich, Germany
pAB1-L1-EMP1- CLk-Li1	Fabian Richter, 2009 unpublished
pAB1-L1-EMP1- hg1e3-Li1	Fabian Richter, 2009 unpublished
pAB1-FabIzI06_Korr_Myc _His	Sabine Munkel, unpublished
pHEN2	15 aa linker, pUC119 backbone

2.13. Primer (acquired from Sigma-Aldrich, Munich, Germany)

Project/Primers	5'> 3' sequence
Epitope Mapping	
AgeI_huTNFR1_CRD1_back	ggaccggtctgggtccctcacctaggcgatcgggag
AgeI_huTNFR1_V14L_back	ggaccggtctgggtccctcacctaggcgatcgggagaagagagatagttgtgtcc ccaagg
AgeI_huTNFR1_I21V_back	ggaccggtctgggtccctcacctaggcgatcgggagaagagagatagttgtgtgtcc ccaaggaaaatatgtccaccctcaaaataattcg
PstI_huTNFR1_G45S_for	tgcactgcagtcctgtatcctgccccgggcttggacagtcattatacaag
XmaI_huTNFR1_Q48R_back	tccccccggggcgggatcaggactgcagggagtg
XmaI_huTNFR1_D51V_back	tccccccggggcgaggatcaggctctgcagggagtg
PstI_huTNFR1_S57K_back	tgcactgcagggagtgtagagagggctccttcaccgcttcag
PstI_huTNFR1_S59T_back	tgcactgcagggagtgtagagagcggcacttcaccgcttcagaaaacc
PstI_huTNFR1_E64Q_back	tgcactgcagggagtgtagagagcggctccttcaccgcttcacagaaccacctcag aactgc
PstI_huTNFR1_H66Y_back	tgcactgcagggagtgtagagagcggctccttcaccgcttcagaaaactacctcag aactgcctcagc
PstI_huTNFR1_H69Q_back	tgcactgcagggagtgtagagagcggctccttcaccgcttcagaaaaccacctcag acagtgcctcagctgctcc
BglII_huTNFR1_G81S_for	ggaagatctccacctgggacatttctcttcggcatttggagc
BglII_huTNFR1_S87P_back	ggaagatctctccttgccacagtgaggccgggacacc
BglII_huTNFR1_T89Q_V90A_back	ggaagatctctctcttgccaagctgaccgggacaccgctgtgtgg
BglII_huTNFR1_R92K_back	ggaagatctctctcttgccacagtgaggacaaggacaccgctgtgtggctgtagg
NotI_huTNFR1_CRD4_for	atttgcggccgctgtggtagctcctcagtgccctaac
QC_P23S_back	caaggaaaatatatccacagtcaaaataattcgatttgc
QC_P23S_for	gcaaatcgaattatcttggactgtggatatacttctcctg
QC_Q24K_back	ggaaaatatatccaccctaaaataattcgatttgc
QC_Q24K_for	cagcaaatcgaattatctttaggggtggatatacttctcc
QC_R68A_back	gcttcagaaaaccacctcgacactgcctcagctgctcc
QC_R68A_for	ggagcagctgagggcagtgtagcaggggtgttcttgaagc
QC_H69A_back	gcttcagaaaaccacctcagagcttgcctcagctgctccaaatgc
QC_H69A_for	gcatttggagcagctgaggcaagctctgaggtggtttctgaagc
QC_L71A_back	ccacctcagacactgcgccagctgctccaaatgccg
QC_L71A_for	cggcatttggagcagctggcgagctgtctgaggtgg
QC_S72A_back	cacctcagacactgcctcgccctgctccaaatgccgaaag
QC_S72A_for	cttctggcatttggagcagggcagggcagtgctgaggtg
QC_S74K_back	gacactgcctcagctgcaagaaatgccgaaaggaaatg
QC_S74K_for	catttctcttggcatttcttgcagctgagggcagtgct
QC_K75T_back	cactgcctcagctgctccacatgccgaaaggaaatgg
QC_K75T_for	ccatttctcttggcatttcttgcagctgagggcagtg
scFv-Fc	
XbaI_L1_VHscFvIzI06.1_back	cgtctagacaccatggagacagacacactcctgctatgggtactgctgctctggg ttccaggttcaccggctcaggttcagctgggttcagagcgggtgcg
NotI_VLscFvIzI06.1_for	ttggggccgctccgctgaaccgccacgtttaatttccactttgg
IgG-FabL	
AgeI_VLIZI06.1_back	Ggaccggtgatattgtgatgaccagagcccgctg
RsrII_Li_CLK_for	gattcgggtccgtccgcccctcctccgctcccaccctgttgaagctcttgtga cgggcg
AgeI_VHIZI06.1_back	ggaccggtcaggtgcagctgggtgcagagcggagccgag

NheI_Li_CH1ZI06.1_for	ccgctagctccgccgctaccgccgctccctcccaccttcttgctccacctgggtgttgctgg
FabATROSAB	
AgeI_VLIZI06.1_back	ggaccggtgatattgtgatgaccagagcccgctg
RsrII_VL-IZI06.1_for	ggcaccaaagtggaaattaaacggaccgccc
AgeI_VHIZI06.1_back	ggaccggtcaggtgcagctgggtgcagagcggagccgag
EcoRI_CH1-ATROSAB_for	ccggaattcttagcagctcttgggctccaccttcttgctcc
2scFvHSA	
AgeI_XhoI_HSA_back	ggaccggtccctcgagtgggtggatcaggcgggtgatgcacacaagagtgg
NotI_BspEI_HSA_for	tttgccggccgaaatccggaccaccgctgccaccggcagcttgacttgacg
AgeI_VHIZI06.1_back	gggaccggtcaggttcagctgggttcagagcgggtgcggaa
Sall_VLIZI06.1_for	agcgtcgaccgtttaattccactttgggtgccacc
BspEI_VHIZI06.1_back	gggtccggacaggttcagctgggttcagagcgggtgcggaa
LMB2	actggccgctcgttttac
Acceptor Vectors	
EcoRI_CH1_ATROSAB_for	ccggaattcttagcagctcttgggctccaccttcttgctcc
HindII-NheI-CH1hg1-back_neu	cccaagcttggggctagcaccaggcccatcgggtcttcc
LMB3	caggaaacagctatgacc
CLK-Li8-for	tccgccgctccctccgctcccaccctgttgaagctctttgtgac
Li8-CLK-back	ggtagggagcggaggaggcggcggacgtaccgttgctgcgccatctgtc
LMB2	actggccgctcgttttac
CH1-Li8-for	tccgccgctaccgccgctccctcccaccttcttgctccaccttgg
Li8-CH1-back	ggagggagcggcggtagcggcggagccagcaccaggcccccagc
XmaI-Li10-CLK-for	cagctcgtcccgggagggggcagggtgtacacctggggctcccgtggctgagagccacctccgctgaaccgctccaccgctcgaccacactctcccctgttgaagctctttgtgac
XmaI-Li10-CH1-for	cagctcgtcccgggagggggcagggtgtacacctggggctcccgtggctgagagccacctccgctgaaccgctccaccgctcgaccgcagctcttgggctccaccttcttgctccaccttgg
FRK13.7 derivatives	
AgeI_VH-T12B_back	ggttccaccggtcatgttcagctgggttcagagc
NheI_VH-T12B_for	cttgggtgctagcgtcgcagaccgtaacggtgg
AgeI_VL-FRK7_back	ggttccaccggtgatgtgcagatgaccagagc
RsrII_VL-FRK7_for	gcagcaacgggtccggttgatttccaccttgggtgcctcc
pHENIS-scFvIG11-fsSTOP	
NcoI_VH-IZI06.1_back	cagccggccatggcccaggttcagctgggtcag
BstZ17I_fsSTOP_BssHII_for	ccaaaggtatacggcacccttaatccagaaaatcccaacgcgcgcaataatacacgcgggtatc
EP03	
LMB2	actggccgctcgttttac
fd-seq1	cctcatacagaaaattc

3. Methods

3.1. Preparation of chemically competent *E. coli* TG1

50 ml LB medium was inoculated at a starting OD [600 nM] of 0.05 to 0.1 from a overnight culture of *E. coli* TG1 (which was in turn started using TG1 freshly streaked on a minimal plate) and incubated shaking at 37 °C until an OD [600 nM] of 0.5 to 0.6 was reached. The culture was chilled on ice for 15 minutes and harvested by centrifugation at 1000 *g for 5 minutes. Subsequently, the supernatant was discarded and the pellet was resuspended in 50 ml of 100 mM CaCl₂ in H₂O, again incubated on ice for 30 minutes and centrifuged as described. This time, the pellet was resuspended in 10 ml 20 % glycerin containing 50 mM CaCl₂. Aliquots of the bacteria suspension were frozen in liquid nitrogen and stored at -80 °C.

3.2. Cloning procedures

DNA preparation was performed using the NucleoSpin® Plasmid kit or NucleoBond® Xtra Midi kit according to the manufacturers protocols. Manipulations were performed by the use of individually designed primers in standard PCR techniques with a T₄-DNA Polymerase in combination with the delivered buffer, strictly following the guidelines of the supplier. Duration of the single steps during the PCR reaction, temperature and cycles were adjusted if necessary. PCR samples were analyzed by agarose gel electrophoresis (0.5 % to 2 % agarose in TAE buffer). Obtained DNA fragments were excised and purified using the NucleoSpin® Gel and PCR Clean-up kit according to the manufacturers protocol.

QuickChange® PCR was performed according to the protocol suggested by StrataGen (Kirkland, WA, USA). In some cases the completion of the whole plasmid did not work during the PCR process, hence a Fusion-PCR was performed. For this three-step PCR procedure, mutagenesis primers were designed as recommended for QuickChange. In addition, primers that annealed to the N- and C-terminal regions of the construct were used. PCR1 was performed using the N-terminal back primer together with the QuickChange_for primer, PCR2 with the QuickChange_back primer and the C-terminal for primer. Both cleaned PCR products were mixed and then subject to an intermediate PCR step of five cycles with 3

minutes elongation time in the absence of primers followed by a 3 minutes incubation on ice. Finally, the N- and C-terminal primers were again added to the reaction mix and PCR3 was performed according to the standard protocol.

Digestions of DNA samples were performed in a standard procedure using a 50 µl sample, containing 5-15 µg DNA. Buffers, Enzymes, Incubation temperature and duration were applied as suggested by the provider. Incubation time was extended over night if necessary (seemed to be of advantage for PCR products but not for plasmids). Linearized vector molecules were dephosphorylated to prevent religation of the empty plasmids by incubation with 1-3 units alkaline phosphatase (FastAP) per 50 µl sample for one to twelve hours (elongated incubation increased ligation efficiency). Digested DNA fragments were separated by agarose gel electrophoresis containing 0.5 % to 2 % agarose in TEA buffer at 80 volts for 30 minutes. Visualization was performed by staining with ethidium bromide (0.1 µg/ml final concentration). Isolated DNA fragments were extracted from the gel matrix using the NucleoSpin® Gel and PCR Clean-up kit as recommended by the manufacturer.

Ligation was performed by incubation with T4 DNA Ligase according to the product manual in a volume of 20 µl, containing 100 to 200 ng of vector DNA in combination with insert DNA at a molar ratio of 1:5 to 1:10 (vector to insert). *E. coli* TG1 were transformed with 7 µl to 20 µl (whole ligation mix) of the ligated DNA by a temperature shift from 4 °C (ice bucket) to 42 °C. Prior to plating to LB agar plates, substituted with the appropriate antibiotic, bacteria were chilled again on ice for a few minutes and incubate in 1 ml LB without selective pressure, shaking at 37 °C for 20-60 minutes. Ligation success was tested by colony PCR with standard primers for the respective vectors, using DreamTaq Green DNA Polymerase MIX or REDTaq® ReadyMix™, according to the manufacturers protocol. Except, instead of the addition of template DNA, a single colony of the transformation plate was picked and tipped into the reaction mix. Cloning success was further verified by sequence analysis using the GATC (Constance, Germany) LIGHTrun system. Sequences were compared using NCBI BLAST to confirm base composition of the cloning product.

3.3. Cloning Strategies

3.3.1. Cloning of huTNFR1-Fc Receptor mutations

Mutations of residues in the sequence of the human TNFR1 were introduced by site-directed mutagenesis. Primers containing the desired mutation in their sequences were used for standard PCR, QuickChange® or Fusion-PCR together with huTNFR1-Fc as template. PCR products were introduced into the sequence of huTNFR1-Fc by restriction digest and ligation (procedure see above). Combinations of primers, PCR reaction type and restriction enzymes are displayed in Table 3.1.

Table 3.1 Cloning of human TNFR1-Fc mutants

Mutation	Primer_back	Primer_for	PCR	RE 1	RE 2
V14L	AgeI_huTNFR1_V14L_back	NotI_huTNFR1_CRD4_for	STD	AgeI	NotI
I21V	AgeI_huTNFR1_I21V_back	NotI_huTNFR1_CRD4_for	STD	AgeI	NotI
P23S	QC_P23S_back	QC_P23S_for	QC	AgeI	NotI
Q24K	QC_Q24K_back	QC_Q24K_for	QC	AgeI	NotI
G45S	AgeI_huTNFR1_CRD1_back	PstI_huTNFR1_G45S_for	STD	AgeI	PstI
Q48R	XmaI_huTNFR1_Q48R_back	NotI_huTNFR1_CRD4_for	STD	XmaI	NotI
D51V	XmaI_huTNFR1_D51V_back	NotI_huTNFR1_CRD4_for	STD	XmaI	NotI
S57K	PstI_huTNFR1_S57K_back	NotI_huTNFR1_CRD4_for	STD	PstI	NotI
S59T	PstI_huTNFR1_S59T_back	NotI_huTNFR1_CRD4_for	STD	PstI	NotI
E64Q	PstI_huTNFR1_E64Q_back	NotI_huTNFR1_CRD4_for	STD	PstI	NotI
H66Y	PstI_huTNFR1_H66Y_back	NotI_huTNFR1_CRD4_for	STD	PstI	NotI
R68A	QC_R68A_back	QC_R68A_for	QC	AgeI	NotI
H69Q	PstI_huTNFR1_H69Q_back	NotI_huTNFR1_CRD4_for	STD	PstI	NotI
H69A	QC_H69A_back	QC_H69A_for	QC	AgeI	NotI
L71A	QC_L71A_back	QC_L71A_for	QC	AgeI	NotI
S72A	QC_S72A_back	QC_S72A_for	QC	AgeI	NotI
S74K	QC_S74K_back	QC_S74K_for	QC	AgeI	NotI
K75T	QC_K75T_back	QC_K75T_for	QC	AgeI	NotI
G81S	AgeI_huTNFR1_CRD1_back	BglII_huTNFR1_G81S_for	STD	AgeI	BglII
S87P	BglII_huTNFR1_S87P_back	NotI_huTNFR1_CRD4_for	STD	BglII	NotI
T89Q/V90A	BglII_huTNFR1_T89Q_V90A_back	NotI_huTNFR1_CRD4_for	STD	BglII	NotI
R92K	BglII_huTNFR1_R92K_back	NotI_huTNFR1_CRD4_for	STD	BglII	NotI

Explanations: Primer_back (5'>3' on plus strand), Primer_for (5'>3' on minus strand), STD (standard PCR), QC (QuickChange), RE (restriction enzyme)

3.3.2. Cloning of moTNFR1-Fc

The Sequence of mouse TNFR2 was acquired from GeneArt AG (Regensburg, Germany) and introduced into pSecTagA-L1-huTNFR1-Fc after digestion with AgeI and NotI followed by ligation, resulting in the expression plasmid pSecTagA-L1-moTNFR2-Fc.

3.3.3. Cloning of scFvZI06.1-Fc

The scFv of ATROSAB (scFvZI06.1) was amplified by PCR from the Template pAB1-scFvZI06.1 using the primers XbaI_L1_VHscFvZI06.1_back and NotI_VLscFvZI06.1_for. The resulting DNA fragment was inserted into the vector pSecTagA upon digestion with the restriction enzymes NheI and NotI for the vector as well as XbaI and NotI in case of the insert. Resulting in pSecTagA-L1-scFvZI06.1-Fc. NheI and XbaI sites contain compatible ends and lead to subsequent elimination of the used restriction site.

3.3.4. Cloning of IgG-FabL

The light chain of an IgG molecule with extended Fab arms was cloned by PCR upon the usage of the primers AgeI_VLZI06.1_back and RsrII_Li_CLK_for and the template pCV072_IZI06_VLCL_VHCH1CH2CH3, followed by digestion with the enzymes AgeI and RsrII and ligation into the Vector pAB1-L1-EMP1-CLK-Li1, resulting in pAB1-L1-VLZI06.1-2CLK. The PCR of the heavy chain was performed with the same template and the primers AgeI_VHIZI06.1_back and NheI_Li_CH1_for. The resulting DNA fragment was digested by AgeI and NheI and inserted into pAB1-L1-EMP1-hg1e3-Li1. The new plasmid was designated pAB1-L1-VHIZI06.1-2CH1CH2CH3. Heavy and light chains, containing either two CH1 or two CLK domains were transferred to the LONZA GS-System™ composed of the expression vectors pEE14.4 and pEE6.4, using the restriction enzymes HindIII and EcoRI followed by ligation to create pEE6.4-VHIZI06.1-2CH1-CH2CH3 and pEE14.4-VLZI06.1-2CLK. Both plasmids were fused in the following, after digestion by NotI and BamHI, resulting in the bicistronic expression vector pEE14.4-VHVLZI06.1-2CLK-2CH1CH2CH3.

3.3.5. Cloning of FabATROSAB

VLZI06.1 was amplified from pAB1-L1-VLZI06.1-2CLK (cloning of IgG-FabL) using the primers AgeI_VLZI06.1_back and RsrII_VLZI06.1_for and inserted into pAB1-L1-EMP1-CLK by digestion with AgeI and RsrII and subsequent ligation (pAB1-L1-VHIZI06.1-CH1). The Primers AgeI_VHIZI06.1_back and EcoRI_CH1-ATROSAB_for were employed for PCR of the VH and CH1 of ATROSAB with the template pCV072_IZI06_VLCL_VHCH1CH2CH3. The resulting DNA fragment was inserted into pAB1-L1-EMP1-hg1e3-Li1 by digestion with AgeI and EcoRI followed by ligation (pAB1-L1-VLZI06.1-CLK). Introduction into the LONZA GS-System™ was performed as described for IgG-FabL.

3.3.6. Cloning of 2scFv-HSA

Firstly, the sequence encoding for HSA was amplified from pAB1-HSA by the use of the primers *AgeI_XhoI_HSA_back* and *NotI_BspEI_HSA_for* and inserted into the plasmid pSecTagA-L1-His after digestion by *AgeI* and *NotI*, resulting in the new plasmid pSecTagA-L1-HSA. Second, the DNA of the N-terminal scFv fragment was produced by PCR with the template pAB1-scFvZI06.1 using the primers *AgeI_VHIZI06.1_back* and *Sall_VLIZI06.1_for* and inserted into pSecTagA-L1-HSA following digestion of the PCR product with *AgeI* and *Sall* and the vector with *AgeI* and *XhoI*. The created plasmid was designated pSecTagA-L1-scFvZI06.1-HSA. The compatible ends of *Sall* and *XhoI* allowed for the elimination of the restriction sites upon ligation. Lastly, the C-terminal scFvZI06.1 was amplified by PCR from the template pAB1-scFvZI06.1 by use of the primers *BspEI-VHIZI06.1_back* and *LMB2*. Insertion into pSecTagA-L1-scFvZI06.1-HSA was accomplished by digestion of vector and insert with the restriction enzymes *BspEI* and *NotI*. Ligation resulted in the expression vector pSecTagA-L1-scFvZI06.1-HSA-scFvZI06.1.

3.3.7. Cloning of scFvT12B

pHENIS-scFvT12B was selected by phage display and the scFv encoding DNA sequence was transferred to the expression vector pAB1 by enzymatic digestion using *NcoI* and *NotI* followed by ligation, resulting in pAB1-scFvT12B.

3.3.8. Cloning of scFvFRK13.1 to scFvFRK13.8

The DNA sequence encoding for scFvFRK13.1 and scFvFRK13.2 was purchased from GeneArt AG (Regensburg, Germany) and sub-cloned into pAB1 using the restriction enzymes *NcoI* and *NotI*, resulting in the vectors pAB1-scFvFRK13.1 and pAB1-scFvFRK13.2. VL domain encoding DNA sequences were excised from pAB1-scFvFRK13.1, pAB1-scFvFRK13.2 and pAB1-scFvT12B using *XhoI* and *NotI* and introduced into the corresponding plasmids to create the expression vectors pAB1-scFvFRK13.3 to pAB1-scFvFRK13.8 (Table 3.2).

Table 3.2. Combinations of scFvFRK

Vector	VH	VL	Vector	VH	VL
pAB1-scFvFRK13.1	FRK1	FRK1	pAB1-scFvFRK13.5	T12B	FRK1
pAB1-scFvFRK13.2	FRK2	FRK2	pAB1-scFvFRK13.6	FRK1	T12B
pAB1-scFvFRK13.3	FRK1	FRK2	pAB1-scFvFRK13.7	T12B	FRK2
pAB1-scFvFRK13.4	FRK2	FRK1	pAB1-scFvFRK13.8	FRK2	T12B

3.3.9. Cloning of Acceptor Vectors

In order to enable rapid conversion of scFv fragments into IgG, Fab, FabL or FabCH3 molecules, a series of acceptor vectors was generated on the basis of EMP1 peptide sequence containing pAB1 plasmids. The advantage of these acceptor vectors was the possibility to observe correct insertion of heavy and light chain variable domain sequences by agarose gel electrophoresis upon a band shift, without the need for time consuming sequence analysis.

Acceptor vectors for the creation of IgG already existed in pAB1-L1-EMP1- CLk-Li1 and pAB1-L1-EMP1- hg1e3-Li1.

As the light chain of the Fab fragment is identical to the light chain of the IgG, the acceptor vector containing only the CH1 domain remained to be created for the generation of Fab acceptor vectors. CH1 domain encoding DNA was amplified from the template pAB1-EMP1-hg13e-Li1 by PCR with the primers EcoRI_CH1_ATROSAB_for and HindII-NheI-CH1hg1-back_neu. After digestion by the restriction enzymes NheI and EcoRI the PCR fragment was inserted into pAB1-EMP1-hg13e-Li1, resulting in the acceptor vector pAB1-L1-EMP1-CH1.

pAB1-L1-EMP1-2CLk was created by ligation of the product of a Fusion-PCR using the primers LMB3 and CLk-Li8-for for PCR1, Li8-CLk-back and LMB2 for PCR2 as well as LMB2 and LMB3 for PCR3, into the plasmid pAB1-L1-EMP1-CLk, after digestion by the enzymes RsrII and EcoRI. Similarly, the Fusion-PCR product, generated with the template pAB1-L1-EMP1-hg1e3-Li1 and the primers LMB3 and CH1-Li8-for (PCR1), Li8-CH1-back and EcoRI-CH1-ATROSAB-for (PCR2) as well as LMB3 and EcoRI-CH1-ATROSAB-for (PCR3), was inserted after NheI/EcoRI digestion into the plasmid pAB1-L1-EMP1-hg1e3-Li1, resulting in pAB1-L1-EMP1-2CH1.

Acceptor vectors for the cloning of FabCH3 constructs were created by PCR using the template pAB1-EMP1-L1-CLk-Li1 together with the primers LMB3 and XmaI-Li10-CLk-for and the template pAB1-FabIZI06_Korr_Myc_His in combination with the primers HindII-NheI-CH1hg1-back_neu and XmaI-Li10-CH1-for, resulting pAB1-L1-EMP1-CLk-CH3 and pAB1-L1-EMP1-CH1-CH3, respectively, after digestion with the enzymes AgeI and XmaI for the light chain vector as well as NheI and XmaI in case of the heavy chain vector, followed by ligation into the vector pAB1-L1-EMP1-hg1e3-Li1.

3.3.10. Cloning of IgG13.7, Fab13.7, Fab13.7L, Fab13.7CH3

The DNA sequences encoding for the variable domains of scFvFRK13.7 were amplified by PCR from pAB1-scFvFRK13.7 using the primers AgeI_VH-T12B_back and NheI_VH-T12B_for for the heavy chain as well as AgeI_VL-FRK7_back and RsrII_VL-FRK7_for in case of the light chain. After digestion with the enzymes AgeI and NheI (heavy chain) or AgeI and RsrII (light chain), the variable domains were introduced into the particular acceptor vectors, which are described above. NheI digestion of the PCR product, containing the VH encoding DNA sequence was performed shortly to allow for partial digestion, as another NheI restriction site was located within the VH. Sub-cloning into the LONZA GS-System™ was performed as described for IgG-FabL.

3.4. Second Humanization of H398

The amino acid sequence of the variable domains of the heavy (VH) and the light chain (VL) were individually aligned to mouse IgG germline genes using the Ig-BLAST algorithm of the NCBI website (<http://www.ncbi.nlm.nih.gov/igblast/>) to identify the closest related mouse genes. The same procedure was performed using human germline genes to identify the genetic sequences, showing the highest sequence identity to VH and VL of H398. In addition, the humanness of the BLAST hits was evaluated on the basis of the Z-score (<http://www.bioinf.org.uk/abs/shab/>). Furthermore, the functionality of the displayed sequences was confirmed by consulting appropriate databases (IMGT/Gene-Db, Gene). Sequences were chosen due to a combination of their BLAST-score, sequence identity and humanness (with priority for higher humanness/Z-score). CDR sequences of H398 were inserted into the human framework in silico (copy and paste), while the D and J segments C-terminal of CDR3 (H and L) were adopted from the sequence of ATROSAB and the Z-score was determined again.

The canonical structure of the newly designed antibody domains were analyzed using another online available tool provided by the group of Andrew C.R. Martin (<http://www.bioinf.org.uk/abs/chothia.html>). The identification of two residues in the sequence, not allowed by the algorithm (see the results section), led to their exchange and thereby the final sequences of scFvFRK13.1 and scFvFRK13.2. DNA encoding for the two scFv antibodies

was ordered from GeneArt AG (Regensburg, Germany) and further cloned as described above.

3.4.1. Homology modelling

Models of the macromolecular structure of scFv antibodies were generated on the basis of the plain sequence information, using the free available online tool PIGS (Prediction of Immunoglobulin Structure, Marcatili et al. 2008). Default settings were used for the modelling method as suggested by the website. The predicted structures were further subject to energy minimization (YASRA Energy Minimization Server, Krieger et al. 2009). Visualization of the model structures was performed using PyMOL molecular graphics (The PyMOL Molecular Graphics System, Version 1504 Schrödinger, LLC).

3.5. Protein Expression

3.5.1. Expression of Antibody Fragments in the Periplasm of *E. coli* TG1

A starting culture of *E. coli* TG1 containing the expression plasmid was incubated overnight in 20 ml 2xTY (100 µg/ml Ampicillin, 1 % glucose) at 37 °C. The next day, 1 liter 2xTY (100 µg/ml Ampicillin, 0.1 % glucose) was inoculated with 10 ml of the over-night culture and incubated shaking at 37 °C until an OD [600 nm] of 0.8 to 1.0 was reached. Subsequent to the addition of 1 ml IPTG (final concentration 1 mM), the culture was incubated at room temperature for additional 3 to 4 hours. Bacteria were harvested by centrifugation at 4500 *g and the pellet was resuspended in PPB to a final volume of 50 ml. To release the antibody fragments from the periplasm, 0.25 ml of lysozyme (10 mg/ml in ddH₂O) were added and the suspension, followed by incubation on ice for 30 minutes. Prior to the next centrifugation step (10,000 *g, 10 minutes, 4 °C), the remaining spheroblasts were stabilized by the addition of 0.5 ml of 1 M MgSO₄. The supernatant was dialyzed over night at 4 °C against PBS. Antibody fragments were purified from the dialyzed solution after an additional centrifugation step (1000 *g, 15 min, 4 °C) as described below.

3.5.2. Expression of Antibodies and Fusion Proteins in Stably Transfected HEK293T Cells

HEK293T cells were seeded into a 6-well plate (10⁶ per well) and incubated in RPMI 1640 + 5 % FCS overnight (37 °C, 5 % CO₂). The medium was then replaced by 1.5 ml Opti-MEM and 3 µg of the expression plasmid as well as 7 µl Lipofectamine were individually

mixed with 170 μ l Opti-MEM, subsequently mixed together and incubated at RT for 30 minutes. The transfection mix was slowly added to the supernatant and the cells were incubated at 37 °C, 5 % CO₂ for additional 6-18 hours. Transfected cells were collected from the 6-well plates and harvested by centrifugation at 500 *g and RT for 5 minutes. Cells were then transferred to a 75 cm² bottle in 10 ml RPMI 1640 + 5 % FCS and after 6-18 hours 300 μ g/ml Zeocin was added. Medium was replaced if necessary until the cells got confluent. For expansion of the transfected cells for the production to reach 70-90 % confluency in 5 175 cm² bottles, the Zoecin concentration was reduced to 50 μ g/ml. RPMI was replaced by Opti-MEM during production (50 ml Opti-MEM per bottle, exchanged every other day, in total at least 1 liter was collected). Supernatants were sterile filtered and purified as described below.

3.5.3. Transient Expression of Antibodies and Fusion Proteins in HEK239T Cells

HEK293 cells were cultivated until five 175 cm² bottles reached 70-90 % confluency. 100 μ g of the vector DNA and 250 μ l Lipofectamine were first mixed individually, each with 7 ml Opti-MEM and then mixed together and incubated for 30 minutes at RT. The transfection mix was adjusted to a volume of 25 ml using Opti-MEM, the culture medium of each bottle was replaced by 5 ml of the transfection solution and the cells were incubated at 37 °C, 5 % CO₂ for 4-6 hours. Production was started by replacing the transfection medium by 50 ml Opti-MEM, which was replaced every second day until at least one liter was collected. Supernatants were sterile filtered and purified as described below.

3.6. Protein purification

3.6.1. Immobilized Metal Affinity Chromatography (IMAC)

Sterile filtered tissue culture supernatants or dialyzed periplasmatic extracts were incubated with Ni-NTA rolling at 4 °C over night. In order to collect the purification resin, the beads containing supernatants were loaded to a Poly-Prep[®] chromatography column by gravity flow or moderate vacuum pressure. Washing was performed using IMAC buffer containing 20 mM Imidazol until almost no protein could be detected in the flow through by a concomitant Bradford test (90 μ l Bradford reagent + 10 μ l sample mixed in a 96-well microtiter plate). Protein was eluted from the resin with 250 mM Imidazol in IMAC buffer

and fractions of 500 μ l were collected. The protein containing fractions (determined by Bradford quick test as described) were pooled and dialyzed against PBS.

3.6.2. Antibody and Protein A Affinity Chromatography

Procedure was performed exactly as described for IMAC, using either TOYOPEARL® AF-rProtein A-650F (protein A resin) or HiTrap KappaSelect (kappa chain selective antibody fragments conjugated to a agarose matrix) resins. Washing was performed using PBS and proteins were eluted from the resin with 100 mM glycine at pH 2-3. Eluted fractions were directly pooled and immediately dialyzed against PBS.

3.6.3. Preparative Size Exclusion Chromatography

In the case of aggregated or multimeric assembled protein in the preparations, an additional size exclusion step was performed using the Äkta purifier. Proteins were separated on a Superdex 200 10/300 GL column at a flow rate of 0.5 ml/min using PBS as liquid phase. Fractions of 200 μ l were collected and the peak containing samples were pooled for further experiments.

3.7. Protein Characterization

3.7.1. Poly-Acrylamide Gel Electrophoresis (SDS-PAGE)

SDS-PAGE was performed strictly according to Laemmli 1970, using 3 μ g of protein preparations and the indicated percentages of stacking and separation gel.

3.7.2. Size Exclusion Chromatography (SEC)

To determine the hydrodynamic radius, 30 μ g purified protein samples were analyzed using the Waters 2695 HPLC in combination with a Phenomenex Yarra SEC-2000 column (300 x 7.8 mm, flow rate of 0.5 ml/min). The mobile phase was 0.1 M Na_2HPO_4 / NaH_2PO_4 , 0.1 M Na_2SO_4 , pH 6.7. The following standard proteins were used: Thyroglobulin (669 kDa), Apoferritin (443 kDa), Alcohol dehydrogenase (150 kDa), BSA (66 kDa), Carbonic anhydrase (29 kDa), FLAG peptide (1 kDa).

3.7.3. Thermal Stability by Dynamic Light Scattering

Stability to increasing temperatures was measured by dynamic light scattering using the ZetaSizer Nano ZS (Malvern, Herrenberg, Germany). Around 100 µg of the purified protein samples were adjusted to a total volume of 1 ml by the use of PBS and applied to a quartz cuvette. Kilo counts per second (kcps) were measured, indicating the size of denatured protein particles in the solution, which increases while the protein aggregates upon heating. Temperature was increased stepwise from 35 °C to 80 °C (1 °C intervals, 2 minutes equilibration prior to each measurement).

3.8. Enzyme-Linked Immunosorbent Assay (ELISA)

Microtiter plates were coated with 100 µl of the indicated protein (1 µg/ml in PBS, see Table 3.3) and incubated at 4 °C over night. The residual binding sites were blocked with 2 % MPBS (skim milk in PBS, 200 µl per well) at room temperature for 2 hours and subsequently washed twice with PBS. 100 µl of the samples diluted in 2 % MPBS were incubated at room temperature for 1 hour prior to the last incubation step with 100 µl of the HRP conjugated detection antibodies in 2 % MPBS. In the case of competition experiments, both analyzed protein samples were prepared individually (either titrated or diluted to a single concentration) and mixed before they were applied to the plate. Bound protein was detected with 100 µl TMB substrate solution, the HRP-reaction was stopped by the addition of 50 µl 1 M H₂SO₄ and the absorption at the wavelength of 450 nm was measured using the Infinite microtiter plate reader (TECAN, Maennedorf, Switzerland). Between each incubation step and in advance of the detection, the plates were washed three times with PBST and twice with PBS.

Table 3.3 ELISA settings

Figure/Table	Coating	Sample	Detection
Fig. 4.1-01	ATROSAB	FcγRIA	Anti-His-HRP
	Trastuzumab	FcγRIIB	Anti-His-HRP
		FcγRIIIA	Anti-His-HRP
		C1q	Anti-C1q-HRP
Fig. 4.1-02	Human TNFR1	serum samples	Anti-hu IgG (Fab-specific) - HRP
Fig. 4.1-06b	Human TNFR1 + 2	ATROSAB	Anti-hu IgG (Fab-specific)- HRP
	Mouse TNFR1 +2	Htr-9	Anti-mo IgG (Fc-specific) - HRP
Fig. 4.1-06d	Human TNFR1	ATROSAB	Anti-hu IgG (Fab-specific) - HRP
		Htr-9	Anti-mo IgG (Fc-specific) - HRP

Fig. 4.1-06e	Human TNFR1	ATROSAB Htr-9	Anti-mo IgG (Fc-specific) - HRP
Fig. 4.1-06f	Human TNFR1	ATROSAB Htr-9 TNF	Anti-hu TNF- HRP
Table 4.1-05 Table 4.1-06	Human TNFR1-Fc mutants	ATROSAB Htr-9 TNF	Anti-hu IgG (Fab-specific) - HRP Anti-mo IgG (Fc-specific) - HRP Anti-hu TNF- HRP
Fig. 4.2-05a	Human TNFR1-Fc	ATROSAB FabATROSAB IgG-FabL Db scFv-Fc scFv-HSA 2scFvHSA	Anti-hu IgG (Fab-specific) - HRP Anti-hu IgG (Fab-specific) - HRP Anti-hu IgG (Fab-specific) - HRP Anti-His-HRP Anti-His-HRP Rabbit anti-HSA + Anti Rabbit IgG-HRP Rabbit anti-HSA + Anti Rabbit IgG-HRP
Fig. 4.3-01a Fig. 4.3-03 Fig. 4.3-04	Human TNFR1-Fc	ATROSAB H398	Anti-hu IgG (Fab-specific) - HRP Anti-mo IgG (Fc-specific) - HRP
Fig. 4.4-03	Human TNFR1-Fc	Precipitated Phages	Anti-M13-HRP
Fig. 4.4-04 Fig. 4.4-05a	Human TNFR1-Fc	Phage containing culture supernatants	Anti-M13-HRP
Fig. 4.4-07b	Human TNFR1-Fc	scFvZI06.1 scFvIG11 scFvT12B	Anti-His-HRP
Fig. 4.5-04a	Human TNFR1-Fc	scFvFRK13.1-8 scFvZI06.1 scFvT12B	Anti-His-HRP
Fig. 4.6-02	Human TNFR1 + 2 Mouse TNFR1 +2	ATROSAB FabATR IgG13.7 Fab13.7	Anti-hu IgG (Fab-specific)- HRP
Fig. 4.6-03	Human TNFR1-Fc	ATROSAB FabATR IgG13.7 Fab13.7	Anti-hu IgG (Fab-specific)- HRP
Fig. 4.6-08a	Fab13.7	Goat anti-hu IgG serum	Anti-goat IgG-HRP
Fig. 4.7-02a	Human TNFR1-Fc	Fab13.7 Fab13.7L Fab13.7CH3	Anti-hu IgG (Fab-specific)- HRP
Fig. 4.7-03	Human TNFR1	serum samples	Anti-hu IgG (Fab-specific) - HRP

3.9. Flow Cytometry

Cells were detached and transferred to a 96-well microtiter plate at a concentration of 100.000 - 250.000 per well in 100 µl PBA. Samples were diluted in PBA at a double to the finally desired concentration and 100 µl were added to the cells for a 1 hour incubation. Subsequently, the cells were incubated with antibodies conjugated to fluorescent dyes prior

to the detection using the Cytomix FC₅₀₀ (Beckman Coulter, Pasadena, CA, USA) or the MACSQuant® Analyzer (Miltenyi Biotec, Bergisch Gladbach, Germany). Cells were washed twice by centrifugation (500 *g, 5 minutes) and resuspension in 150 µl PBA after each incubation step.

3.10. Affinity Measurements using the Quartz Christal Microbalance

Real-time binding dynamics in protein-protein interactions were determined by quartz crystal microbalance measurements (A-100 C-Fast or Cell-200 C-Fast, Attana, Stockholm, Sweden). One of the binding partners (ligand) was chemically immobilized on a carboxyl sensor chip according to the manufacturer's protocol at different densities. Binding experiments were performed with samples (analyte) diluted in PBST (0.1 % Tween 20) at pH 7.4 with a flow rate of 25 µl/min at 37°C. The chip was regenerated with 25 µl 5 mM NaOH or 20 mM glycine, pH 2.0. Every third measurement, an injection of running buffer was measured which was subtracted from the binding curve. Data were collected using the software provided by Attana for the particular device and analyzed by Attaché Office Evaluation software (Attana, Stockholm, Sweden) and TraceDrawe (ridgview instruments, Vange, Sweden).

3.11. Competition of ¹²⁵I-labeled TNF

TNF was labeled with Na¹²⁵I using iodination beads (IODO-BEADS) to obtain specific activities of 1-2 x 10⁴ cpm/ng. The retained biologic activity (40–60%) was determined in cytotoxicity assays with Kym-1 cells (Grell et al. 1994). The iodination beads were washed with 1 ml PBS and two of the beads were pre-incubated with 10 µl Na¹²⁵I and 50 µl PBA for 5 min at RT. 10 µg TNF was incubated for 4-10 min with iodination beads and Na¹²⁵I. The supernatant was applied to a PD-10 Column (Sephadex™ G-25 M) and eluted with 10 x 1 ml PBS. The eluted fractions were analyzed in a gamma counter (Berthold, Wildbad, Germany) and the 2-3 main fractions were pooled. The final concentration of ¹²⁵I-TNF was adjusted to 2 ng/µl. For competition assays, 2 x 10⁵ HT1080 cells per well were used in a PFA suspension (PBS, 1 % BSA, 0.1 % NaN₃). Samples were diluted as well in PFA together with labeled TNF and added to the cells. The non specific binding was determined using a 200 fold molar excess of unlabeled TNF. 0.1 nM ¹²⁵I-TNF alone served as 100 % binding control. The samples

were incubated for 3 hours at 4 °C or 37 °C. The cells and the supernatant were separated by centrifugation at 13200 rpm in micro-tubes (Sarstedt), containing 150 µl of an oil mixture (Dibutylphthalate/Dioctylphthalate) with a density of 1.014 g/cm³ (adjusted to let the cells settle to the ground, separated from the aqueous phase on top of the oil). The binding was analyzed in a gamma counter (Berthold, Wildbad, Germany).

3.12. Interleukin Release Assay

2 x 10⁴ HeLa or HT1080 cells per well were seeded into a 96 well microtiter plate and grown in 100 µl RPMI 1640 + 5 % FCS over night. The next day, the supernatants were exchanged in order to remove constitutively produced IL-8. The cells were incubated with dilution series of samples in RPMI 1640 + 5 % FCS at 37 °C, 5 % CO₂. In the case of competition experiments, both analyzed protein samples were prepared individually (either titrated or diluted to a single concentration) and mixed before they were applied to the plate. Non-stimulated cells served as control. After 16-20 hours the plates were centrifuged at 500 * g for 5 minutes and cell supernatants were analyzed directly by ELISA, which was performed according to the protocol of the manufacturer. Supernatants were diluted in RPMI 1640 (without FCS) and antibodies were diluted in Reagent Diluent. The coated microtiter plates were blocked using 2 % BSA (Bovine Serum Albumine) in PBS and washing as well as detection and measuring were performed as described above for ELISA.

3.13. Kym-1 Cytotoxicity Assay

Kym-1 cells (1*10⁴ per well) were seeded into 96-well microtiter plates and incubated over night at 37 °C and 5 % CO₂. The proteins were diluted in RPMI 1640 + 10 % FCS. If two protein species were used together in competition experiments, both samples were prepared individually (either titrated or diluted to a single concentration) and mixed before they were applied to the plate. Cytotoxicity assays were incubated at 37 °C, 5 % CO₂ for 24 hours before the supernatant was discarded and 50 µl crystal violet solution was added to the cells. Subsequently, the plates were washed in ddH₂O for 20 times and dried. The remaining violet dye, resulting from living and adherent cells, which were fixed by the methanol contained in the staining solution, was dissolved by the addition of 100 µl

methanol upon shaking at RT for 10 minutes. Plates were measured using the Infinite microtiterplate reader (Tecan, Maennedorf, Switzerland).

3.14. Complement-dependent Cytolysis (CDC)

Kym-1 target cells, bearing TNFR-1 were labeled with cell-permeant calcein for 30 minutes at 1 mM final calcein concentration in assay medium (RPMI, 2% FCS). Cells were washed twice in assay medium and then seeded onto 96-well microtiter plates ($1 \cdot 10^4$ cells/well). Sample dilutions were carried out in assay medium and added to the cells. Medium for sample dilution was diluted itself with the formulation buffer of the sample, equivalent to the highest sample concentration, thus, each well contained the same amount of formulation buffer, compensating for potential buffer effects on cell viability *per se*. Then, human serum was added to the cell-antibody mixture and release of calcein was measured after 2 h. Three different dilutions of each of the two serum batches were carried out in medium supplemented with 10% FCS prior to addition of serum to the cell-antibody mixture. A commercially available anti- CD20 antibody (Rituximab), which is known to induce cell lysis by CDC in CD20-expressing cells, served as positive control. The target cell line for this antibody was DOHH-2. Cells treated with 0.5% final concentration of Triton X-100 (maximal release of calcein=100% relative cell lysis/positive control) or the medium-buffer mixture (containing formulation buffer equivalent to the highest sample concentration) served as controls, representing the condition of spontaneous calcein release (i.e. 0% relative cell lysis/negative control). Statistical analysis was performed with Student's t-test. Experiments were performed by Dr. Timo Liebig (Celonic, Basel, Switzerland).

3.15. Antibody-Dependent Cellular Cytotoxicity (ADCC)

PBMCs were purified from fresh human whole blood as source of NK cells. Kym-1 target cells bearing TNFR-1 were labeled for 30 minutes with calcein (1 mM final calcein concentration in assay medium, see also CDC) and subsequently washed prior to seeding onto 96-well microtiter plates (10^4 cells/well). Samples were diluted in medium and formulation buffer as described for CDC and added to the cells. The PBMC effector cell fraction was applied to the cell-antibody mixture at the indicated effector-to-target cell (E:T) ratios and calcein release was measured after 4 h of incubation. Controls and analysis were

performed as described above for CDC. Experiments were performed by Timo Liebig (Celonic, Basel, Switzerland).

3.16. I κ B α Immunoblot

One million HT1080 cells in 2 ml RPMI 1640 (5% FCS) were seeded in a 6-well plate one day prior to the assay. Cells were then stimulated for 0, 5, 10, 25, 30 and 60 min at 37 °C, 5% CO₂. Subsequently, the supernatants were replaced by 1 ml ice cold PBS and the cells were detached mechanically. After centrifugation (500 *g, 4 °C, 5 min), the pellets were resuspended in “Solubi Shu” lysis buffer and incubated on ice for 30 minutes. Cell debris was separated by centrifugation (16.000 *g, 4 °C, 10 min) and the total protein content was determined by Bradford assay. 40 mg of the total protein was analyzed by SDS-PAGE and transferred to a nitrocellulose membrane using a semidry-blotter (110 mA/gel, 30 minutes). Residual binding sites were blocked with 5 % MPBS. Phospho-specific mouse monoclonal antibody (mAb) for plkB α , mouse mAb for total I κ B α , mouse mAb for tubulin-a (loading control), and HRP- conjugated rabbit anti-mouse IgG (Fc-specific) antibodies were used for detecting the particular protein species. Between each detection step, the membranes were stripped (5 min incubated with ddH₂O, 5 min 0.2 M NaOH, 5 min dd H₂O) and blocked again with 5 % MPBS. Signals were detected with ECL substrate solution (incubated for 2 min).

3.17. Pharmacokinetics

Transgenic C57BL/6J mice, bearing the gene of the extracellular domain of human TNFR-1 at the locus of the particular mouse gene (C57BL/6J-huTNFRSF1A_{eccd}^{tm1UEG}/izi), were injected intravenously with 12 μ g to 25 μ g of the analyzed proteins. C57BL/6J of an unaltered genetic background served as control. Blood samples were collected after 3 min, 30 min, 1 h, 3 h and 6 h as well as after 3 days and 7 days and incubated on ice immediately. Serum was separated by centrifugation (13.000 *g, 4 °C, 10 minutes) and stored at -20 °C. Remaining protein in the serum was detected by binding ELISA as described above. Data were displayed as percentage of the 3 min value. Alternatively, the ELISA signal at the injection time was interpolated from the obtained curves and set to the initial *in vivo* concentration on the basis of the injected dose and the average blood volume of the mice, resulting in the indicated concentrations at the measurement time points. Experiments were

performed by Dr. Oliver Seifert (Institute of Cell Biology and Immunology, University of Stuttgart).

3.18. Phage Display

3.18.1. Cloning of Acceptor Vector pHENIS_scFvIG11-fsSTOP

The DNA sequence encoding for scFvIG11 was amplified by PCR (described above) from the template pHENIS-scFvL2a_huBR6_IG11 (Zettlitz 2010b) using the primers NcoI_VH-IZI06.1_back and BstZ17I_fsSTOP_BssHII_for. The obtained DNA fragment, containing a frame shift in combination with stop a codon, was inserted again into pHENIS-scFvL2a_huBR6_IG11 after digestion with NcoI and BstZ17I, resulting in the acceptor vector pHENIS_scFvIG11-fsSTOP.

3.18.2. Generation of Selection Library EP03

The selection library EP03 for the affinity maturation of scFvIG11, resulting in scFvT12B was generated by error prone PCR using the GeneMorph II Random Mutagenesis Kit according to the manufacturers protocol. The Template DNA pHENIS-scFvLib2a_huBR6_IG11 was amplified by the use of the primers LMB2 and fdSeq1. Intended to generate a moderate incidence of mutations, 0.1 µg template DNA were used in a 30 cycles PCR reaction. The resulting PCR-Product was cloned into the acceptor vector pHENIS_scFvIG11_ fsSTOP after digestion by the enzymes NcoI and NotI. Ligation was performed over night at 16 °C. The next day, ligated DNA was precipitated by the addition of 1/10 of the ligation mix volume (LMV) of 3 M NaAc pH 5.2, 5 µl Glycogen (20 µg/µl) and 2.7 LMV of 100 % Ethanol. Following an 1 hour incubation at - 80 °C, the DNA was centrifuged (13.000 *g, RT, 5 minutes) and the air-dried pellet was resuspended in 40 µl ddH₂O and frozen again at -20 °C in 2-4 µl aliquots.

3.18.3. Preparation of Electrocompetent *E. coli* TG1

Transferring 5 ml of an over-night culture of *E. coli* TG1 grown in SOB medium (containing 1 % glucose) to 500 ml fresh SOB, a culture was inoculated and grown until an OD [600 nm] of 0.5 - 1.0 was reached. Cells were chilled on ice subsequently for at least 15 minutes and harvested by centrifugation (2000 *g, 4 °C, 15 min). The cell pellet was gently resuspended in 200 ml ice cold ddH₂O (firstly using 20 ml, another 180 ml were added after resuspension). The centrifugation/resuspension cycle was repeated for a second time exactly

as described, the resuspended cells were then kept on ice for 30 minutes and centrifuged again (2000 *g, 4 °C, 15 min). Bacteria were resuspended in 50 ml of 10 % glycerol, incubated on ice for another 30 minutes and collected again by centrifugation (1500 *g, 4 °C, 15 min). The resulting pellet was resuspended to a final volume of 500 to 1000 µl, kept on ice and used directly for electroporation.

3.18.4. Electroporation of *E. coli* TG1

Electrocompetent *E. coli* TG1 were freshly prepared and 40 µl of the cell suspension was mixed with a frozen aliquot of ligated DNA. After 1 minute incubation on ice, the DNA bacteria mix was transferred to an electroporation cuvette (BIO-RAD, Munich, Germany) and electroporated immediately (1.8 kV/cm, 200 Ω, 25 µF, GenePulser® XCell, BIO-RAD, Munich, Germany). Subsequently, the transformed cells were rescued by flushing the cuvette with 1 ml of LB, transferred to a culture tube and incubated shaking at 37 °C for 1 hour, prior to plating on LB_{amp} agar plates. For control purposes, 10 µl, 1 µl and 0.1 µl of a transformed sample were plated separately onto LB_{amp} agar plates, as well as 2.5 µl of electroporation samples containing either 2 µl ddH₂O or 1 µl pUC DNA (0.1 ng/µl) mixed with the competent cells.

3.18.5. Preparation of helper Phages

E. coli TG from an over-night culture, which was started with bacteria freshly streaked on a minimal plate, were used to inoculate a 500 ml 2xTY culture (OD [600 nm] 0.05 - 0.07). At an OD [600 nm] of 0.4 to 0.5, 1 ml VSC M13 helper phages were added and the culture was incubated for 30 minutes without shaking at 37 °C and for another 30 minutes, shaking at 37 °C. Subsequently, Kanamycin was added to a final concentration of 30 µg/ml and the culture was incubated shaking at 30 °C over night. Finally, bacteria were separated by centrifugation (4000 *g, 45 min, RT) and the phage containing supernatant was stored at -20 °C in 1 ml aliquots.

3.18.6. Phage Rescue and Precipitation

Transformed bacteria were collected from LB agar plates and 50 ml 2xTY (2 % glucose, 100 µg/ml Ampicillin) were inoculated to a starting OD [500 nm] of 0.05 - 0.07. When the culture reached an OD [600 nm] of 0.4 - 0.5 after shaking incubation at 37 °C, 1 ml of VSC M13 helper phages were added and the culture was incubated at 37 °C first without shaking

(30 minutes) and then shaking (30 min). Subsequently, the bacteria were harvested by centrifugation (4000 *g, RT, 15 min), resuspended in 50 ml fresh 2xTY containing 100 µg/ml Ampicillin and 30 µg/ml Kanamycin and incubated, shaking, at 30 °C over night.

The next day, bacteria were centrifuged (4000 *g, RT, 30 min) and 10 ml of 20 % PEG₆₀₀₀ were added to 40 ml of the supernatant, gently mixed and rolled at 4 °C for 1 hour. Precipitated phages were dissolved in 1 ml PBS after centrifugation (4000 *g, RT, 30 min) and centrifuged again at 13.000 *g and RT for 10 min. The bacteria-free supernatant, containing the amplified phages was used immediately for selection (or stored at 4 °C for later usage).

3.18.7. Immunotube Selection

Immunotubes were coated with human TNFR1-Fc or human TNFR2-Fc at concentrations decreasing with each selection round (Round 1: 1 and 0.1 µg/ml, round 2: 0.1 and 0.01 µg/ml, etc.; huTNFR2 always was coated using 2 µg/ml). Tubes were blocked with 2 % MPBS. 1 or 10 µl precipitated phages were added to 1 ml 2 % MPBS and incubated in human TNFR2-Fc coated tubes to eliminate cross-reactive phages. This negative selection was performed exclusively prior to the first round of selection. Following 1 hour incubation at RT, the supernatant was transferred to immunotubes coated with human TNFR1-Fc and incubated for an additional hour. Starting at round 2, soluble human TNFR1-Fc was added to the immunotube at a final concentration of 5 µg/ml in order to capture quickly dissociating phages and to hinder their binding to the immobilized receptors. The supernatant was subsequently discarded and the tubes were washed 10 times with PBST (0.1 % Tween 20) and 10 times with PBS. Phages were eluted with 1 ml of 100 mM TEA (triethylamine) upon incubation for 7 minutes. The eluted phages were neutralized immediately using 500 µl of 1 M TrisHCl buffer (pH 7.5) and added to 8.5 ml of early log phase *E. coli* TG1. Incubation was performed as described above for transduction (37 °C, standing, 30 min; 37 °C, shaking, 30 min). Bacteria were separated by centrifugation (4000 *g, RT, 10 min) and plated to LB_{amp} plates.

3.18.8. Biotinylation of Receptor-Fc Fusion Proteins

Human TNFR1-Fc and human TNFR2-Fc were biotinylated upon mixing protein samples with a 20-fold molar excess of Sulfo-NHS-SS-Biotin and incubation at RT for 2 hours. Remaining free Sulfo-NHS-SS-Biotin was removed from the sample by dialysis against PBS at

4 °C over night. Successful biotinylation of TNFR1-Fc and TNFR2-Fc was tested in standard binding ELISA to immobilized TNF. Bound receptor-Fc fusion proteins were detected by Poly-HRP-Strep. ELISA was performed as described above.

3.18.9. Equilibrium Selection on Magnetic Dynabeads

In order to remove phages binding to human TNFR2 or the fused Fc moiety in a cross-reactive manner, 1 µl or 10 µl of precipitated phages were added to 1 ml 2 % MPBS, containing 0.1 µM human TNFR2-Fc and incubated rolling at RT for 1 hour. Subsequently, 50 µl of magnetic streptavidin-coated Dynabeads were added to the selection mix and rolled for another 5 minutes. Beads were then separated by placing the 2 ml reaction tube into an magnetic device (DYNAL® MPC®-S, Life Technologies, Carlsbad, CA, USA), the selection mix was transferred to a new 2 ml reaction tube and human TNFR1-Fc was added to the selection mix (Round 1: 10 nM/1 nM, round 2: 1 nM/0.1 nM, round 3: 0.1 nM/0.01 nM). After incubation at RT (rolling for 1 hour), 10 µl Dynabeads were added to the selection mix and incubated and separated as described for the negative selection round with human TNFR2-Fc. The supernatant was discarded and 1 ml 10 mM DTT (Dithiothreitol) was added to the beads to release the bound phages from the antigen. Transduction was performed as described for the immunotube selection.

3.18.10. Polyclonal Phage ELISA

Changes in over all binding of the phage pool was tested by polyclonal phage ELISA. The experimental procedure is described in the ELISA section, here the antigen which was subject to phage display selection was used for coating. 10 µl of precipitated phages were mixed with 90 µl of 2 % MPBS, applied to the microtiter plate and the bound phages were detected using an anti-M13-HRP antibody.

3.18.11. Screening of Phage Display Selections

100 µl 2xTY LB_{amp} per well of 1 to 4 microtiter plates were inoculated by single clones (100 to 400 colonies), which were picked from the plates after transduction of the final selection round and incubated shaking at 37 °C. When clouding was visible, 25 µl LB containing VCS M13 helper phages (1 ml per microtiter plate) were added and incubated for transduction as described. Subsequently, 25 µl LB containing 240 µg/ml Kanamycin (final concentration 30 µg/ml) were added to the microtiter plate and the plate was incubated at

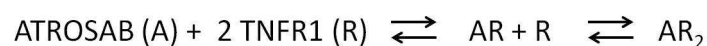
30 °C, shaking over night. The next day, bacteria were separated by centrifugation (500 *g, RT, 5 min) and the supernatants were mixed 1:1 with 2 % MPBS and analyzed by ELISA as described in the polyclonal phage ELSIA, either in one point measurements or titrated.

3.18.12. Off-Rate Screening of Phage Containing Bacteria Culture Supernatants

The dissociation rate constant of scFv-bearing phages was determined by off-rate screening, using the QCM technology. Phage rescue was performed similar to the described protocol, however, it was down scaled to a 5 ml LB culture. 100 µl of an overnight culture (or a purified scFv preparation) were used for inoculation and VSC M13 helper phages were added when the cultures showed visible clouding. The following steps were carried out as above mentioned. Without precipitation, phage containing supernatants were diluted 1:2 in PBST (0.1 % Tween 20) and applied to a sensor chip, immobilized with huTNFR1-Fc at a moderate density of (48 Hz). The running buffer was mixed 1:1 with LB as well, to minimize buffer effects. The mean value of three measurements was analyzed using the Attaché office software (Attana, Stockholm, Sweden).

3.18.13. Calculation of ATROSAB-TNFR1 Complexes on the Cell Surface

According to the law of mass action, a two step equation of the binding of ATORSAB to TNFR1 was given by



We defined two equations for each equilibrium, while statistical factors were introduced due to the possibility of ATROSAB to bind with either one arm in the first step but to dissociate with the only one arm and vice versa in the second step (see also Crothers and Metzger 1972, Kaufman and Jain 1992).

$$K_{D1} = \frac{2*[A]*[R]}{[AR]} \quad ; \quad K_{D2} = \frac{[AR]*[R]}{2*[AR_2]}$$

The concentrations of ATROSAB [A] and TNFR1 [R] had to be replaced with respect to the initial used concentration for each data point:

$$[A] = [A_0] + [AR] + [AR_2] \quad ; \quad [R] = [R_0] + [AR] + 2*[AR_2]$$

This system of non-linear equations was solved using Scilab (Scilab Enterprises, Free and Open Source software for numerical computation, Version 5.5.1):

```
deff('y=complexes2(x)', ['m=a-x(1)-x(2)',
'n=b-x(1)-2*x(2)',
'y1=(2*m*n)-(kD1*x(1))',
'y2=(n*x(1))-(2*kD2*x(2))',
'y=[y1;y2]'])

//definition of the described equations
//m=[ATROSAB]
//a=[ATROSAB]₀
//n=[TNFR1]
//n=[TNFR1]₀
//x(1)=[AR]
//x(2)=[AR2]
//initial concentration of TNFR1
//(1/Keq) of first part
//(1/Keq) of second part
//initial values for fsolve
//initial concentration of ATROSAB
//solver for the system of non-linear equations
//display concentrations of ATROSAB, and both complexes

b=0.00332;
kD1=72.36;
kD2=0.0029;
x0=[0,0];
a=[200];
[x,v,info]=fsolve(x0,complexes2);
disp([a,x]);
```

4. Results

4.1. Receptor Binding and *in vitro* Bioactivity of ATROSAB

4.1.1. ATROSAB Lacks Fc-Mediated Effector Functions

The inherent ability of antibodies to activate the immune system via their Fc region is a rather obstructive feature, considering ATROSAB as a drug for diseases affected by excessive TNF mediated inflammation. Thus, the Fc region of ATROSAB (Zettlitz et al. 2010a) was modified in order to inactivate immune effector functions (ADCP, ADCC and CDC, Armour et al. 1999, Shields et al. 2001). In ELISA binding studies, ATROSAB did not bind to human FcγRIA (CD64, Fig. 4.1-01a) and human C1q (Fig. 4.1-01d), while binding to FcγRIIB (CD32b, Fig. 4.1-01b) and FcγRIIIA (CD16a, Fig. 4.1-01c) was strongly reduced. In contrast, the positive control trastuzumab (possessing a human wild-type IgG1 Fc) showed binding to FcγRIA (Fig. 4.1-01a), FcγRIIB (Fig. 4.1-01b), FcγRIIIA (Fig. 4.1-01c) and C1q with EC₅₀ values of 7.06 nM, >1 mM, 825.4 nM and 4.04 nM, respectively. Immobilization of ATROSAB and trastuzumab was confirmed with an anti-human IgG antibody, binding specifically to the Fc fragment.

The depletion of the ADCC effector function was demonstrated by testing the potential of ATROSAB to elicit killing of TNFR1-expressing Kym-1 cells and thereby the release of previously incorporated calcein. Rituximab, a chimeric anti-CD20 IgG1, and DOHH-2 cells (CD-20 positive) were included as positive controls. The control antibody induced lysis of its target cells in the presence of peripheral blood mononuclear effector cells (PBMC), depending on the effector to target cell ratio (E:T) at 50 µg/ml (Fig. 4.1-01e). In contrast, ATROSAB induced significantly less calcein release from Kym-1 cells, even when added at 600 µg/ml in combination with a high E:T ratio (Fig. 4.1-01e). Similar results were obtained with lower ATROSAB concentrations (120 µg/ml and further 1:5 dilutions), whereas lower concentrations of rituximab were still able to elicit ADCC in DOHH-2 cells, particularly at the highest E:T ratio (data not shown).

The potential of ATROSAB to induce complement-dependent cytolysis (CDC) was also tested, employing calcein-labeled Kym-1 as target cells. Again, rituximab and CD20-expressing DOHH-2 cells served as positive control. Rituximab led to cytolysis of the target

cells using serum of two different donors (Fig. 4.1-01f). ATROSAB, however, elicited significantly lower CDC of antigen-expressing Kym-1 cells (Fig. 4.1-01f). Similar results were

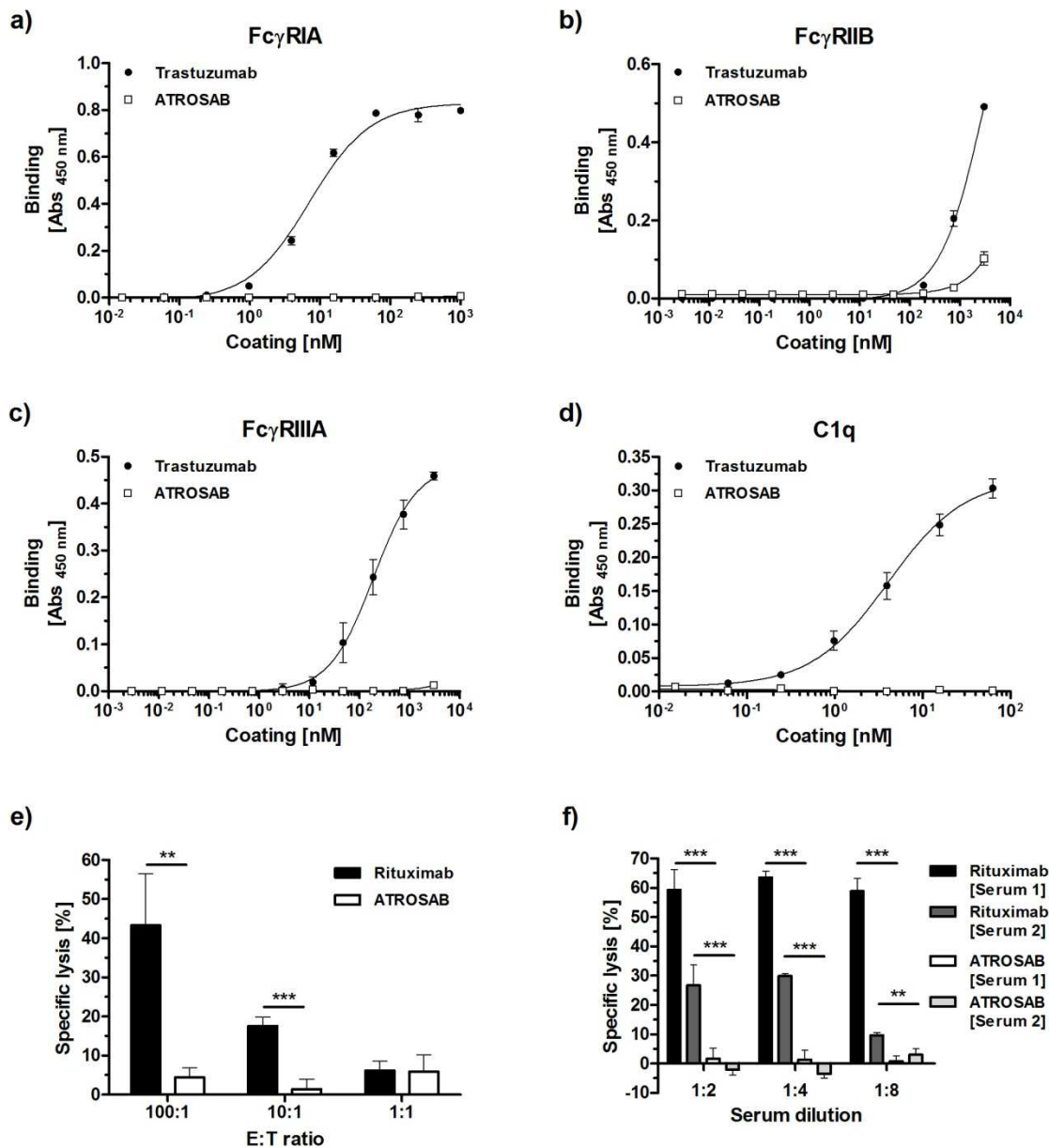


Figure 4.1-01. Analysis of Human Soluble Fc γ Receptor and C1q Binding of ATROSAB and Mediation of Effector Functions. 3 μ M Fc gamma receptor IA (Fc γ RIA, a), 3 μ M Fc γ RIIB (b), 3 μ M Fc γ receptor IIIA (c), and 5 μ g/ml human C1q (d) were analyzed for binding to ATROSAB and Trastuzumab, immobilized at the indicated concentrations. e) ADCC of ATROSAB and the anti-CD20 monoclonal antibody Rituximab to Kym-1 and DOHH-2 cells, respectively, using different effector to target cell ratios (n = 4). f) CDC of ATROSAB and Rituximab to Kym-1 cells and DOHH-2 cells, respectively, using sera from two different donors at various dilutions (n = 4). Asterisks indicate statistically significant differences (** p < 0.01, *** p < 0.001). ADCC and CDC data (e and f) were kindly provided and analyzed by Dr. Timo Liebig, Celonic GmbH, Basel, Switzerland.

obtained with reduced ATROSAB concentrations (60 µg/ml and further dilutions), whereas lower concentrations of rituximab were still able to kill DOHH-2 cells by CDC (not shown). Taken together, these data confirm that binding of ATROSAB to Fcγ receptors and the complement protein C1q is significantly reduced and that ATROSAB does not mediate substantial CDC and ADCC activity against TNFR-1 expressing target cells.

4.1.2. ATROSAB Shows Target Mediated Clearance From the Blood

The effect of the presence or absence of human TNFR1 on the pharmacokinetic profile of ATROSAB was analyzed, using transgenic C57BL/6J mice, homozygously carrying the gene of the extracellular domain (ecd) of human TNFR1 at the locus of the respective mouse gene. Over a period of 7 days after single-dose injection of 25 µg antibody, serum samples were analyzed in binding ELISA for remaining functional protein molecules (Fig. 4.1-02). In human TNFR1_{ecd} knock-in mice, ATROSAB revealed an identical initial half-life of 0.07 ± 0.01 days, compared with the value observed in wild-type C57BL/6J mice, serving as negative control. In contrast, the terminal half-life and the area under the curve (AUC), which indicates the bioavailability of the therapeutic agent, were reduced in knock-in mice by a factor of 4.6 and 1.25, respectively (Table 4.1-01), compared with the situation in wild-type C57BL/6J mice. Hence, over-all serum half-life and bioavailability (area under the curve) of ATROSAB are reduced in mice, expressing the extracellular domain of human TNFR1.

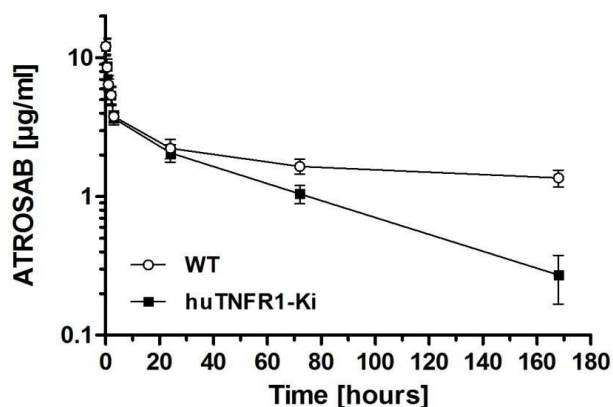


Figure 4.1-02. Pharmacokinetics of ATROSAB. Initial and terminal plasma half-live after single-dose injection (25 µg), as well as bioavailability (area under the curve) of ATROSAB were determined using C57BL/6J mice, homozygously bearing the extracellular domain of human TNFR1 instead of the mouse receptor (n=3). Wild-type C57BL/6J mice were included as control. Remaining active antibody in serum samples was detected by ELISA. Experiments were performed in cooperation with Dr. Oliver Seifert.

Table 4.1-01: Pharmacokinetic Study of ATROSAB

	WT		huTNFR1-ki +/+	
T1/2α [d]	0.07	± 0.01	0.07	± 0.01
T1/2β [d]	9.43	± 2.21	2.04	± 0.32
AUC [$\mu\text{g}\cdot\text{d}/\text{ml}$]	36.84	± 2.10	29.56	± 3.71

4.1.3. Binding of ATROSAB to Human TNF Receptor 1

Binding of ATROSAB to human TNFR1 was analyzed by quartz crystal microbalance (QCM) measurements at high and low densities of immobilized receptor (Fig. 4.1-03a). The dissociation curve revealed characteristics of a biphasic decay, clearly visible in particular on the low density chip (ldc). In order to generate robust kinetic data, considering all information of measurements on the high and low density chip, both data sets were superimposed and analyzed simultaneously using the "one to two" algorithm of the TraceDrawer software. The resulting fit described a high and a low affinity binding event, reflected by K_D values of 0.2 nM and 72.6 nM, respectively. The low K_D value of the higher affinity interaction originated from slower dissociation of the antibody-receptor complex, indicated by a smaller k_{off} value, compared with the data set obtained for the lower affinity interaction (Fig. 4.1-03a, Table 4.1-02).

Moreover, the interaction of ATROSAB with human TNFR1 on the surface of the HT1080 cells was analyzed by flow cytometry. In addition to standard assay conditions (4 °C), the experiments were performed at 37 °C, consistent with the QCM measurements. Similar to the biosensor data, two phases of binding were observed, with EC_{50} values of 0.15 nM and 148 nM at 4 °C as well as 0.32 nM and 91 nM at 37 °C (Fig. 4.1-03b). These findings further indicated heterogeneity in the binding of ATROSAB to human TNFR1, attributable to high and low affinity interactions.

Table 4.1-02: QCM Affinity Measurements of ATROSAB

Interaction	$B_{\text{max}}_{\text{hdc}}$ (Hz)	$B_{\text{max}}_{\text{ldc}}$ (Hz)	k_{on} ($\text{M}^{-1}\text{s}^{-1}$)	k_{off} (s^{-1})	K_D (nM)
Low affinity	6.0	12.3	2.5×10^5	1.8×10^{-2}	73
High affinity	46	4.2	8.2×10^5	1.7×10^{-4}	0.21

hdc: high density chip; ldc: low density chip

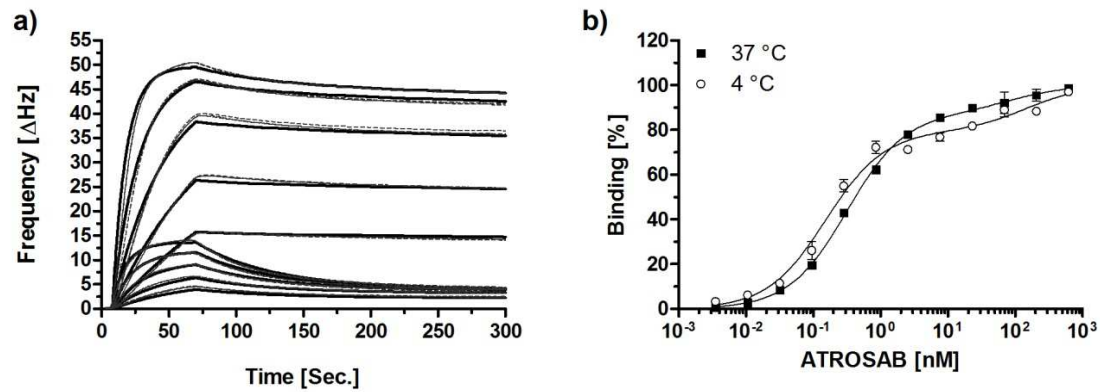


Figure 4.1-03. Receptor Binding by ATROSAB. Binding of ATROSAB to human TNFR1 was analyzed by QCM at high (215 Hz) and low (69 Hz) density of immobilized human TNFR1-Fc. ATROSAB was analyzed at concentrations between 256 nM and 16 nM at 37 °C (a), in triplicates for each concentration (dashed lines = data curves, solid lines = fitted curves). Binding of ATROSAB to human TNFR1 on the surface of HT1080 cells was analyzed by flow cytometry (b) at 4 °C and 37 °C

4.1.4. Inhibition of TNF Binding, Signaling and TNFR1-Mediated Interleukin Release

To address the inhibitory activity of ATROSAB on TNF binding, HT1080 cells were used in combination with 125 I-labeled TNF. Approximately 1500 binding sites for 125 I-labeled TNF were determined on HT1080 cells in an equilibrium binding experiment (Fig. 4.1-04a). Interpolation of the acquired data points revealed a concentration of half-maximum binding for TNF of 0.11 nM. Subsequent Scatchard analysis gave no evidence for TNF binding sites with different affinities (Fig. 4.1-04b). Binding of 125 I-labeled TNF at a concentration of 0.1 nM was inhibited by ATROSAB in a concentration-dependent manner (Fig. 4.1-04c). Analysis of the binding-inhibition curves revealed a two-step characteristic, with IC_{50} values of 0.15 nM and 6.01 nM at 4 °C. Similar values were determined at 37 °C (0.11 nM and 9.58 nM). These results confirm that ATROSAB directly blocks the binding of TNF to its receptor.

Moreover, the neutralizing activity of ATROSAB on IL-8 and IL-6 secretion, induced by lymphotoxin alpha ($LT\alpha$, $LT\alpha_3$) was analyzed in comparison with the inhibition of cytokine release in response to TNF. $LT\alpha$ -induced IL-8, released from HT1080 cells, reached approximately 40 % of the maximum response triggered by TNF (Fig. 4.1-05a). Similarly, $LT\alpha$ -induced release of IL-6 in the HeLa cell model reached approximately 65 % of the maximum answer provoked by TNF (Fig. 4.1-05b). ATROSAB inhibited IL-8 and IL-6 secretion, induced by 0.1 nM $LT\alpha$ (5.7 ng/ml), in a concentration dependent manner with equal IC_{50} values of 7.6 nM. IL-8 and IL-6 release induced by TNF, applied at the same molarity, was inhibited by

ATROSAB less efficiently, depicted by IC_{50} values of 42.0 nM and 125.6 nM, respectively (Fig. 4.1-05c and d).

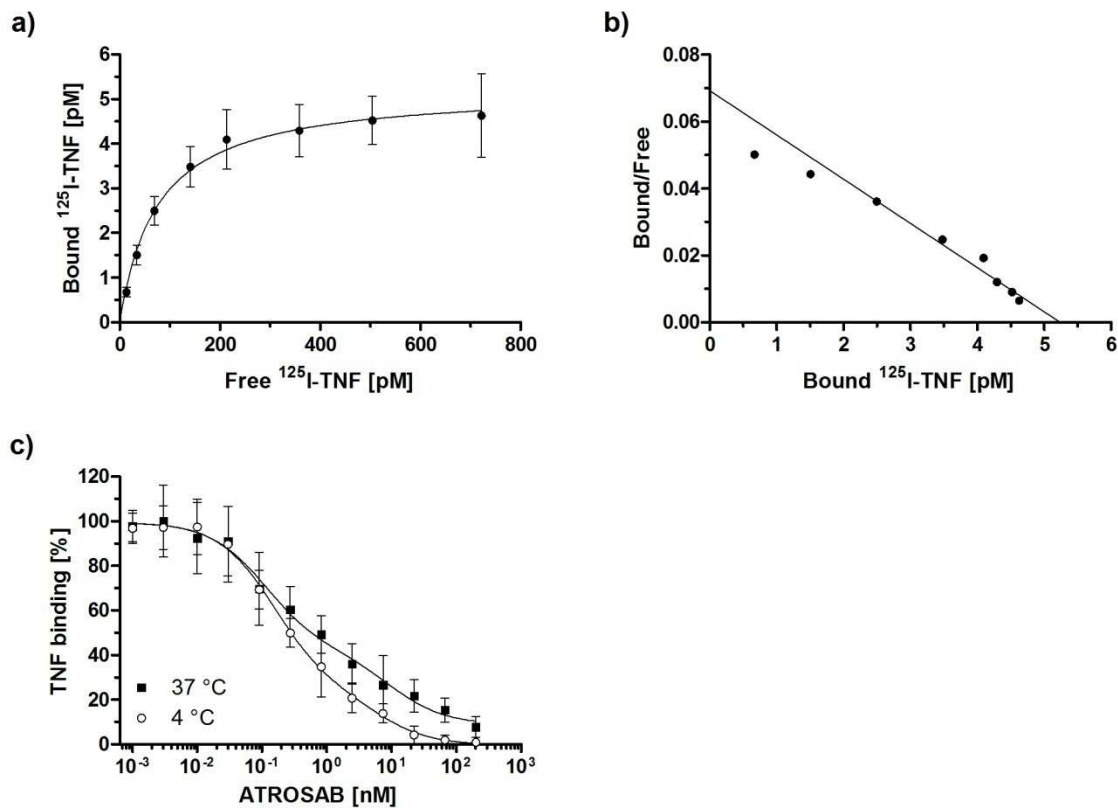


Figure 4.1-04. Inhibition of ^{125}I -TNF Binding to HT1080 Cells by ATROSAB. a) Specific binding of ^{125}I -labeled TNF to HT1080 cells (non-specific has been subtracted). b) Scatchard plot of the binding of ^{125}I -labeled TNF to HT1080 cells. c) Inhibition of binding of ^{125}I -labeled TNF to HT1080 cells by ATROSAB at 4°C and 37°C, respectively. Displayed are mean values of three individual experiments in percent of maximum TNF binding.

Next, the effects of ATROSAB on TNF-mediated signal transduction were investigated at the level of I κ B α phosphorylation. In HT1080 cells, incubated with 0.1 nM TNF, rapid phosphorylation and subsequent degradation of I κ B α was detected by immunoblotting experiments, using anti-I κ B α and anti-pI κ B α antibodies (Fig. 4.1-05e). In the presence of excess amounts of ATROSAB (500 nM), phosphorylation and degradation of I κ B α was strongly reduced and delayed over time. ATROSAB alone did not induce any detectable I κ B α phosphorylation or degradation.

The described experiments demonstrated, that i) ATROSAB blocks the binding of TNF to TNFR1 on the cell surface, ii) ATROSAB inhibits TNF-induced signal transduction and iii) ATROSAB eliminates pro-inflammatory cellular responses like IL-8 or IL-6 release.

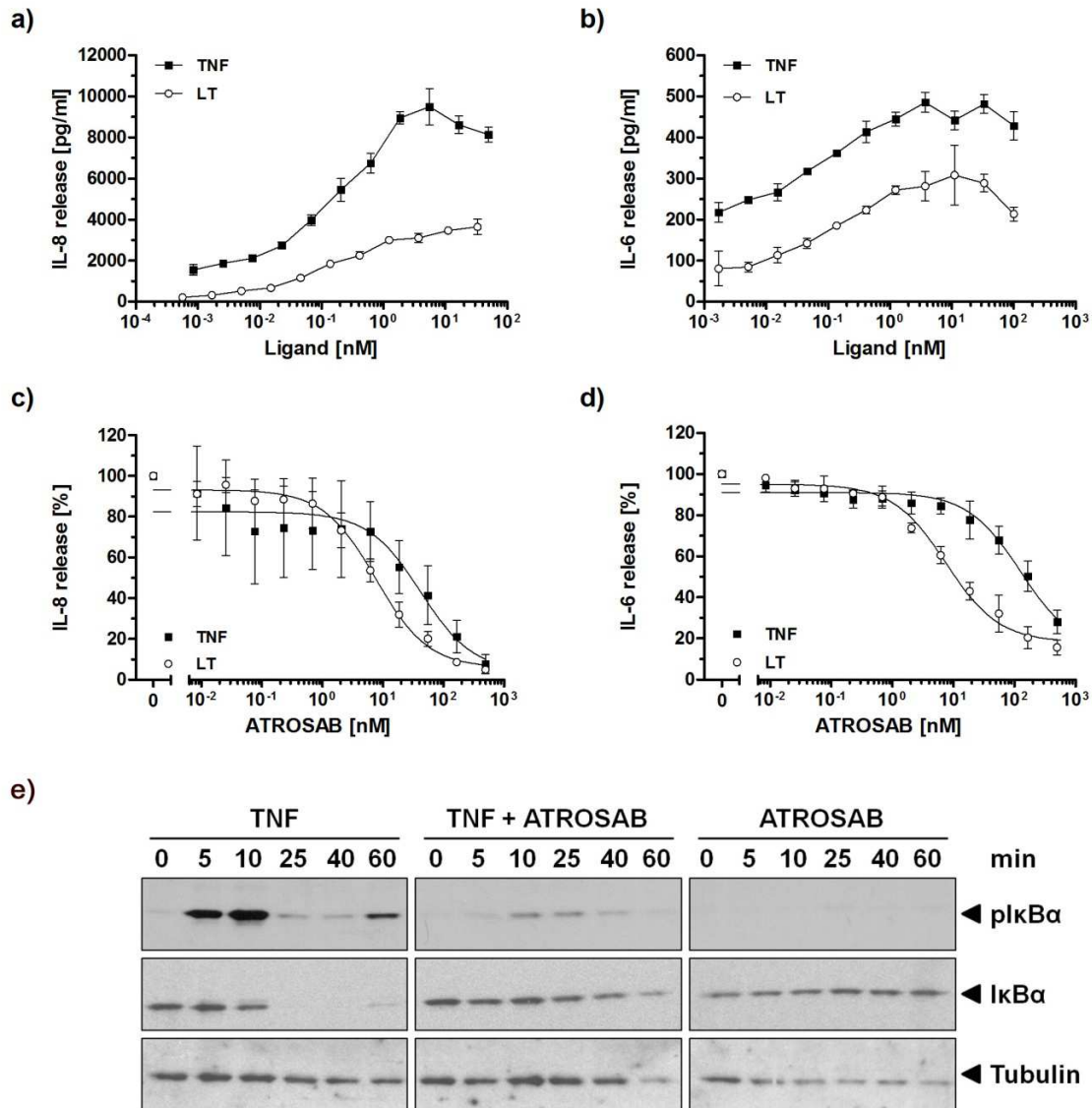


Figure 4.1-05. Inhibition of TNF and LT α Action by ATROSAB. a) IL-8 release from HT1080 cells, stimulated with TNF and LT α . b) IL-6 release from HeLa cells stimulated TNF and LT α . c) Inhibition of TNF- and LT α -induced IL-8 secretion from HT1080 cells with increasing concentrations of ATROSAB, using 0.1 nM of TNF and LT α . d) Inhibition of TNF- and LT α -induced IL-6 secretion from HeLa cells with increasing concentrations of ATROSAB using 0.1 nM of TNF and LT α . Data from $n = 3$ experiments are shown as percent of maximum IL release, triggered by TNF or LT α alone (c, d). Shown are mean values and standard deviation. e) Immunoblot analysis of the inhibition of TNF-induced phosphorylation (pI κ B α) and degradation of I κ B α by excess amounts of ATROSAB in HT1080 cells. Tubulin was included as loading control.

4.1.5. Comparison of ATROSAB with the Agonistic Antibody Htr-9

The monoclonal antibody Htr-9 was previously characterized as a human TNFR1-specific agonist (Brockhaus et al. 1990, Espevik et al. 1990). Purified Htr-9 showed in size

exclusion chromatography (SEC) a major peak, corresponding to the molecular weight of intact IgG (Fig. 4.1-06a). Equivalent to ATROSAB, Htr-9 revealed selectivity for human TNFR1, without binding to human TNFR2, mouse TNFR1 or mouse TNFR2, as determined by ELISA (Fig. 4.1-06b). A K_D value of 14 nM was determined by QCM for the binding of Htr-9 to human TNFR1-Fc at a receptor density of 48 Hz (Fig. 4.1-06c). Htr-9 showed dose-dependent binding to immobilized TNFR1-Fc in standard ELISA (Fig. 4.1-06d), however, the detected

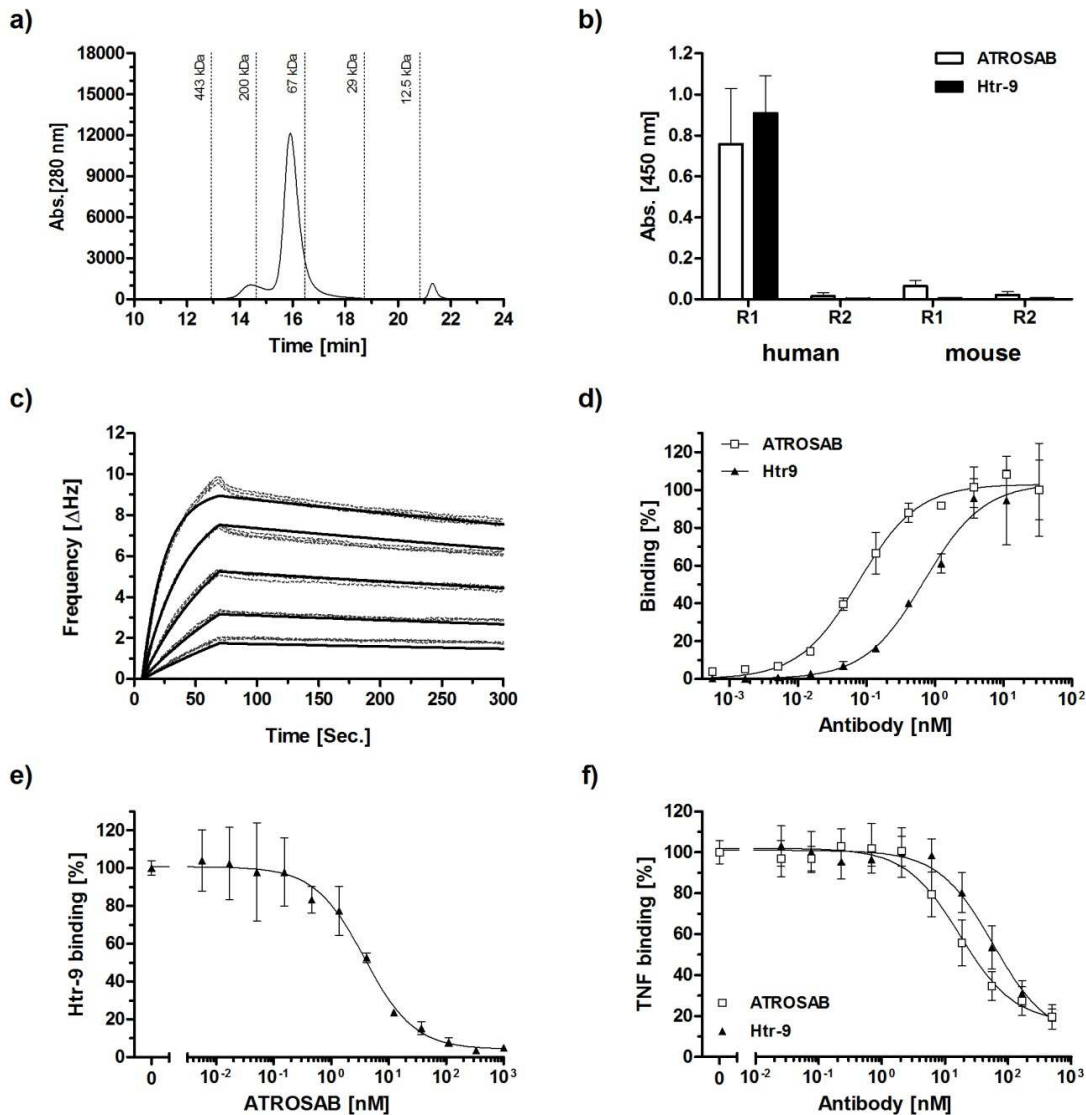


Figure 4.1-06. TNFR1-specific Agonistic Antibody Htr-9. a) SEC of purified Htr-9. b) Receptor-selectivity of 200 nM ATROSAB and Htr-9, determined by ELISA (R1 = TNFR1; R2 = TNFR2). c) Binding of Htr-9 to human TNFR1-Fc analyzed by QCM at a receptor density of 48 Hz. Htr-9 was analyzed at concentrations between 1 μ M and 62.5 nM. d) Dose-dependent Binding of ATROSAB and Htr-9 to immobilized human TNFR1-Fc in ELISA. e) Inhibition of binding of 7 nM Htr-9 to human TNFR1-Fc by increasing concentrations of ATROSAB. f) ELISA study, showing the binding of 1 nM TNF to human TNFR1 inhibited by increasing concentrations of Htr-9 and ATROSAB.

EC₅₀ value of 0.7 nM was about 10-fold higher than the EC₅₀ value observed for ATROSAB (0.08 nM). ATROSAB competed with Htr-9 for binding to human TNFR1-Fc (IC₅₀ = 3.8 nM), indicating closely located or overlapping epitopes of the two antibodies (Fig. 4.1-06e). Accordingly, Htr-9 also inhibited binding of TNF to TNFR1-Fc with an IC₅₀ value of 58 nM, demonstrated by ELISA. ATROSAB, included as control, showed inhibition of TNF binding with an IC₅₀ value of 17 nM (Fig. 4.1-06f).

In the next Step, ATROSAB and Htr-9 were analyzed for their potential to induce cytokine secretion *in vitro*, using the cell lines HeLa (IL-6) and HT1080 (IL-8). Human TNF, which was included as control, induced strong release of IL-6 and IL-8 in the performed experiments (Fig. 4.1-07). Maximum cytokine release was observed at a TNF concentration of approximately 10 nM, resulting in IL-8 and IL-6 concentrations in the cell culture supernatant of roughly 11 ng/ml and 500 pg/ml, respectively. Htr-9 showed strong induction of IL-6 and IL-8 secretion, reaching a maximum of 2-3 ng/ml for IL-8 and 200-300 pg/ml in the case of IL-6, both stimulated by a concentration of around 30 nM. Considering the maximum interleukin concentration, detected in response to TNF, the highest cytokine release triggered by Htr-9 corresponded to approximately 27 % in the IL-8 assay as well as to 50 % in the IL-6 assay (Fig. 4.1-07). In contrast, stimulation by ATROSAB led only to a marginal cytokine release, reaching at the maximum a concentration of 140-160 pg/ml IL-8 and 40-80 pg/ml IL-6. After subtraction of the cellular background, this weak activity represented approximately 1 % and 6 % of the maximum *in vitro* activity of TNF, detected in IL-8 (HT1080) and IL-6 release (HeLa) assays, respectively. Background values of 50-70 pg/ml

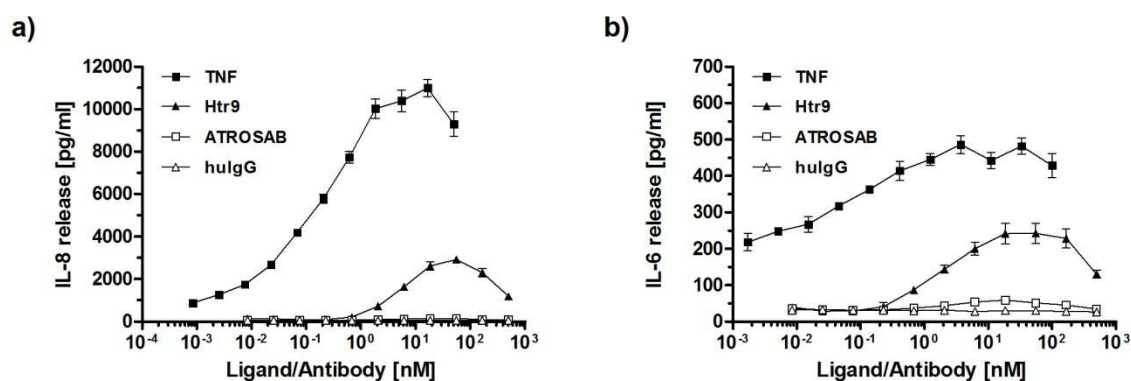


Figure 4.1-07. Cytokine Release Induced by TNF, Htr-9 and ATROSAB. Effects of increasing concentrations of TNF, Htr-9 and ATROSAB on the release of IL-8 from HT1080 (a) and IL-6 from HeLa cells (b). Human serum IgG was included as negative control. Cells were incubated for 16 h with the proteins and released cytokines were determined by ELISA.

IL-8 and 25-40 pg/ml IL-6 were determined for unstimulated cells. Control IgG had no detectable effect on cytokine secretion (Fig. 4.1-07).

4.1.6. Crosslinking of ATROSAB by an Anti-human IgG Antibody

Stimulation of HT1080 cells by ATROSAB in the presence of a crosslinking antibody, specifically binding to human IgG, was investigated to clarify the potential risk of enforced receptor stimulation in case of patients, developing an anti-drug antibody (ADA) response. ATROSAB was incubated at increasing concentrations (0.05 nM to 200 nM) in combination with the crosslinking antibody, applied as well in the concentration range from 0.05 nM to 200 nM to each concentration of ATROSAB (Fig. 4.1-08). For control purposes, ATROSAB in the absence of IgG-specific antibody was included, leading to a maximum IL-8 release of 290 pg/ml at a concentration of around 18.5 nM. In the presence of the crosslinking antibody, the maximum amount of IL-8, detected in the cell culture supernatant, increased with the concentration of the anti-human IgG antibody in a dose-dependent manner (Fig. 4.1-08a).

In order to gain further insight into the mechanism behind the increased receptor activation, IL-8 release as well as the ratio of ATROSAB to anti-human IgG antibody was calculated for the maxima of the fitted arguments of ATROSAB titration curves at any given concentration of crosslinking antibody (Table 4.1-03). Interestingly, the ratio of ATROSAB to anti-human IgG antibody was highly dependent on the concentration of both candidates. The highest ratio of 1:0.008 (ATROSAB to crosslinker) was observed for the curve obtained for 0.05 nM anti-human IgG antibody and led to an IL-8 release of 353 pg/ml at an ATROSAB concentration of 6.3 nM. In the presence of 0.8 nM crosslinking antibody, already 2.9 nM ATROSAB yielded an IL-8 release of 2.2 ng/ml at a ratio of ATROSAB to crosslinker of 1:0.28 (Table 4.1-03). However, as much as 83.9 nM ATROSAB were determined to induce maximum IL-8 release together with 200 nM of anti-human IgG antibody, revealing a ratio of 1:2.4 (ATROSAB to crosslinker). This combination resulted in the highest calculated concentration of 6.6 ng/ml IL-8, which still represented less than 21 % of the maximum IL-8 release, triggered by TNF in these experiments (Fig. 4.1-08b). For better understanding of the cellular response under the tested conditions, the release of IL-8 was visualized in a 3D graph, according to the values, derived from the Gaussian-fit of the experimental data (Fig. 4.1-08c and d).

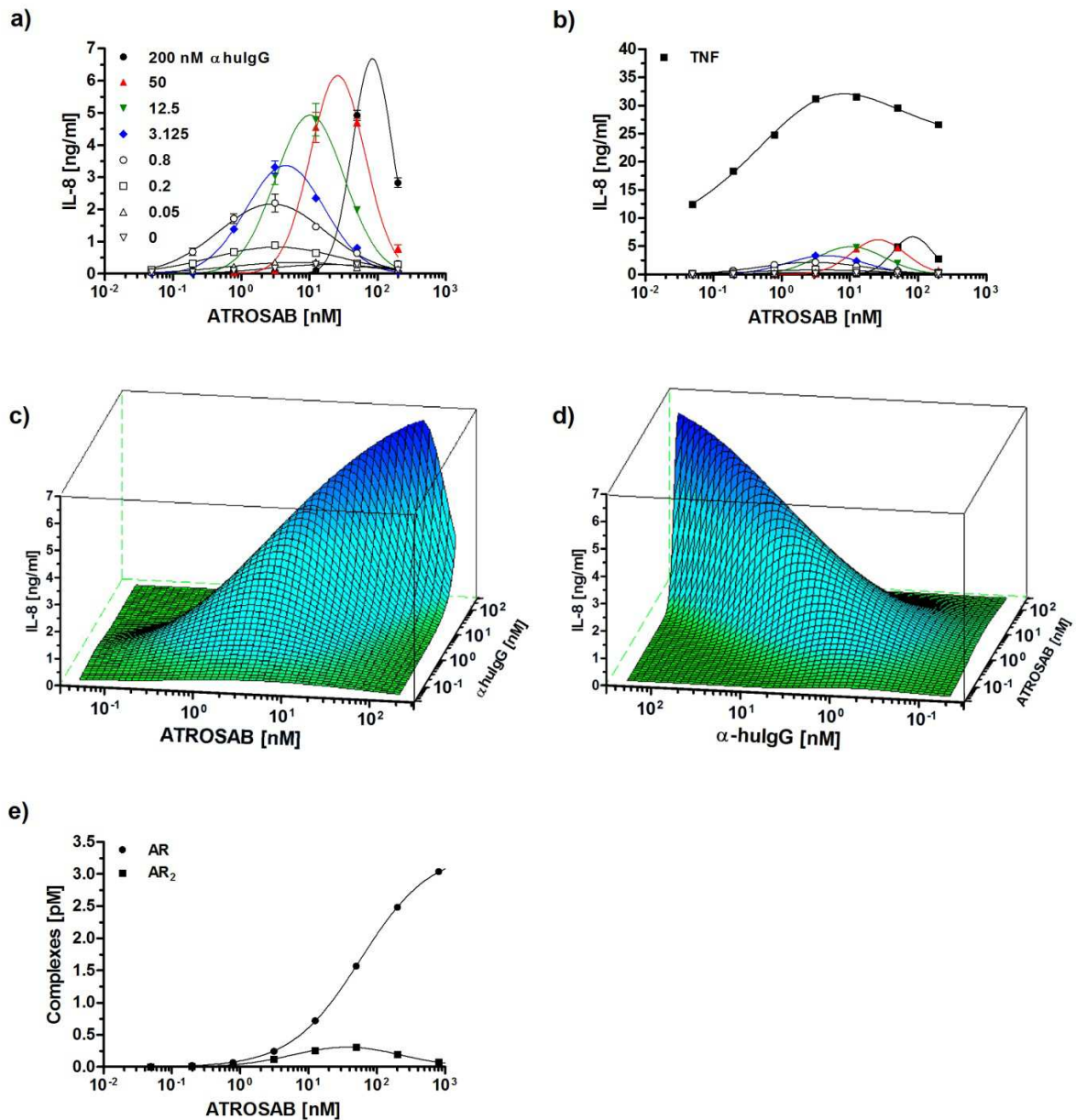


Figure 4.1-08. Crosslinking of ATROSAB by an Anti-human IgG Antibody. a) IL-8 release from HT1080 cells triggered by ATROSAB in the presence of a crosslinking antibody at concentrations from 0.05 nM to 200 nM. b) Comparison to the observed IL-8 release in response to increasing concentrations of TNF. Data in a) and b) were fitted to a Gaussian distribution. c) and d) 3D simulation of IL-8 release induced by ATROSAB and anti-human IgG antibody is shown in two different perspectives. e) Calculation of cell surface complexes of ATROSAB, mono- (AR) and bivalently (AR₂) bound to TNFR1, fitted to a Gaussian distribution in the case of AR and to a log(agonist) vs. response algorithm for [AR₂].

Table 4.1-03: ATROSAB Crosslinking

Anti-hulG (nM)	Maximum IL-8 release (pg/ml)	ATROSAB (nM)	Ratio (ATROSAB/ crosslinker)
200	6685	83.9	2.4
50	6159	26.1	1.9
12.5	4930	10.3	1.2
3.125	3365	4.5	0.7
0.8	2169	2.9	0.3
0.2	828.2	3.3	0.06
0.05	353.3	6.3	0.008
0	290.6	18.5	

Furthermore, on the basis of the law of mass action, the formation of mono- and bivalent complexes between ATROSAB and TNFR1 on the cell surface was calculated (Fig. 4.1-08e). Binding affinities of ATROSAB (4.1.3) and the number of TNFR1 molecules (4.1.4) originated from earlier presented experiments of this study. The monovalent ATROSAB-TNFR1 complex (AR) was formed in a dose-dependent manner, revealing an EC₅₀ value of 58 nM. In contrast, the bivalent complex, consisting of ATROSAB, bound to two TNFR1 molecules (AR₂), appeared transiently with a maximum in the presence 36 nM ATROSAB. Surprisingly, at the highest level of ATROSAB mediated TNFR1-crosslinking, only 9.3 % percent of all available receptors were connected in a bivalent fashion (Table 4.1-04). Finally, high ATROSAB concentrations induced the predominant formation of the monovalent

Table 4.1-04: Calculation of ATROSAB-TNFR1 Complexes

ATROAB [nM]	AR [pM]*	AR [%]	AR ₂ [pM]*	AR ₂ [%]	Free ATR [%]	Free TNFR1 [%]
200	2.485	75.29	0.193	11.70	98.7	13.0
50	1.569	47.54	0.308	18.66	96.2	33.8
12.5	0.720	21.80	0.259	15.70	92.2	62.5
3.125	0.245	7.42	0.120	7.27	88.3	85.3
0.78125	0.069	2.08	0.038	2.28	86.4	95.6
0.1953125	0.018	0.54	0.010	0.61	85.8	98.9
0.048828125	0.005	0.14	0.003	0.16	85.5	99.7

*Receptor concentration in one well: 3.3 pM (according to 1500 receptors per cell and 20,000 cells per well in a 100 µl volume). AR (monovalent ATROSAB-TNFR1 complex), AR₂ (bivalent ATROSAB-TNFR1 complex), ATR (ATROSAB).

4.1.7. Epitope Mapping of ATROSAB and Htr-9

A panel of mutant human TNFR1-Fc fusion proteins was generated to identify the epitopes of ATROSAB and Htr-9. The introduced mutations substituted one or two residues either with the residues of mouse TNFR1 (Fig. 4.1-09a, Table 4.1-05) or with alanine. All proteins were produced in stably or transiently transfected HEK293T cells and purified by protein A affinity chromatography. Purity of all fusion proteins was confirmed by SDS-PAGE (data not shown). Binding of ATROSAB, Htr-9 and human TNF to immobilized mutant receptor-Fc fusion proteins was analyzed by ELISA using 1 nM ATROSAB, Htr-9 or TNF. In

Table 4.1-05: Epitope Fine Mapping of ATROSAB Analyzed by Binding to TNFR1 Mutants in ELISA

Receptor	mutation	TNF	ATROSAB	Htr-9
		Binding		
moTNFR1	wt	+	-	-
huTNFR1	wt	+	+	+
huTNFR1	V14L	+	+	+
huTNFR1	I21V	+	+	+
huTNFR1	P23S	+	-	+
huTNFR1	Q24K	+	+	+
huTNFR1	G45S	+	+	+
huTNFR1	Q48R	+	+	+
huTNFR1	D51V	+	+	+
huTNFR1	S57K	+	+	+
huTNFR1	S59T	+	+	+
huTNFR1	E64Q	+	+	+
huTNFR1	H66Y	+	+	+
huTNFR1	R68A	+	-	+
huTNFR1	H69Q	+	-	+
huTNFR1	H69A	+	-	+
huTNFR1	L71A	+	+	-
huTNFR1	S72A	+	+	+
huTNFR1	S74K	+	+	-
huTNFR1	K75T	+	+	+
huTNFR1	G81S	+	+	+
huTNFR1	S87P	+	+	+
huTNFR1	T89Q/V90A	+	+	+
huTNFR1	R92K	+	+	+

Binding to the receptor mutants compared to huTNFR1-Fc wild type is indicated as similar (+) or strongly reduced (-), respectively. Receptors were immobilized at 1 µg/ml and incubated with antibodies or TNF at a concentration of 1 nM.

order to enable robust quantitative comparison, binding data were standardized to the coating control (anti-human IgG Fc-specific antibody, Table 4.1-05).

In a previous study, the double mutation P23S/Q24K was identified in a chimeric human/mouse TNFR1 background to completely abrogate ATROSAB binding (Zettlitz et al. 2010a). This was narrowed down to a single amino acid by analyzing the same residues in the fully human TNFR1 background. Single mutations of P23 or Q24 to either the mouse residue or an alanine revealed that P23 is critical for ATROSAB binding, while mutation of Q24 to lysine or alanine did not affect binding. Furthermore, exchange of residue H69 (mutated to Q or A) also strongly reduced binding of ATROSAB, which was similarly observed in the case of the conserved residue R68, mutated to alanine. In the following, binding of ATROSAB and TNF to selected mutants was further analyzed by titration experiments (Table 4.1-06). The wild-type receptor was bound by ATROSAB and TNF in the sub-nanomolar range, whereas mutation of H69 to alanine reduced binding of ATROSAB approximately 440-fold. In addition, an 18-fold reduction was observed for the mutation R68A. Expectedly, all mutants bound TNF with similar EC_{50} values compared with wild-type TNFR1 (Table 4.1-06).

Table 4.1-06: Binding of ATROSAB and TNF to Human TNFR1 Mutants in ELISA

TNFR1 Mutant	ATROSAB binding EC_{50} (nM)	TNF binding EC_{50} (nM)
wt	0.27	0.19
P23S	11.0	0.16
Q24K	0.23	0.17
H66Y	0.18	0.14
R68A	5.0	0.16
H69Q	8.6	0.15
H69A	118.5	0.14
R92K	0.12	0.08

Details of binding studies are described in Materials and Methods.

Epitope fine mapping was also performed for the described agonistic TNFR1 antibody Htr-9. Using human-mouse chimeric TNFR1 molecules (Zettlitz et al. 2010a), the epitope of Htr-9 was located as well between residues 29 and 137 (B2 of CRD1, CRD2 and CRD3, data not shown). Using TNFR1 mutants, two residues (L71 and S74) were found to be part of the Htr-9 epitope, discriminating the epitope of ATROSAB from that of the agonistic antibody

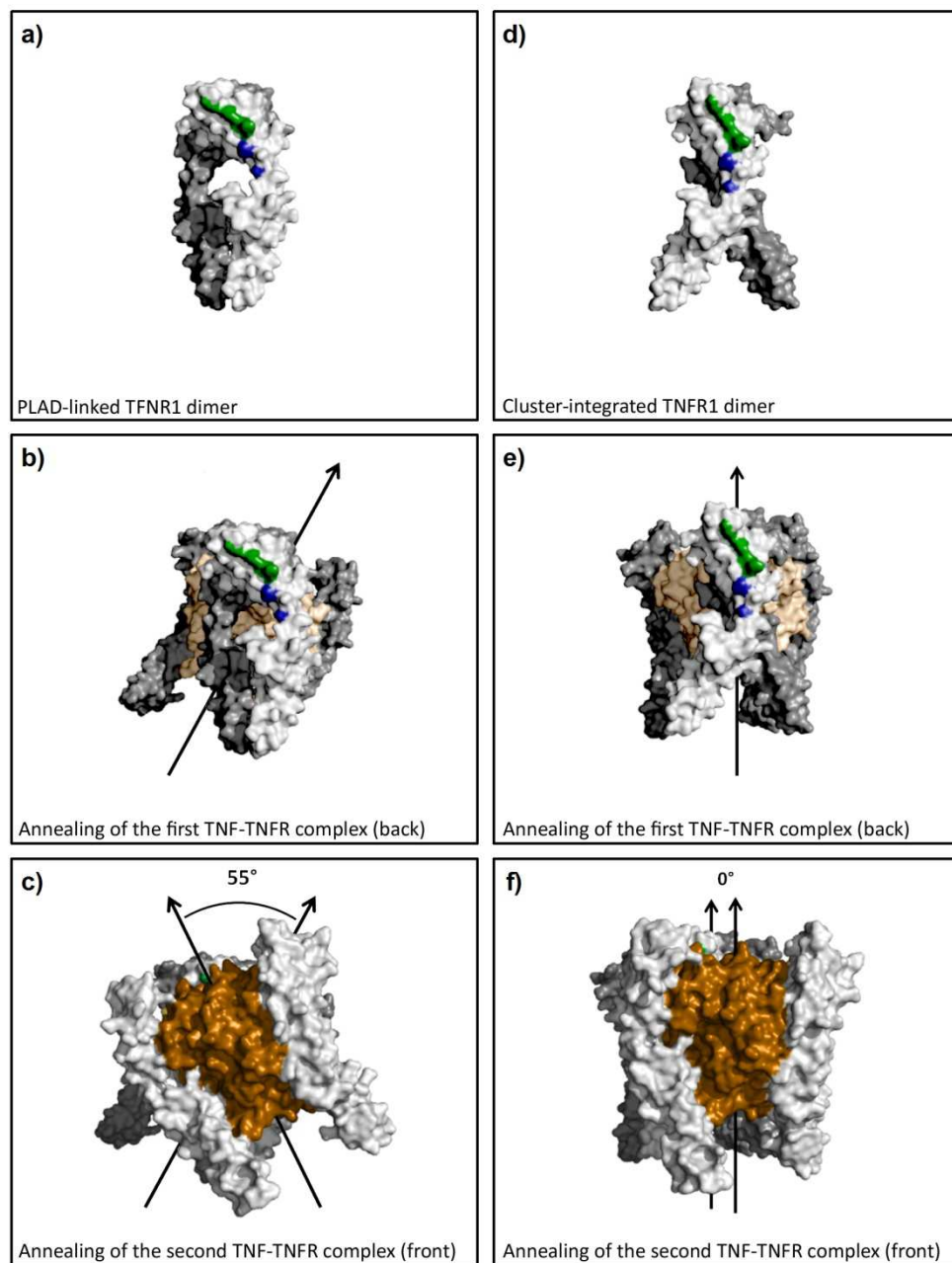


Figure 4.1-10. Conformational Change of the TNFR1 Dimer in the TNF-TNFR1 Complex. Structural analysis of the TNF (bright and dark brown)-TNFR (bright and dark grey) complex. Indicated are the binding sites of ATROSAB (green) and Htr-9 (blue), the center axes of the trimeric TNF molecules (arrows) and the relative angle between the center axes. a) Ligand-independent PLAD-linked TNFR1 dimer (1NCF). b) Annealing of a hexameric TNF-TNFR complex (3ALQ), whereof one receptor molecule of the complex was aligned to the rear receptor molecule of the PLAD-linked TNFR1 dimer. c) Annealing of the second TNF-TNFR complex in the front, as described in b). The center axes of the assembled TNF molecules revealed a relative angle of 55°. d) PLAD-linked TNFR1 dimer, manually arranged to allow for parallel orientation of the TNF molecules and thus, the formation of larger signaling clusters. e) and f) annealed TNF-TNFR complexes as described for b) and c). The employed trimeric TNF molecules show parallel orientation. Structures were visualized using PyMOL (The PyMOL Molecular Graphics System, Version 1504 Schrödinger, LLC).

molecule of each complex with one TNFR molecule of the PLAD-linked TNFR1 dimer (Fig. 4.1-10b and c). Surprisingly, the adjacent trimeric TNF molecules revealed a twisted orientation with an estimated relative angle of 55° between their center axes. In addition to the used TNF-TNFR complex structure 3ALQ, which is composed of TNF and TNFR2, the same analysis was performed for the complex of $LT\alpha$ and TNFR1 (1TNR), revealing the identical orientation of the adjacent $LT\alpha$ molecules.

The formation of higher order signaling networks in case of TNFR1 activation, however, requires parallel fixation of multiple receptor-bound TNF molecules on the cellular surface. Hence, two TNFR1 molecules were manually arranged in an orientation, allowing for parallel orientation of the adjacent TNF-TNFR complexes (Fig. 4.1-10d-f). In summary, these results indicate the requirement of fundamental changes in the orientation and/or conformation for interacting TNFR1 molecules and thus, for the residues of the ATROSAB and Htr-9 epitopes, between ligand-independent, inactive and cluster-integrated, activated status.

4.2. Alternative Antibody Formats

In order to investigate the influence of the molecular architecture on the *a priori* antagonistic activity of ATROSAB, several mono- and bivalent antibody fusion proteins were created. All constructs were cloned using standard PCR and cloning techniques (Fig. 4.2-01a). Constructs like the Diabody (Db) and the scFv-Fc fusion protein, presenting their binding sites for human TNFR1 in smaller distance compared with ATROSAB, were included into the set of derivatives, as well as constructs with increased space between the two binding sites, namely IgG-FabL and 2scFv-HSA (Fig. 4.2-01b). The Fab fragment of ATROSAB and the previously described scFv-HSA construct (Berger et al. 2013) were used as monovalent control proteins (Fig. 4.2-01b).

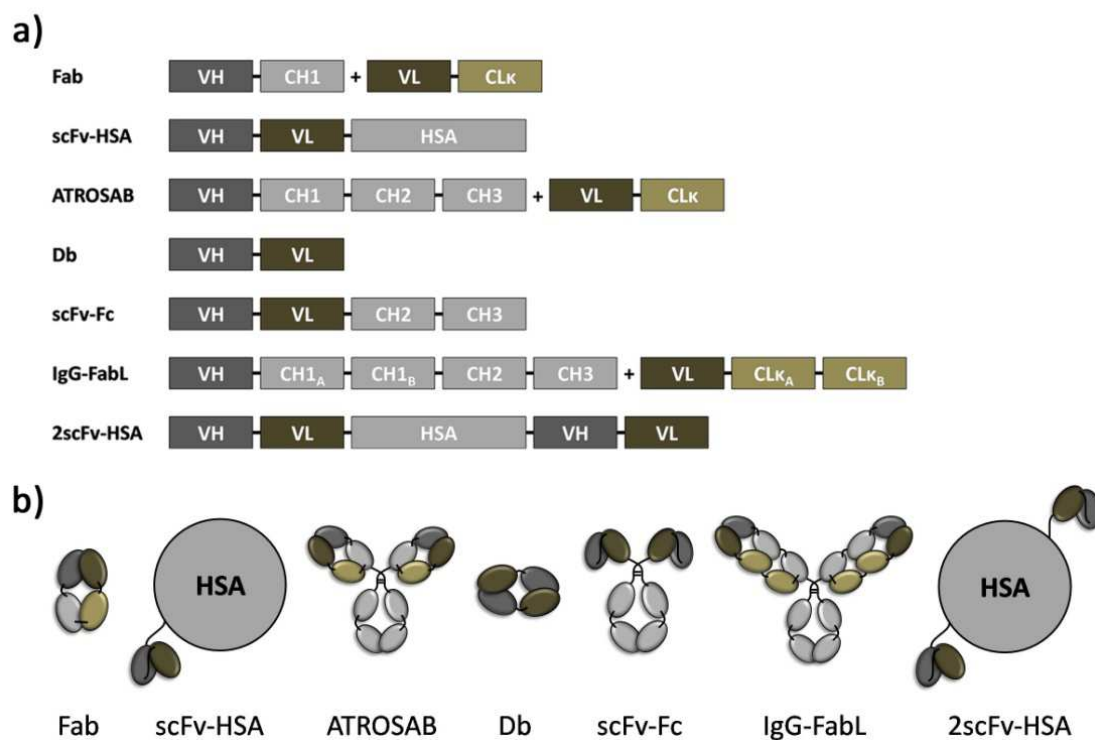


Figure 4.2-01. Overview of Alternative Antibody Formats with ATROSAB Binding Site. a) represents the genotype and b) the architecture of the protein molecules, containing one or two binding sites for human TNFR1. Heavy and light chain antibody domains of the variable and constant regions as well as human serum albumin (HSA, grey) are colored and marked. VH, variable domain, heavy chain, dark grey. VL, variable domain, light chain, dark brown. CH1-CH3, constant domains of the heavy chain, bright grey. CLk, constant domain, light chain, gold. Solid black connections indicate expression as one single amino acid chain.

4.2.1. Purification and Expression of ATROSAB Derivatives

All proteins were produced in HEK239T cells after stable or transient transfection and purified from the tissue culture supernatant by affinity chromatography or immobilized metal ion affinity chromatography. Correct expression of the polypeptide chains was confirmed by SDS-PAGE under reducing and non-reducing conditions (Fig. 4.2-02). All constructs showed bands corresponding to the calculated molecular weights (Table 4.2-01). In the case of scFv-Fc and 2scFv-HSA under reducing conditions, minor bands of lower molecular weight were observed, indicating partly degraded protein (Fig. 4.2-02a). However, under non-reducing conditions, exclusively bands of the whole length fusion proteins were present (Fig. 4.2-02b).

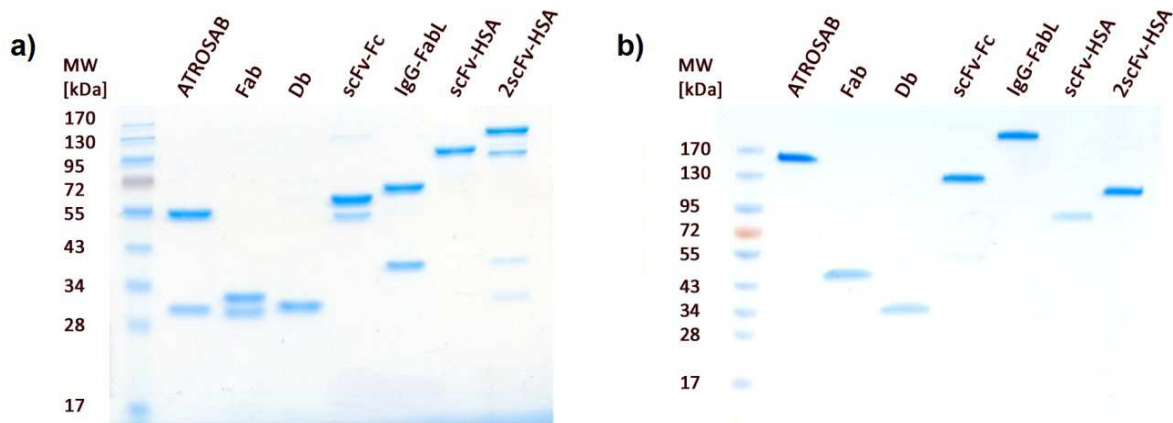


Figure 4.2-02. SDS-PAGE of ATROSAB Derivatives. 3 μ g of denatured protein samples were analyzed under reducing conditions (a) on a 12 % Acryl-/Bisacryl separation gel and under non-reducing conditions using a pre-cast 4-15 % gradient TGX™ gel (b). Proteins were stained with coomassie brilliant blue and de-stained with H₂O.

Furthermore, the alternative antibody formats were subjected to size exclusion chromatography (SEC) to monitor protein integrity under native conditions. All constructs showed a major peak at a retention time, attributable to the calculated molecular sizes (Fig. 4.2-03, Table 4.2-01). Except, the scFv-Fc fusion protein exhibited an unclear trend over the whole measurement time, accounting usually for disordered expression, incorrect assembly, degradation or aggregation of the protein molecule. The residual minor peaks in the SEC measurements of other fusion proteins could result from background noise and marginal degradation or aggregation of the protein samples.

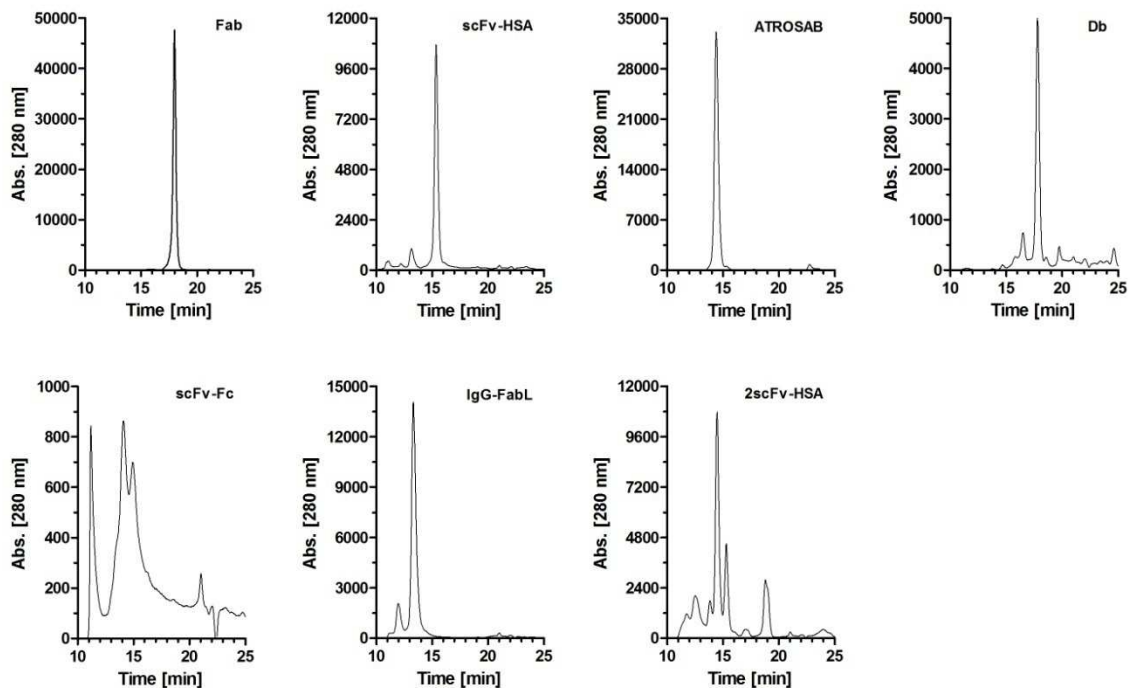


Figure 4.2-03. Size-Exclusion Chromatography of ATROSAB Derivatives. Native protein molecules were analyzed on a Yarra SEC-2000 column at a flow rate of 0.5 ml/min. Absorption of UV light was measured at 280 nm.

Table 4.2-01: Overview Alternative Antibody Formats

Construct	Fab	scFv-HSA	ATROSAB	Db	scFv-Fc	IgG-FabL	2scFv-HSA
Binding sites	1	1	2	2	2	2	2
MW_{subunits} [kDa]	24	-	49; 24	28	53	59; 36	-
MW_{molecule} [kDa]	50	98	160	62	108	192	123
MW_{SEC} [kDa]	42	101	140	44	n.d.	215	135
Span [nm]	-	-	12	7	8	18	18
EC₅₀ [nM]	6.1	3.2	0.83	1.6	1	1	0.36
K_D [nM]_{low affinity}	22	37.1	73	50	175	178	71
K_D [nM]_{high affinity}	-	-	0.20	0.09	1.26	0.36	0.69
IL-8 release [%]	1.7	1.7	2.4	6.2	71	33	46

4.2.2. Receptor Selectivity of Antibody Fusion Proteins with ATROSAB Variable Domains

In the set of ATROSAB derivatives, all constructs retained their specificity for TNFR1, as demonstrated in flow cytometry (Fig. 4.2-04). Binding studies were performed using immortalized mouse embryonic fibroblasts, stably transfected with either the extracellular domain (ecd) of human TNFR1, fused to the intracellular domain (icd) of Fas, or a human TNFR2_{ecd}-Fas_{icd} fusion protein (Krippner-Heidenreich et al. 2002). Bound antibody fusion

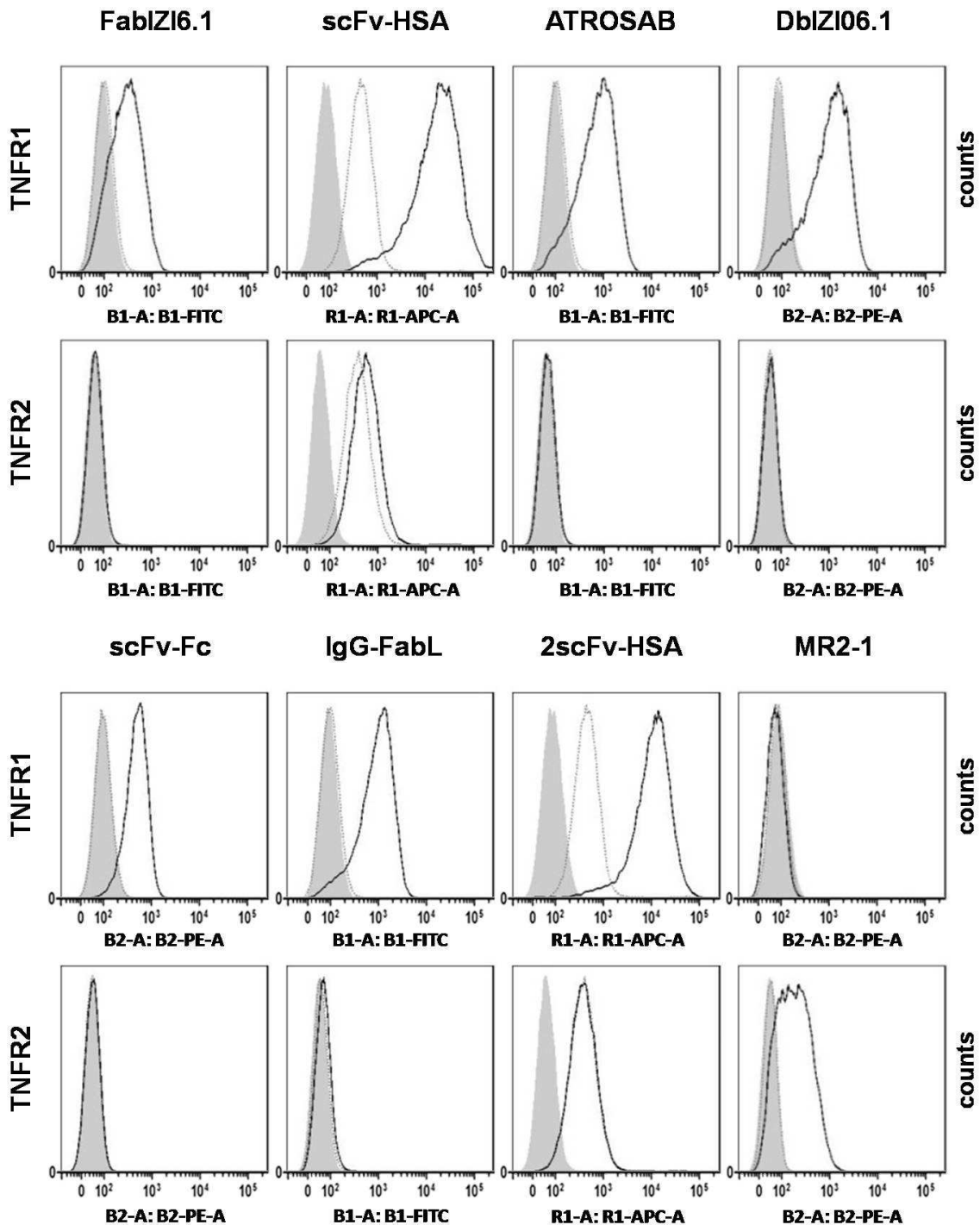


Figure 4.2-04. Receptor-Selectivity of Constructs with ATROSAB Binding Sites. Binding of ATROSAB derivatives (200 nM) to mouse embryonic fibroblasts, stably transfected with either human TNFR1-Fas or human TNFR2-Fas was tested in flow cytometry. Protein samples are shown as solid black lines. Cells alone (grey, filled histogram) and the detection system (dotted line, grey) served as controls. The TNFR2-specific control antibody MR2-1 was used at 50 nM.

proteins were detected either via the Fab fragment, the Fc fragment, the His-tag or the HSA moiety. In contrast to all other fluorescently labeled antibodies, the combination of rabbit anti-HSA and goat anti-rabbit antibodies caused an increased background signal, due to

unspecific binding of the detection antibodies to the cells (applied for scFv-HSA and 2scFv-HSA). However, the signal of the bound protein was clearly above the level of detection (Fig. 4.2-04). The TNFR2-specific antibody MR2-1 was used as control (Fig. 4.2-04, lower right).

4.2.3. Characterization of TNFR1 Binding by Alternative Antibody Formats

A concentration-dependent binding to huTNFR1-Fc was shown for all tested proteins by ELISA (Fig. 4.2-05a). ATROSAB, Db, scFv-Fc and IgG-FabL showed similar binding with EC_{50} values between 0.83 and 1.6 nM (Table 4.2-01). 2scFv-HSA showed slightly stronger binding to huTNFR1-Fc, indicated by the lower EC_{50} value of 0.36 nM. In contrast, the monovalent Fab fragment showed weaker binding to the human TNFR1-Fc (EC_{50} 6.1 nM), compared with the proteins comprising two binding sites for the receptor. Surprisingly, the albumin fusion protein scFv-HSA, also harboring only one binding site for huTNFR1-Fc, showed an 1.9-fold lower EC_{50} value of 3.2 nM compared with the Fab fragment.

In addition, the dynamics of the binding process to human TNFR1 were analyzed by Quartz Crystal Microbalance (QCM) measurements to further line out differences between the investigated molecules. All ATROSAB derivatives were tested on two sensor chips, presenting different amounts of immobilized antigen on their surface. Data sets from both chips were evaluated simultaneously, to receive reliable results, independent from receptor density. Exclusively the obtained data of the monovalent formats, namely Fab and scFv-HSA, could be described on both chips by a fitting algorithm, based on a "one to one" binding model (Fig. 4.2-05b and c). The kinetic constants for both molecules were in the similar range with K_D values of 22 nM for the Fab fragment and 37 nM in case of the scFv-HSA fusion protein (Table 4.2-02). ATROSAB, Db and scFv-Fc revealed biphasic dissociation characteristics on both chips (Fig. 4.2-05d, e and f), which converged towards a "one to two" binding model. The analyzed binding curves resulted in two different data sets, either with higher affinity K_D values of 0.20 nM, 0.088 nM and 1.3 nM or lower affinity dissociation constants of 73 nM, 50 nM and 175 nM, for ATROSAB, Db and scFv-Fc, respectively. Measurements of IgG-FabL and 2scFv-HSA, binding to sensor chips immobilized with human TNFR1 at high density, have been excluded due to hardly detectable dissociation, which led to overestimated affinities during the fitting process (data not shown). However, on the low density TNFR1 chip, both molecules exhibited biphasic binding characteristics of sufficient

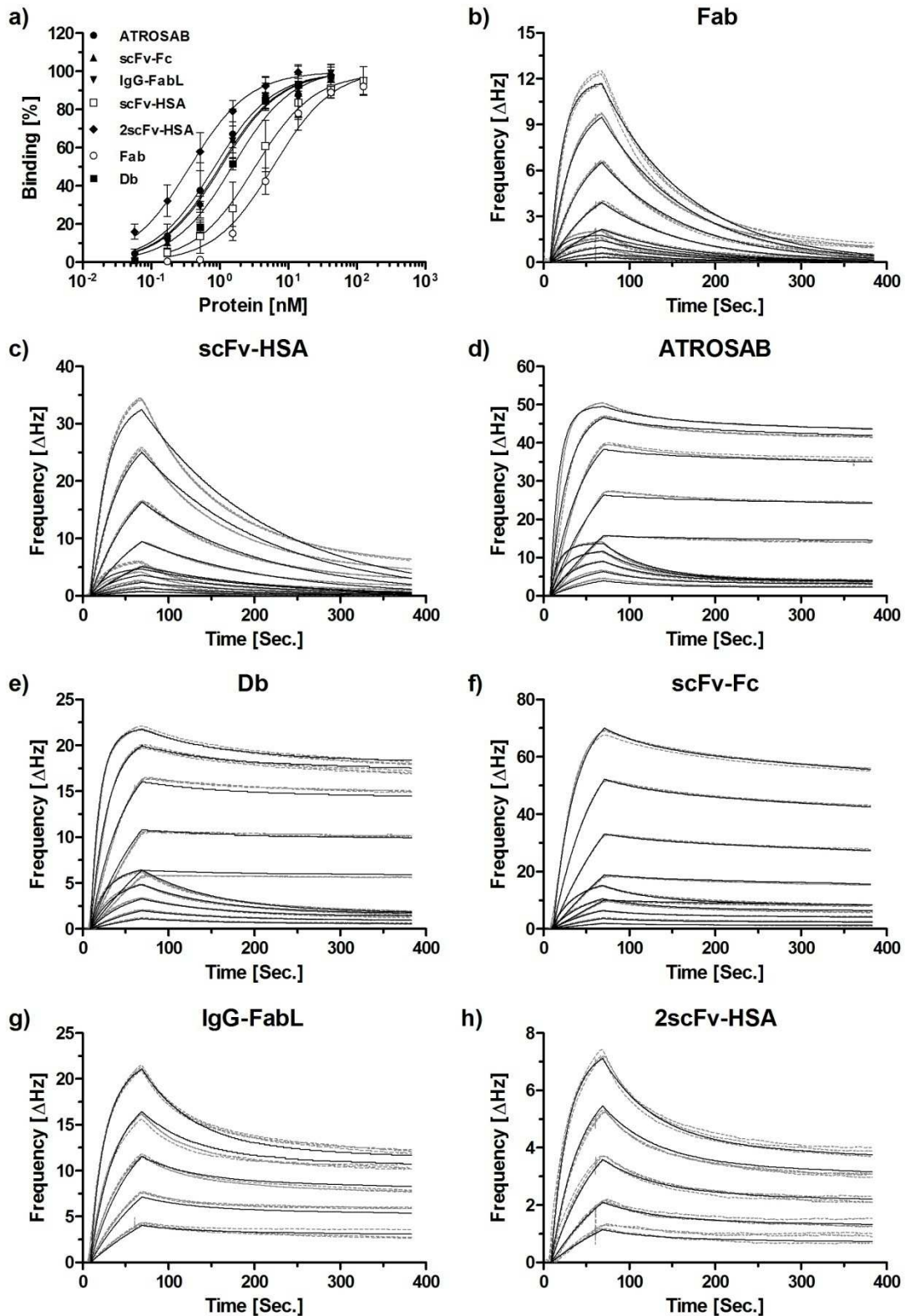


Figure 4.2-05. Binding of ATROSAB Derivatives to Human TNFR1-Fc. a) Binding analysis by ELISA in serial dilutions starting at 125 nM or 41,7 nM (mean \pm SD, n = 3). Quartz crystal microbalance based biosensor investigation of the Fab fragment (b), scFv-HSA (c), ATROSAB (d), Diabody (e), scFv-Fc (f), IgG-FabL (g) and 2scFv-HSA (h) on one or two sensor chips of either high or low receptor density. Five different concentrations (256 nM to 16 nM or 128 nM to 8 nM) were analyzed in triplicates.

curvature for robust evaluation. High and low affinity interactions were represented by K_D values of 0.36 nM and 178 nM for IgG-FabL (Fig. 4.2-05g) as well as 0.69 nM and 71 nM in the case of 2scFv-HSA (Fig. 4.2-05h), respectively. The K_D values of the high affinity binding compared with the low affinity situation were improved by factors from 103 for the 2scFv-HSA to 573 for the Db. This difference could be mainly attributed to changes in the dissociation rate constant k_{off} , which was reduced from 47 fold (scFv-Fc) to 162 fold (Db). The association rate constant k_{on} varied less during the performed experiments (1.9 fold for 2scFv-HSA to 6.7 fold for IgG-FabL, see also Table 4.2-02).

Table 4.2-02: QCM measurements of Alternative Antibody Formats.

	Fab	scFv-HSA	ATORSAB	Db	scFv-Fc	IgG-FabL	2scFv-HSA
$B_{max1_{idc}}$ (Hz)	2.1	5.6	12	7.1	16	25	5.0
$B_{max2_{idc}}$ (Hz)	-	-	4.2	1.8	10.5	12.6	4.3
$B_{max1_{hdc}}$ (Hz)	14	39	6.0	4.7	21	-	-
$B_{max2_{hdc}}$ (Hz)	-	-	46	19	67	-	-
k_{on1} ($M^{-1}s^{-1}$)	4.7×10^5	1.8×10^5	2.5×10^5	2.3×10^5	1.0×10^5	9.6×10^4	2.4×10^5
k_{off1} (s^{-1})	1.0×10^{-2}	6.7×10^{-3}	1.8×10^{-2}	1.2×10^{-2}	1.8×10^{-2}	1.7×10^{-2}	1.7×10^{-2}
K_D1 (nM)	22	37	73	50	175	178	71
k_{on2} ($M^{-1}s^{-1}$)	-	-	8.2×10^5	8.1×10^5	3.1×10^5	6.4×10^5	4.4×10^5
k_{off2} (s^{-1})	-	-	1.7×10^{-4}	7.1×10^{-5}	3.9×10^{-4}	2.3×10^{-4}	3.0×10^{-4}
K_D2 (nM)	-	-	0.20	0.08	1.3	0.36	0.69

4.2.4. Activity of ATROSAB Derivatives on Interleukin-8 Release from HT1080 Cells

ATROSAB and the related mono- and bivalent molecules were tested for their *in vitro* bioactivity on HT1080 cells, compared with human soluble TNF. In an established interleukin-8 release assay, cells alone showed low basal activity of approximately 1.6 % of the maximum response to TNF, observed at a concentration of 18.5 nM. ATROSAB at a concentration of 56 nM stimulated HT1080 cells to a marginal IL-8 production of about 2.4 % of the maximum TNF response. No stimulatory activity above the cellular background was detected for the monovalent constructs Fab and scFv-HSA (Fig. 4.2-06b). All newly designed bivalent reagents, however, showed increased agonistic activity, compared with the parental IgG ATROSAB. The Db displayed a minor increase in IL-8 production of up to 6.2 % of the maximum TNF response, when applied at a concentration of 6.2 nM. In contrast, the

derivatives scFv-Fc, IgG-FabL and 2scFv-HSA stimulated IL-8 production in HT1080 cells of 71 %, 33 % and 46 % of the maximum response to TNF, respectively, when present in concentrations ranging from 6.2 to 56 nM (Fig. 4.2-06a, Table 4.2-01). In summary, among the tested bivalent TNFR1 specific molecules, exclusively the IgG molecule ATROSAB did not induce profound stimulation of a cellular response.

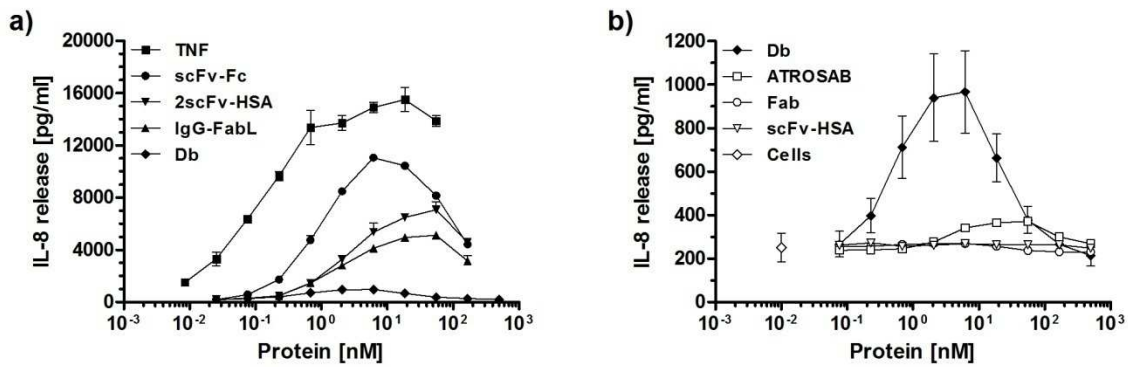


Figure 4.2-06. IL-8 Release Triggered by Alternative ATROSAB Molecules. IL-8 release from HT1080 cells in the cell culture supernatant was analyzed by ELISA. a) Agonistic activity of bivalent ATROSAB derivatives was compared to the release triggered by the positive control TNF. b) Response to treatment with low and non-agonistic molecules of the same experiments are displayed on a smaller scale Y-axis.

4.3. Superior Bioactivity of H398

ATROSAB was initially generated by humanization of the mouse monoclonal antibody H398 (Kontermann et al. 2008). In standard ELISA, both antibodies exhibited similar binding activities to human TNFR1 with EC_{50} values of 0.25 nM in the case of ATROSAB and 0.15 nM for H398 (Fig. 4.3-01a). Furthermore, similar affinities (K_D values) of ATROSAB and its parental mouse antibody H398 of 0.35 nM and 0.23 nM, respectively, were determined by QCM technology, under conditions of high receptor density (Fig. 4.3-01). In contrast, unlike the similarity observed in binding assays, comparable inhibition of TNF- or LT-induced IL-8 release from HT1080 cells was only achieved, using 10- to 12-fold higher concentrations of ATROSAB, compared with H398 (Fig. 4.3-02).

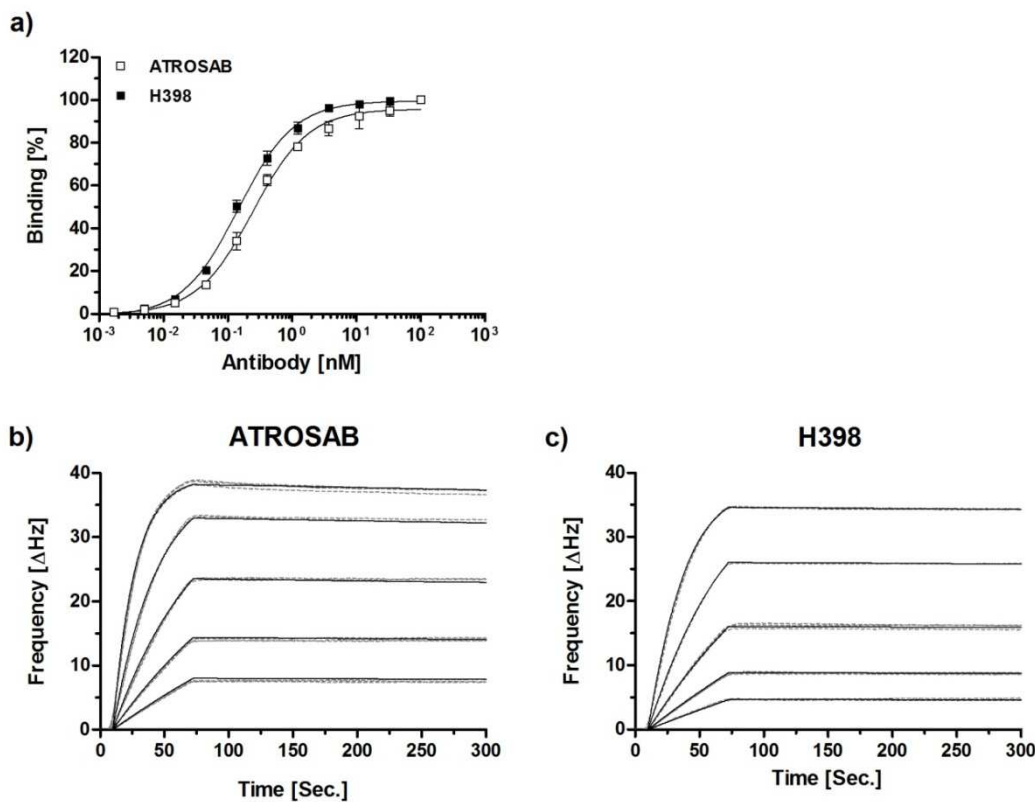


Figure 4.3-01. Binding of H398 and ATROSAB to Human TNFR1-Fc. a) Equilibrium binding of ATROSAB and H398 was analyzed by standard ELISA ($n=3$, mean + SD). QCM binding kinetics of ATROSAB (b) and H398 (c), tested under conditions of high receptor density (195 Hz). Applied were triplicates of five concentrations between 62.5 nM and 3.9 nM.

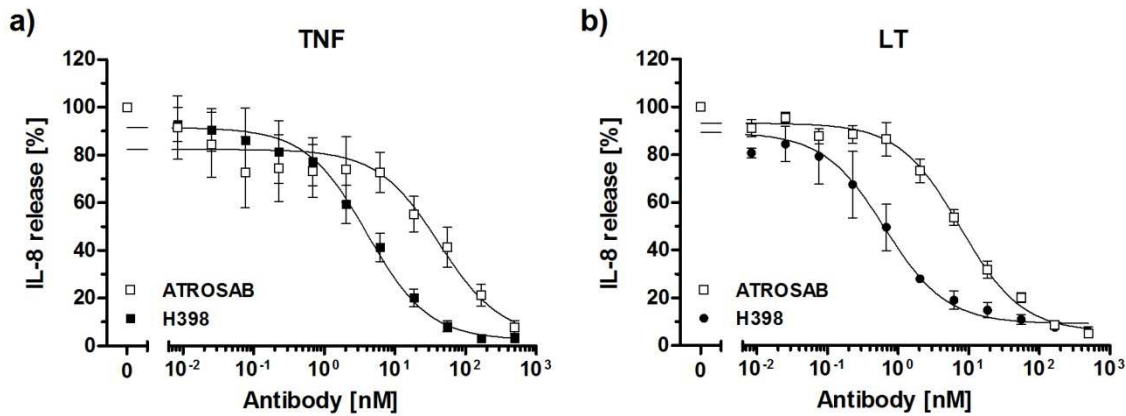


Figure 4.3-02. Inhibition of TNF and LT Action by ATROSAB and H398. Inhibition of IL-8 secretion from HT1080 cells with increasing concentrations of ATROSAB and H398, induced by 0.1 nM TNF (a) and LT α (b). Data from $n=3$ experiments are shown as percent of maximum IL release, triggered by TNF or LT α alone (Mean + SD).

4.3.1. Serum Stability, pH-value and Incubation Time in the Bioactivity of ATROSAB and H398

ELISA binding studies were carried out in 2 % skim milk on the basis of phosphate buffered saline (PBS) at room temperature in the range of a few hours. In contrast, during IL-8 release experiments, the antibodies were exposed for longer periods of time to culture medium, containing fetal bovine serum (FCS) at higher temperatures (16-18 hours, 37 °C). Hence, it was investigated whether the reduced inhibitory potential, observed for ATROSAB in IL-8 release assays, resulted from a loss in activity due to a lower stability in the presence of serum proteases. Nevertheless, similar binding to human TNFR1-Fc in ELISA was detected after the incubation of ATROSAB and H398 in human (Fig. 4.3-03a) or fetal bovine serum

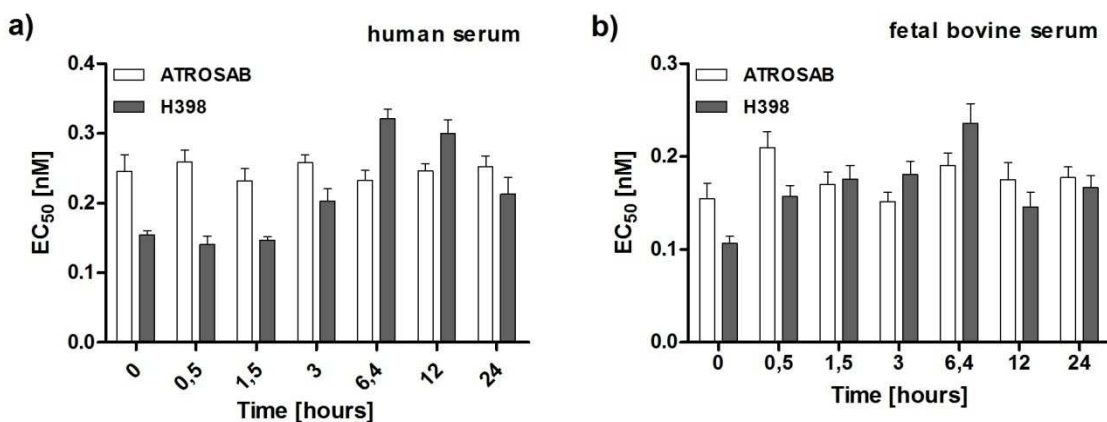


Figure 4.3-03. Serum Stability of ATROSAB and H398. Comparison of EC₅₀ values of ATROSAB and H398, measured by binding ELISA (titration from 100 nM to 1.7 pM) to human TNFR1-Fc, after incubation in human serum (a) or fetal bovine serum (b) for the indicated time periods ($n=1$, duplicates, Mean + SD).

(Fig. 4.3-03b) for up to 24 hours, revealed by slightly varying EC_{50} values ranging from 0.1 nM to 0.3 nM.

Furthermore, in the setting of the standard IL-8 release assay, the tested antibodies underlie target cell-mediated secondary effects like continuous internalization of bound receptor complexes. Taking into account that internalized receptors could still contribute to signaling, the acidified conditions in the endosomal compartment might play a role in the superior bioactivity of H398. A pH-dependent effect could yet be excluded, as binding of ATROSAB and H398 to human TNFR1-Fc in ELISA did not differ significantly among each other in experiments, performed at pH 5.4, pH 6.4, pH 7.4 and pH 8.4 (Fig. 4.3-04).

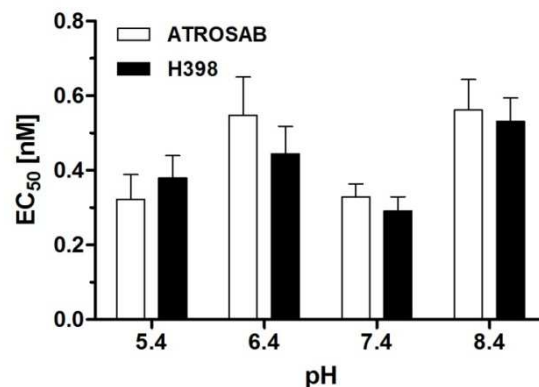


Figure 4.3-04. Influence of the pH-Value on the Binding of ATROSAB and H398 to huTNFR1. Comparison of EC_{50} values of ATROSAB and H398 (titrated from 500 nM to 8.5 pM), binding to human TNFR1-Fc in ELISA, at the indicated pH-values ($n=1$, duplicates, Mean + SD).

Alternatively, the differing bioactivities of ATROSAB and H398 in the IL-8 release assays might accumulate over time, eventually due to a varying impact of internalization-mediated degradation on the human and mouse antibodies. Therefore, the time-dependent IL-8 release, triggered by 1 nM and 0.1 nM TNF, was analyzed during the usually applied incubation time of 16 hours (Fig. 4.3-05). Already two hours after the start of the experiment, IL-8 levels induced by both concentrations of TNF were detected clearly above the cellular background. Consequently, the inhibition of TNF- (Fig. 4.3-06a) and LT-induced (Fig. 4.3-06b) IL-8 release from HT1080 cells by ATROSAB and H398 was tested after a reduced incubation time of 2 hours. However, the detected IC_{50} values and, even more striking, the predominance of H398 were almost identical compared with the data acquired after 16 hours of incubation (Fig. 4.3-06c).

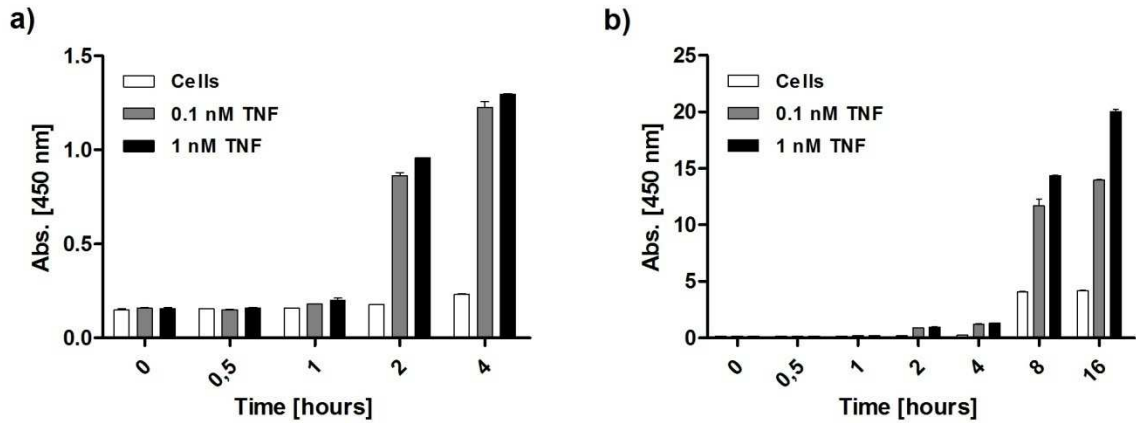


Figure 4.3-05. Time Course of TNF-induced IL-8 Release from HT1080 Cells. IL-8 release in response to TNF, detected by ELISA after incubation for a) 0 to 4 hours and b) 0 to 16 hours (n=1, duplicates, Mean + SD).

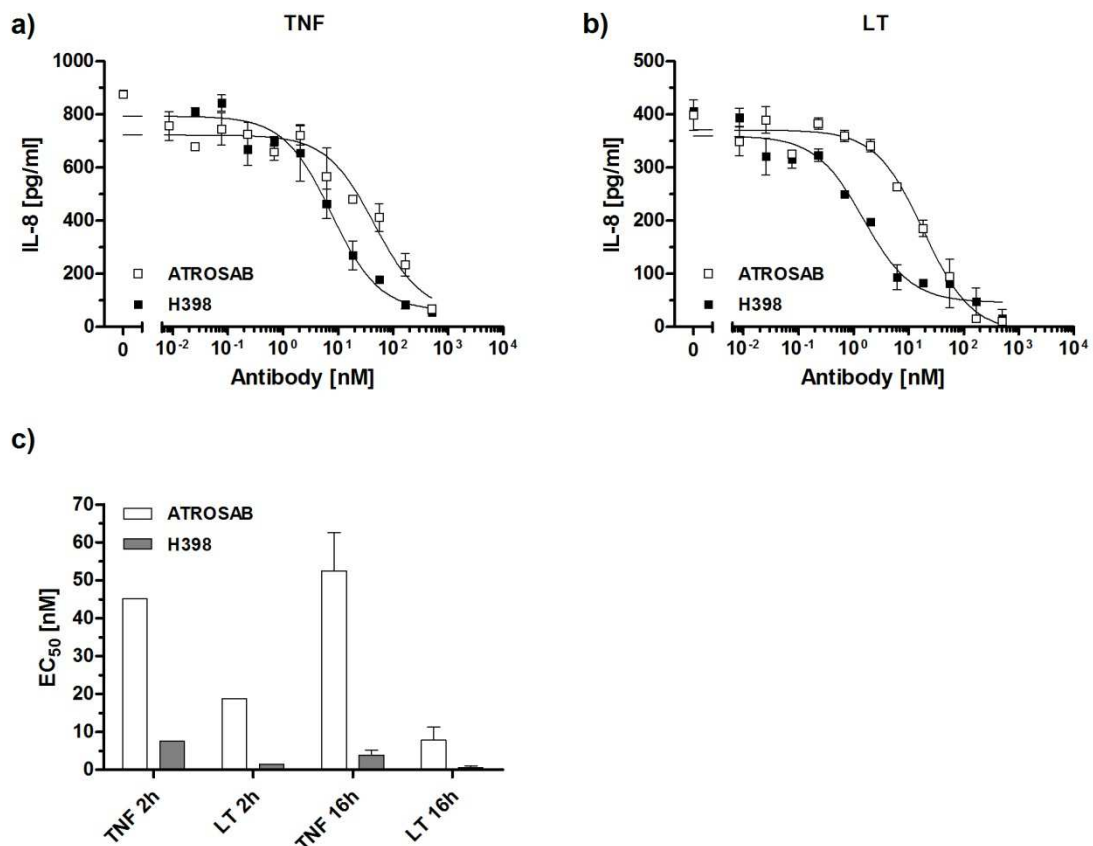


Figure 4.3-06. Neutralization of TNF-or LT-Mediated IL-8 Release from HT1080 Cells. Differences of the inhibitory potency of ATROSAB and H398 after two hours incubation in an IL-8 release assay, performed as presented in Fig. 4.3-02. a) Inhibition of TNF action. b) inhibition of LT action (Mean + SD of a single experiment with duplicates). c) comparison of neutralization after 2 h (n=1) or 16 h of incubation (n=2, Mean + SD).

4.3.2. Binding of ATROSAB and H398 to huTNFR1 at Low Receptor Density

Considering that the receptors in ELISA and QCM measurements (performed on a high density chip) are overrepresented, compared with the *in vitro* situation on HT1080 cells in the IL-8 release assay, QCM measurements were repeated, using a chip with lower receptor density (Fig. 4.3-07). A K_D value of 4.5 nM was obtained for ATROSAB and a K_D value 1.6 nM in the case of H398 (Table 4.3-01). Interestingly, while the K_D value and the association rate constant (k_{on}) of ATROSAB and H398 similarly differed by a factor of 2.8 and 2.6, respectively, the dissociation (described by k_{off}) of H398 was about 7.6-fold slower than the dissociation of ATROSAB (Fig. 4.3-07, Table 4.3-01).

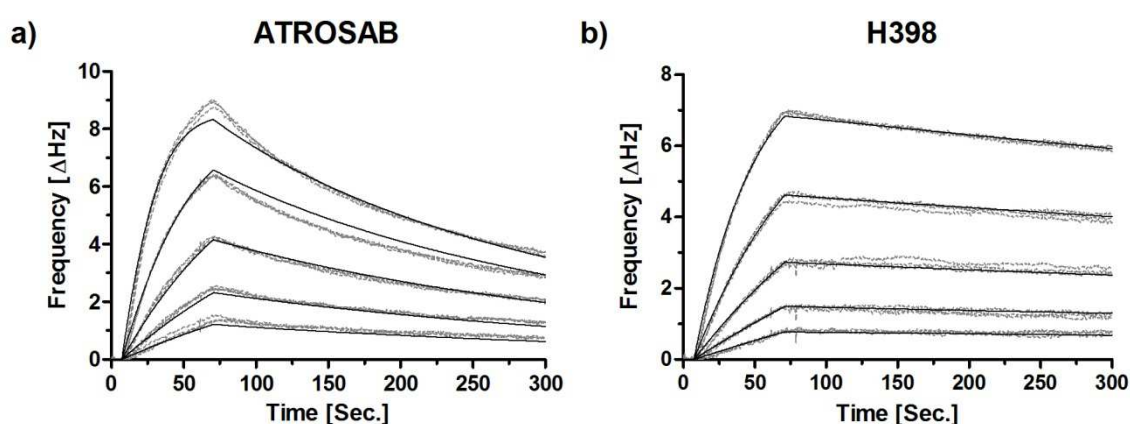


Figure 4.3-07. Binding Kinetics at Low Receptor Density. Determination of the affinity of ATROSAB (a) and H398 (b) for human TNFR1-Fc by QCM at a receptor density of 48 Hz. Analyzed were five concentrations between 62.5 nM and 3.9 nM in triplicates. Measurements (grey, dotted line) and fit (black, solid line) are displayed.

Table 4.3-01. Binding and Bioactivity of ATROSAB and H398

	ATROSAB	H398	Factor
EC_{50} , ELISA [nM]	0.25	0.15	1.7
K_D , high density chip [nM]	0.35	0.23	1.5
IC_{50} , TNF [nM]	42	4.1	10
IC_{50} , LT [nM]	7.6	0.65	12
K_D , low density chip [nM]	4.5	1.6	2.8
k_{off} , low density chip [s^{-1}]	4.7×10^{-3}	6.2×10^{-4}	7.6

Taking together, the influence of serum stability, changed pH and incubation time on the observed superiority of H398 over ATROSAB in the inhibition of TNFR1-mediated cellular responses could be excluded. But, lastly, it was possible to demonstrate that H398 dissociates slower from the antibody receptor complex, compared with ATROSAB. Hence, this feature was specifically addressed in the subsequent affinity maturation studies.

4.4. Affinity Maturation of ATROSAB

In previous work (Zettlitz 2010b), ATROSAB was subjected to affinity maturation using phage display libraries of individually randomized CDRH1, CDRH2, CDRL1, and CDRL2. Within these CDRs, positions were randomized, which were identified in a model structure of scFvIZI06.1 (ATROSAB) to be exposed to the antigen-binding site. Although preferred residues were identified for all four CDRs, only mutations in CDRH2 were found to show some improvements in TNFR1 binding. ScFvIG11 revealed binding to TNFR1-Fc with a two-fold higher K_D compared with scFvIZI06.1, as determined by QCM. ScFvIG11 was selected for further experiments due to its nearly three-fold reduced off-rate constant k_{off} , compared with scFvIZI06.1, indicating slower dissociation of the antibody from the antibody-receptor complex. A sequence alignment of scFvIZI06.1 and scFvIG11 is shown in Figure 4.4-01.

a)

	FR1	CDRH1	FR2	CDRH2
Kabat	123456789102345678920234567893	02345	67894023456789	502a3456789602345
scFvIZI06.1	QVQLVQSGAEVKKPGSSVKVSKASGYTFT	DFYIN	WVRQAPGQGLEWIG	EIYPYSGHAYYNEKFKA
scFvIG11V.TQ.E.K..D....

	FR3	CDRH3	FR4
Kabat	67897023456789802abc345678990234	567891	003456789110
scFvIZI06.1	RVTITADKSTSTAYMELSSLRSEDTAVYYCAR	WDFLDY	WGQGTTVTVSS
scFvIG11

b)

	FR1	CDRL1	FR2	CDRL2
Kabat	12345678910234567892023	4567abcde8930234	567894023456789	5023456
scFvIZI06.1	DIVMTQSPVSLPVPTEPEASIS	RSSQSLLSNGNTYLH	WYLQKPGQSPQLLIY	TVSNRFS
scFvIG11

	FR3	CDRL3	FR4
Kabat	78960234567897023456789802345678	990234567	89100345678
scFvIZI06.1	GVPDRFSGSGSGTDFTLKISRVEAEDVGVYYC	SQSTHVPYT	FGGGTKVEIKR
scFvIG11

Figure 4.4-01. Sequence Alignment of scFvIZI06.1 and scFvIG11. a) aligned VH sequences of ATROSAB (scFvIZI06.1) and scFvIG11. b) Alignment of VL sequences. Residues are numbered according to the Kabat numbering scheme and dots represent identical amino acids compared with scFvIZI06.1. Letters in red/bold indicate newly introduced mutations.

The library used for the following selection experiments was generated by error-prone PCR of the whole sequence comprising VH and VL of scFvIG11 (6.2×10^5 colony forming units). Ten analyzed single clones revealed an overall mutagenesis rate of 7.5 mutations per kilo base pair (7.5/kbp). Within the CDRs, covering 25 % of the whole scFv sequence (180 of 729 bp), 15 of 55 mutations were observed (27 %), indicating a rather equal distribution of mutations (Fig. 4.4-02).

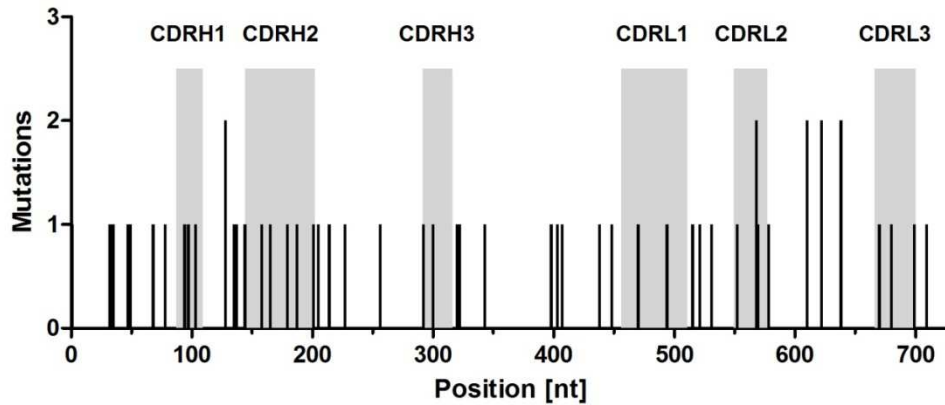


Figure 4.4-02. Mutational Analysis of Phage Display Library EP03. Frequency of mutations, randomly introduced by error-prone PCR, at the indicated positions of the scFv sequence. Ten clones were analyzed. The positions of the complementarity determining regions (CDR) are marked by the bright grey background color.

4.4.1. Selection of the Affinity Matured Clone scFvT12B

A negative selection round, using human TNFR2, was performed prior to panning against human TNFR1, to retain receptor specificity during the selection process. Displayed scFv fragments with improved binding behavior were selected, employing either biotinylated human TNFR1-Fc in combination with streptavidin-coated magnetic dynabeads or human TNFR1-Fc, immobilized to immunotubes. Total binding changes of the selection pool were recorded by polyclonal phage ELISA after each round (Fig. 4.4-03). Binding was improved about two-fold using dynabeads and approximately three-fold after selection in immunotubes.

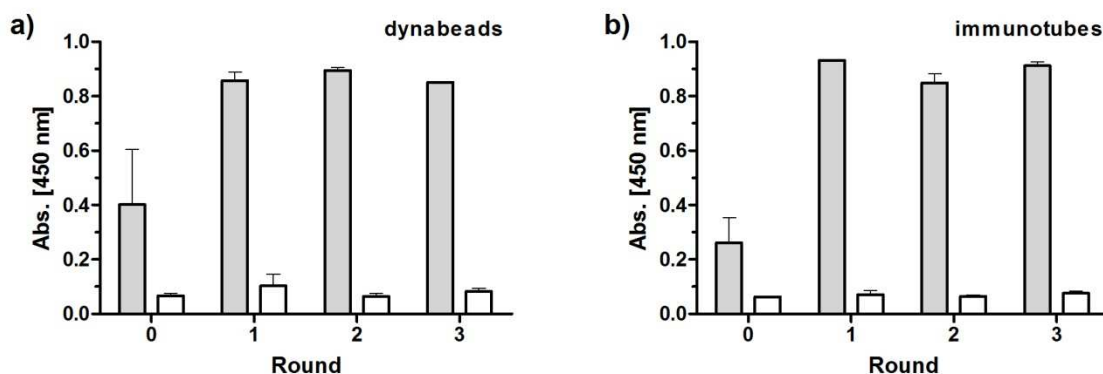


Figure 4.4-03. Polyclonal Phage ELISA of Selection Against Human TNFR1. The pool of amplified phages was analyzed for total binding to human TNFR1-Fc in ELISA after each round of selection, using soluble biotinylated antigen in combination with dynabeads (a) or immobilized antigen in immunotubes (b). Grey bars represent binding to human TNFR1, white bars show binding to human TNFR2. Shown are mean \pm SD of a single experiment with duplicates.

Subsequently to selection round three (selection conditions are reviewed in Table 4.4-01), single clone culture supernatants were screened in an ELISA against human TNFR1 and TNFR2, revealing numerous binders with retained receptor specificity (Fig. 4.4-04). Clones from dynabead and immunotube selections were chosen for further analysis

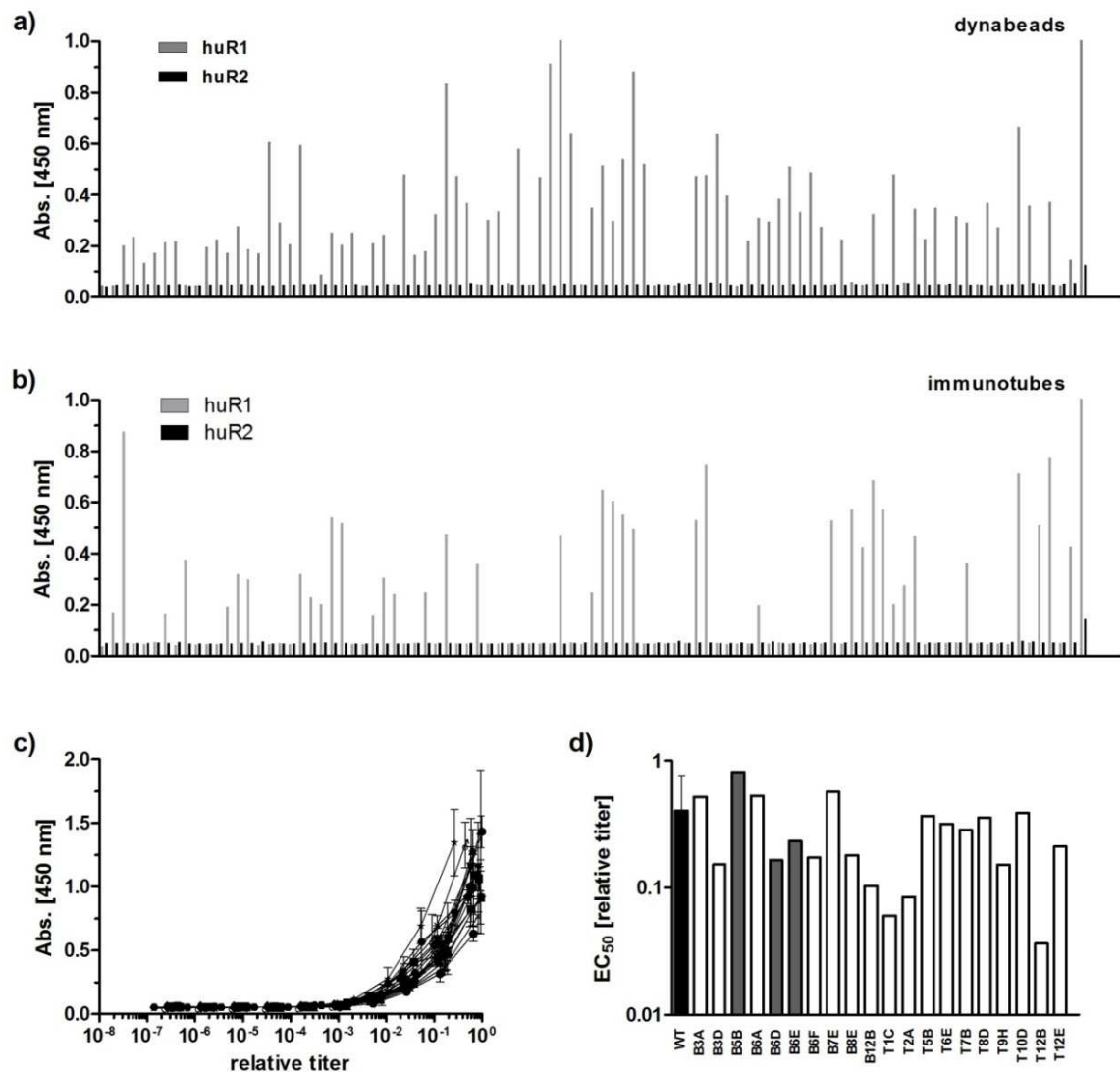


Figure 4.4-04. Screening of Single Clone Phages for Human TNFR1 Binding. Phage containing supernatants of small scale single clone cultures, originating from dynabead (a) or immunotube (b) selections, were tested for binding to human TNFR1-Fc in ELISA. Increasing concentrations of the selected candidates were further analyzed for their interaction with huTNFR1 (c) and the EC_{50} values are shown in d). The phage concentration was determined by anti-His/anti M13-HRP sandwich ELISA and normalized to the highest titer (relative titer). Dark bars indicate genetic wild type (scFvIG11) sequence. All graphs show single experiments, c) and d) were performed in duplicates. Displayed are mean \pm SD.

according to signal intensity and phages were amplified in a larger scale cultures. Supernatants were titrated and analyzed in an ELISA against huTNFR1. Relative phage concentrations (relative titer) were determined by an anti-His/anti-M13-HRP sandwich ELISA and normalized to the sample with the highest phage titer (Fig. 4.4-04c). Clone T12B showed the strongest binding, indicated by the lowest EC_{50} value (Fig. 4.4-04d), which was determined on the basis of the normalized phage concentration (relative titer). Subsequent sequence analysis identified three clones of identical DNA composition compared with the wild type scFvIG11 (Fig. 4.4-04d).

Table 4.4-01. Selection Conditions

Round	Antigen	Phages	Competition	Antigen	Phages	Competition
	DynaBeads			Immunotubes		
1	10 nM	10 μ l	-	1 μ g/ml	10 μ l	-
2	1 nM	10 μ l	-	0.1 μ g/ml	1 μ l	-
3	0.1 nM	1 μ l	10 nM*	0.01 μ g/ml	1 μ l	10 nM*

* Unlabeled human TNFR1 in solution was used for competition for both, selection on DynaBeads and in Immunotubes.

Candidate phages, showing the strongest binding to human TNFR1 were expressed as soluble scFv fragments and subject to an additional ELISA experiment. Here, clone T10D was found to bind with the lowest EC_{50} value to human TNFR1 (Fig. 4.4-05a, Table 4.4-02).

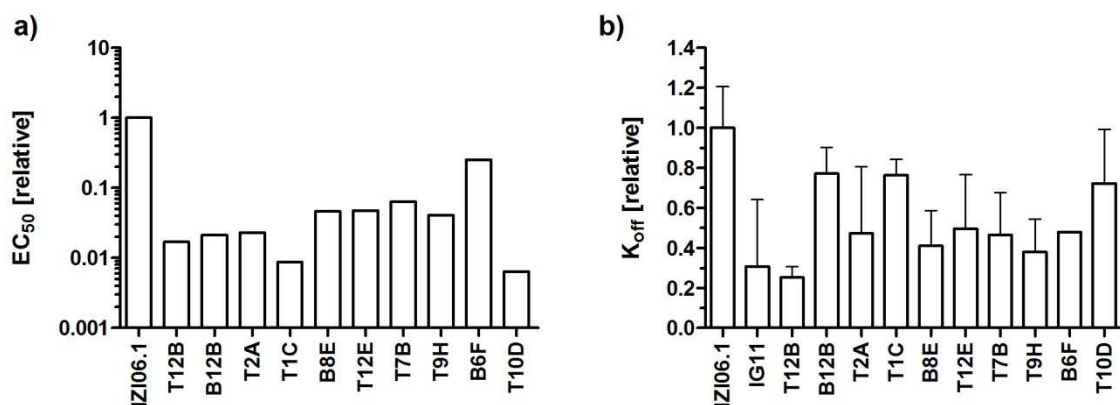


Figure 4.4-05. Characterization of Candidate scFv Antibodies. Selected candidates were expressed as soluble scFv antibodies and tested for binding to human TNFR1-Fc in ELISA (a) and QCM measurements (b). EC_{50} (ELISA, scFv were titrated using a maximum concentration of 100 nM) and K_{off} (QCM) values were determined from single experiments with duplicates. Error bars in b) represent SD, scFvIZI06.1 and scFvIG11 served as controls. Detected EC_{50} and K_{off} values were standardized to the values scFvIZI06.1.

Unfortunately, in the shown experiment binding of scFvIG11 could not be detected. Moreover, soluble scFv antibodies were tested by QCM for their dissociation behavior, using a sensor chip with a moderate receptor density. Clone T12B revealed the slowest release from the receptor, indicated by the most strongly reduced k_{off} value (Fig. 4.4-05b, Table 4.4-02).

Taken together, scFvT12B showed best binding characteristics in two of three experiments. More important, in the QCM off-rate screening, T12B revealed the slowest dissociation kinetics, supposed to be the key attribute for the improvement of receptor blockade. The DNA sequence of scFvT12B was changed at three positions compared with scFvIG11, as demonstrated in the alignment in Figure 4.4-06, i.e. Q1H and T53S in the CDR2 of the heavy chain variable domain (VH) as well as S91G in the CDR3 of the light chain variable domain (VL).

a)

	FR1	CDRH1	FR2	CDRH2
Kabat	123456789102345678920234567893	02345	67894023456789	502a3456789602345
scFvIZI06.1	QVQLVQSGAEVKKPGSSVKVSKASGYTFT	DFYIN	WVRQAPGQGLEWIG	EIYPYSGHAYYNEKFKA
scFvIG11V.TQ.E.K..D....
scFvT12B	HV. SQ .E.K..D....

	FR3	CDRH3	FR4
Kabat	67897023456789802abc345678990234	567891	003456789110
scFvIZI06.1	RVTITADKSTSTAYMELSSLRSEDVAVYYCAR	WDFLDY	WGQGTTVTVSS
scFvIG11
scFvT12B

b)

	FR1	CDRL1	FR2	CDRL2
Kabat	12345678910234567892023	4567abcde8930234	567894023456789	5023456
scFvIZI06.1	DIVMTQSPLSLPVTPGEPASIS	RSSQSLLSNGNTYLH	WYLQKPGQSPQLLIY	TVSNRFS
scFvIG11
scFvT12B

	FR3	CDRL3	FR4
Kabat	78960234567897023456789802345678	990234567	89100345678
scFvIZI06.1	GVPDRFSGSGSGTDFTLKISRVEAEDVGVYYC	SQSTHVPYT	FGGGTKVEIKR
scFvIG11
scFvT12B G

Figure 4.4-06. Sequence Alignment of scFvT12B. a) aligned VH sequences of ATROSAB (scFvIZI06.1), scFvIG11 and scFvT12B. b) Alignment of VL sequences. Residues are numbered according to the Kabat numbering scheme and dots represent identical amino acids compared with scFvIZI06.1. Letters in red/bold indicate newly introduced mutations.

Table 4.4-02. EC₅₀ and k_{off} Values of Candidates of Phage Display Library EP03

Clone	EC ₅₀ (relative)	k _{off} (relative)
IZI06.1	1	1
IG11	n.d.	0.31
T12B	0.017	0.25
B12B	0.021	0.77
T2A	0.023	0.47
T1C	0.009	0.76
B8E	0.046	0.41
T12E	0.047	0.49
T7B	0.062	0.47
T9H	0.041	0.38
B6F	0.251	0.48
T10D	0.006	0.72

4.4.2. Characterization of scFvT12B

The soluble antibody fragments scFvT12B, scFvIZI06.1 and scFvIG11 were produced in the periplasm of *E. coli* TG1 and proper expression was confirmed by SDS-PAGE, where minor contaminations in the purified samples could be observed (Fig. 4.4-07a). Concentration dependent binding to human TNFR1 was demonstrated in ELISA, revealing EC₅₀ values of 3.8 nM, 2.6 nM and 2.0 nM for scFvIZI06.1, scFvIG11 and scFvT12B, respectively (Fig. 4.4-07b, Table 4.4-03). Hence, scFvT12B showed an improved binding under the applied conditions of 1.3-fold compared with scFvIG11. K_D values of 29 nM for scFvIZI06.1, 25 for scFvIG11 and 6.0 in the case of scFvT12B were determined by QCM, representing and 4.1-fold improved binding of scFvT12B compared with scFvIG11 (Fig. 4.4-07c, Table 4.4-03). The change in affinity originated equally from an improved association- (2.1-fold increased k_{on}) and dissociation rate constant (2.0-fold decreased k_{off}, Table 4.4-03).

Finally, scFvT12B blocked TNF induced interleukin-8 release *in vitro* with an obviously improved antagonistic potency compared with scFvIZI06.1 and scFvIG11 (Fig. 4.4-07d). IC₅₀ values could poorly be determined, due to an increasing signal at high concentrations of applied scFv, leading to insufficient convergence of the observed data towards a standard inhibition curve. However, roughly estimated concentrations of half-maximum inhibition

reflected an about seven-fold stronger blockade of human TNFR1 by scFvT12B compared with scFvIG11 (Table 4.4-03).

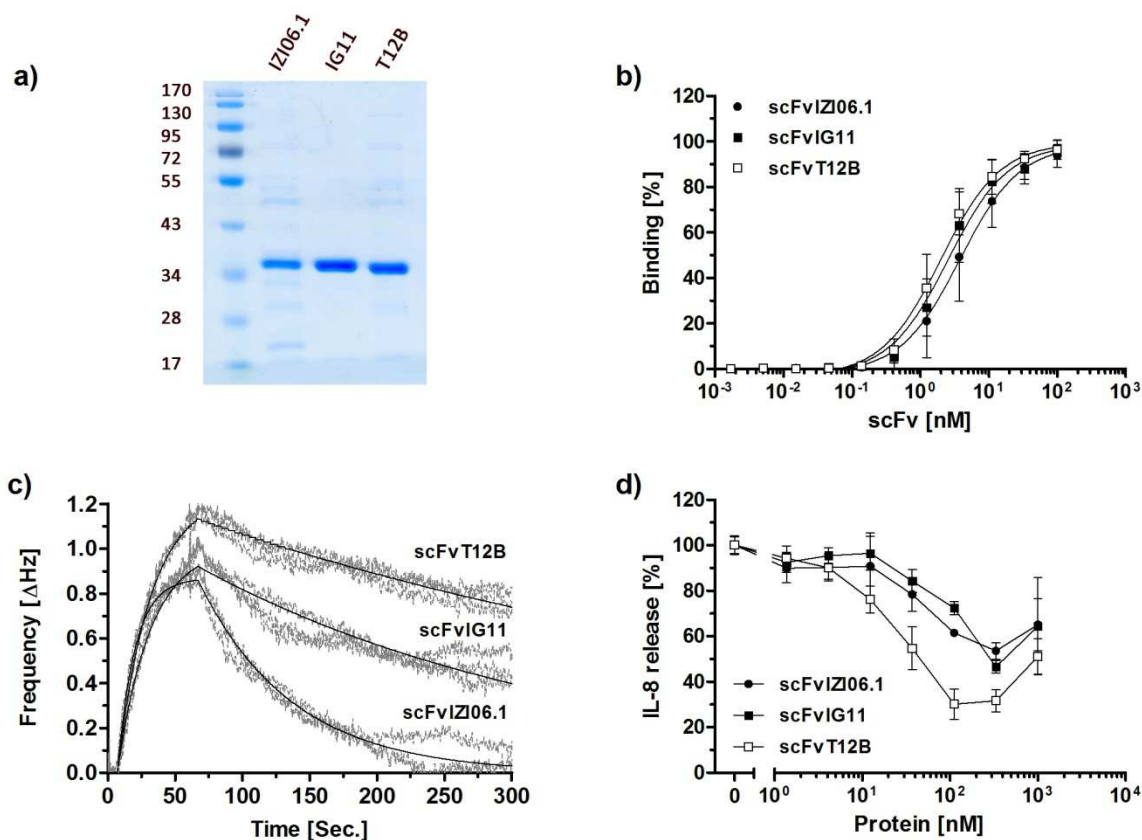


Figure 4.4-07. Expression and Characterization of scFvT12B. a) Coomassie-stained SDS-PAGE (12 %) of scFvT12B and the control antibodies scFvZI06.1 and scFvIG11. Binding to human TNFR-Fc was tested in ELISA (b) and by QCM analysis (c). In c), measurement (dashed grey line) and fit (solid black line) are displayed. d) Inhibition of TNF-induced (0.1 nM) release of IL-8. b) and d) show mean \pm SD of two (d) or three (b) individual experiments performed in duplicates.

Table 4.4-03 Characterization of scFvT12B Compared with scFvZI06.1 and scFvIG11. Improvement is Indicated as Factor Regarding the Values of scFvIG11.

	scFvZI06.1	scFvIG11	scFvT12B	Improved
EC_{50} (nM)	3.8	2.6	2.0	1.3
k_{on} ($M^{-1}s^{-1}$)	5.0×10^5	1.5×10^5	3.0×10^5	2.1
k_{off} (s^{-1})	1.4×10^{-2}	3.6×10^{-3}	1.8×10^{-3}	2.0
K_D (nM)	29	25	6.0	4.1
IC_{50} (nM)*	~200	~300	~45	6.7

*estimated IC_{50} values, originating from evaluation of the obtained IL-8 data upon exclusion of the last 1-2 data points.

4.5. Repeated Humanization of H398

H398, the parental mouse monoclonal antibody of ATROSAB and scFvIZI06.1, proved to be more efficient in blocking TNF-mediated cellular responses compared with ATROSAB (see also Zettlitz et al. 2010a), hence, the process of humanization was recapitulated. The variable domains of heavy and light chain of H398 showed closest similarity to mouse germline genes 1-18*01 for VH and 1-110*01 in the case of VL (Fig. 4.5-01 top line). Human germline genes of sequence similarity to H398 ranging from 46 % to 62 % (VH) and 54 % to 80 % (VL) were included into the analysis. In addition, the selected sequences were compared with the genes 1-69*01 (Fig. 4.5-01a, green) and 2D-28*01 (Fig. 4.5-01b, green), which were used for the initial humanization of H398, resulting in scFvIZI06.1 (ATROSAB).

a)

	FR1	CDRH1	FR2	CDRH2
Kabat	123456789102345678920234567893	02345	67894023456789	502a3456789602345
1-81*1Q.....	SYG.SR.NT.....G
>H398 VH	QVQLQESGAEIARPGASVKLSCKASGYTFT	DFYIN	WVKQRTGQGLEWIG	EIYPGSGHAYYNEKFKA
1-69*1VQ.....VKK..S...V.....G..S	SYA.S	..R.AP.....M	G.I.IF.T.N.AQ..QG
1-8*1VQ.....VKK.....V.....	SYD..	..R.A.....M	WMN.N.NTG.AQ..QG
3-11*1V...GG.VK..G.LR...A...F..S	.Y.MS	.IR.AP.K....VS	Y.SSSGSTI..ADSV.G
3-30.3*1V...GGVVQ..R.LR...A...F..S	SYAMH	..R.AP.K....VA	V.SYDGSNK..ADSV.G

	FR3
Kabat	67897023456789802abc345678990234
1-81*1Y.E.R.....A.
>H398 VH	KATLTADKSSSTAFMQLNSLTSEDSAVYFCVR
1-69*1	RV.I.....T...Y.E.S..R...T...Y.A.
1-8*1	RV.M.RNT.I...Y.E.S..R...T...Y.A.
3-11*1	RF.ISR.NAKNSLYL.M...RA..T...Y.A.
3-30.3*1	RF.ISR.N.KN.LYL.M...RA..T...Y.A.

b)

	FR1	CDRL1	FR2	CDRL2
Kabat	12345678910234567892023	4567abcde8930234	567894023456789	5023456
1-110*1	.V...TP.....V.....L.....	K.....
>H398 VL	DIVMTQDELSPVSLGDQASISC	RSSQSLLSHNSGNTYLH	WYVQKPGQSPKLLIY	TVSNRFS
2D-28*1SP.....TP.EP.....YN..D..L.....Q.....L.....P.Q.....	LG...A.
2D-29*2TP...S.TP.QP.....	K.....D.K...Y..L.....P.Q.....	E.....
2-30*1	.V...SP.....T..QP.....VY.D...N	FQ.R...RR...K...D.	
1-39*2	..Q...SPS...SA.V..RVT.T..	A...I-----SS..N	..Q...KA.....AA.SLQ.	

	FR3
Kabat	78960234567897023456789802345678
1-110*1
>H398 VL	GVPDRFSGSGTDFTLTKISRVEAEDLGVYFC
2D-28*1V...Y.
2D-29*2V...Y.
2-30*1V...Y.
1-39*2	...S.....T..SLQP..FAT.Y.

Figure 4.5-01. BLAST Sequence Alignment of H398. Alignment of heavy (a) and light chain (b) variable domains of H398 to mouse (top line, clones 1-81*1 and 1-110*1) and human germline genes. Displayed are the candidates, selected due to sequence identity or humanness (Z-score, see also Table 4.5-01 and Table 4.5-02). Identical residues are represented by dots. Changed amino acids are shown as letters in red/bold. The sequences, used for the initial humanization of ATROSAB are indicated in green.

To identify alternative human germline genes, humanness (positive z-scores of higher value, Abhinandan and Martin 2007) was prioritized over sequence identity and used clones of rather low homology to scFvH398 for the repeated humanization of VH and VL. Germline gene 3-11*01 was selected for the repeated humanization of VH due to its profound humanness, indicated by the z-score of 1.987 and the higher BLAST score and sequence identity in CDRH1, compared with clone 3-30.3*01 (Table 4.5-01). Furthermore, germline gene 1-39*02 was chosen for the humanization of the light chain variable domain, revealing 54 % sequence identity and a z-score of 1.204 (Table 4.5-02).

Table 4.5-01. Humanization of the VH of H398.

Locus	Clone	Identity	BLAST score	z-score
H398-VH	-	-	-	-2.023
1-69*08 [#]	DP88	60.2%	127	0.317
1-8*01	DP15	62.2%	132	-0.343
3-11*01	DP35	45.9%	109	1.987
3-30.3*01	DP46	45.9%	104	2.196
FRK13.1	DP35	-	-	0.760
FRK13.2	DP35	-	-	0.698

[#]*germline-gene used for the humanized IZI06.1 (ATROSAB)*

Table 4.5-02. Humanization of the VL of H398.

Locus	Clone	Identity	BLAST score	Z-score
H398	-	-	-	-1.829
2D-28*01 [#]	DPK15	79.0%	161	-1.401
2D-29*02	DPK12	80.0%	165	-1.773
2-30*01	DPK18	79.0%	163	-1.971
1-39*02	DPK9	54.0%	109	1.204
FRK13.1	DPK9	-	-	0.188
FRK13.2	DPK9	-	-	0.051

[#]*germline-gene used for the humanized IZI06.1 (ATROSAB)*

4.5.1. *In Silico* Evaluation of Humanized VH and VL Sequences

CDR sequences of the mouse antibody H398 were transferred *in silico* to the framework of germline sequences 3-11*01 (VH) and 1-39*02 (VL), resulting in the sequence of scFvFRK13. Analysis of the canonical structures of the newly generated scFv using auto-

generated SDR templates (Copyright© 1995, Andrew C.R. Martin, UCL) indicated atypical amino acids at position H71 and L2. Hence, these residues were substituted to the residues used for the generation of ATROSAB (VH: R71A, VL: I2V, Fig. 4.5-02). Classification of CDR structures is reviewed in Table 4.5-03. Heavy and light chain of the humanized scFv before (scFvFRK13.1) and after amino acid substitution (scFvFRK13.2) showed reduced humanness compared with the germline genes (VH, Table 4.5-01 and VL, Table 4.5-02). However, z-scores were improved in the range of 0.443 to 2.017 for scFvFRK13.1 and 2 compared with scFvIZI06.1 (ATROSAB).

Table 4.5-03. Canonical Evaluation of Humanized scFv Antibodies

	scFvFRK13.1	scFvFRK13.2
CDR L1	n.d.	Class 4/16A [1rmf]
CDR L2	Class 1/7A [1lmk]	Class 1/7A [1lmk]
CDR L3	Class 1/9A [1tet]	Class 1/9A [1tet]
CDR H1	Class 1/10A [2fbj]	Class 1/10A [2fbj]
CDR H2	n.d.	n.d.

a)

	FR1	CDRH1	FR2	CDRH2
Kabat	123456789102345678920234567893	02345	67894023456789	502a3456789602345
scFvIZI06.1	QVQLVQSGAEVKKPGSSVKVSKASGYTFT	DFYIN	WVRQAPGQGLEWIG	EIYPYSGHAYYNEKFKA
FRK13.1 E..GGLV...G.LRL..A...F..SI.....K....VSG.....
FRK13.2 E..GGLV...G.LRL..A...F..SI.....K....VSG.....
Kabat	67897023456789802abc345678990234	567891	003456789110	
scFvIZI06.1	RVTITADKSTSTAYMELSSLRSEDVAVYYCAR	WDFLDY	WGQTTVTVSS	
FRK13.1	.F..SR.NAKNSL.LQMN...A.....
FRK13.2	.F..SA.NAKNSL.LQMN...A.....

b)

	FR1	CDRL1	FR2	CDRL2
Kabat	12345678910234567892023	4567abcde8930234	567894023456789	5023456
scFvIZI06.1	DIVMTQSPLSLPVTPEPASISC	RSSQSLHLSNGNTYLH	WYLQKPGQSPQLLIY	TVSNRFS
FRK13.1	.IQ.....S..SASV.DRVT.T.Q....KA.K.....
FRK13.2	.VQ.....S..SASV.DRVT.T.Q....KA.K.....
Kabat	78960234567897023456789802345678	990234567	89100345678	
scFvIZI06.1	GVPDRFSGSGSDFTLTKISRVEAEDVGVYYC	SQSTHVPYT	FGGGTKVEIKR	
FRK13.1	...S.....T..SLQP..FAT...
FRK13.2	...S.....T..SLQP..FAT...

Figure 4.5-02. Alignment of H398 with the Humanized Sequences . The humanized sequences of VH (a) and VL (b) were aligned to the sequence of the single chain variable fragment of ATROSAB (IZI906.1) Identical residues are represented by dots. Changed amino acids are shown as letters in red/bold.

4.5.2. Expression and Characterization of scFvFRK13

Besides scFvFRK13.1 and scFvFRK13.2, combinations of their heavy and light chain variable domains and combinations with the heavy and light chain variable domains of scFvT12B were cloned and produced (Fig. 4.5-03a). ScFv fragments were analyzed in SDS-PAGE under reducing conditions, demonstrating integer expression and clean purification only for scFvFRK13.5 and scFvFRK13.7 (Fig. 4.5-03b). Bands of higher and lower molecular weight were observed for all other constructs, indicating contaminations of the purification process or degradation products. In addition, scFvFRK13.5 and scFvFRK13.7 showed major peaks in size exclusion chromatography, corresponding to the calculated molecular weight (Fig. 4.5-03c). Lower signals of shorter retention time were detected for both proteins, possibly representing the existence of dimeric scFv or aggregates of higher order.

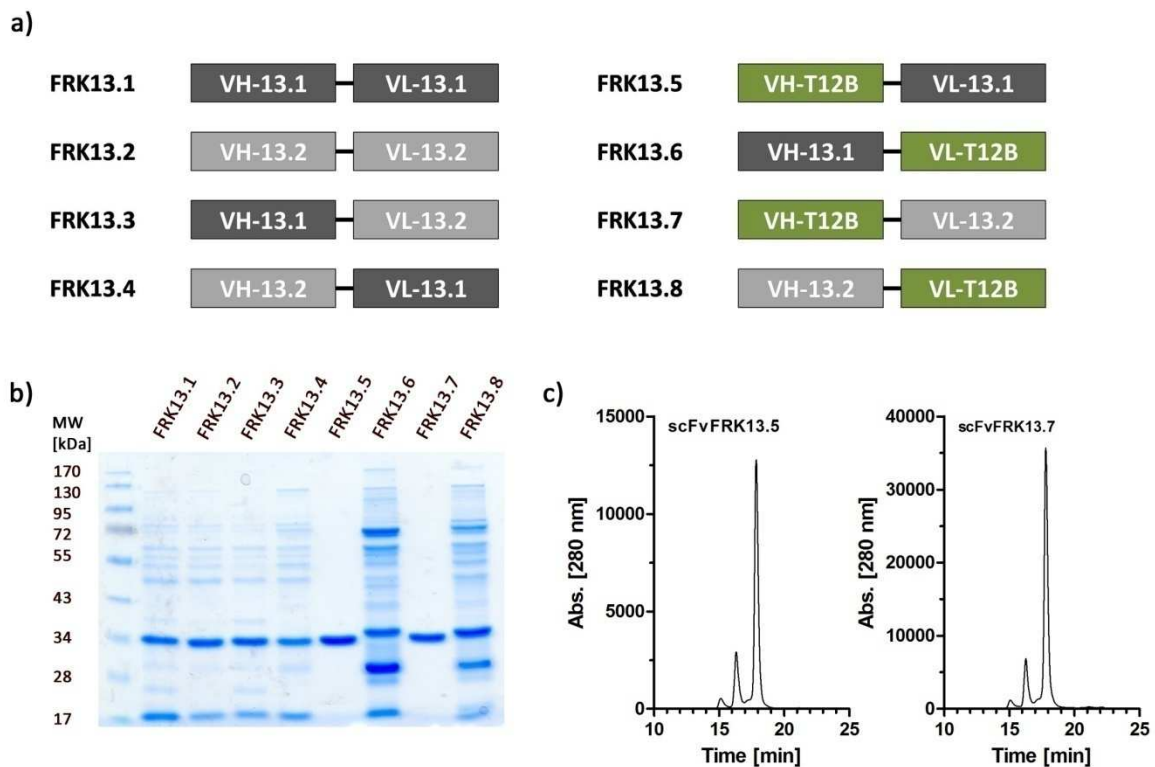


Figure 4.5-03. Production of Humanized scFv Antibodies. a) genotype of humanized scFv variants (bright and dark grey) combined with scFvT12B (green). Purified scFv fragments were analyzed by SDS-PAGE (b, 12 %, coomassie-stained) and subsequently by SEC (c, Yarra SEC-2000 column, flow rate 0.5 ml/min) in the case of proper expression.

Receptor binding of scFvFRK13.1-8 was further analyzed in ELSIA (Fig. 4.5-04a). While scFvFRK13.5 and scFvFRK13.7 bound to human TNFR1 with EC_{50} values of around 1 nM (Table 4.5-04), the remaining set of scFvs showed weak binding only at concentrations above

100 nM. The scFv antibodies T12B and IZI06.1 were included as controls. ScFvT12B bound with a similar EC_{50} value to TNFR1, compared with scFvFRK13.1 and scFvFRK13.2, while scFvIZI06.1 revealed around three-fold weaker binding. Similarly, scFvFRK13.5, scFvFRK13.7 and scFvT12B inhibited TNF-induced IL-8 release from HT1080 cells with comparable IC_{50} values of around 300 nM. The second control protein scFvIZI06.1 showed TNFR1 blockade with an IC_{50} value of 932 nM (Fig. 4.5-04b, Table 4.5-04).

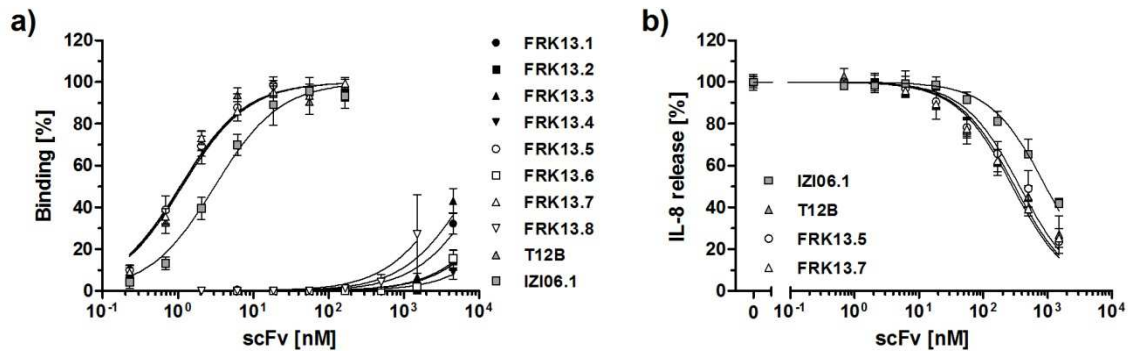


Figure 4.5-04. Binding and Blockade of Human TNFR1. a) Humanized scFv antibodies were tested by ELISA for binding to human TNFR1-Fc and b) for the inhibition of IL-8 release from HT1080 cells induced by 0.1 nM TNF (performed only for strongly binding scFvs). ScFvIZI06.1 and scFvT12B served as controls (displayed are mean \pm SD, $n=3$).

Moreover, thermal stability of the scFvs was investigated by dynamic light scattering. ScFvFRK13.5 and scFvFRK13.7 displayed melting temperatures of 63 °C and 65 °C, compared with 59 °C and 55 °C in the case of scFvIZI06.1 and scFvT12B, respectively (Fig. 4.5-05). Interestingly, scFvIZI06.1 showed increasing mean count rates already at lower temperatures, indicating partial destabilization of the protein structure. In contrast, the

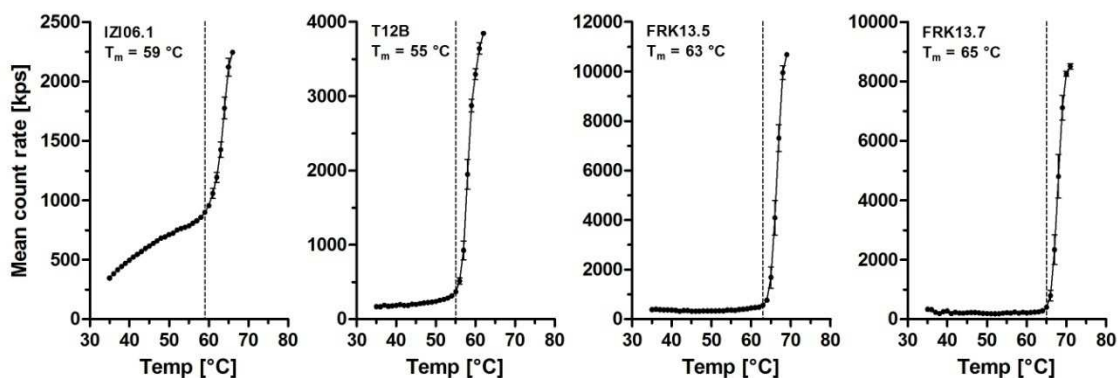


Figure 4.5-05. Thermal Stability of Humanized scFv Fragments. Molecular stability of the scFv antibodies was analyzed by dynamic light scattering. The melting temperature (T_m) was determined by visual interpretation of the displayed data points.

signals of scFvT12B, scFvFKR13.5 and scFvFRK13.7 were nearly constant below the melting point, revealing improved stability also at the lower temperature range.

Table 4.5-04. Characterization of Humanized scFvH398 Antibody Fragments.

	H398	IZI	T12B	FRK13.5	FRK13.7
Z-score VH	-2.023	-0.419	-0.500	0.760	0.698
Z-score VL	-1.829	-1.172	-1.225	0.188	0.051
EC₅₀ (nM)	n.d.	3.07	1.14	1.06	1.09
IC₅₀ (nM)	n.d.	932	309	367	284
T_m (°C)	n.d.	59	55	63	65

4.5.3. Structural Analysis of Homology Modeled scFvFRK13 Variants

Analysis of the humanized sequences was further performed on the basis of *in silico* modeled structures (PIGS, Marcatili et al. 2008), which were refined by energy minimization (YASARA, Krieger et al. 2009). The different model structures revealed a high level of overall structural similarity between scFvH398, scFvT12B and scFvFRK13.1/-2/-7 (Fig. 4.5-06). In addition, the CDRs H1, H3, L1, L2 and L3 of all analyzed scFvs covered comparable surface areas, and the polypeptide backbone revealed similar conformation. However, the loop comprising CDRH2 and the flanking beta sheets showed spatial differences of 1.2 nm or 1.8 nm, between scFvH398 and scFvFRK13.1 or scFvFRK13.2, respectively (Fig. 4.5-06, right panel). The left panel of Figure 4.5-06 demonstrates the impact of this partial change in the antibody structure, leading to an altered arrangement of the whole binding site.

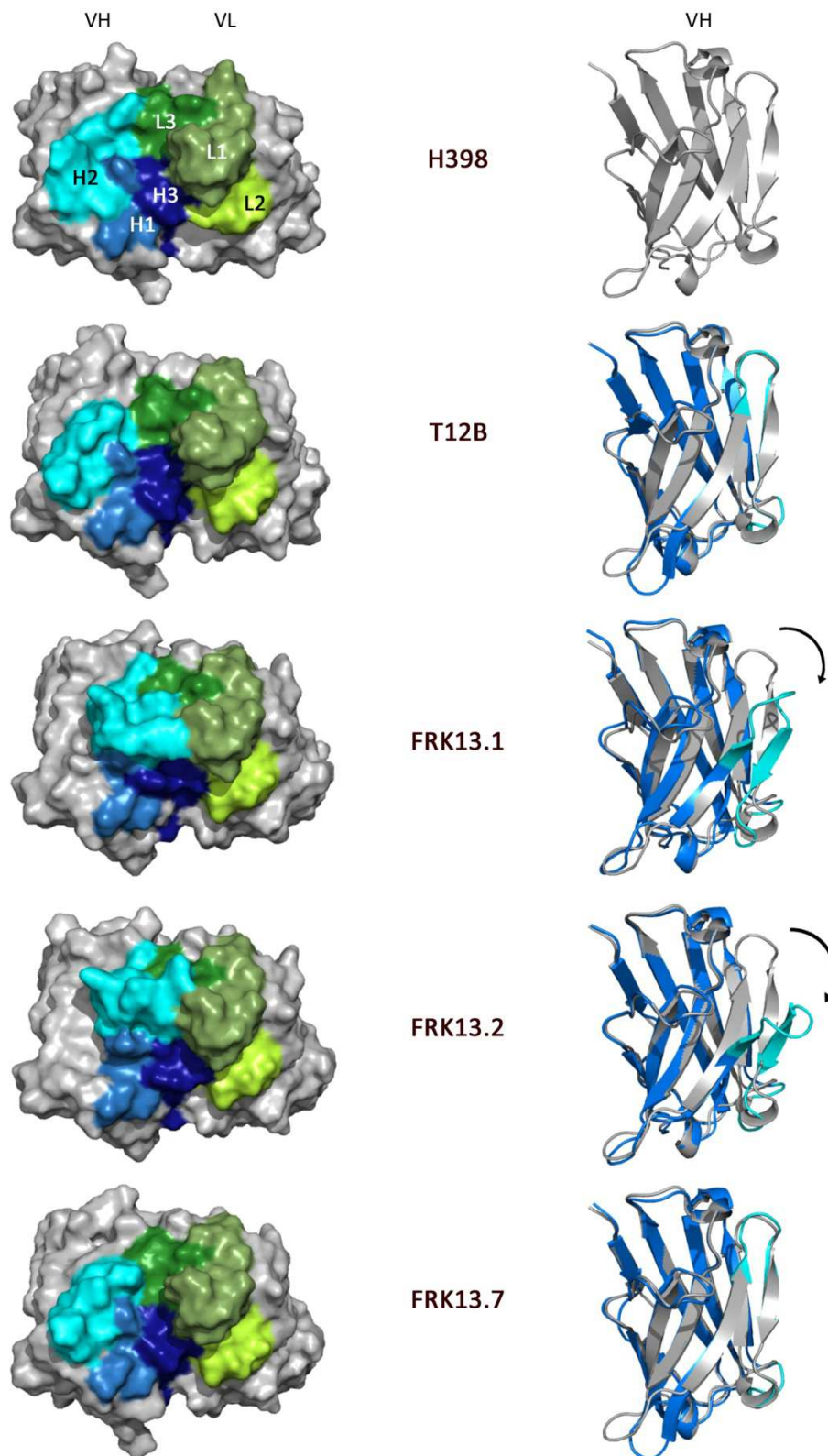


Figure 4.5-06. Homology Modeling of scFv Antibodies. The left panel shows the surface area containing the antigen binding site with color-labeled CDRs as assigned for H398 (CDRH1, bright blue; H2, cyan; H3 dark blue; CDRL1, bright green; L2, lemon; L3, dark green). Cartoons on the right panel show the structural alignment of the backbone of the heavy chain variable domains (VH) of H398 (gray) and the indicated scFv (blue). The beta-sheet and the loop comprising CDRH2 are colored in cyan.

4.6. Conversion of scFvFRK13.7 into the IgG and Fab-Format

Heavy and light chain variable domains of scFvFRK13.7 were introduced into the constant region background of ATROSAB IgG and ATROSAB Fab by standard cloning and PCR techniques. IgG-FRK13.7 and Fab-FRK13.7 are in the following referred to as IgG13.7 and Fab13.7, respectively. Proteins were produced transiently in HEK293T cells and purified by protein A (IgG13.7) or antibody (Fab13.7) affinity chromatography (KappaSelect, GE Healthcare). IgG13.7 was subject to an additional preparative size exclusion chromatography (SEC; FPLC), due to minor peaks at higher molecular weight in the initial SEC profile. Expression and protein integrity was monitored by SDS-PAGE under reducing (Fig. 4.6-01a) and non-reducing conditions (Fig. 4.6-01b), as well as by SEC (Fig. 4.6-01c). ATROSAB and FabATROSAB (FabATR) were used as controls in all experiments. All four proteins showed bands correlating with the calculated molecular weight during electrophoresis. Similarly, the observed absorption peaks in gel filtration confirmed homogenous protein preparations, all

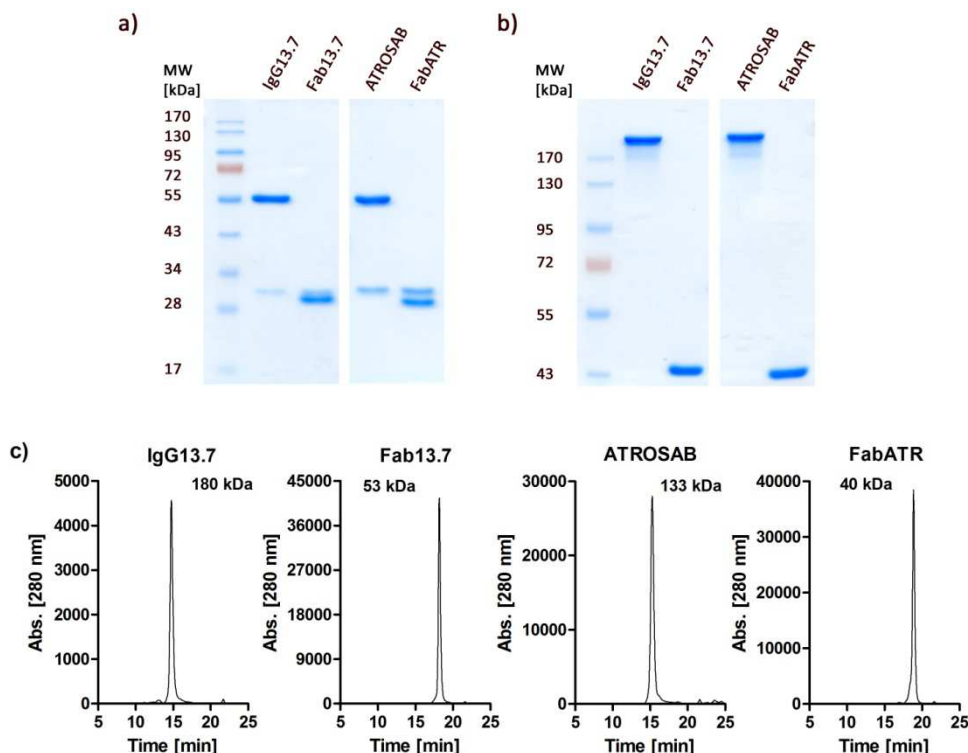


Figure 4.6-01. Expression and Purification of FRK13.7 Derived IgG and Fab. Expression and purification of Fab13.7 and IgG13.7 was evaluated by SDS-PAGE (a, 12% separation gel, reducing conditions; b, 8 % separation gel, non-reducing conditions) and size exclusion chromatography (c, Yarra SEC-2000 column, flow rate 0,5 ml/min). The indicated molecular weight was interpolated according to standard proteins of known mass and retention time.

of apparent molecular weights in agreement with the expected sizes. Fab13.7 and IgG13.7 retained their specificity for human TNFR1 in ELISA, compared with human TNFR2 and both mouse TNF receptors (Fig. 4.6-02).

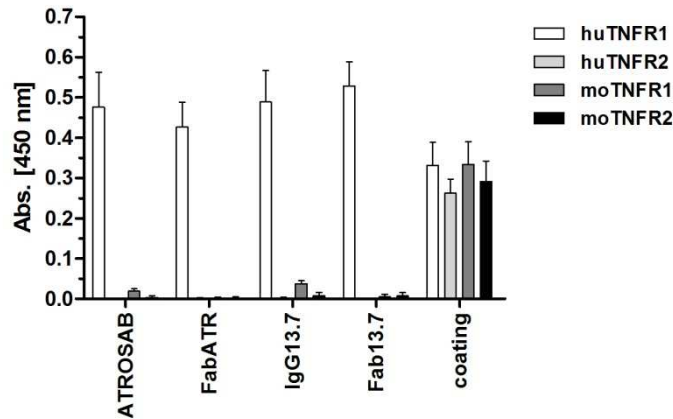


Figure 4.6-02. Species Selectivity of FRK13.7 Antibodies. Binding of 50 nM IgG13.7 and Fab13.7 to TNFR1-Fc and TNFR2-Fc each of both, human and mouse origin, was tested by ELISA and detected using an anti-human IgG (Fab specific) antibody. Coating of receptor fusion proteins was detected by an anti-human IgG (Fc specific) antibody. ATROSAB (50 nM) and FabATROSAB (FabATR, 200 nM) served as controls.

4.6.1. Binding of FRK13.7 Antibodies to Human TNFR1

IgG13.7 and Fab13.7 bound to human TNFR1-Fc in ELISA with EC_{50} values of 1.4 nM for Fab13.7 as well as 0.76 nM in the case of IgG13.7. The control proteins ATROSAB and FabATR showed weaker binding compared with IgG13.7 and Fab13.7 as indicated by 1.4-fold and 8.7-fold higher EC_{50} values, respectively (Fig. 4.6-03).

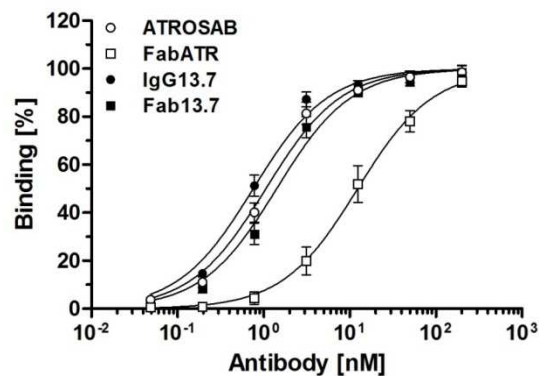


Figure 4.6-03. Equilibrium Binding of FRK13.7 Antibodies to Human TNFR1-Fc. Increasing concentrations of Fab13.7, IgG13.7, FabATR and ATROSAB were tested for their binding to huTNFR1-Fc in ELISA ($n=3$, mean \pm SD).

Moreover, evaluation of the binding dynamics was performed by quartz crystal microbalance, using sensor chips of moderate (86 Hz) or high (184 Hz) receptor density. The control antibody ATROSAB revealed a clear biphasic interaction with human TNFR1-Fc at moderate receptor density, composed of proportions with either high or low affinity, as represented by K_D values of 0.38 nM and 78 nM, respectively (Fig. 4.6-04a, Table 4.6-01). IgG13.7, tested on the chip of moderate receptor density, showed in an "one to two" binding analysis k_{off} values in the range of 1.8×10^{-4} to 9.3×10^{-4} (data not shown), resulting in very low amounts of dissociating protein and thereby hardly detectable differences between high and low affinity binding and dissociating subpopulations. Therefore, IgG13.7 was tested on a high-density chip, on which the high affinity interaction was clearly dominating and the contribution of the low affinity interaction to the binding signal could be largely disregarded, allowing for the evaluation in an "one to one" analysis. The determined K_D value of 0.11 nM reflected a 3.5-fold improvement compared with ATROSAB, considering the high affinity binding situation (Fig. 4.6-04c). The monovalent control protein FabATR dissociated almost completely from the chip of moderate receptor density during the detection period (five minutes), revealing a dissociation rate constant (k_{off}) of $1.5 \times 10^{-2} \text{ s}^{-1}$ and a K_D value of 30 nM (Fig. 4.6-04b). In contrast, the dissociation of Fab13.7 from the antibody-receptor complex was considerably slower, indicated by the k_{off} value of $7.3 \times 10^{-4} \text{ s}^{-1}$, while the association rate constant (k_{on}) was nearly identical compared with FabATR. This resulted in a 19-fold higher affinity of Fab13.7 to human TNFR1, in comparison with FabATR, revealed by a K_D value of 1.6 nM (Fig. 4.6-04d, Table 4.6-01).

Table 4.6-01. Affinity Determination of IgG13.7 and Fab13.7

	ATROSAB	IgG13.7	FabATR	Fab13.7
Bmax1 (Hz)	16.8		6.4	8.9
Bmax2 (Hz)	10.7	55.9		
$k_{on1} (M^{-1}s^{-1})$	2.8×10^5		5.0×10^5	4.7×10^5
$k_{off1} (s^{-1})$	2.2×10^{-2}		1.5×10^{-2}	7.3×10^{-4}
K_D1 (nM)	78		30	1.6
$k_{on2} (M^{-1}s^{-1})$	1.1×10^6	5.4×10^5		
$k_{off2} (s^{-1})$	4.1×10^{-4}	5.9×10^{-5}		
K_D2 (nM)	0.38	0.11		

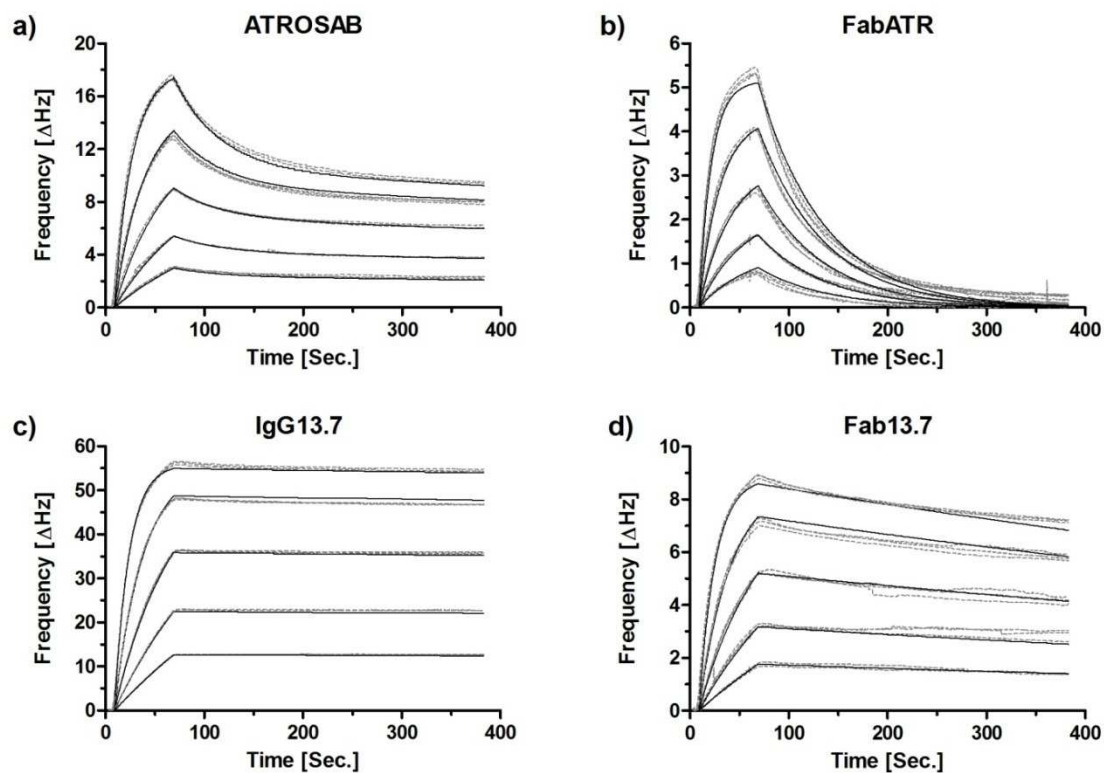


Figure 4.6-04. QCM Analysis of IgG and Fab Derived from scFvFRK13.7. Real-time kinetic data of the interaction of ATROSAB (a), FabATR (b), IgG13.7 (c) and Fab13.7 (d) with human TNFR1-Fc were collected using the quartz crystal microbalance. Analyzed were triplicates of concentrations between 64 nM and 4 nM (ATROSAB and IgG13.7) or 128 nM to 8 nM (FabATR and Fab13.7). Measurements (grey, dotted line) and fit (black, solid) are shown.

4.6.2. *In vitro* Bioactivity of scFvFRK13.7 Derived Proteins

To investigate the influence of affinity maturation and re-humanization on the *per se* antagonistic antibody ATROSAB, the potential of scFvFRK13.7-derived IgG and Fab was tested for the induction of interleukin-8 and -6 release from HT1080 and HeLa cells, respectively. ATROSAB, which was included as control, showed the described marginal receptor activation only in the case of IL-8 (Richter et al. 2013). In the performed IL-6 release experiments stimulation above the cellular background could not be observed (Fig. 4.6-05b and c). The monovalent control protein FabATR did neither stimulate IL-8 nor IL-6 release from the respective cell type. Consistently, interleukin release induced by Fab13.7 was not increased, compared with untreated cells. However, IgG13.7 clearly stimulated the release of IL-8 and IL-6, resulting in interleukin levels of 20 % to 87 %, compared with the effect of 33 nM TNF (not shown), which was around the maximum response stimulated by TNF in previous experiments (Fig. 4.6-05a and c).

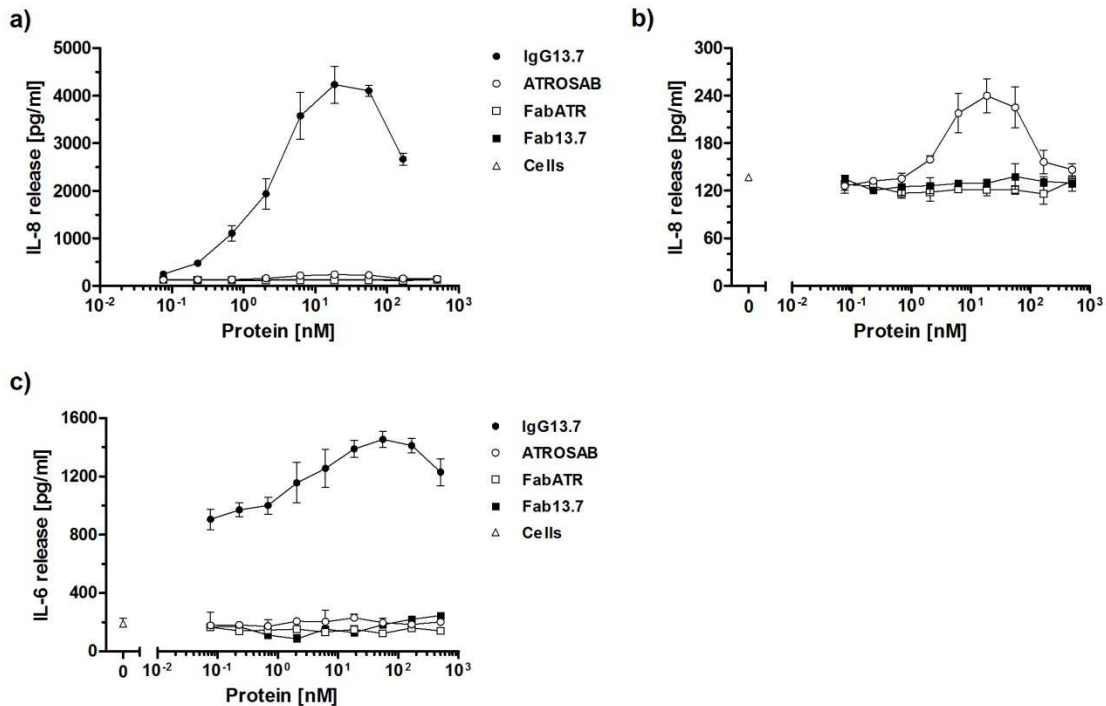


Figure 4.6-05. Bioactivity of FRK13.7 Antibodies. IL-8 release from HT1080 cells triggered by FRK13.7 antibody formats is displayed in a and b (b was increased in size to show low and non-agonistic constructs) together with IL-6 release from HeLa cells (c). TNF (not shown), ATROSAB and FabATR served as controls. Presented are mean \pm SD of two individual experiments with duplicates.

Interestingly, IL-8 release from HT1080 cells triggered by 0.1 nM TNF was inhibited by ATROSAB and FabATR with comparable IC₅₀ values of 118 nM and 151 nM, respectively (Fig. 4.6-06a). Similarly, ATROSAB and FabATR revealed equally strong inhibition of IL-6

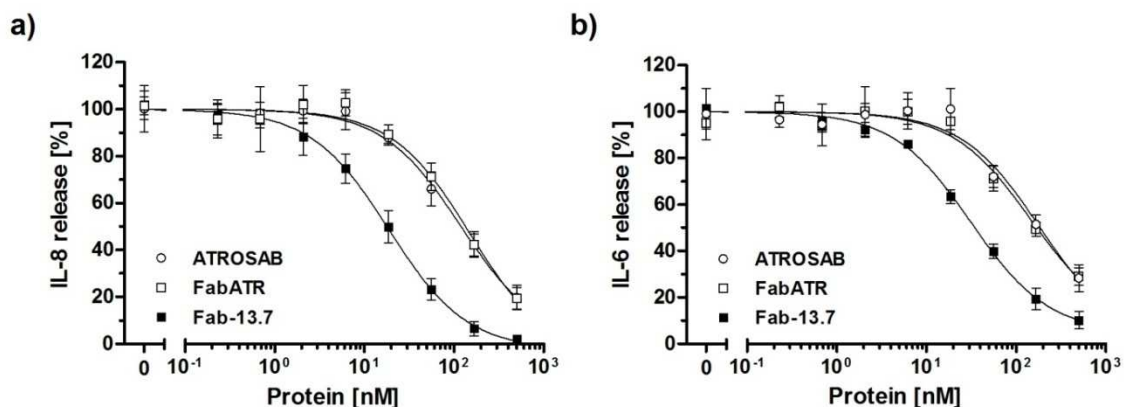


Figure 4.6-06. Inhibition of TNF-Induced Cytokine Release by Fab13.7. Presented is the inhibition of IL-8 (a) and IL-6 release (b), induced by 0.1 nM TNF. ATROSAB and FabATR served as controls. Shown are mean \pm SD of three individual experiments.

release from HeLa cells, caused by 0.1 nM TNF (Fig. 4.6-06b, Table 4.6-02). Due to its agonistic activity, a concentration of half-maximum inhibition (IC_{50}) of IgG13.7 was not determined. In contrast, Fab13.7 inhibited IL-8 and IL-6 release in response to 0.1 nM TNF in a dose-dependent manner with IC_{50} values of 19 nM and 31 nM, respectively, revealing a 5.8-fold to 6.2-fold improved TNF neutralization, compared with the IgG ATROSAB.

Table 4.6-02. Bioactivity of ATROSAB and FRK13.7 Antibodies

	TNF (33 nM)	ATROSAB	FabATR	IgG13.7	Fab13.7	Cells
IL-8 release (pg/ml)	20850	240	128	4231	138	137
$IC_{50, IL-8}$ (nM)	-	118	151	-	19	-
IL-6 release (pg/ml)	1667	231	179	1454	101	191
$IC_{50, IL-6}$ (nM)	-	179	145	-	31	-
Cytotoxicity (%)	92	-	-	up to 100	-	-
$IC_{50, Cytotox}$ (nM)	-	24	37	-	4.7	-

Furthermore, the potential of the IgG molecule and the Fab fragment originating from scFvFRK13.7 to promote or inhibit TNFR1 mediated cell death in Kym-1 cells was investigated. Consistent with the control proteins ATROSAB and FabATR, stimulation by Fab13.7 did not lead to any detectable cytotoxicity (Fig. 4.6-07a). On the other hand, IgG13.7 eradicated nearly 100 % of Kym-1 cells at a broad range of concentrations, equivalent to the positive control TNF, which was used at 33 nM. To investigate the inhibitory capacity of the

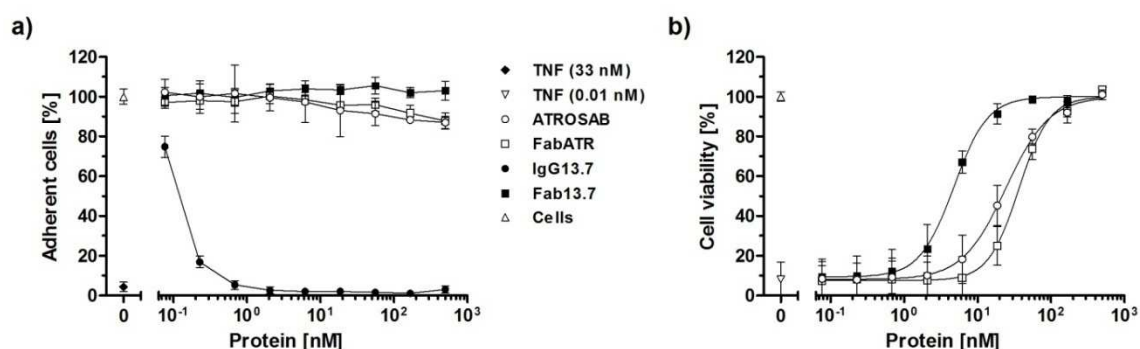


Figure 4.6-07. Induction and Inhibition of Kym-1 Cytotoxicity. The potential of IgG13.7 and Fab13.7 to trigger cell death in Kym-1 cells was analyzed by KV staining of the remaining adherent cells (a). In the same assay the inhibitory potential of Fab13.7 to inhibit cytotoxicity induced by 0.01 nM TNF was analyzed (b). ATROSAB and FabATR served as controls. Presented are mean \pm SD of two to three individual experiments with duplicates (a, stimulation of cytotoxicity, $n=2$; b, inhibition, $n=3$).

non-agonistic Fab13.7, Kym-1 cells were incubated with 0.01 nM TNF, killing around 90 % of the cells in single treatment. Fab13.7 and the control proteins ATROSAB and FabATR inhibited TNF-mediated cell death with IC_{50} values of 4.7 nM, 24 nM and 37 nM, respectively (Fig. 4.6-07b, Table 4.6-02).

Protein drugs, in general, hold the potential to induce anti-drug immune responses. Thereby produced antibodies could lead to the formation of molecular clusters of higher order by crosslinking of the protein therapeutic. In order to evaluate the potential risk of crosslinked Fab13.7 to activate TNFR1, the bioactivity of the Fab fragment on HT1080 cells in the presence of a polyclonal anti-human Fab serum was tested. In standard binding ELISA, strong binding of the Fab-specific goat serum to Fab13.7 was shown (EC_{50} 6.3 nM, Fig. 4.6-08a). However, up to 500 nM Fab13.7 together with the serum did not stimulate IL-8 release above the cellular background (Fig. 4.6-08b). Whereas, ATROSAB showed clearly increased induction of IL-8 from HT1080 cells in response to co-treatment with the serum antibodies (Fig. 4.6-08b).

Taken together, these data revealed on the one hand a higher antagonistic potency of Fab13.7 compared with both, ATROSAB and FabATR, and on the other hand, a lack in any TNFR1 agonism, even in the presence of crosslinking antibodies.

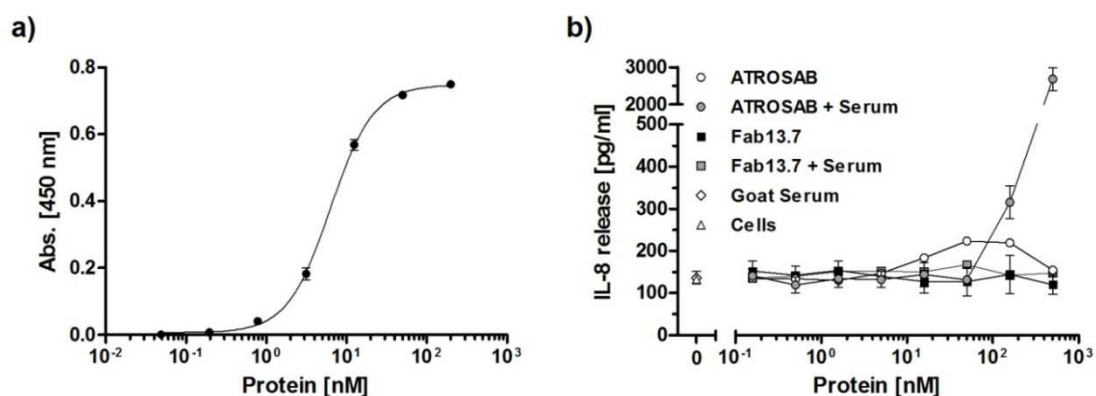


Figure 4.6-08. Crosslinking of ATROSAB and Fab13.7. a) concentration-dependent binding of a Fab-specific polyclonal goat serum to Fab3.7 was demonstrated by ELISA. In an IL-8 release assay the effect of Fab13.7 on HT1080 in the presence of 64 µg/ml cross-linking goat anti-human Fab was analyzed and compared with ATROSAB (n=2, mean ± SD).

4.7. Half-life Extension of Fab13.7

The relatively small molecular weight of the Fab fragment of around 50 kDa is, in general, accompanied by rapid clearance from the circulation. Considering a potential therapeutic application, the molecular structure of Fab13.7 was further modified, in order to improve its serum half-life. Therefore, an extended Fab fragment was created, designated Fab13.7L (Fab13.7"long"), containing additional copies of both, CH1 and CL_K, to circumvent renal filtration due to the increased hydrodynamic radius. Identical to the regular Fab fragment, the heterodimer of Fab13.7L was stabilized by a single disulfide bond between cysteines, located at the C-terminal end of the sequences of CH1_B and CL_K_B (Fig. 4.7-01a). In addition, Fab13.7CH3 was generated by the fusion of the third constant domain of the IgG1 heavy chain (CH3) to CH1 and CL_K of Fab13.7 (Fig. 4.7-01a). Besides the sheer increase of the molecular weight, the appended CH3 domains in Fab13.7CH3 harbor essential parts of the IgG binding site for the neonatal Fc receptor (FcRn, Schields et al. 2001), possibly providing the benefit of half-life extension by FcRn-mediated recycling.

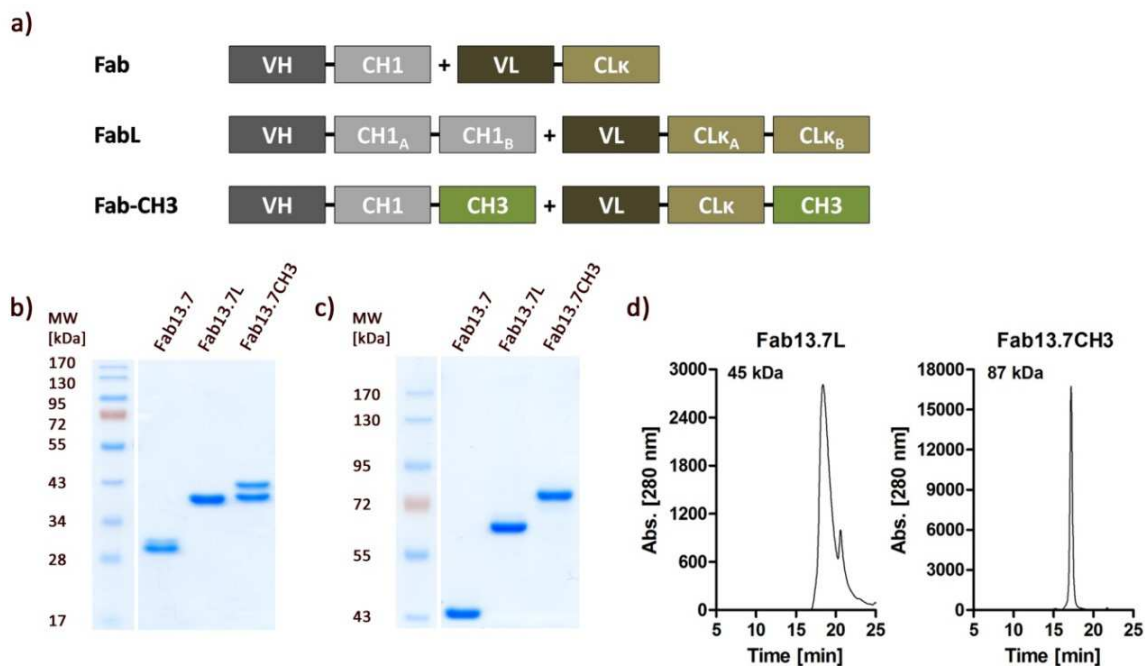


Figure 4.7-01. Production of Fab13.7L and Fab13.7CH3. a) Composition of the genetic arrangement of Fab13.7L and Fab13.7CH3. b) SDS-PAGE under reducing and c) under non-reducing conditions (12 % reducing, 8 % non-reducing). d) Size exclusion chromatography (SEC, Yarra SEC-2000 column, flow rate 0,5 ml/min).

Both proteins were expressed tag-free in HEK239T cells after transient transfection. Purification was performed in a two-step process of antibody affinity chromatography (KappaSelect, GE Healthcare), followed by a preparative size exclusion chromatography

(FPLC-SEC), in order to eliminate aggregated or multimeric assembled protein fractions. Proper expression and purity was confirmed by SDS-PAGE under reducing (Fig. 4.7-01b) and non-reducing (Fig. 4.7-01c) conditions, as well as by HPLC-SEC (Fig. 4.7-01d). The bands observed in the SDS-PAGE correlated with the calculated molecular masses of subunits and fully assembled proteins, which was also the case for the peak of Fab13.7CH3 in the SEC analysis. In contrast, the peak of Fab13.7L revealed a considerably low value compared with the calculated molecular weight, according to the molecular weights of the applied standard proteins. This indicated a low hydrodynamic radius, in relation to the molecular mass. Furthermore, the peak appeared less discrete, compared with Fab13.7CH3. The minor peak at higher retention time possibly indicated monomeric heavy or light chains or a degradation product.

Fab13.7L and Fab13.7CH3 interacted equally strong with human TNFR1 in standard ELISA, compared with Fab13.7 (Fig. 4.7-02a, Table 4.7-01). Moreover, Fab13.7 and Fab13.7L similarly inhibited the IL-8 release from HT1080 cells in response to 0.1 nM TNF, revealed by IC_{50} values of 26 nM and 24 nM, respectively. Fab13.7CH3 inhibited TNF-mediated IL-8 release with a 1.7-fold higher IC_{50} value of 45 nM, compared with Fab13.7 (Fig. 4.7-02b). These results indicated an unaffected or only slightly reduced bioactivity of Fab13.7L and Fab13.7CH3 upon addition of additional immunoglobulin domains.

Transgenic C57BL/6J mice, expressing the extracellular domain of human TNFR1 instead of the respective mouse protein, were injected with 12 μ g to 25 μ g of FabATR, Fab13.7, Fab13.7L and Fab13.7CH3, to determine their pharmacokinetic profile (Fig. 4.7-03).

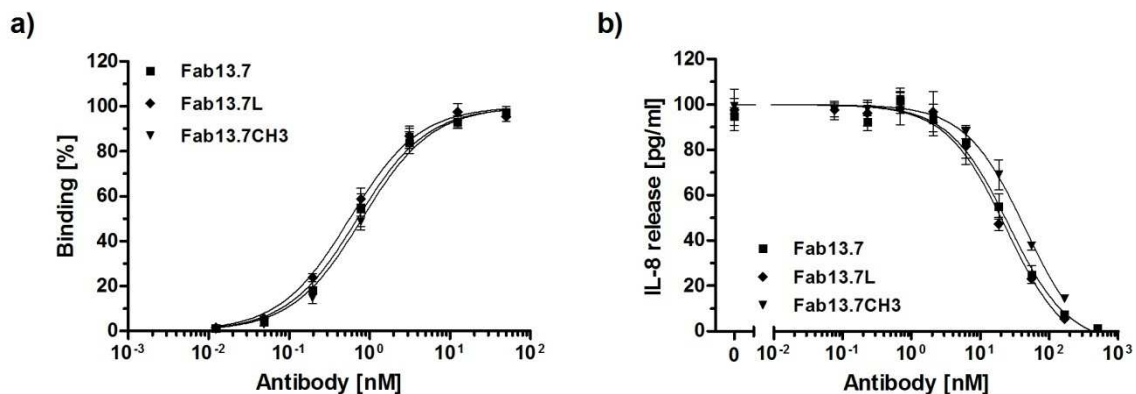


Figure 4.7-02. Binding and Bioactivity of Fab Variants. a) interaction of Fab13.7L and Fab13.7CH3 with huTNFR1 in binding ELISA. b) Inhibition of IL-8 release from HT1080 cells induced by 0.1 nM TNF. Fab13.7 served as control in all experiments (n=2 with duplicates, mean \pm SD).

Fab13.7 revealed an almost identical pharmacokinetic behavior compared with FabATR (used as control), indicated by comparable values of initial and terminal half-life as well as of the area under the curve (Table 4.7-01). In addition, the increased molecular weight of Fab13.7L did not further sequester the antibody in the circulation, which is reflected by similar values for initial and terminal half-lives, compared with Fab13.7 and FabATR. Whereas, the fusion of two CH3 domains to the C-terminus of CH1 and CL κ , resulting in a comparable molecular weight as calculated for FabL, led to 3.6-fold and 2.5-fold increases in initial and terminal half-life, respectively, compared with Fab13.7 (Table 4.7-01).

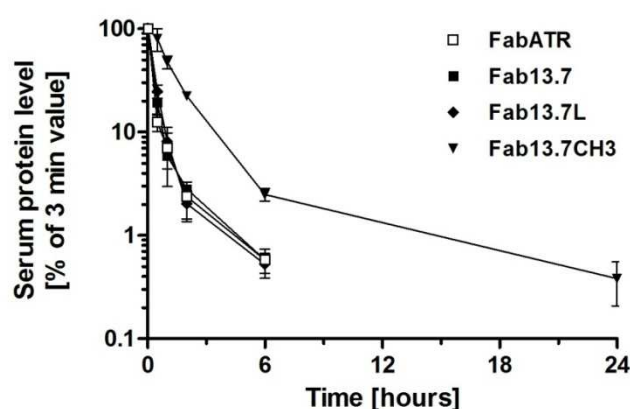


Figure 4.7-03. Pharmacokinetic Analysis of Fab13.7L and Fab13.7CH3. Transgenic C57BL/6J mice, bearing the extracellular domain of human TNFR1, were injected (i. v.) with 12 μ g (Fab13.7L), 15 μ g (Fab13.7CH3) or 25 μ g (Fab13.7/FabATR) protein. Remaining functional antibody molecules were detected by standard binding ELISA (Mean \pm SD of 3 mice per molecule). For better comparison, data were normalized to the 3 min value. Experiments were performed and analyzed by Dr. Oliver Seifert.

In Summary, fusion of either another CH1 and CL κ (Fab3.7L) or two CH3 domains (Fab13.7CH3) to Fab13.7 did not influence the bioactivity of the antibody fragment. However, only Fab13.7CH3 showed an improved pharmacokinetic behavior.

Table 4.7-01. Bioactivity and Pharmacokinetic of Fab13.7 Variants

	FabATR	Fab13.7	Fab13.7L	Fab13.7CH3
EC₅₀ [nM]		0.70	0.57	0.81
IC₅₀ [nM]		25.7	23.6	45.0
T_{1/2, initial} [h]	0.24 \pm 0.02	0.25 \pm 0.06	0.27 \pm 0.02	0.91 \pm 0.18
T_{1/2, terminal} [h]	1.56 \pm 0.07	1.70 \pm 0.15	1.44 \pm 0.20	4.29 \pm 0.59
AUC_{0-6h} [%*h]	45.24 \pm 2.68	41.99 \pm 5.53	47.98 \pm 0.92	158.4 \pm 16.4

AUC values are displayed as % of the 3 min value.

5. Discussion

This thesis presents further data on the *in vitro* characterization of the humanized TNFR1-specific IgG1 antibody ATROSAB (Kontermann et al. 2008, Zettlitz et al. 2010a, Richter et al. 2013), which contribute to better understanding of the mechanism of action of TNFR1-activation and result in the development of a promising candidate for therapeutic application by affinity maturation and the exchange of the light chain framework sequences. This novel approach of selective intervention at the site of TNF receptor 1 (TNFR1) holds great therapeutic potential for the treatment of inflammatory and autoimmune diseases. In contrast to the established anti-tumor necrosis factor (TNF) therapy, selective blockade of TNFR1 activation inhibits pro-inflammatory and cytotoxic responses, while circumventing the immunological drawbacks of TNFR2 blockade (for review see van Hauwermeiren 2011).

5.1. Reduced Induction of ADCC/CDC and Target Mediated Clearance

ATROSAB was provided with a mutated IgG1 Fc part. The amino acids on positions 233-236 or 327, 330 and 331 were exchanged by the residues of IgG2 or IgG4, respectively (Armour et al. 1999, Shields et al. 2001, Zettlitz et al. 2010a). The described effect of the introduced mutations was confirmed by demonstrating the lack of binding to FcγRIA and C1q, the dramatically reduced binding to FcγRIIB and FcγRIIIA and the significantly diminished killing of target cells. Similar results of reduced binding to Fcγ receptors and C1q protein were earlier reported, using an antibody Fc part on the basis of IgG2 with four residues, mutated into the IgG4 amino acids (H268Q, V309L, A330S and P331S; An et al. 2009). The resulting lack of cytolytic activity is fundamental for TNFR1-targeting therapeutics, as TNFR1 is ubiquitously expressed, also by resident cells of inflamed tissue, and their antibody-mediated removal would cause further damage. In addition, abrogating the interaction with FcγRIA on the surface of e.g. monocytes and macrophages, prevents crosslinking-induced expression of pro-inflammatory cytokines like IL-8 (interleukin-8) and MCP-1 (monocyte chemoattractant protein-1; Wojtal et al. 2012, Hristodorov et al. 2014). Moreover, blockade of FcγRIIB binding prevents antibody hyper-crosslinking on the cellular surface, as described for anti-CD40 antibodies (White et al. 2013) to result in increased agonism towards the TNFRSF (TNFR superfamily) member CD40 (for review see Willcocks et

al. 2009). Similarly, binding to FcγRIIB was reported for a DR5-specific agonistic antibody to be necessary for the exhibition of pro-apoptotic activity (Li and Ravetch 2012). In contrast, a fully functional Fc part could be of importance in the case of antibodies, directly targeting tumor necrosis factor, in order to redirect the complement system (via C1q) and immune effector cells (e.g. via FcγRIIIA) to membrane bound TNF, mainly expressed by cells of the immune system. Consequently, the elimination of mTNF expressing cells was shown to contribute to the anti-inflammatory power of these drugs (Lügering et al. 2001, ten Hove et al. 2002, Di Sabatino et al. 2004). However, the here cited reports suggested an ADCC-/CDC-independent mechanism of action.

In addition, the ability of the antibody Fc part to bind to the neonatal Fc receptor (FcRn) has great influence on *in vivo* pharmacokinetics (Kim et al. 2006). In wild type C57BL/6J mice, ATROSAB showed a terminal half-life of 9.43 ± 2.1 days, which is in good accordance with earlier published data of ATROSAB and wild type IgG in CD1 mice (Zettlitz et al. 2010a, Unverdorben et al. 2012). Thus, the reduced terminal half-life of 2.04 ± 0.32 days in mice expressing the extracellular domain of human TNFR1 strongly suggests that ATROSAB underlies a mechanism of target-specific clearance. This broadly described phenomenon concerning antibody pharmacokinetics (e.g. Mager et al. 2001, Hansen et al. 2014) is dependent on the applied dose and only observable for amounts of injected protein below a threshold of target saturation (Kamath et al. 2014). Hence, high doses of protein therapeutic above this threshold (250 mg/m^2 in the case of cetuximab, described in a clinical phase I study; Fracasso et al. 2007) need to be administered in order to eliminate this target-mediated clearing effect. Alternatively, engineering of the antibody paratope to bind to the antigen in a pH-dependent manner was reported to result in enhanced circulation time and increased duration of the biological effect (Chaparro-Riggers et al. 2012). This strategy of strong binding at a physiological pH-value of 7.4 and reduced affinity at lower pH-values (5.5 - 6.0) benefits from the acidification of the endosome following phagocytosis and results in dissociation of the antibody from the target antigen after receptor internalization, enabling FcRn-mediated drug recycling.

In general, pharmacokinetic data originating from animal models are the basis of predictions concerning clinical dosage of drugs under development. However, interspecies scaling still is a demanding challenge (Lin 1998, Mahmood 2007, Tam et al. 2013). Thus,

monitoring of individual pharmacokinetics and adjustment of dosing is required during clinical practice to provide optimal drug efficacy (Vande Casteele and Gils 2015).

5.2. High and Low Affinity Interaction of ATROSAB to TNFR1 Inhibits Binding of TNF

Key feature of an antibody is the specific binding to defined target structures. The nature of these interactions is described in terms of binding kinetics and affinity, varying in general over several orders of magnitude, even among antibodies directed against the same antigen (van Regenmortel 2000, Zhou et al. 2012). Selectivity of ATROSAB for TNFR1, when compared with TNFR2, was previously described (Zettlitz et al. 2010a). In this study, analyses of the interaction between ATROSAB and huTNFR1 by quartz crystal microbalance (QCM) and flow cytometry were performed and revealed biphasic characteristics, indicating the existence of mono- and bivalent binding events. This is supported by extensive literature data (e.g. Nygren et al. 1985, Kaufman and Jain 1992, MacKenzie et al. 1996), allocating the lower affinity to the monovalent interaction, while the bivalent binding is associated with higher affinity. High and low affinity data of ATROSAB showed K_D values correlating well between the experimental systems of QCM and flow cytometry. Compared with earlier published data, minor differences were observed for the QCM-derived low affinity K_D value of 73.0 nM (Richter et al. 2013; 14.2 nM), resulting most likely from different measurement and analysis settings. The determined values of high and low affinity binding events of 0.2 nM and 73 nM, respectively, indicate an overall moderate intensity for ATROSAB binding to TNFR1, when compared with cetuximab, targeting EGFR with an intrinsic monovalent affinity of 0.013 nM and a bivalent avidity of 0.006 nM (Zhou et al. 2012).

Similar to the high affinity binding of ATROSAB, TNF bound to TNFR1 with a K_D value of 0.1 nM, comparable with diverging literature data, covering the entire picomolar range (Kull et al. 1995, Grell et al. 1998, Kontermann et al. 2008, Boschert et al. 2010). In addition, half-maximal ATROSAB concentrations, inhibiting the binding of TNF to TNFR1 (0.11 nM to 9.6 nM), were similar to earlier reported data on its precursor molecules H398 (0.06 nM; Thoma et al. 1990) and IZI06.1-Fab (2.7 nM; Kontermann et al. 2008). The observed multiphasic dose-inhibition curves possibly indicate different potencies of mono- or bivalently binding ATROSAB in the competition with TNF for binding to TNFR1. Alternatively, the multi-step binding-inhibition curves could also indicate different susceptibilities of TNF-TNFR1 complexes of different stoichiometry to ATROSAB-mediated liberation of TNF. The

latter is supported by the 25- to 100-fold higher association rate constant of TNF to TNFR1 (Grell et al. 1998), in comparison with ATROSAB, suggesting that TNF-TNFR1 complexes may be formed rather quickly during the experiment and that TNF would have to be liberated from assembled complexes by ATROSAB subsequently.

5.3. Intra- and Extracellular Effects of TNFR1 Inhibition

In order to investigate the inhibition of TNF-mediated cellular responses, the cell lines HeLa and HT1080 were stimulated with TNF and lymphotoxin α (LT α), resulting in the release of IL-6 and IL-8, respectively. The blockade of this cytokine release by ATROSAB was analyzed in ELISA experiments. LT α -induced interleukin release was inhibited by ATROSAB more efficiently than interleukin release induced by TNF. This reflects the weaker binding affinity of LT α to TNFR1, compared with TNF, resulting from an 8-fold higher dissociation rate constant (Grell et al. 1998). Interestingly, TNF-induced IL-6 and IL-8 release was not reduced at concentrations, where ^{125}I -TNF binding was already clearly inhibited (0.01 - 1 nM), indicating the existence of a large proportion of TNF-TNFR1 complexes, that do not contribute to signaling. Thus, activation of a rather low number of TNFR1 molecules may already induce a sustained cellular response. Figure 5.2-01 presents a simplified binding and activation sequence of TNF and TNFR1, which is in agreement with recent literature on the initial steps of TNF-TNFR1 complex formation (Winkel et al. 2012) and shows the different possible ligand receptor stoichiometries. The formation of highly ordered ligand receptor clusters, as depicted in Figure 5.2-01, was suggested for several TNF/TNFR superfamily members to be responsible for the induction of intracellular signaling (Krippner-Heidenreich et al. 2002, Siegel et al. 2004, Henkler et al. 2005). Hence, ATROSAB might rather inhibit monovalent binding of TNF to TNFR1, in comparison with multivalent binding, which is involved in the formation of multimeric, and thus signaling competent complexes. This is supported by the observation that mono- and multimeric interactions between TNF and TNFR1 reveal different affinities (Chan et al. 2000, Scheurich, unpublished). Alternatively, the inhomogeneous distribution and motility of TNFR1 with respect to its location to membrane microdomains might also influence the susceptibility to inhibition by ATROSAB (Legler et al. 2003, Ranzinger et al. 2009, Gerken et al. 2010).

In addition, the efficient inhibition of TNFR1-signaling by ATROSAB at the level of I κ B α -phosphorylation was demonstrated, in order to confirm the intracellular connection

between the inhibition of receptor binding on the one hand and the cellular response of interleukin release on the other hand. This observation is in great accordance with earlier publications, reporting I κ -B α phosphorylation in response to TNFR1-activation to eventually result in the translocation of the transcription factor NF- κ B to the nucleus and hence to induce the expression of pro-inflammatory cytokines (for review see Baeuerle and Henkel 1994 or Roebuck 1999).

Finally, supporting the therapeutic relevance of the used assay systems, IL-6 and IL-8 levels were found to be elevated in the serum and the synovial fluid of patients under rheumatic conditions (Takahashi et al. 1999, Vierboom et al. 2007, Baillet et al. 2014). Moreover, the applied ATROSAB concentrations correlated well with observed infliximab serum-levels in patients (0.3 - 10 nM, Elberdin et al. 2015), whereas TNF levels reported from the clinic were at least 25-fold lower, compared with the experimental situation (0.4 - 4 pM, Schiattino et al. 2005).

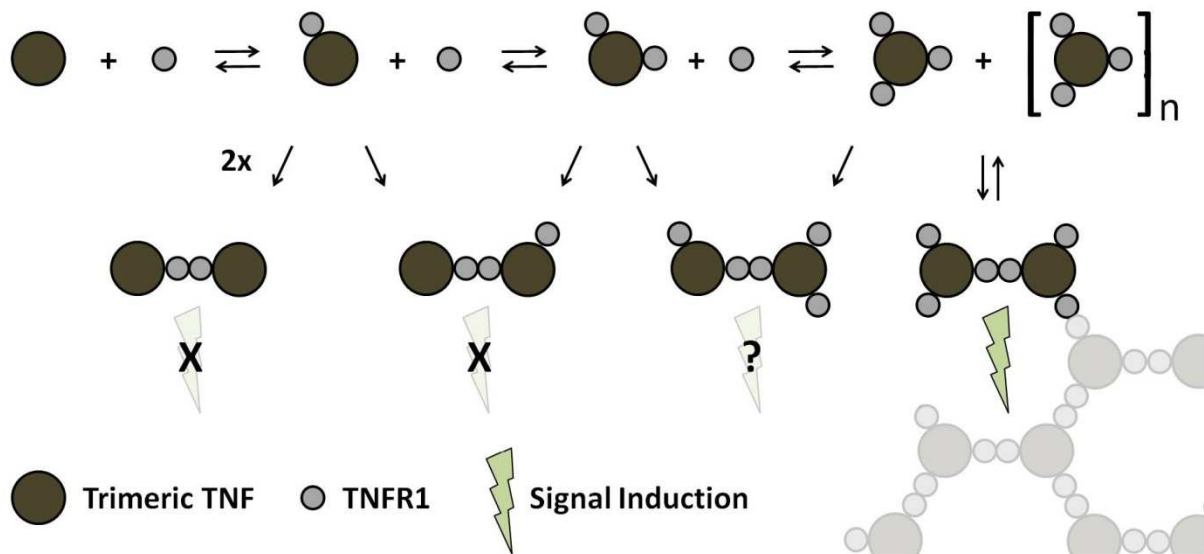


Figure 5.2-01. Binding Sequence of TNF to TNFR1 and Signal Induction. Binding of trimeric TNF to three TNFR1 molecules on the cell surface leads to the formation of hexameric complexes and their assembly into higher order clusters (lower right). Intracellular signal transduction requires at least two dimerized and TNF-bound TNFR1 molecules. However, two trimeric TNF-molecules each bound exclusively to one receptor of a TNFR1-dimer seem to be insufficient for receptor activation (lower left). Thus, it remains to be determined how many additional TNFR1 molecules are required for the stabilization of the TNF-TNFR complex in order to induce signal transduction.

5.4. Agonism and Antagonism at the Site of TNFR1

The comparison of ATROSAB with the TNFR1-specific mouse IgG1 Htr-9 (Brockhaus et al. 1990, Espevik et al. 1990), underlined the *per se* antagonistic potential of ATROSAB, which induced only 1 % and 6 % of the maximal IL-8 and IL-6 release observed after stimulation by TNF, respectively, compared with 27 % and 50 % in the case of Htr-9. The opposite biological activities of Htr-9 and ATROSAB might result from one or more of the following factors: (i) the epitope of Htr-9 is located in closer proximity to the center of the TNF-TNFR1 interface, implying a more TNF-like interaction, (ii) compared with ATROSAB, Htr-9 revealed a lower affinity to TNFR1, which is in accordance with a published model of antibody-mediated Fas activation, associating higher affinity with antagonism (Chodorge et al. 2012), (iii) human and mouse IgG1 molecules possess only about 64 % sequence similarity, containing most mismatches in the hinge region and hence, potentially apply different steric effects to TNFR1 due to their individual molecular geometry or flexibility, which was described to differ already considerably between the IgG subclasses of one species (Sosnick et al. 1992, Roux et al. 1997, Sapphire et al. 2002).

Remarkably, the sustained release of IL-8 from HT1080 cells, induced by ATROSAB in the presence of a monoclonal anti-human IgG1 (α huIgG) antibody, underlined the challenge of preexisting or newly developed anti-drug antibodies (ADA) in terms of clinical application. The observed receptor stimulation was in good accordance with a report from the clinic by Holland and coworkers in 2013, concerning a single VH domain antibody drug for the inhibition of TNFR1 activation. In this study, two out of five patients, treated with 2 - 10 μ g/kg of the domain antibody, experienced mild to moderate signs of cytokine release syndrome, due to preexisting autoantibodies directed against the VH, which were subsequently detected in 50 % of all patients. In general, ADAs are a well documented phenomenon for protein therapeutics. For example in a study on TNF inhibitors like infliximab and adalimumab, 50 % and 31 % of the patients developed such antibodies, respectively, resulting in ineffective treatment and drug withdrawal (Mok et al. 2013). Moreover, in the special case of TNFR1-blocking protein drugs, ADA-mediated crosslinking could in addition lead to TNFR1 activation and hence, the exacerbation of pathologic symptoms.

For better understanding of anti-IgG antibody-mediated ATROSAB crosslinking, the numbers of antibody receptor complexes on the cell surface were calculated, taking into

account that ATROSAB can bind to TNFR1 in a mono- (AR) and bivalent (AR₂) fashion. The obtained results correlated well with IL-8 release data and disclosed the events on the cell surface, reversing the principle of ATROSAB's antagonism. Notably, the strongest induction of IL-8 release was detected at high concentrations of ATROSAB, where the vast majority of the receptors seem to exist as AR rather than AR₂ complexes, indicating a prominent role of the AR complex in α hulgG-induced agonism.

5.5. Alternative Antibody Formats and Avidity

One possible explanation for the agonistic activity of Htr-9 could be the different molecular architecture, when compared with ATROSAB. Hence, several antibody-like formats derived from ATROSAB with one or two binding sites for TNFR1 were analyzed. Equilibrium binding studies revealed obvious differences between binding of mono- and bivalent constructs, accompanied by characteristic dissociation profiles in QCM experiments, which were discussed earlier for ATROSAB and are well established in the literature (see above, Nygren et al. 1985, Kaufman and Jain 1992, MacKenzie et al. 1996, Zhou et al. 2012). In addition, increased induction of IL-8 release was exhibited by all bivalent ATROSAB variants, supporting the impact of molecular geometry on TNFR1 binding and activation and underlining the unique inhibitory potential of ATROSAB. Moreover, the amounts of the maximum IL-8 release detected for the individual bivalent antibody formats correlated with the affinities/avidities of the bivalent interactions with TNFR1 (scFv-Fc > 2scFv-HSA > IgG-FabL > Db), further indicating an influence of affinity under conditions of bivalent receptor activation.

Interestingly, molecules containing HSA moieties showed higher affinity, compared with other mono- or bivalent molecules, possibly resulting from partial HSA dimerization, as described for bovine serum albumin (Andersson 1966, Janatova et al. 1968, Levi et al. 2002). However, this assumed partial dimerization did not result in TNFR1 activation in the case of monomeric scFv-HSA. In addition, minor signals of higher molecular weight, observed in size exclusion chromatography (SEC) for Db, 2scFv-HSA and IgG-FabL, might indicate protein aggregation, possibly contributing to TNFR1 activation. This observation will be investigated in future studies. Moreover, the ambiguous SEC profile of scFv-Fc correlated well with unpublished experiments, which was accompanied under certain conditions by unspecific

binding in flow cytometry analysis. Hence, further effort should be made revising the molecular design of the scFv-Fc format.

5.6. Affinity Maturation and Framework Exchange

ATROSAB and its parental mouse antibody H398 revealed similar affinities in equilibrium binding studies and in QCM at high receptor density, while H398 inhibited TNFR1 activation about ten-fold more efficiently *in vitro* (see also Zettlitz et al. 2010a, Zettlitz 2010b). Intrinsic affinities, determined by QCM at lower receptor density, also differed only by a factor of two, however, ATROSAB showed a 7.6-fold faster dissociation rate from TNFR1, supporting the hypothesis of a particular importance of the monovalent dissociation behavior on biologic activity in general (Moore et al. 2011). This difference in binding kinetics might be due to minimal alterations in the reconstructed complementarity determining regions (CDR) of ATROSAB following the process of humanization (Kontermann et al. 2008), which was demonstrated to be a major challenge of this technique (Fransson et al. 2010).

In spite of the reported potent inhibition of TNF activity by ATROSAB (Kontermann et al. 2008, Zettlitz et al. 2010a), two different strategies were pursued to further improve its ability for TNFR1 binding and blockade. First, on the basis of scFvIG11, a combinatorial phage display library was generated by error-prone PCR in order to introduce random mutations into the whole sequence of scFvIG11. ScFvIG11 was also isolated by phage display after the randomization of six residues in the CDR-H2 sequence of scFvIZI06.1 (scFv of ATROSAB, Zettlitz 2010b) and exhibited a 3.9-fold reduction of the dissociation rate constant, as determined by QCM. In this study, the further affinity matured scFvT12B was isolated by specific off-rate selection and revealed an additional 2-fold reduced dissociation rate constant due to three amino acid exchanges (FRH1: Q1H; CDRH2: T53S; CDRL3: S91G). The resulting increase in inhibition of TNFR1-mediated interleukin release is in accordance with a large body of literature, connecting reduced dissociation from the antigen with increased biological activity (e.g. Hawkins et al. 1992, Marks et al. 1992, Thie et al. 2009). However, the observed moderate K_D value of 6 nM for scFvT12B after affinity maturation indicates further potential for the development of antibody candidates with improved binding characteristics, when compared with reported data on scFv or Fab molecules after affinity maturation, revealing K_D values of 0.4 to 100 pM (Luginbühl et al. 2006, Steidl et al. 2009, Lou et al. 2010). Interestingly, the reported studies used DNA, CDR or chain shuffling techniques for

the generation of phage or yeast display libraries, suggesting alternative methods for further affinity maturation of scFvT12B. Moreover, sequential randomization and phage display selection of all CDR sequences successively (CDR walking) was published to result in a 15 pM affinity for an anti-HIV gp120 Fab fragment (Yang et al. 1995). In general, the here applied method of immunotube selection under competitive conditions, using immobilized and soluble TNFR1-Fc for off-rate improvement, was in line with previously published data (Zahnd et al. 2010), identifying the competition time after equilibrium binding of antibody-expressing phages to the receptor as crucial factor. However, due to inconsistent numbers of scFv copies on the surface of the filamentous phages and the described partial dimerization of scFv fragments (Essig et al. 1993, Schier et al. 1996), the limits of the available selection and screening techniques to further identify improved dissociation behavior were reached. In addition, limited library size represented a major hurdle for further maturation of scFvT12B affinity (Perelson and Oster 1979, for review see Bradbury and Marks 2004). The described limitations of the applied selection technologies were overcome in a report on single residue mutations, introducing all possible amino acids into any position of the CDR sequences, followed by intensive screening of the rather low number of 2,336 resulting clones (Wu et al. 1998). In addition, alanine scanning of an scFv fragment directed against CD22 resulted in a 56 pM affinity (10-fold increased) after one single amino acid exchange in the surface area of the VH-VL interface (Kawa et al. 2011), further supporting the approach of site-specifically mutated antibody fragments.

In a second approach, the experimental procedure of humanization was repeated with respect to human germline gene sequences of higher humanness-scores (Abhinandan and Martin 2007), in order to overcome the reduced inhibitory activity of ATROSAB, when compared with H398. The resulting scFvFRK13.7 was composed of the VH of the affinity matured scFvT12B together with a newly humanized light chain variable domain and revealed similar efficacy in binding to TNFR1 and in inhibition of TNF mediated IL-8 release, compared with scFvT12B. Interestingly, the good producibility of scFvFRK13.7 and its low tendency to aggregation were confirmed by the determination of sustained molecular stability at lower temperatures and a rather high melting temperature (T_m) of 65 °C. In contrast, scFvZI06.1 (scFv of ATROSAB) showed a T_m of 59 °C, accompanied by partial destabilization at lower temperatures, while scFvT12B already revealed better stability below the T_m but aggregated already at 55 °C. However, repeated humanization of the heavy

chain variable domain, not only led to a lack in binding to TNFR1, but also impaired the expression of the newly designed scFv antibodies. Structural analysis on the basis of *in silico* modeled scFv structures revealed a tremendous displacement of CDR-H2 for scFvFRK13.1 and scFvFRK13.2, both containing newly humanized VH and VL domains. Given the restricted accuracy of model structures, leading to differences between models and crystal structures of less than 2.0 Å (Zhao et al. 2012), the observed aberration in CDR-H2 of 16.5 Å indeed indicates a structural change, possibly responsible for the molecular disintegration. This is in accordance with a report by Fransson and colleagues in 2010 on IgG humanization and the impact of structural changes on antibody characteristics. In contrast, a structural explanation for the increased melting temperature of scFvFRK13.7 could not be derived from the models, although this issue could certainly be addressed by sophisticated mathematical approaches e.g. with a reported algorithm including an empirical function of free energy levels and side chain conformational entropy (Filikov et al. 2002, for review see Bhanothu et al. 2014). Moreover, these results suggest the comprehensive consideration of structural integrity of the CDRs for future humanization experiments. This is facilitated by the growing number of available modeling tools, providing results within the range of minutes, compared with several days to weeks, required by established platforms.

5.7. IgG13.7 and Fab13.7

IgG (IgG13.7) and Fab (Fab13.7) formats were derived from scFvFRK13.7 and analyzed in direct comparison with ATROSAB and FabATROSAB (FabATR) in order to evaluate the suggested improvement of their therapeutic potential. In spite of its monovalent molecular architecture, Fab13.7 revealed improved antagonistic potency, compared with both control proteins FabATR and ATROSAB, presumably originating from a considerably slower dissociation of the antibody receptor complex. However, improved binding in case of the bivalent IgG13.7 resulted in massive TNFR1 activation. In contrast, Fab13.7 exhibited no agonistic potency at all, even in the presence of a human Fab-specific polyclonal goat serum, intended to restore bi- or multivalency by antibody mediated cross-linking. The observed difference in TNFR1 activation between IgG13.7 and ATROSAB could possibly be explained by a phenomenon called epitope drift, describing minor or larger differences between the epitopes of *in vivo* affinity matured antibodies (Bock et al. 1988, Root-Bernstein 2014). IgG13.7 presumably binds to a slightly drifted epitope, resulting in an altered structural

influence of the antibody on the receptor and its activation. This suggested change in TNFR1 activation may be due to a changed influence of antibody binding on the receptor structure, possibly resulting from an induced-fit mechanism, as published previously for the interaction between antibody and antigen (Rini et al. 1992, Wang et al. 2013). Alternatively, a change in the applied intermolecular forces upon receptor crosslinking in terms of altered direction or relative angle between the epitopes before and after affinity maturation could cause the stimulatory activity of IgG13.7.

Interestingly, both control proteins ATROSAB and FabATR inhibited interleukin release and cytotoxicity with similar IC_{50} values, suggesting that the presence of only one TNFR1 binding site instead of two does not reduce the capacity to inhibit TNF-mediated receptor activation. Considering the requirement for multivalent interactions in signaling competent TNF-TNFR1 complexes, the first interaction between an antagonistic antibody and one of the receptor molecules involved in such complexes might already abrogate proper signal induction and thus, the second binding event in case of bivalent antagonists would not result in further suppression of the cellular effect. This hypothesis, however, cannot be generalized and applied to other ligand-receptor systems, as literature data concerning inhibitory antibodies targeted to EGFR (epidermal growth factor receptor; Harms et al. 2012, Zhou et al. 2012), underline the impact of both, intrinsic affinity on the one hand, and bivalent molecule structure on the other hand for sustained blockade of EGF signaling.

Due to the reduced hydrodynamic radius and the lack of FcRn-mediated drug recycling (Kontermann et al. 2009b, Stork et al. 2009), Fab13.7 exhibited a rather short circulation time in the blood of transgenic human TNFR1_{ecd} knock-in mice, compared with ATROSAB, restricting its further applicability in therapeutic settings. In addition, the fusion of additional Ig domains to the C-terminus of CH1 and CLk of Fab13.7 did not result in promising *in vivo* circulation times. However, there are numerous established half-life extension strategies to overcome this disadvantage (Kontermann et al. 2009b), e.g. PEGylation (chemical modification with polyethylene glycol), which was reported for a TNF-specific Fab fragment to result in a terminal half-life of 14 days in humans (Choy et al. 2002).

5.8. Implications on the Model of TNFR1 Activation

The TNF-TNFR1 system is a well studied field, however, the exact mechanism of action of TNFR1 activation remains not fully understood. A puzzling question is e.g. the

identification of the minimal signaling unit. This study demonstrated that (monovalent) binding of TNF alone does not initiate signaling, supporting the requirement for TNF-mediated crosslinking of at least two TNFR1 molecules. Moreover, here presented observations concerning TNFR1 activation by antibodies and antibody-derived molecules, possessing the binding sites for TNFR1 in varying distances, indicated a minor importance for the space between crosslinked TNFR1 molecules. Accordingly, recent literature congruently proposed ligand-bound receptor dimers, associated via their pre-ligand binding assembly domain (PLAD), to represent the smallest signaling-competent unit in the TNF-TNFR1 system (Naismith et al. 1995, Chan et al. 2000, Branschädel et al. 2010, Lewis et al. 2012), which is in clear contrast to the long standing dogma of trimeric receptor assembly. Interestingly, Lewis and colleagues (2012) suggested that TNFR1 has to be switched "ON" by a ligand-induced conformational change, meaning that monomeric but also PLAD-dimerized TNFR1 molecules remain in an "OFF" conformation in the absence of TNF. Key result of this ON-OFF transition was proposed to be the effect on the intracellular parts of the PLAD-linked receptors, separating the two adjacent death domains in a way that allows TRADD association exclusively in the ON state. This is supported by the observation, that the residues of the TNFR1 death domain which are responsible for the interaction with TRADD, also mediate self-association of the intracellular part of the receptor (Telliez et al. 2000). However, considering the relative position of the extracellular TNFR1 domains in the published structure of the PLAD-linked dimer (Naismith et al. 1995), two trimeric TNF molecules, each bound to one of the presented receptors, reveal a relative angle between their threefold axis of symmetry of around 55° . The observed twisted assembly of TNF molecules renders the direct integration of these initial TNF-TNFR complexes into higher ordered ligand-receptor clusters impossible. However, clustering of TNF-TNFR complexes was proposed by various authors to be important for sustained signal induction (Siegel et al. 2000, Krippner-Heidenreich et al. 2002, Valley et al. 2012, Fricke et al. 2014). Hence, in addition to the proposed ligand-induced conformational change, the twisted orientations of the aligned TNF molecules suggest major conformational alterations in the structure of the described complexes, e.g. in the alignment of the four CRDs of TNFR1 between ligand-free PLAD-dimerized receptors and activated TNFR1 molecules, assembled into signaling clusters (see also Lewis et al. 2012). Alternatively, a dramatic change in the PLAD-PLAD interaction could be proposed when PLAD-dimerized TNFR1 molecules as shown by Naismith and coworkers

(1995) are incorporated into large, planar membrane signaling complexes. These hypotheses are supported by a FRET (Förster resonance energy transfer) study of N-terminally labeled TNFR1 molecules, reporting increased FRET signaling after TNF binding and thus, a change of the relative positions or the conformations of the dimerizing PLAD domains (Chan et al. 2000). Furthermore, it has to be mentioned that these hypotheses are based on crystal structures of soluble proteins (Banner et al. 1993, Naismith et al. 1995, Mukai et al. 2010) and that actual fixation of TNFR1 molecules at the cellular membrane could have a considerable influence on the resulting complex structures. In addition, the TNFR molecules used for the generation of the discussed structures were expressed either in *E. coli* or in insect cells and hence did not possess a mammalian glycosylation pattern, which was shown to be important for ligand binding and bioactivity of several members of the TNFR superfamily, including TNFR1 (Corti et al. 1995, Wagner et al. 2007, Vaitaitis and Wagner 2010). Finally, a mechanism of membrane-proximal cysteine-mediated covalent receptor dimerization, as described for DR5 (death receptor 5; Valley et al. 2012, Lewis et al. 2014), would also have a strong impact on the proposed hypotheses on TNFR1 activation.

The before discussed ON and OFF conformations of TNFR1 (Richter et al. 2013) might rather be designated ON and OFF states, representing e.g. alternative structural conformations of receptor molecules or alternative PLAD-PLAD interactions, differing in the orientations of the interacting receptors. Presumably, monomeric and PLAD-dimerized TNFR1 molecules preferentially adopt the OFF state in the absence of TNF, preventing sustained ligand-independent receptor activation. Moreover, trimeric TNF must be able to bind to a first TNFR1 molecule in either the ON or the OFF state, regardless of the actual state of the receptor. However, subsequent association of the second and/or third receptor to the TNF trimer requires all three involved receptors to adopt the ON state to enable a perpendicular fixation of the TNF-TNFR1 complex at the membrane and hence, to enable further formation of larger clusters. Accordingly, TNFR1 molecules must be able to transiently switch from OFF to ON state independent of ligand binding. Hence, an equilibrium between ON and OFF state would have to be proposed, residing far on the inactive side for unligated receptor molecules in both, monomeric and dimerized forms.

In agreement with the proposed modes of TNFR1 activation, antibodies could stabilize PLAD-linked dimers in either the ON or the OFF state, highly dependent on the respective epitope or the inherent molecular geometry. Thus, agonistic antibodies like Htr-9 or IgG13.7

shift the equilibrium between ON and OFF state to the active side, while antagonists like ATROSAB keep TNFR1 dimers in the preferred OFF state and in addition, block the binding of the activating cytokine TNF (Fig. 5.8-01a-c). Notably, Htr-9 and ATROSAB possess overlapping epitopes, both interfering with TNF binding and IgG13.7, derived from ATROSAB by affinity maturation, also binds to similar amino acids of TNFR1. These observations indicate that already subtle differences in the epitope or the binding mode may determine the character of a particular antibody to be agonistic or antagonistic.

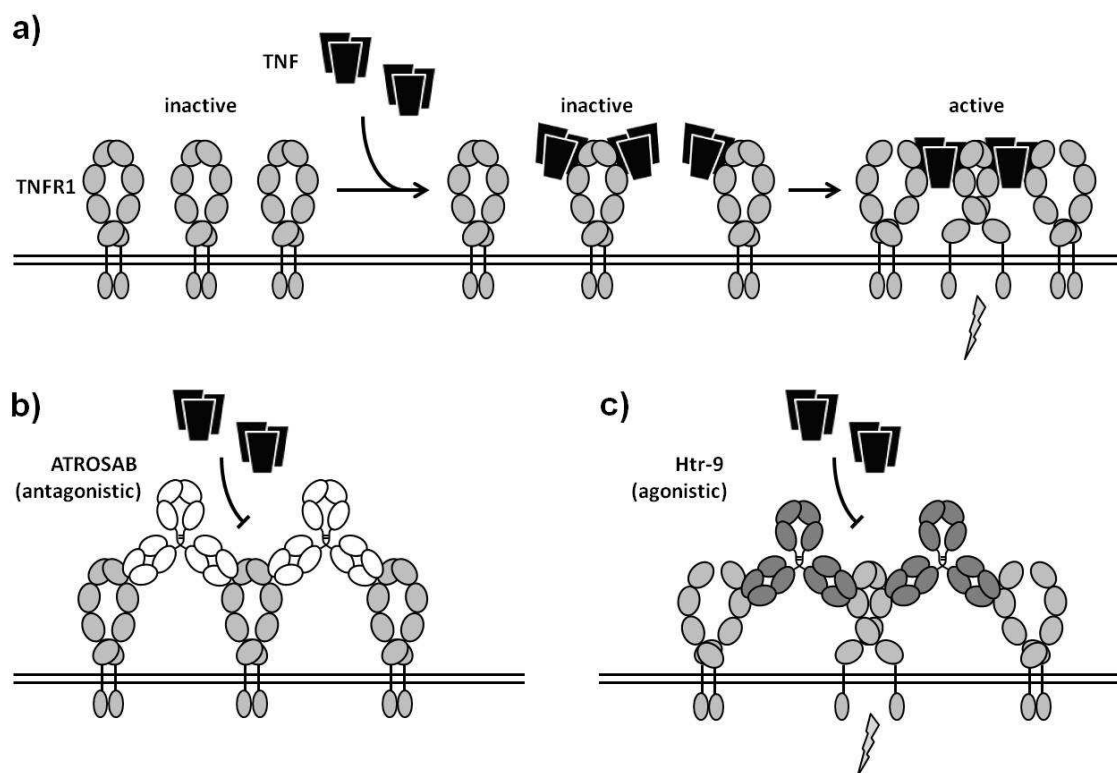


Figure 5.8-01. Model of TNFR1 Activation. Proposed model for the interaction, activation and inhibition of TNF and TNFR1. a) TNFR1 activation by TNF binding and receptor crosslinking, due to a changed receptor conformation or a changed PLAD-PLAD interaction after TNFR1 re-organization. b) Formation of inactive complexes upon binding of antagonistic antibody ATROSAB. c) Htr-9 mimics TNF binding and mediates TNFR1 activation by the formation of signaling competent complexes.

Boschert and colleagues (2010) reported signaling competent scTNF (single-chain TNF) molecules with only one active binding site for TNFR1, which would clearly contradict the proposed hypotheses. However, no SEC data were presented in order to exclude the formation of polyvalent multimers. In addition, the introduced mutations, intended to disrupt two of the three possible interactions with TNFR1, might have resulted in significantly decreased affinity rather than in total elimination of TNF binding (Peter

Scheurich, unpublished). Hence, the formation of larger TNF-TNFR1 clusters could still lead to stabilization of these weak interactions and thereby induce receptor activation. Moreover, antagonistic TNFR1-specific TNF molecules (R1antTNF) were reported to inhibit TNFR1 activation and still bind to three receptor molecules, which has yet to be confirmed by the solution of a crystal structure (Shibata et al. 2008a, Shibata et al. 2008b, Mukai et al. 2009). Furthermore, the described decrease in affinity, due to largely increased dissociation of R1antTNF from TNFR1, indicates a loss of the ability for multivalent binding.

5.9. Outlook and Conclusions

Prospective studies will focus, for example, on the generation of antibodies comprising ATROSAB heavy and light chain variable domains with backbone sequences of all four IgG subclasses, in order to shed light on the influence of molecular geometry on the marginal agonistic activity observed for ATROSAB. Further efforts might also be made on the improvement of TNFR1 binding. The restricted success of affinity maturation after randomization of CDR-H3 and L3 (data not shown), however, indicated a limited potential for further modification of the inner paratope. Similarly, separate randomization and subsequent combination of the matured CDRs hardly resulted in candidates possessing higher affinity (Zettlitz 2010b), which could possibly be overcome by a sequential randomization-selection process of all loops involved in antigen binding, called CDR-walking (Barbas et al. 1994). Alternatively, Chowdhury and Pastan recommended in 1999 to focus on the randomization of so called "hot spots", which are subject to somatic hypermutation *in vivo*, for rapid isolation of improved antibody fragments, particularly in the case of small size libraries. In addition, site-directed mutagenesis of selected residues might also represent a future approach, as certain positions in the antibody sequence were identified to contribute to antigen binding in general (Robin et al. 2014). Moreover, the S91G mutation in the VL (variable domain of the light chain) of Fab13.7, which was inserted by phage display (scFvT12B) and subsequently lost after repeated humanization (scFvFRK13.7), could be reintroduced in a following study. Furthermore, besides the previously mentioned PEGylation (Choy et al. 2002), several strategies concerning the extension of *in vivo* half-life were described (Kontermann et al. 2009b), among them are the genetic fusion to (i) albumin binding domains (Stork et al. 2009), (ii) IgG binding domains (Unverdorben et al. 2012, Hutt et al. 2012) or (iii) polypeptides, forming random coil repeats (e.g. Schlapschy et al. 2013).

In summary, the here presented Fab13.7 blocks all TNFR1-mediated pro-inflammatory effects in response to both, TNF and LT α , which is in clear contrast to the five TNF-targeting biologicals approved for clinical treatment. In addition, TNFR2-induced signals supporting cellular proliferation, regeneration and homeostasis remain unaffected. This is of particular interest, considering the important pro-inflammatory role of LT α (Robak et al. 1998, O'Rourke et al. 2008), which was shown e.g. in mouse models of collagen induced arthritis (CIA) or experimental autoimmune encephalomyelitis (EAE; Powell et al. 1990, Suen et al. 1997, Chiang et al. 2009). The clinical relevance of LT α neutralization is further supported by a report on RA remission after treatment with the TNFR2 fusion protein etanercept, that also inhibits LT α activity, observed in patients with previously reported resistance to infliximab (Buch et al. 2004). Moreover, Fab13.7 might also be applied in certain oncological settings, as suggested by investigations e.g. on the involvement of TNFR1 in tumor-associated lymphangiogenesis (Ji et al. 2014) or *Helicobacter pylori* infection-mediated development of gastric cancer in mouse models (Oshima et al. 2014). In conclusion, Fab13.7 combines the beneficial effects of specific TNFR1 blockade with inhibition of TNF and LT α , completely eliminated agonistic potential and reduced susceptibility to crosslinking-induced TNFR1 activation in the presence of anti-drug antibodies.

6. References

- Abhinandan KR, Martin AC. Analyzing the "degree of humanness" of antibody sequences. *J Mol Biol.* 2007 Jun 8;369(3):852-62. Epub 2007 Mar 14.
- Aggarwal BB, Kohr WJ, Hass PE, Moffat B, Spencer SA, Henzel WJ, Bringman TS, Nedwin GE, Goeddel DV, Harkins RN. Human tumor necrosis factor. Production, purification, and characterization. *J Biol Chem.* 1985 Feb 25;260(4):2345-54.
- Algire GH, Legallais FY, Anderson BF. Vascular reactions of normal and malignant tissues in vivo. V. The rôle of hypotension in the action of a bacterial polysaccharide on tumors. *J Natl Cancer Inst.* 1952 Jun;12(6):1279-95.
- An Z, Forrest G, Moore R, Cukan M, Haytko P, Huang L, Vitelli S, Zhao JZ, Lu P, Hua J, Gibson CR, Harvey BR, Montgomery D, Zaller D, Wang F, Strohl W. IgG2m4, an engineered antibody isotype with reduced Fc function. *MAbs.* 2009 Nov-Dec;1(6):572-9.
- Andersson LO. The heterogeneity of bovine serum albumin. *Biochim Biophys Acta.* 1966 Mar 28;117(1):115-33.
- Armour KL, Clark MR, Hadley AG, Williamson LM. Recombinant human IgG molecules lacking Fc γ receptor I binding and monocyte triggering activities. *Eur J Immunol.* 1999 Aug;29(8):2613-24.
- Arnett HA, Mason J, Marino M, Suzuki K, Matsushima GK, Ting JP. TNF alpha promotes proliferation of oligodendrocyte progenitors and remyelination. *Nat Neurosci.* 2001 Nov;4(11):1116-22.
- Arntz OJ, Geurts J, Veenbergen S, Bennink MB, van den Brand BT, Abdollahi-Roodsaz S, van den Berg WB, van de Loo FA. A crucial role for tumor necrosis factor receptor 1 in synovial lining cells and the reticuloendothelial system in mediating experimental arthritis. *Arthritis Res Ther.* 2010;12(2):R61. doi: 10.1186/ar2974. Epub 2010 Apr 6.
- Aspalter RM, Wolf HM, Eibl MM. Chronic TNF-alpha exposure impairs TCR-signaling via TNF-RII but not TNF-RI. *Cell Immunol.* 2005 Sep;237(1):55-67. Epub 2005 Dec 1.
- Baeuerle PA, Henkel T. Function and activation of NF-kappa B in the immune system. *Annu Rev Immunol.* 1994;12:141-79.
- Baillet A, Gossec L, Paternotte S, Etcheto A, Combe B, Meyer O, Mariette X, Gottenberg JE, Dougados M. Evaluation of serum IL-6 level as a surrogate marker of synovial inflammation and as a factor of structural progression in early rheumatoid arthritis: Results from the ESPOIR cohort. *Arthritis Care Res (Hoboken).* 2014 Nov 10. doi: 10.1002/acr.22513.
- Banner DW, D'Arcy A, Janes W, Gentz R, Schoenfeld HJ, Broger C, Loetscher H, Lesslauer W. Crystal structure of the soluble human 55 kd TNF receptor-human TNF beta complex: implications for TNF receptor activation. *Cell.* 1993 May 7;73(3):431-45.
- Barbas CF 3rd, Hu D, Dunlop N, Sawyer L, Cababa D, Hendry RM, Nara PL, Burton DR. In vitro evolution of a neutralizing human antibody to human immunodeficiency virus type 1 to enhance affinity and broaden strain cross-reactivity. *Proc Natl Acad Sci U S A.* 1994 Apr 26;91(9):3809-13.
- Berger V, Richter F, Zettlitz K, Unverdorben F, Scheurich P, Herrmann A, Pfizenmaier K, Kontermann RE. An anti-TNFR1 scFv-HSA fusion protein as selective antagonist of TNF action. *Protein Eng Des Sel.* 2013 Oct;26(10):581-7. doi: 10.1093/protein/gzt044. Epub 2013 Sep 4.
- Bhanothu V, Theophilus JP, Rozati R. Review On Characteristic Developments Of Computational Protein Engineering. *Journal of Pharmaceutical Research & Opinion*, 2014, 2. Jg., Nr. 8.
- Bianchi K, Meier P. A tangled web of ubiquitin chains: breaking news in TNF-R1 signaling. *Mol Cell.* 2009 Dec 11;36(5):736-42. doi: 10.1016/j.molcel.2009.11.029.
- Black RA, Rauch CT, Kozlosky CJ, Peschon JJ, Slack JL, Wolfson MF, Castner BJ, Stocking KL, Reddy P, Srinivasan S, Nelson N, Boiani N, Schooley KA, Gerhart M, Davis R, Fitzner JN, Johnson RS, Paxton RJ, March CJ, Cerretti DP. A metalloproteinase disintegrin that releases tumour-necrosis factor-alpha from cells. *Nature.* 1997 Feb 20;385(6618):729-33.

- Bock K, Karlsson KA, Strömberg N, Teneberg S. Interaction of viruses, bacteria and bacterial toxins with host cell surface glycolipids. Aspects on receptor identification and dissection of binding epitopes. *Adv Exp Med Biol.* 1988;228:153-86.
- Bongartz T, Sutton AJ, Sweeting MJ, Buchan I, Matteson EL, Montori V. Anti-TNF antibody therapy in rheumatoid arthritis and the risk of serious infections and malignancies: systematic review and meta-analysis of rare harmful effects in randomized controlled trials. *JAMA.* 2006 May 17;295(19):2275-85.
- Boschert V, Krippner-Heidenreich A, Branschädel M, Tepperink J, Aird A, Scheurich P. Single chain TNF derivatives with individually mutated receptor binding sites reveal differential stoichiometry of ligand receptor complex formation for TNFR1 and TNFR2. *Cell Signal.* 2010 Jul;22(7):1088-96. doi: 10.1016/j.cellsig.2010.02.011. Epub 2010 Mar 4.
- Bradbury AR, Marks JD. Antibodies from phage antibody libraries. *J Immunol Methods.* 2004 Jul;290(1-2):29-49.
- Brakebusch C, Nophar Y, Kemper O, Engelmann H, Wallach D. Cytoplasmic truncation of the p55 tumour necrosis factor (TNF) receptor abolishes signalling, but not induced shedding of the receptor. *EMBO J.* 1992 Mar;11(3):943-50.
- Branschädel M, Aird A, Zappe A, Tietz C, Krippner-Heidenreich A, Scheurich P. Dual function of cysteine rich domain (CRD) 1 of TNF receptor type 1: conformational stabilization of CRD2 and control of receptor responsiveness. *Cell Signal.* 2010 Mar;22(3):404-14. doi: 10.1016/j.cellsig.2009.10.011.
- Brockhaus M, Schoenfeld HJ, Schlaeger EJ, Hunziker W, Lesslauer W, Loetscher H. Identification of two types of tumor necrosis factor receptors on human cell lines by monoclonal antibodies. *Proc Natl Acad Sci U S A.* 1990 Apr;87(8):3127-31.
- Bruns P. Die Heilwirkung des Erysipels auf Geschwulste. *Beitr. Klin. Chir.* 1868 3; 443-446.
- Buch MH, Conaghan PG, Quinn MA, Bingham SJ, Veale D, Emery P. True infliximab resistance in rheumatoid arthritis: a role for lymphotoxin alpha? *Ann Rheum Dis.* 2004 Oct;63(10):1344-6. Epub 2004 Mar 19.
- Cabal-Hierro L, Lazo PS. Signal transduction by tumor necrosis factor receptors. *Cell Signal.* 2012 Jun;24(6):1297-305. doi: 10.1016/j.cellsig.2012.02.006. Epub 2012 Feb 20.
- Calmon-Hamaty F, Combe B, Hahne M, Morel J. Lymphotoxin α revisited: general features and implications in rheumatoid arthritis. *Arthritis Res Ther.* 2011 Jul 26;13(4):232. doi: 10.1186/ar3376.
- Calzascia T, Pellegrini M, Hall H, Sabbagh L, Ono N, Elford AR, Mak TW, Ohashi PS. TNF-alpha is critical for antitumor but not antiviral T cell immunity in mice. *J Clin Invest.* 2007 Dec;117(12):3833-45.
- Cao J, Meng F, Gao X, Dong H, Yao W. Expression and purification of a natural N-terminal pre-ligand assembly domain of tumor necrosis factor receptor 1 (TNFR1 PLAD) and preliminary activity determination. *Protein J.* 2011 Apr;30(4):281-9. doi: 10.1007/s10930-011-9330-4.
- Carswell EA, Old LJ, Kassel RL, Green S, Fiore N, Williamson B. An endotoxin-induced serum factor that causes necrosis of tumors. *Proc Natl Acad Sci U S A.* 1975 Sep;72(9):3666-70.
- Carter PH, Scherle PA, Muckelbauer JK, Voss ME, Liu RQ, Thompson LA, Tebben AJ, Solomon KA, Lo YC, Li Z, Strzemienski P, Yang G, Falahatpisheh N, Xu M, Wu Z, Farrow NA, Ramnarayan K, Wang J, Rideout D, Yalamoori V, Domaille P, Underwood DJ, Trzaskos JM, Friedman SM, Newton RC, Decicco CP. Photochemically enhanced binding of small molecules to the tumor necrosis factor receptor-1 inhibits the binding of TNF-alpha. *Proc Natl Acad Sci U S A.* 2001 Oct 9;98(21):11879-84.
- Carter PJ. Potent antibody therapeutics by design. *Nat Rev Immunol.* 2006 May;6(5):343-57.
- Chan FK, Chun HJ, Zheng L, Siegel RM, Bui KL, Lenardo MJ. A domain in TNF receptors that mediates ligand-independent receptor assembly and signaling. *Science.* 2000 Jun 30;288(5475):2351-4.
- Chaparro-Riggers J, Liang H, DeVay RM, Bai L, Sutton JE, Chen W, Geng T, Lindquist K, Casas MG, Boustany LM, Brown CL, Chabot J, Gomes B, Garzone P, Rossi A, Strop P, Shelton D, Pons J, Rajpal A. Increasing serum half-life and extending cholesterol lowering in vivo by engineering antibody with pH-sensitive binding to PCSK9. *J Biol Chem.* 2012 Mar 30;287(14):11090-7. doi: 10.1074/jbc.M111.319764. Epub 2012 Jan 31.

- Chen X, Bäumel M, Männel DN, Howard OM, Oppenheim JJ. Interaction of TNF with TNF receptor type 2 promotes expansion and function of mouse CD4+CD25+ T regulatory cells. *J Immunol*. 2007 Jul 1;179(1):154-61.
- Chen X, Chang J, Deng Q, Xu J, Nguyen TA, Martens LH, Cenik B, Taylor G, Hudson KF, Chung J, Yu K, Yu P, Herz J, Farese RV Jr, Kukar T, Tansey MG. Progranulin does not bind tumor necrosis factor (TNF) receptors and is not a direct regulator of TNF-dependent signaling or bioactivity in immune or neuronal cells. *J Neurosci*. 2013 May 22;33(21):9202-13. doi: 10.1523/JNEUROSCI.5336-12.2013.
- Chiang EY, Kolumam GA, Yu X, Francesco M, Ivelja S, Peng I, Gribling P, Shu J, Lee WP, Refino CJ, Balazs M, Paler-Martinez A, Nguyen A, Young J, Barck KH, Carano RA, Ferrando R, Diehl L, Chatterjea D, Grogan JL. Targeted depletion of lymphotoxin-alpha-expressing TH1 and TH17 cells inhibits autoimmune disease. *Nat Med*. 2009 Jul;15(7):766-73. doi: 10.1038/nm.1984. Epub 2009 Jun 28.
- Chodorge M, Züger S, Stirnimann C, Briand C, Jermutus L, Grütter MG, Minter RR. A series of Fas receptor agonist antibodies that demonstrate an inverse correlation between affinity and potency. *Cell Death Differ*. 2012 Jul;19(7):1187-95. doi: 10.1038/cdd.2011.208. Epub 2012 Jan 20.
- Chowdhury PS, Pastan I. Improving antibody affinity by mimicking somatic hypermutation in vitro. *Nat Biotechnol*. 1999 Jun;17(6):568-72.
- Chowdhury PS, Wu H. Tailor-made antibody therapeutics. *Methods*. 2005 May;36(1):11-24.
- Choy EH, Hazleman B, Smith M, Moss K, Lisi L, Scott DG, Patel J, Sopwith M, Isenberg DA. Efficacy of a novel PEGylated humanized anti-TNF fragment (CDP870) in patients with rheumatoid arthritis: a phase II double-blinded, randomized, dose-escalating trial. *Rheumatology (Oxford)*. 2002 Oct;41(10):1133-7.
- Clark J, Vagenas P, Panesar M, Cope AP. What does tumour necrosis factor excess do to the immune system long term? *Ann Rheum Dis*. 2005 Nov;64 Suppl 4:iv70-6.
- Coley WB. II. Contribution to the Knowledge of Sarcoma. *Ann Surg*. 1891 Sep;14(3):199-220.
- Cope AP, Liblau RS, Yang XD, Congia M, Laudanna C, Schreiber RD, Probert L, Kollias G, McDevitt HO. Chronic tumor necrosis factor alters T cell responses by attenuating T cell receptor signaling. *J Exp Med*. 1997 May 5;185(9):1573-84.
- Corti A, Merli S, Bagnasco L, D'Ambrosio F, Marino M, Cassani G. Identification of two forms (31-33 and 48 kD) of the urinary soluble p55 tumor necrosis factor receptor that are differentially N- and O-glycosylated. *J Interferon Cytokine Res*. 1995 Feb;15(2):143-52.
- Crothers DM, Metzger H. The influence of polyvalency on the binding properties of antibodies. *Immunochemistry*. 1972 Mar;9(3):341-57.
- de Gannes GC, Ghoreishi M, Pope J, Russell A, Bell D, Adams S, Shojania K, Martinka M, Dutz JP. Psoriasis and pustular dermatitis triggered by TNF- α inhibitors in patients with rheumatologic conditions. *Arch Dermatol*. 2007 Feb;143(2):223-31.
- Deng GM, Zheng L, Chan FK, Lenardo M. Amelioration of inflammatory arthritis by targeting the pre-ligand assembly domain of tumor necrosis factor receptors. *Nat Med*. 2005 Oct;11(10):1066-72. Epub 2005 Sep 18.
- Desai SB, Furst DE. Problems encountered during anti-tumour necrosis factor therapy. *Best Pract Res Clin Rheumatol*. 2006 Aug;20(4):757-90.
- Di Sabatino A, Ciccocioppo R, Cinque B, Millimaggi D, Morera R, Ricevuti L, Cifone MG, Corazza GR. Defective mucosal T cell death is sustainably reverted by infliximab in a caspase dependent pathway in Crohn's disease. *Gut*. 2004 Jan;53(1):70-7.
- Diak P, Siegel J, La Grenade L, Choi L, Lemery S, McMahan A. Tumor necrosis factor alpha blockers and malignancy in children: forty-eight cases reported to the Food and Drug Administration. *Arthritis Rheum*. 2010 Aug;62(8):2517-24. doi: 10.1002/art.27511.
- Dumitru CD, Ceci JD, Tsatsanis C, Kontoyiannis D, Stamatakis K, Lin JH, Patriotis C, Jenkins NA, Copeland NG, Kollias G, Tsichlis PN. TNF-alpha induction by LPS is regulated posttranscriptionally via a Tpl2/ERK-dependent pathway. *Cell*. 2000 Dec 22;103(7):1071-83.

- Eggermont AM, de Wilt JH, ten Hagen TL. Current uses of isolated limb perfusion in the clinic and a model system for new strategies. *Lancet Oncol.* 2003 Jul;4(7):429-37.
- Elberdín L, Outeda M, Salvador P, Paradela S, Fernández-Torres RM, Iglesias R, Fonseca E, Martín I. Infliximab drug and antibody levels in patients with dermatological conditions. *Int J Clin Pharm.* 2015 Jan 23. [Epub ahead of print]
- Emanuelli B, Peraldi P, Filloux C, Chavey C, Freidinger K, Hilton DJ, Hotamisligil GS, Van Obberghen E. SOCS-3 inhibits insulin signaling and is up-regulated in response to tumor necrosis factor-alpha in the adipose tissue of obese mice. *J Biol Chem.* 2001 Dec 21;276(51):47944-9. Epub 2001 Oct 16.
- Espevik T, Brockhaus M, Loetscher H, Nonstad U, Shalaby R. Characterization of binding and biological effects of monoclonal antibodies against a human tumor necrosis factor receptor. *J Exp Med.* 1990 Feb 1;171(2):415-26.
- Essig NZ, Wood JF, Howard AJ, Raag R, Whitlow M. Crystallization of single-chain Fv proteins. *J Mol Biol.* 1993 Dec 5;234(3):897-901.
- Etemadi N, Webb A, Bankovacki A, Silke J, Nachbur U. Progranulin does not inhibit TNF and lymphotoxin- α signalling through TNF receptor 1. *Immunol Cell Biol.* 2013 Nov-Dec;91(10):661-4. doi: 10.1038/icb.2013.53. Epub 2013 Oct 8.
- Feinberg B, Kurzrock R, Talpaz M, Blick M, Saks S, Gutterman JU. A phase I trial of intravenously-administered recombinant tumor necrosis factor-alpha in cancer patients. *J Clin Oncol.* 1988 Aug;6(8):1328-34.
- Feldmann M. Development of anti-TNF therapy for rheumatoid arthritis. *Nat Rev Immunol.* 2002 May;2(5):364-71.
- Filikov AV, Hayes RJ, Luo P, Stark DM, Chan C, Kundu A, Dahiyat BI. Computational stabilization of human growth hormone. *Protein Sci.* 2002 Jun;11(6):1452-61.
- Fracasso PM, Burris H 3rd, Arquette MA, Govindan R, Gao F, Wright LP, Goodner SA, Greco FA, Jones SF, Willcut N, Chodkiewicz C, Pathak A, Springett GM, Simon GR, Sullivan DM, Marcelpoil R, Mayfield SD, Mauro D, Garrett CR. A phase 1 escalating single-dose and weekly fixed-dose study of cetuximab: pharmacokinetic and pharmacodynamic rationale for dosing. *Clin Cancer Res.* 2007 Feb 1;13(3):986-93.
- Fransson J, Teplyakov A, Raghunathan G, Chi E, Cordier W, Dinh T, Feng Y, Giles-Komar J, Gilliland G, Lollo B, Malia TJ, Nishioka W, Obmolova G, Zhao S, Zhao Y, Swanson RV, Almagro JC. Human framework adaptation of a mouse anti-human IL-13 antibody. *J Mol Biol.* 2010 Apr 30;398(2):214-31. doi: 10.1016/j.jmb.2010.03.004. Epub 2010 Mar 10.
- Fricke F, Malkusch S, Wangorsch G, Greiner JF, Kaltschmidt B, Kaltschmidt C, Widera D, Dandekar T, Heilemann M. Quantitative single-molecule localization microscopy combined with rule-based modeling reveals ligand-induced TNF-R1 reorganization toward higher-order oligomers. *Histochem Cell Biol.* 2014 Jul;142(1):91-101. doi: 10.1007/s00418-014-1195-0. Epub 2014 Feb 12.
- Fu YX, Chaplin DD. Development and maturation of secondary lymphoid tissues. *Annu Rev Immunol.* 1999;17:399-433.
- Gardam MA, Keystone EC, Menzies R, Manners S, Skamene E, Long R, Vinh DC. Anti-tumour necrosis factor agents and tuberculosis risk: mechanisms of action and clinical management. *Lancet Infect Dis.* 2003 Mar;3(3):148-55.
- Gerken M, Krippner-Heidenreich A, Steinert S, Willi S, Neugart F, Zappe A, Wrachtrup J, Tietz C, Scheurich P. Fluorescence correlation spectroscopy reveals topological segregation of the two tumor necrosis factor membrane receptors. *Biochim Biophys Acta.* 2010 Jun;1798(6):1081-9. doi: 10.1016/j.bbame.2010.02.021. Epub 2010 Feb 23.
- Gratia A, Linz RCR. *Seances. Sec. Biol. Ses Fil.* 1931 108;421-428
- Grell M, Zimmermann G, Hülser D, Pfizenmaier K, Scheurich P. TNF receptors TR60 and TR80 can mediate apoptosis via induction of distinct signal pathways. *J Immunol.* 1994 Sep 1;153(5):1963-72.

- Grell M, Douni E, Wajant H, Löhden M, Clauss M, Maxeiner B, Georgopoulos S, Lesslauer W, Kollias G, Pfizenmaier K, Scheurich P. The transmembrane form of tumor necrosis factor is the prime activating ligand of the 80 kDa tumor necrosis factor receptor. *Cell*. 1995 Dec 1;83(5):793-802.
- Grell M, Wajant H, Zimmermann G, Scheurich P. The type 1 receptor (CD120a) is the high-affinity receptor for soluble tumor necrosis factor. *Proc Natl Acad Sci U S A*. 1998 Jan 20;95(2):570-5.
- Hansen L, Petersen LC, Lauritzen B, Clausen JT, Grell SN, Agersø H, Sørensen BB, Hilden I, Almholt K. Target-mediated clearance and bio-distribution of a monoclonal antibody against the Kunitz-type protease inhibitor 2 domain of Tissue Factor Pathway Inhibitor. *Thromb Res*. 2014 Mar;133(3):464-71. doi: 10.1016/j.thromres.2013.12.015. Epub 2013 Dec 17.
- Harms BD1, Kearns JD, Su SV, Kohli N, Nielsen UB, Schoeberl B. Optimizing properties of antireceptor antibodies using kinetic computational models and experiments. *Methods Enzymol*. 2012;502:67-87. doi: 10.1016/B978-0-12-416039-2.00004-5.
- Havell EA. Evidence that tumor necrosis factor has an important role in antibacterial resistance. *J Immunol*. 1989 Nov 1;143(9):2894-9.
- Hawkins RE, Russell SJ, Winter G. Selection of phage antibodies by binding affinity. Mimicking affinity maturation. *J Mol Biol*. 1992 Aug 5;226(3):889-96.
- Hehlhans T, Männel DN. The TNF-TNF receptor system. *Biol Chem*. 2002 Oct;383(10):1581-5.
- Henkler F, Behrle E, Dennehy KM, Wicovsky A, Peters N, Warnke C, Pfizenmaier K, Wajant H. The extracellular domains of FasL and Fas are sufficient for the formation of supramolecular FasL-Fas clusters of high stability. *J Cell Biol*. 2005 Mar 28;168(7):1087-98.
- Himmeler A, Maurer-Fogy I, Krönke M, Scheurich P, Pfizenmaier K, Lantz M, Olsson I, Hauptmann R, Stratowa C, Adolf GR. Molecular cloning and expression of human and rat tumor necrosis factor receptor chain (p60) and its soluble derivative, tumor necrosis factor-binding protein. *DNA Cell Biol*. 1990 Dec;9(10):705-15.
- Hock H, Dorsch M, Kunzendorf U, Qin Z, Diamantstein T, Blankenstein T. Mechanisms of rejection induced by tumor cell-targeted gene transfer of interleukin 2, interleukin 4, interleukin 7, tumor necrosis factor, or interferon gamma. *Proc Natl Acad Sci U S A*. 1993 Apr 1;90(7):2774-8.
- Holland MC, Wurthner JU, Morley PJ, Birchler MA, Lambert J, Albayaty M, Serone AP, Wilson R, Chen Y, Forrest RM, Cordy JC, Lipson DA, Bayliffe AI. Autoantibodies to variable heavy (VH) chain Ig sequences in humans impact the safety and clinical pharmacology of a VH domain antibody antagonist of TNF- α receptor 1. *J Clin Immunol*. 2013 Oct;33(7):1192-203. doi: 10.1007/s10875-013-9915-0. Epub 2013 Jul 6.
- Hotamisligil GS, Murray DL, Choy LN, Spiegelman BM. Tumor necrosis factor alpha inhibits signaling from the insulin receptor. *Proc Natl Acad Sci U S A*. 1994 May 24;91(11):4854-8.
- Hristodorov D, Mladenov R, Brehm H, Fischer R, Barth S, Thepen T. Recombinant H22(scFv) blocks CD64 and prevents the capture of anti-TNF monoclonal antibody. *MAbs*. 2014 Sep 3;6(5):1283-9. doi: 10.4161/mabs.32182.
- Huang XW, Yang J, Dragovic AF, Zhang H, Lawrence TS, Zhang M. Antisense oligonucleotide inhibition of tumor necrosis factor receptor 1 protects the liver from radiation-induced apoptosis. *Clin Cancer Res*. 2006 May 1;12(9):2849-55.
- Hutt M, Färber-Schwarz A, Unverdorben F, Richter F, Kontermann RE. Plasma half-life extension of small recombinant antibodies by fusion to immunoglobulin-binding domains. *J Biol Chem*. 2012 Feb 10;287(7):4462-9. doi: 10.1074/jbc.M111.311522. Epub 2011 Dec 6.
- Hwang YG, Moreland LW. Induction therapy with combination TNF inhibitor and methotrexate in early rheumatoid arthritis. *Curr Rheumatol Rep*. 2014 May;16(5):417. doi: 10.1007/s11926-014-0417-8.
- Jacob CO, Lewis GD, McDevitt HO. MHC class II-associated variation in the production of tumor necrosis factor in mice and humans: relevance to the pathogenesis of autoimmune diseases. *Immunol Res*. 1991;10(2):156-68.
- Janatova J, Fuller JK, Hunter MJ. The heterogeneity of bovine albumin with respect to sulfhydryl and dimer content. *J Biol Chem*. 1968 Jul 10;243(13):3612-22.

- Ji H, Cao R, Yang Y, Zhang Y, Iwamoto H, Lim S, Nakamura M, Andersson P, Wang J, Sun Y, Dissing S, He X, Yang X, Cao Y. TNFR1 mediates TNF- α -induced tumour lymphangiogenesis and metastasis by modulating VEGF-C-VEGFR3 signalling. *Nat Commun.* 2014 Sep 17;5:4944. doi: 10.1038/ncomms5944.
- Kamath AV, Yip V, Gupta P, Boswell CA, Bumbaca D, Haughney P, Castro J, Tsai SP, Pacheco G, Ross S, Yan M, Damico-Beyer LA, Khawli L, Shen BQ. Dose dependent pharmacokinetics, tissue distribution, and anti-tumor efficacy of a humanized monoclonal antibody against DLL4 in mice. *MAbs.* 2014;6(6):1631-7. doi: 10.4161/mabs.36107.
- Kassiotis G1, Kollias G. Uncoupling the proinflammatory from the immunosuppressive properties of tumor necrosis factor (TNF) at the p55 TNF receptor level: implications for pathogenesis and therapy of autoimmune demyelination. *J Exp Med.* 2001 Feb 19;193(4):427-34.
- Kaufman EN, Jain RK. Effect of bivalent interaction upon apparent antibody affinity: experimental confirmation of theory using fluorescence photobleaching and implications for antibody binding assays. *Cancer Res.* 1992 Aug 1;52(15):4157-67.
- Kawa S, Onda M, Ho M, Kreitman RJ, Bera TK, Pastan I. The improvement of an anti-CD22 immunotoxin: conversion to single-chain and disulfide stabilized form and affinity maturation by alanine scan. *MAbs.* 2011 Sep-Oct;3(5):479-86. doi: 10.4161/mabs.3.5.17228. Epub 2011 Sep 1.
- Kim J, Hayton WL, Robinson JM, Anderson CL. Kinetics of FcRn-mediated recycling of IgG and albumin in human: pathophysiology and therapeutic implications using a simplified mechanism-based model. *Clin Immunol.* 2007 Feb;122(2):146-55. Epub 2006 Oct 13.
- Kitagaki M, Isoda K, Kamada H, Kobayashi T, Tsunoda S, Tsutsumi Y, Niida T, Kujiraoka T, Ishigami N, Ishihara M, Matsubara O, Ohsuzu F, Kikuchi M. Novel TNF- α receptor 1 antagonist treatment attenuates arterial inflammation and intimal hyperplasia in mice. *J Atheroscler Thromb.* 2012;19(1):36-46. Epub 2011 Dec 7.
- Kontermann RE, Martineau P, Cummings CE, Karpas A, Allen D, Derbyshire E, Winter G. Enzyme immunoassays using bispecific diabodies. *Immunotechnology.* 1997 Jun;3(2):137-44.
- Kontermann RE, Münkkel S, Neumeyer J, Müller D, Branschädel M, Scheurich P, Pfizenmaier K. A humanized tumor necrosis factor receptor 1 (TNFR1)-specific antagonistic antibody for selective inhibition of tumor necrosis factor (TNF) action. *J Immunother.* 2008 Apr;31(3):225-34. doi: 10.1097/CJI.0b013e31816a88f9.
- Kontermann RE, Scheurich P, Pfizenmaier K. Antagonists of TNF action: clinical experience and new developments. *Expert Opin Drug Discov.* 2009a Mar;4(3):279-92. doi: 10.1517/17460440902785167.
- Kontermann RE. Strategies to extend plasma half-lives of recombinant antibodies. *BioDrugs.* 2009b;23(2):93-109. doi: 10.2165/00063030-200923020-00003.
- Kotsovilis S, Andreakos E. Therapeutic human monoclonal antibodies in inflammatory diseases. *Methods Mol Biol.* 2014;1060:37-59. doi: 10.1007/978-1-62703-586-6_3.
- Krieger E, Joo K, Lee J, Lee J, Raman S, Thompson J, Tyka M, Baker D, Karplus K. Improving physical realism, stereochemistry, and side-chain accuracy in homology modeling: Four approaches that performed well in CASP8. *Proteins.* 2009;77 Suppl 9:114-22. doi: 10.1002/prot.22570.
- Kriegler M, Perez C, DeFay K, Albert I, Lu SD. A novel form of TNF/cachectin is a cell surface cytotoxic transmembrane protein: ramifications for the complex physiology of TNF. *Cell.* 1988 Apr 8;53(1):45-53.
- Krippner-Heidenreich A, Tübing F, Bryde S, Willi S, Zimmermann G, Scheurich P. Control of receptor-induced signaling complex formation by the kinetics of ligand/receptor interaction. *J Biol Chem.* 2002 Nov 15;277(46):44155-63. Epub 2002 Sep 4.
- Kruppa G, Thoma B, Machleidt T, Wiegmann K, Krönke M. Inhibition of tumor necrosis factor (TNF)-mediated NF- κ B activation by selective blockade of the human 55-kDa TNF receptor. *J Immunol.* 1992 May 15;148(10):3152-7.
- Kull FC Jr, Jacobs S, Cuatrecasas P. Cellular receptor for ¹²⁵I-labeled tumor necrosis factor: specific binding, affinity labeling, and relationship to sensitivity. *Proc Natl Acad Sci U S A.* 1985 Sep;82(17):5756-60.

- Laemmli UK. Cleavage of structural proteins during the assembly of the head of bacteriophage T4. *Nature*. 1970 Aug 15;227(5259):680-5.
- Legler DF, Micheau O, Doucey MA, Tschopp J, Bron C. Recruitment of TNF receptor 1 to lipid rafts is essential for TNF α -mediated NF- κ B activation. *Immunity*. 2003 May;18(5):655-64.
- Lenercept MS Study Group. TNF neutralization in MS: results of a randomized, placebo-controlled multicenter study. The Lenercept Multiple Sclerosis Study Group and The University of British Columbia MS/MRI Analysis Group. *Neurology*. 1999 Aug 11;53(3):457-65.
- Levi V, González Flecha FL. Reversible fast-dimerization of bovine serum albumin detected by fluorescence resonance energy transfer. *Biochim Biophys Acta*. 2002 Sep 23;1599(1-2):141-8.
- Lewis AK, Valley CC, Sachs JN. TNFR1 signaling is associated with backbone conformational changes of receptor dimers consistent with overactivation in the R92Q TRAPS mutant. *Biochemistry*. 2012 Aug 21;51(33):6545-55. doi: 10.1021/bi3006626. Epub 2012 Aug 8.
- Lewis AK, James ZM, McCaffrey JE2, Braun AR, Karim CB2, Thomas DD2, Sachs JN3. Open and closed conformations of the isolated transmembrane domain of death receptor 5 support a new model of activation. *Biophys J*. 2014 Mar 18;106(6):L21-4. doi: 10.1016/j.bpj.2014.01.044.
- Li F, Ravetch JV. Apoptotic and antitumor activity of death receptor antibodies require inhibitory Fc γ receptor engagement. *Proc Natl Acad Sci U S A*. 2012 Jul 3;109(27):10966-71. doi: 10.1073/pnas.1208698109. Epub 2012 Jun 20.
- Lin JH. Applications and limitations of interspecies scaling and in vitro extrapolation in pharmacokinetics. *Drug Metab Dispos*. 1998 Dec;26(12):1202-12.
- Locksley RM, Killeen N, Lenardo MJ. The TNF and TNF receptor superfamilies: integrating mammalian biology. *Cell*. 2001 Feb 23;104(4):487-501.
- Loetscher H, Schlaeger EJ, Lahm HW, Pan YC, Lesslauer W, Brockhaus M. Purification and partial amino acid sequence analysis of two distinct tumor necrosis factor receptors from HL60 cells. *J Biol Chem*. 1990a Nov 25;265(33):20131-8.
- Loetscher H, Pan YC, Lahm HW, Gentz R, Brockhaus M, Tabuchi H, Lesslauer W. Molecular cloning and expression of the human 55 kd tumor necrosis factor receptor. *Cell*. 1990b Apr 20;61(2):351-9.
- Lou J, Geren I, Garcia-Rodriguez C, Forsyth CM, Wen W, Knopp K, Brown J, Smith T, Smith LA, Marks JD. Affinity maturation of human botulinum neurotoxin antibodies by light chain shuffling via yeast mating. *Protein Eng Des Sel*. 2010 Apr;23(4):311-9. doi: 10.1093/protein/gzq001. Epub 2010 Feb 15.
- Lügering A, Schmidt M, Lügering N, Pauels HG, Domschke W, Kucharzik T. Infliximab induces apoptosis in monocytes from patients with chronic active Crohn's disease by using a caspase-dependent pathway. *Gastroenterology*. 2001 Nov;121(5):1145-57.
- Luginbühl B, Kanyo Z, Jones RM, Fletterick RJ, Prusiner SB, Cohen FE, Williamson RA, Burton DR, Plückthun A. Directed evolution of an anti-prion protein scFv fragment to an affinity of 1 pM and its structural interpretation. *J Mol Biol*. 2006 Oct 13;363(1):75-97. Epub 2006 Jul 21.
- MacKenzie CR, Hiramata T, Deng SJ, Bundle DR, Narang SA, Young NM. Analysis by surface plasmon resonance of the influence of valence on the ligand binding affinity and kinetics of an anti-carbohydrate antibody. *J Biol Chem*. 1996 Jan 19;271(3):1527-33.
- Mager DE, Jusko WJ. General pharmacokinetic model for drugs exhibiting target-mediated drug disposition. *J Pharmacokinet Pharmacodyn*. 2001 Dec;28(6):507-32.
- Mahmood I. Application of allometric principles for the prediction of pharmacokinetics in human and veterinary drug development. *Adv Drug Deliv Rev*. 2007 Sep 30;59(11):1177-92. Epub 2007 Aug 16.
- Marcatili P, Rosi A, Tramontano A. PIGS: automatic prediction of antibody structures. *Bioinformatics*. 2008 Sep 1;24(17):1953-4. doi: 10.1093/bioinformatics/btn341. Epub 2008 Jul 19.
- Marino MW, Dunn A, Grail D, Inglese M, Noguchi Y, Richards E, Jungbluth A, Wada H, Moore M, Williamson B, Basu S, Old LJ. Characterization of tumor necrosis factor-deficient mice. *Proc Natl Acad Sci U S A*. 1997 Jul 22;94(15):8093-8.

- Marks JD, Griffiths AD, Malmqvist M, Clackson TP, Bye JM, Winter G. By-passing immunization: building high affinity human antibodies by chain shuffling. *Biotechnology (N Y)*. 1992 Jul;10(7):779-83.
- Medvedev AE, Espevik T, Ranges G, Sundan A. Distinct roles of the two tumor necrosis factor (TNF) receptors in modulating TNF and lymphotoxin alpha effects. *J Biol Chem*. 1996 Apr 19;271(16):9778-84.
- Mok CC, van der Kleij D, Wolbink GJ. Drug levels, anti-drug antibodies, and clinical efficacy of the anti-TNF α biologics in rheumatic diseases. *Clin Rheumatol*. 2013 Oct;32(10):1429-35. doi: 10.1007/s10067-013-2336-x. Epub 2013 Jul 26.
- Moore RJ, Owens DM, Stamp G, Arnott C, Burke F, East N, Holdsworth H, Turner L, Rollins B, Pasparakis M, Kollias G, Balkwill F. Mice deficient in tumor necrosis factor-alpha are resistant to skin carcinogenesis. *Nat Med*. 1999 Jul;5(7):828-31.
- Moore GL, Bautista C, Pong E, Nguyen DH, Jacinto J, Eivazi A, Muchhal US, Karki S, Chu SY, Lazar GA. A novel bispecific antibody format enables simultaneous bivalent and monovalent co-engagement of distinct target antigens. *MAbs*. 2011 Nov-Dec;3(6):546-57. doi: 10.4161/mabs.3.6.18123. Epub 2011 Nov 1.
- Moosmayer D, Dübel S, Brocks B, Watzka H, Hampp C, Scheurich P, Little M, Pfizenmaier K. A single-chain TNF receptor antagonist is an effective inhibitor of TNF mediated cytotoxicity. *Ther Immunol*. 1995 Feb;2(1):31-40.
- Mukai Y, Nakamura T, Yoshikawa M, Yoshioka Y, Tsunoda S, Nakagawa S, Yamagata Y, Tsutsumi Y. Solution of the structure of the TNF-TNFR2 complex. *Sci Signal*. 2010 Nov 16;3(148):ra83. doi: 10.1126/scisignal.2000954.
- Mukai Y, Nakamura T, Yoshioka Y, Shibata H, Abe Y, Nomura T, Taniai M, Ohta T, Nakagawa S, Tsunoda S, Kamada H, Yamagata Y, Tsutsumi Y. Fast binding kinetics and conserved 3D structure underlie the antagonistic activity of mutant TNF: useful information for designing artificial proteo-antagonists. *J Biochem*. 2009 Aug;146(2):167-72. doi: 10.1093/jb/mvp065. Epub 2009 Apr 22.
- Müssener A, Litton MJ, Lindroos E, Klareskog L. Cytokine production in synovial tissue of mice with collagen-induced arthritis (CIA). *Clin Exp Immunol*. 1997 Mar;107(3):485-93.
- Naismith JH, Devine TQ, Brandhuber BJ, Sprang SR. Crystallographic evidence for dimerization of unliganded tumor necrosis factor receptor. *J Biol Chem*. 1995 Jun 2;270(22):13303-7.
- Nomura T, Abe Y, Kamada H, Shibata H, Kayamuro H, Inoue M, Kawara T, Arita S, Furuya T, Yamashita T, Nagano K, Yoshikawa T, Yoshioka Y, Mukai Y, Nakagawa S, Taniai M, Ohta T, Serada S, Naka T, Tsunoda S, Tsutsumi Y. Therapeutic effect of PEGylated TNFR1-selective antagonistic mutant TNF in experimental autoimmune encephalomyelitis mice. *J Control Release*. 2011 Jan 5;149(1):8-14. doi: 10.1016/j.jconrel.2009.12.015. Epub 2009 Dec 24.
- Nygren H, Czerkinsky C, Stenberg M. Dissociation of antibodies bound to surface-immobilized antigen. *J Immunol Methods*. 1985 Dec 17;85(1):87-95.
- O'Malley WE, Achinstein B, Shear MJ. Action of bacterial polysaccharide on tumors. II. Damage of sarcoma 37 by serum of mice treated with *Serratia marcescens* polysaccharide, and induced tolerance. *Nutr Rev*. 1988 Nov;46(11):389-91. *Journal of the National Cancer Institute, Vol. 29, 1962:*
- O'Rourke KP, O'Donoghue G, Adams C, Mulcahy H, Molloy C, Silke C, Molloy M, Shanahan F, O'Gara F. High levels of Lymphotoxin-Beta (LT-Beta) gene expression in rheumatoid arthritis synovium: clinical and cytokine correlations. *Rheumatol Int*. 2008 Aug;28(10):979-86. doi: 10.1007/s00296-008-0574-z. Epub 2008 Apr 1.
- Oshima H, Ishikawa T, Yoshida GJ, Naoi K, Maeda Y, Naka K, Ju X, Yamada Y, Minamoto T, Mukaida N, Saya H, Oshima M. TNF- α /TNFR1 signaling promotes gastric tumorigenesis through induction of Nox1 and Gna14 in tumor cells. *Oncogene*. 2014 Jul 17;33(29):3820-9. doi: 10.1038/onc.2013.356. Epub 2013 Aug 26.

- Pasparakis M, Alexopoulou L, Episkopou V, Kollias G. Immune and inflammatory responses in TNF alpha-deficient mice: a critical requirement for TNF alpha in the formation of primary B cell follicles, follicular dendritic cell networks and germinal centers, and in the maturation of the humoral immune response. *J Exp Med*. 1996 Oct 1;184(4):1397-411.
- Pennica D, Nedwin GE, Hayflick JS, Seeburg PH, Derynck R, Palladino MA, Kohr WJ, Aggarwal BB, Goeddel DV. Human tumour necrosis factor: precursor structure, expression and homology to lymphotoxin. *Nature*. 1984 Dec 20-1985 Jan 2;312(5996):724-9.
- Perelson AS, Oster GF. Theoretical studies of clonal selection: minimal antibody repertoire size and reliability of self-non-self discrimination. *J Theor Biol*. 1979 Dec 21;81(4):645-70.
- Pfeffer K, Matsuyama T, Kündig TM, Wakeham A, Kishihara K, Shahinian A, Wiegmann K, Ohashi PS, Krönke M, Mak TW. Mice deficient for the 55 kd tumor necrosis factor receptor are resistant to endotoxic shock, yet succumb to *L. monocytogenes* infection. *Cell*. 1993 May 7;73(3):457-67.
- Picarella DE, Kratz A, Li CB, Ruddle NH, Flavell RA. Insulinitis in transgenic mice expressing tumor necrosis factor beta (lymphotoxin) in the pancreas. *Proc Natl Acad Sci U S A*. 1992 Nov 1;89(21):10036-40.
- Pinckard JK, Sheehan KC, Arthur CD, Schreiber RD. Constitutive shedding of both p55 and p75 murine TNF receptors in vivo. *J Immunol*. 1997 Apr 15;158(8):3869-73.
- Powell MB, Mitchell D, Lederman J, Buckmeier J, Zamvil SS, Graham M, Ruddle NH, Steinman L. Lymphotoxin and tumor necrosis factor-alpha production by myelin basic protein-specific T cell clones correlates with encephalitogenicity. *Int Immunol*. 1990;2(6):539-44.
- Probert L, Akassoglou K, Pasparakis M, Kontogeorgos G, Kollias G. Spontaneous inflammatory demyelinating disease in transgenic mice showing central nervous system-specific expression of tumor necrosis factor alpha. *Proc Natl Acad Sci U S A*. 1995 Nov 21;92(24):11294-8.
- Ramos-Casals M, Brito-Zerón P, Muñoz S, Soria N, Galiana D, Bertolaccini L, Cuadrado MJ, Khamashta MA. Autoimmune diseases induced by TNF-targeted therapies: analysis of 233 cases. *Medicine (Baltimore)*. 2007 Jul;86(4):242-51.
- Ranzinger J, Krippner-Heidenreich A, Haraszi T, Bock E, Tepperink J, Spatz JP, Scheurich P. Nanoscale arrangement of apoptotic ligands reveals a demand for a minimal lateral distance for efficient death receptor activation. *Nano Lett*. 2009 Dec;9(12):4240-5. doi: 10.1021/nl902429b.
- Razani B, Reichardt AD, Cheng G. Non-canonical NF- κ B signaling activation and regulation: principles and perspectives. *Immunol Rev*. 2011 Nov;244(1):44-54. doi: 10.1111/j.1600-065X.2011.01059.x.
- Richter F, Liebig T, Guenzi E, Herrmann A, Scheurich P, Pfizenmaier K, Kontermann RE. Antagonistic TNF receptor one-specific antibody (ATROSAB): receptor binding and in vitro bioactivity. *PLoS One*. 2013 Aug 19;8(8):e72156. doi: 10.1371/journal.pone.0072156. eCollection 2013.
- Rini JM, Schulze-Gahmen U, Wilson IA. Structural evidence for induced fit as a mechanism for antibody-antigen recognition. *Science*. 1992 Feb 21;255(5047):959-65.
- Robak T1, Gladalska A, Stepień H. The tumour necrosis factor family of receptors/ligands in the serum of patients with rheumatoid arthritis. *Eur Cytokine Netw*. 1998 Jun;9(2):145-54.
- Robin G, Sato Y, Desplancq D, Rochel N, Weiss E, Martineau P. Restricted diversity of antigen binding residues of antibodies revealed by computational alanine scanning of 227 antibody-antigen complexes. *J Mol Biol*. 2014 Nov 11;426(22):3729-43. doi: 10.1016/j.jmb.2014.08.013. Epub 2014 Aug 29.
- Roebuck KA. Regulation of interleukin-8 gene expression. *J Interferon Cytokine Res*. 1999 May;19(5):429-38.
- Romas E, Gillespie MT, Martin TJ. Involvement of receptor activator of NFkappaB ligand and tumor necrosis factor-alpha in bone destruction in rheumatoid arthritis. *Bone*. 2002 Feb;30(2):340-6.
- Root-Bernstein R. Rethinking Molecular Mimicry in Rheumatic Heart Disease and Autoimmune Myocarditis: Laminin, Collagen IV, CAR, and B1AR as Initial Targets of Disease. *Front Pediatr*. 2014 Aug 19;2:85. doi: 10.3389/fped.2014.00085. eCollection 2014.
- Rosenblum H, Amital H. Anti-TNF therapy: safety aspects of taking the risk. *Autoimmun Rev*. 2011 Jul;10(9):563-8. doi: 10.1016/j.autrev.2011.04.010. Epub 2011 May 5.

- Rothe J, Lesslauer W, Lötscher H, Lang Y, Koebel P, Köntgen F, Althage A, Zinkernagel R, Steinmetz M, Bluethmann H. Mice lacking the tumour necrosis factor receptor 1 are resistant to TNF-mediated toxicity but highly susceptible to infection by *Listeria monocytogenes*. *Nature*. 1993 Aug 26;364(6440):798-802.
- Roux KH, Strelets L, Michaelsen TE. Flexibility of human IgG subclasses. *J Immunol*. 1997 Oct 1;159(7):3372-82.
- Sacca R, Cuff CA, Lesslauer W, Ruddle NH. Differential activities of secreted lymphotoxin-alpha3 and membrane lymphotoxin-alpha1beta2 in lymphotoxin-induced inflammation: critical role of TNF receptor 1 signaling. *J Immunol*. 1998 Jan 1;160(1):485-91.
- Saphire EO, Stanfield RL, Crispin MD, Parren PW, Rudd PM, Dwek RA, Burton DR, Wilson IA. Contrasting IgG structures reveal extreme asymmetry and flexibility. *J Mol Biol*. 2002 May 24;319(1):9-18.
- Schiattino I, Villegas R, Cruzat A, Cuenca J, Salazar L, Aravena O, Pesce B, Catalán D, Llanos C, Cuchacovich M, Aguillón JC. Multiple imputation procedures allow the rescue of missing data: an application to determine serum tumor necrosis factor (TNF) concentration values during the treatment of rheumatoid arthritis patients with anti-TNF therapy. *Biol Res*. 2005;38(1):7-12.
- Schier R, Bye J, Apell G, McCall A, Adams GP, Malmqvist M, Weiner LM, Marks JD. Isolation of high-affinity monomeric human anti-c-erbB-2 single chain Fv using affinity-driven selection. *J Mol Biol*. 1996 Jan 12;255(1):28-43.
- Schlapschy M, Binder U, Börger C, Theobald I, Wachinger K, Kisling S, Haller D, Skerra A. PASylation: a biological alternative to PEGylation for extending the plasma half-life of pharmaceutically active proteins. *Protein Eng Des Sel*. 2013 Aug;26(8):489-501. doi: 10.1093/protein/gzt023. Epub 2013 Jun 10.
- Shakoor N, Michalska M, Harris CA, Block JA. Drug-induced systemic lupus erythematosus associated with etanercept therapy. *Lancet*. 2002 Feb 16;359(9306):579-80.
- Shear MJ, Turner FC. Chemical treatment of tumors. V. Isolation of the hemorrhage-producing fraction from *Serratia marcescens* (*Bacillus prodigiosus*) culture filtrate. *J. Natl Cancer Inst*. 1943 4;81-97
- Shibata H, Yoshioka Y, Ohkawa A, Minowa K, Mukai Y, Abe Y, Taniai M, Nomura T, Kayamuro H, Nabeshi H, Sugita T, Imai S, Nagano K, Yoshikawa T, Fujita T, Nakagawa S, Yamamoto A, Ohta T, Hayakawa T, Mayumi T, Vandenabeele P, Aggarwal BB, Nakamura T, Yamagata Y, Tsunoda S, Kamada H, Tsutsumi Y. Creation and X-ray structure analysis of the tumor necrosis factor receptor-1-selective mutant of a tumor necrosis factor-alpha antagonist. *J Biol Chem*. 2008a Jan 11;283(2):998-1007. Epub 2007 Nov 14.
- Shibata H, Yoshioka Y, Ohkawa A, Abe Y, Nomura T, Mukai Y, Nakagawa S, Taniai M, Ohta T, Mayumi T, Kamada H, Tsunoda S, Tsutsumi Y. The therapeutic effect of TNFR1-selective antagonistic mutant TNF-alpha in murine hepatitis models. *Cytokine*. 2008b Nov;44(2):229-33. doi: 10.1016/j.cyto.2008.07.003. Epub 2008 Sep 23.
- Shields RL, Namenuk AK, Hong K, Meng YG, Rae J, Briggs J, Xie D, Lai J, Stadlen A, Li B, Fox JA, Presta LG. High resolution mapping of the binding site on human IgG1 for Fc gamma RI, Fc gamma RII, Fc gamma RIII, and FcRn and design of IgG1 variants with improved binding to the Fc gamma R. *J Biol Chem*. 2001 Mar 2;276(9):6591-604. Epub 2000 Nov 28.
- Siegel RM, Frederiksen JK, Zacharias DA, Chan FK, Johnson M, Lynch D, Tsien RY, Lenardo MJ. Fas preassociation required for apoptosis signaling and dominant inhibition by pathogenic mutations. *Science*. 2000 Jun 30;288(5475):2354-7.
- Siegel RM, Muppidi JR, Sarker M, Lobito A, Jen M, Martin D, Straus SE, Lenardo MJ. SPOTS: signaling protein oligomeric transduction structures are early mediators of death receptor-induced apoptosis at the plasma membrane. *J Cell Biol*. 2004 Nov 22;167(4):735-44.
- Sosnick TR, Benjamin DC, Novotny J, Seeger PA, Trehwella J. Distances between the antigen-binding sites of three murine antibody subclasses measured using neutron and X-ray scattering. *Biochemistry*. 1992 Feb 18;31(6):1779-86.

- Steeland S, Puimège L, Vandenbroucke RE, Van Hauwermeiren F, Haustraete J, Devoogdt N, Hulpiau P, Leroux-Roels G, Laukens D, Meuleman P, De Vos M, Libert C. Generation and characterization of small single domain antibodies inhibiting human TNF receptor 1. *J Biol Chem*. 2014 Dec 23. pii: jbc.M114.617787. [Epub ahead of print]
- Steidl S1, Ratsch O, Brocks B, Dürr M, Thomassen-Wolf E. In vitro affinity maturation of human GM-CSF antibodies by targeted CDR-diversification. *Mol Immunol*. 2008 Nov;46(1):135-44. doi: 10.1016/j.molimm.2008.07.013. Epub 2008 Aug 21.
- Stork R, Campigna E, Robert B, Müller D, Kontermann RE. Biodistribution of a bispecific single-chain diabody and its half-life extended derivatives. *J Biol Chem*. 2009 Sep 18;284(38):25612-9. doi: 10.1074/jbc.M109.027078. Epub 2009 Jul 23.
- Suen WE, Bergman CM, Hjelmström P, Ruddle NH. A critical role for lymphotoxin in experimental allergic encephalomyelitis. *J Exp Med*. 1997 Oct 20;186(8):1233-40.
- Tack CJ, Kleijwegt FS, Van Riel PL, Roep BO. Development of type 1 diabetes in a patient treated with anti-TNF-alpha therapy for active rheumatoid arthritis. *Diabetologia*. 2009 Jul;52(7):1442-4. doi: 10.1007/s00125-009-1381-0. Epub 2009 May 14.
- Takahashi Y, Kasahara T, Sawai T, Rikimaru A, Mukaida N, Matsushima K, Sasaki T. The participation of IL-8 in the synovial lesions at an early stage of rheumatoid arthritis. *Tohoku J Exp Med*. 1999 May;188(1):75-87.
- Tam SH, McCarthy SG, Brosnan K, Goldberg KM, Scallon BJ. Correlations between pharmacokinetics of IgG antibodies in primates vs. FcRn-transgenic mice reveal a rodent model with predictive capabilities. *MAbs*. 2013 May-Jun;5(3):397-405. doi: 10.4161/mabs.23836. Epub 2013 Apr 2.
- Tang P, Hung M-C, Klostergaard J. Human pro-tumor necrosis factor is a homotrimer. *Biochemistry*. 1996 Jun 25;35(25):8216-25.
- Tang W, Lu Y, Tian QY, Zhang Y, Guo FJ, Liu GY, Syed NM, Lai Y, Lin EA, Kong L, Su J, Yin F, Ding AH, Zanin-Zhorov A, Dustin ML, Tao J, Craft J, Yin Z, Feng JQ, Abramson SB, Yu XP, Liu CJ. The growth factor progranulin binds to TNF receptors and is therapeutic against inflammatory arthritis in mice. *Science*. 2011 Apr 22;332(6028):478-84. doi: 10.1126/science.1199214. Epub 2011 Mar 10.
- Telliez JB, Xu GY, Woronicz JD, Hsu S, Wu JL, Lin L, Sukits SF, Powers R, Lin LL. Mutational analysis and NMR studies of the death domain of the tumor necrosis factor receptor-1. *J Mol Biol*. 2000 Jul 28;300(5):1323-33.
- ten Hove T, van Montfrans C, Peppelenbosch MP, van Deventer SJ. Infliximab treatment induces apoptosis of lamina propria T lymphocytes in Crohn's disease. *Gut*. 2002 Feb;50(2):206-11.
- Thie H, Voedisch B, Dübel S, Hust M, Schirrmann T. Affinity maturation by phage display. *Methods Mol Biol*. 2009;525:309-22, xv. doi: 10.1007/978-1-59745-554-1_16.
- Thoma B, Grell M, Pfizenmaier K, Scheurich P. Identification of a 60-kD tumor necrosis factor (TNF) receptor as the major signal transducing component in TNF responses. *J Exp Med*. 1990 Oct 1;172(4):1019-23.
- Tracey KJ, Fong Y, Hesse DG, Manogue KR, Lee AT, Kuo GC, Lowry SF, Cerami A. Anti-cachectin/TNF monoclonal antibodies prevent septic shock during lethal bacteraemia. *Nature*. 1987 Dec 17-23;330(6149):662-4.
- Unverdorben F, Färber-Schwarz A, Richter F, Hutt M, Kontermann RE. Half-life extension of a single-chain diabody by fusion to domain B of staphylococcal protein A. *Protein Eng Des Sel*. 2012 Feb;25(2):81-8. doi: 10.1093/protein/gzr061. Epub 2012 Jan 11.
- Vaitaitis GM, Wagner DH Jr. CD40 glycoforms and TNF-receptors 1 and 2 in the formation of CD40 receptor(s) in autoimmunity. *Mol Immunol*. 2010 Aug;47(14):2303-13. doi: 10.1016/j.molimm.2010.05.288. Epub 2010 Jun 19.
- Valley CC, Lewis AK, Mudaliar DJ, Perlmutter JD, Braun AR, Karim CB, Thomas DD, Brody JR, Sachs JN. Tumor necrosis factor-related apoptosis-inducing ligand (TRAIL) induces death receptor 5 networks that are highly organized. *J Biol Chem*. 2012 Jun 15;287(25):21265-78. doi: 10.1074/jbc.M111.306480. Epub 2012 Apr 10.

- van der Heijde D, Breedveld FC, Kavanaugh A, Keystone EC, Landewé R, Patra K, Pangan AL. Disease activity, physical function, and radiographic progression after longterm therapy with adalimumab plus methotrexate: 5-year results of PREMIER. *J Rheumatol*. 2010 Nov;37(11):2237-46. doi: 10.3899/jrheum.100208. Epub 2010 Oct 1.
- Van Hauwermeiren F1, Vandenbroucke RE, Libert C. Treatment of TNF mediated diseases by selective inhibition of soluble TNF or TNFR1. *Cytokine Growth Factor Rev*. 2011 Oct-Dec;22(5-6):311-9. doi: 10.1016/j.cytogfr.2011.09.004. Epub 2011 Oct 1.
- van Regenmortel MH, Azimzadeh A. Determination of antibody affinity. *J Immunoassay*. 2000 May-Aug;21(2-3):211-34.
- Vande Castele N, Gils A. Pharmacokinetics of anti-TNF monoclonal antibodies in inflammatory bowel disease: Adding value to current practice. *J Clin Pharmacol*. 2015 Mar;55 Suppl 3:S39-50. doi: 10.1002/jcph.374.
- Verhelst K1, Carpentier I, Beyaert R. Regulation of TNF-induced NF- κ B activation by different cytoplasmic ubiquitination events. *Cytokine Growth Factor Rev*. 2011 Oct-Dec;22(5-6):277-86. doi: 10.1016/j.cytogfr.2011.11.002. Epub 2011 Nov 25.
- Vierboom MP, Jonker M, Tak PP, 't Hart BA. Preclinical models of arthritic disease in non-human primates. *Drug Discov Today*. 2007 Apr;12(7-8):327-35. Epub 2007 Mar 8.
- Wagner KW, Punnoose EA, Januario T, Lawrence DA, Pitti RM, Lancaster K, Lee D, von Goetz M, Yee SF, Totpal K, Huw L, Katta V, Cavet G, Hymowitz SG, Amler L, Ashkenazi A. Death-receptor O-glycosylation controls tumor-cell sensitivity to the proapoptotic ligand Apo2L/TRAIL. *Nat Med*. 2007 Sep;13(9):1070-7. Epub 2007 Sep 2.
- Wajant H, Pfizenmaier K, Scheurich P. Tumor necrosis factor signaling. *Cell Death Differ*. 2003 Jan;10(1):45-65.
- Walczak H. TNF and ubiquitin at the crossroads of gene activation, cell death, inflammation, and cancer. *Immunol Rev*. 2011 Nov;244(1):9-28. doi: 10.1111/j.1600-065X.2011.01066.x.
- Wallis RS. Tumour necrosis factor antagonists: structure, function, and tuberculosis risks. *Lancet Infect Dis*. 2008 Oct;8(10):601-11. doi: 10.1016/S1473-3099(08)70227-5.
- Wang W, Ye W, Yu Q, Jiang C, Zhang J, Luo R, Chen HF. Conformational selection and induced fit in specific antibody and antigen recognition: SPE7 as a case study. *J Phys Chem B*. 2013 May 2;117(17):4912-23. doi: 10.1021/jp4010967. Epub 2013 Apr 12.
- White AL1, Chan HT, French RR, Beers SA, Cragg MS, Johnson PW, Glennie MJ. Fc γ RIIB controls the potency of agonistic anti-TNFR mAbs. *Cancer Immunol Immunother*. 2013 May;62(5):941-8. doi: 10.1007/s00262-013-1398-6. Epub 2013 Mar 31.
- Willcocks LC, Smith KG, Clatworthy MR. Low-affinity Fc γ receptors, autoimmunity and infection. *Expert Rev Mol Med*. 2009 Aug 13;11:e24. doi: 10.1017/S1462399409001161.
- Wilson NS, Dixit V, Ashkenazi A. Death receptor signal transducers: nodes of coordination in immune signaling networks. *Nat Immunol*. 2009 Apr;10(4):348-55. doi: 10.1038/ni.1714. Epub 2009 Mar 19.
- Winkel C, Neumann S, Surulescu C, Scheurich P. A minimal mathematical model for the initial molecular interactions of death receptor signalling. *Math Biosci Eng*. 2012 Jul;9(3):663-83. doi: 10.3934/mbe.2012.9.663.
- Wojtal KA, Rogler G, Scharl M, Biedermann L, Frei P, Fried M, Weber A, Eloranta JJ, Kullak-Ublick GA, Vavricka SR. Fc gamma receptor CD64 modulates the inhibitory activity of infliximab. *PLoS One*. 2012;7(8):e43361. doi: 10.1371/journal.pone.0043361. Epub 2012 Aug 24.
- Workman LM, Habelhah H. TNFR1 signaling kinetics: spatiotemporal control of three phases of IKK activation by posttranslational modification. *Cell Signal*. 2013 Aug;25(8):1654-64. doi: 10.1016/j.cellsig.2013.04.005. Epub 2013 Apr 21.
- Wu H, Beuerlein G, Nie Y, Smith H, Lee BA, Hensler M, Huse WD, Watkins JD. Stepwise in vitro affinity maturation of Vitaxin, an α beta3-specific humanized mAb. *Proc Natl Acad Sci U S A*. 1998 May 26;95(11):6037-42.

- Xanthoulea S, Pasparakis M, Kousteni S, Brakebusch C, Wallach D, Bauer J, Lassmann H, Kollias G. Tumor necrosis factor (TNF) receptor shedding controls thresholds of innate immune activation that balance opposing TNF functions in infectious and inflammatory diseases. *J Exp Med*. 2004 Aug 2;200(3):367-76.
- Xu J, Chakrabarti AK, Tan JL, Ge L, Gambotto A, Vujanovic NL. Essential role of the TNF-TNFR2 cognate interaction in mouse dendritic cell-natural killer cell crosstalk. *Blood*. 2007 Apr 15;109(8):3333-41. Epub 2006 Dec 12.
- Yang WP, Green K, Pinz-Sweeney S, Briones AT, Burton DR, Barbas CF 3rd. CDR walking mutagenesis for the affinity maturation of a potent human anti-HIV-1 antibody into the picomolar range. *J Mol Biol*. 1995 Dec 1;254(3):392-403.
- Zahnd C1, Sarkar CA, Plückthun A. Computational analysis of off-rate selection experiments to optimize affinity maturation by directed evolution. *Protein Eng Des Sel*. 2010 Apr;23(4):175-84. doi: 10.1093/protein/gzp087. Epub 2010 Feb 3.
- Zettlitz KA, Lorenz V, Landauer K, Münkler S, Herrmann A, Scheurich P, Pfizenmaier K, Kontermann R. ATROSAB, a humanized antagonistic anti-tumor necrosis factor receptor one-specific antibody. *MAbs*. 2010 Nov-Dec;2(6):639-47. Epub 2010 Nov 1.
- Zettlitz KA, 2010, Dissertation. Engineered Antibodies for the Therapy of Cancer and Inflammatory Disease. Institute of Cellbiology and Immunology, University of Stuttgart. Dissertation 2010.
- Zganiacz A, Santosuosso M, Wang J, Yang T, Chen L, Anzulovic M, Alexander S, Gicquel B, Wan Y, Bramson J, Inman M, Xing Z. TNF-alpha is a critical negative regulator of type 1 immune activation during intracellular bacterial infection. *J Clin Invest*. 2004 Feb;113(3):401-13.
- Zhao Z, Worthylake D, LeCour L Jr, Maresh GA, Pincus SH. Crystal structure and computational modeling of the fab fragment from a protective anti-ricin monoclonal antibody. *PLoS One*. 2012;7(12):e52613. doi: 10.1371/journal.pone.0052613. Epub 2012 Dec 19.
- Zhou Y, Goenaga AL, Harms BD, Zou H, Lou J, Conrad F, Adams GP, Schoeberl B, Nielsen UB, Marks JD. Impact of intrinsic affinity on functional binding and biological activity of EGFR antibodies. *Mol Cancer Ther*. 2012 Jul;11(7):1467-76. doi: 10.1158/1535-7163.MCT-11-1038. Epub 2012 May 7.
- Zidi I, Bouaziz A, Mnif W, Bartegi A, Ben Amor N. Golimumab and malignancies: true or false association? *Med Oncol*. 2011 Jun;28(2):641-8. doi: 10.1007/s12032-010-9490-7. Epub 2010 Apr 7.

7. Sequences

7.1. Legend

DNA-Sequence:	Black or red (special regions), small letters
Changed Nucleotides:	Red, capital letters
Amino Acid-Sequence:	Green, capital letters
Restriction Sites:	Blue
Eliminated Restriction Sites:	Grey with asterisk
Abbreviations:	Igk-Leader (Leader peptide of the IgG kappa light chain), huTNFR1 (human TNF Receptor 1), CRD (Cystein rich domain), Stem (stem region of the TNFR1, next to the membrane), Hinge (flexible region of the IgG molecule), CH1-3 (constant domains 1 to 3 of the IgG heavy chain), moTNFR2_ecd (extracellular domain of the mouse TNF receptor 2), scFv (single chain fragment variable), VL (variable domain of the light chain), VH (variable domain of the heavy chain), CLk (constant domain of the IgG kappa light chain), HSA (human serum albumin), CDR H1/L3 (complementarity determining region 1 to 3 of either heavy or light chain), EMP1 (EPO mimetic peptide)

7.2. Human TNFR1-Fc mutants

```

                                Igk-Leader
                                +-+-----
                                AgeI
1  atg gag aca gac aca ctc ctg cta tgg gta ctg ctg tgg gtt cca ggt tcc acc ggt ctg gtc
   M  E  T  D  T  L  L  L  W  V  L  L  L  W  V  P  G  S  T  G  L  V
                                >>.....>
Mutant (amino acid)                V14L                I21V    P23S Q24K
Mutant (nucleic acid)                gtT                Gtc    AGt Aaa
67  cct cac cta ggc gat cgg gag aag aga gat agt gtg tgt ccc caa gga aaa tat atc cac cct caa
   P  H  L  G  D  R  E  K  R  D  S  V  C  P  Q  G  K  Y  I  H  P  Q
   >.....N-terminal peptide.....>> >>.....CRD1.....>>

```

```

                                                    XmaI
                                                    --+----
Mutant
Mutant
133  aat aat tcg att tgc tgt aca aag tgc cac aaa gga acc tac ttg tat aat gac tgt cca ggc ccg
    N  N  S  I  C  C  T  K  C  H  K  G  T  Y  L  Y  N  D  C  P  G  P
    >.....CRD1.....>

                PstI
                -+-----
Mutant  Q48R          D51V          S57K  S59T          E64Q  H66Y  R68A
Mutant  cGg          gTc          gAG   Acc          CaG   Tac   GCa
199  ggg cag gat acg gac tgc agg gag tgt gag agc ggc tcc ttc acc gct tca gaa aac cac ctc aga
    G  Q  D  T  D  C  R  E  C  E  S  G  S  F  T  A  S  E  N  H  L  R
    >.....CRD1.....>> >>.....CRD2.....>

                                BglII
                                +-----
Mut.H69Q
Mut. caG
Mut.H69A  L71A S72A  S74K K75T          G81S          S87P  T89Q_V90A
Mut. GCT  GCc GCc  AAG aCa          TCC          Cct  CAa gCT
265  cac tgc ctc agc tgc tcc aaa tgc cga aag gaa atg ggt cag cag gtg gag atc tct tct tgc aca gtg
    H  C  L  S  C  S  K  C  R  K  E  M  G  Q  V  E  I  S  S  C  T  V
    >.....CRD2.....>

Mutant  R92K
Mutant  AAg
331  gac cgg gac acc gtg tgt ggc tgt agg aag aac cag tac cgg cat tat tgg agt gaa aac ctt ttc
    D  R  D  T  V  C  G  C  R  K  N  Q  Y  R  H  Y  W  S  E  N  L  F
    >.....CRD2.....>> >>.....CRD3.....>

397  cag tgc ttc aat tgc agc ctc tgc ctc aat ggg acc gtg cac ctc tcc tgc cag gag aaa cag aat
    Q  C  F  N  C  S  L  C  L  N  G  T  V  H  L  S  C  Q  E  K  Q  N
    >.....CRD3.....>

463  acc gtg tgc acc tgc cat gca ggt ttc ttt cta aga gaa aac gag tgt gtc tcc tgt agt aac tgt
    T  V  C  T  C  H  A  G  F  F  L  R  E  N  E  C  V  S  C  S  N  C
    >....CRD3....>> >>.....CRD4.....>

529  aag aaa agc ctg gag tgc acg aag ttg tgc cta ccc cag att gag aat gtt aag ggc act gag gac
    K  K  S  L  E  C  T  K  L  C  L  P  Q  I  E  N  V  K  G  T  E  D
    >.....CRD4.....>> >>.....stem.....>

                NotI
                -+-----
595  tca ggt acc aca gcg gcc gca gac aaa act cac aca tgc cca ccg tgc cca gca cct gaa ctc ctg
    S  G  T  T  A  A  A  D  K  T  H  T  C  P  P  C  P  A  P  E  L  L
    >....stem....>> >>.....hinge.....>> >>.....CH2.....>

661  ggg gga ccg tca gtc ttc ctc ttc ccc cca aaa ccc aag gac acc ctc atg atc tcc cgg acc cct
    G  G  P  S  V  F  L  F  P  P  K  P  K  D  T  L  M  I  S  R  T  P
    >.....CH2.....>

727  gag gtc aca tgc gtg gtg gtg gac gtg agc cac gaa gac cct gag gtc aag ttc aac tgg tac gtg
    E  V  T  C  V  V  V  D  V  S  H  E  D  P  E  V  K  F  N  W  Y  V
    >.....CH2.....>

793  gac ggc gtg gag gtg cat aat gcc aag aca aag ccg cgg gag gag cag tac aac agc acg tac cgg
    D  G  V  E  V  H  N  A  K  T  K  P  R  E  E  Q  Y  N  S  T  Y  R
    >.....CH2.....>

859  gtg gtc agc gtc ctc acc gtc ctg cac cag gac tgg ctg aat ggc aag gag tac aag tgc aag gtc
    V  V  S  V  L  T  V  L  H  Q  D  W  L  N  G  K  E  Y  K  C  K  V
    >.....CH2.....>

925  tcc aac aaa gcc ctc cca gcc ccc atc gag aaa acc atc tcc aaa gcc aaa ggg cag ccc cga gaa
    S  N  K  A  L  P  A  P  I  E  K  T  I  S  K  A  K  G  Q  P  R  E
    >.....CH2.....>> >>.....CH3.....>

                XmaI
                -+-----
991  cca cag gtg tac acc ctg ccc cca tcc cgg gag gag atg acc aag aac cag gtc agc ctg acc tgc
    P  Q  V  Y  T  L  P  P  S  R  E  E  M  T  K  N  Q  V  S  L  T  C
    >.....CH3.....>

```



```

1057 ctg gtc aaa ggc ttc tat ccc agc gac atc gcc gtg gag tgg gag agc aat ggg cag ccg gag aac
      L V K G F Y P S D I A V E W E S N G Q P E N
      >.....CH3.....>
1123 aac tac aag acc acg cct ccc gtg ctg gac tcc gac ggc tcc ttc ttc ctc tat agc aag ctc acc
      N Y K T T P P V L D S D G S F F L Y S K L T
      >.....CH3.....>
1189 gtg gac aag agc agg tgg cag cag ggg aac gtc ttc tca tgc tcc gtg atg cat gag gct ctg cac
      V D K S R W Q Q G N V F S C S V M H E A L H
      >.....CH3.....>
1255 aac cac tac acg cag aag agc ctc tcc ctg tct ccg ggt aaa taa
      N H Y T Q K S L S L S P G K -
      >.....CH3.....>>

```

7.3. moTNFR2-Fc

```

                                     Igk-Leader
                                     AgeI
                                     -+-----
1  atg gag aca gac aca ctc ctg cta tgg gta ctg ctg ctc tgg gtt cca ggt tcc acc ggt gtg ccc
      M E T D T L L L W V L L L W V P G S T G V P
                                     moTNFR2_ecd >>.....>
67 gcc cag gtt gtc ttg aca ccc tac aaa ccg gaa cct ggg tac gag tgc cag atc tca cag gaa tac
      A Q V V L T P Y K P E P G Y E C Q I S Q E Y
      >..... moTNFR2_ecd.....>
133 tat gac agg aag gct cag atg tgc tgt gct aag tgt cct cct ggc caa tat gtg aaa cat ttc tgc
      Y D R K A Q M C C A K C P P G Q Y V K H F C
      >..... moTNFR2_ecd.....>
199 aac aag acc tcg gac acc gtg tgt gcg gac tgt gag gca agc atg tat acc cag gtc tgg aac cag
      N K T S D T V C A D C E A S M Y T Q V W N Q
      >..... moTNFR2_ecd.....>
265 ttt cgt aca tgt ttg agc tgc agt tct tcc tgt acc act gac cag gtg gag atc cgc gcc tgc act
      F R T C L S C S S C T T D Q V E I R A C T
      >..... moTNFR2_ecd.....>
331 aaa cag cag aac cga gtg tgt gct tgc gaa gct ggc agg tac tgc gcc ttg aaa acc cat tct ggc
      K Q Q N R V C A C E A G R Y C A L K T H S G
      >..... moTNFR2_ecd.....>
397 agc tgt cga cag tgc atg agg ctg agc aag tgc ggc cct ggc ttc gga gtg gcc agt tca aga gcc
      S C R Q C M R L S K C G P G F G V A S S R A
      >..... moTNFR2_ecd.....>
463 cca aat gga aat gtg cta tgc aag gcc tgt gcc cca ggg acg ttc tct gac acc aca tca tcc act
      P N G N V L C K A C A P G T F S D T T S S T
      >..... moTNFR2_ecd.....>
529 gat gtg tgc agg ccc cac cgc atc tgt agc atc ctg gct att ccc gga aat gca agc aca gat gca
      D V C R P H R I C S I L A I P G N A S T D A
      >..... moTNFR2_ecd.....>
595 gtc tgt gcg ccc gag tcc cca act cta agt gcc atc cca agg aca ctc tac gta tct cag cca gag
      V C A P E S P T L S A I P R T L Y V S Q P E
      >..... moTNFR2_ecd.....>
661 ccc aca aga tcc caa ccc ctg gat caa gag cca ggg ccc agc caa act cca agc atc ctt aca tcg
      P T R S Q P L D Q E P G P S Q T P S I L T S
      >..... moTNFR2_ecd.....>
                                     NotI
                                     --+-----
727 ttg ggt tca acc ccc att att gaa caa agt acc aag ggt gcc gcg gcc gca
      L G S T P I I E Q S T K G G A A A
      >..... moTNFR2_ecd.....>>

```

7.4. scFvIZI06.1-Fc

```

      NheI*
      +-+-----
      XbaI*
      +-+-----
1  tgg cta gac acc atg gag aca gac aca ctc ctg cta tgg gta ctg ctg ctc tgg gtt cca ggt tcc
   W  L  D  T  M  E  T  D  T  L  L  L  W  V  L  L  L  W  V  P  G  S
67  acc ggt cag gtt cag ctg gtt cag agc ggt gcg gaa gtg aaa aaa ccg ggc agc agc gtg aaa gtg
   T  G  Q  V  Q  L  V  Q  S  G  A  E  V  K  K  P  G  S  S  V  K  V
   >>.....scFv_IZI06.1.....>>
133 agc tgc aaa gct agc ggc tat acc ttt acc gat ttc tac att aac tgg gtg cgt cag gca ccc ggg
   S  C  K  A  S  G  Y  T  F  T  D  F  Y  I  N  W  V  R  Q  A  P  G
   >.....scFv_IZI06.1.....>
199 cag ggc ctg gaa tgg att ggc gaa att tat ccg tat agc ggc cat gca tat tac aac gaa aaa ttc
   Q  G  L  E  W  I  G  E  I  Y  P  Y  S  G  H  A  Y  Y  N  E  K  F
   >.....scFv_IZI06.1.....>
265 aaa gcg cgt gtg acc att acc gcg gat aaa agc acc agc acc gcg tat atg gaa ctg agc agc ctg
   K  A  R  V  T  I  T  A  D  K  S  T  S  T  A  Y  M  E  L  S  S  L
   >.....scFv_IZI06.1.....>
331 cgt agc gaa gat acc gcg gtg tat tat tgc gcg cgt tgg gat ttt ctg gat tat tgg ggc cag ggc
   R  S  E  D  T  A  V  Y  Y  C  A  R  W  D  F  L  D  Y  W  G  Q  G
   >.....scFv_IZI06.1.....>
397 acc acc gtt acg gtc tcg agt ggt gga ggc ggt tca ggc gga ggt ggc tct ggc ggt agt gca caa
   T  T  V  T  V  S  S  G  G  G  G  S  G  G  G  G  S  G  G  S  A  Q
   >.....scFv_IZI06.1.....>
463 gat att gtg atg acc cag agc ccg ctg tct ctg ccg gtc acg ccg ggt gaa ccg gcg agc att agc
   D  I  V  M  T  Q  S  P  L  S  L  P  V  T  P  G  E  P  A  S  I  S
   >.....scFv_IZI06.1.....>
529 tgc cgt agc agc cag agc ctg ctg cat agc aac ggc aac acc tat ctg cat tgg tat ctg cag aaa
   C  R  S  S  Q  S  L  L  H  S  N  G  N  T  Y  L  H  W  Y  L  Q  K
   >.....scFv_IZI06.1.....>
595 ccg ggc cag agc ccg cag ctg ctg att tat acc gtg agc aac cgt ttt agc ggc gtg ccg gat cgc
   P  G  Q  S  P  Q  L  L  I  Y  T  V  S  N  R  F  S  G  V  P  D  R
   >.....scFv_IZI06.1.....>
661 ttt agc gga tcc ggt agc ggc acc gat ttt acc ctg aaa att agc cgt gtg gaa gcg gaa gat gtg
   F  S  G  S  G  S  G  T  D  F  T  L  K  I  S  R  V  E  A  E  D  V
   >.....scFv_IZI06.1.....>
727 ggc gtg tat tat tgc agc cag agc acc cat gtg ccg tat acc ttt ggc ggt ggc acc aaa gtg gaa
   G  V  Y  Y  C  S  Q  S  T  H  V  P  Y  T  F  G  G  G  T  K  V  E
   >.....scFv_IZI06.1.....>

      NotI
      +-+-----
793 att aaa cgt ggc ggt tca ggc gga gcg gcc gca
   I  K  R  G  G  S  G  G  A  A  A
   >.....>>

```

7.5. IgG-FabL Light Chain

```

      HindIII
      +-+-----
1  aag ctt gcc gcc acc atg gag aca gac aca ctc ctg cta tgg gta ctg ctg ctc tgg gtt cca ggt
   K  L  A  A  T  M  E  T  D  T  L  L  L  W  V  L  L  L  W  V  P  G
      AgeI
      +-+-----
67  tcc acc ggt gat att gtg atg acc cag agc ccg ctg tct ctg ccg gtc acg ccg ggt gaa ccg gcg
   S  T  G  D  I  V  M  T  Q  S  P  L  S  L  P  V  T  P  G  E  P  A
   >>.....VL.....>>

```

```

133 agc att agc tgc cgt agc agc cag agc ctg ctg cat agc aac ggc aac acc tat ctg cat tgg tat
    S I S C R S S Q S L L H S N G N T Y L H W Y
    >.....VL.....>

199 ctg cag aaa ccg ggc cag agc ccg cag ctg ctg att tat acc gtg agc aac cgt ttt agc ggc gtg
    L Q K P G Q S P Q L L I Y T V S N R F S G V
    >.....VL.....>

265 ccg gat cgc ttt agc ggc agc ggt agc ggc acc gat ttt acc ctg aaa att agc cgt gtg gaa gcg
    P D R F S G S G S G T D F T L K I S R V E A
    >.....VL.....>

331 gaa gat gtg ggc gtg tat tat tgc agc cag agc acc cat gtg ccg tat acc ttt ggc ggt ggc acc
    E D V G V Y Y C S Q S T H V P Y T F G G G T
    >.....VL.....>

397 aaa gtg gaa att aaa cgt acc gtt gct gcg cca tct gtc ttc atc ttc ccg cca tct gat gag cag
    K V E I K R T V A A P S V F I F P P S D E Q
    >.....VL.....>>>.....CLk.....>

463 ttg aaa tct gga act gcc tct gtt gtg tgc ctg ctg aat aac ttc tat ccc aga gag gcc aaa gta
    L K S G T A S V V C L L N N F Y P R E A K V
    >.....CLk.....>

529 cag tgg aag gtg gat aac gcc ctc caa tcg ggt aac tcc cag gag agt gtc aca gag cag gac agc
    Q W K V D N A L Q S G N S Q E S V T E Q D S
    >.....CLk.....>

595 aag gac agc acc tac agc ctc agc agc acc ctg acg ctg agc aaa gca gac tac gag aaa cac aaa
    K D S T Y S L S S T L T L S K A D Y E K H K
    >.....CLk.....>

661 gtc tac gcc tgc gaa gtc acc cat cag ggc ctg agc tcg ccc gtc aca aag agc ttc aac agg ggt
    V Y A C E V T H Q G L S S P V T K S F N R G
    >.....CLk.....>>>

                                RsrII
                                -+-----
727 ggg agc gga ggg agc ggc gga cgg acc gtt gct gcg cca tct gtc ttc atc ttc ccg cca tct gat
    G S G G S G G R T V A A P S V F I F P P S D
    >.....linker.....>>>.....CLk.....>

793 gag cag ttg aaa tct gga act gcc tct gtt gtg tgc ctg ctg aat aac ttc tat ccc aga gag gcc
    E Q L K S G T A S V V C L L N N F Y P R E A
    >.....CLk.....>

859 aaa gta cag tgg aag gtg gat aac gcc ctc caa tcg ggt aac tcc cag gag agt gtc aca gag cag
    K V Q W K V D N A L Q S G N S Q E S V T E Q
    >.....CLk.....>

925 gac agc aag gac agc acc tac agc ctc agc agc acc ctg acg ctg agc aaa gca gac tac gag aaa
    D S K D S T Y S L S S T L T L S K A D Y E K
    >.....CLk.....>

991 cac aaa gtc tac gcc tgc gaa gtc acc cat cag ggc ctg agc tcg ccc gtc aca aag agc ttc aac
    H K V Y A C E V T H Q G L S S P V T K S F N
    >.....CLk.....>

                                EcoRI
                                -+-----
1057 agg gga gag tgt taa gaa ttc
     R G E C - E F
    >....CLk.....>>

```

7.6. gG-FabL Heavy Chain

```

HindIII
-+-----
1 aag ctt gcc gcc acc atg gag aca gac aca ctc ctg cta tgg gta ctg ctg ctc tgg gtt cca ggt
  K L A A T M E T D T L L L W V L L L W V P G
                                Igk-Leader

```

```

      AgeI
    +-----
67  tcc acc ggt cag gtg cag ctg gtg cag agc gga gcc gag gtg aag aag ccc ggc agc tcc gtc aag
    S T G Q V Q L V Q S G A E V K K P G S S V K
    >>.....VHIZI06.1.....>

133  gtg tcc tgc aag gcc agc ggc tac acc ttc acc gac ttc tac atc aac tgg gtg cgc cag gtg cca
    V S C K A S G Y T F T D F Y I N W V R Q V P
    >.....VHIZI06.1.....>

199  gga cag gga ctg gag tgg atc ggc gag atc tac ccc tac agc ggc cac gcc tac tac aac gag aag
    G Q G L E W I G E I Y P Y S G H A Y Y N E K
    >.....VHIZI06.1.....>

265  ttc aag gcc aga gtg acc atc acc gcc gac aag agc acc agc acc gcc tac atg gaa ctg tcc agc
    F K A R V T I T A D K S T S T A Y M E L S S
    >.....VHIZI06.1.....>

331  ctg aga agc gag gac acc gcc gtg tac tac tgc gcc aga tgg gac ttc ctg gac tac tgg gga cag
    L R S E D T A V Y Y C A R W D F L D Y W G Q
    >.....VHIZI06.1.....>

397  ggc acc acc gtg aca gtc tgc agc gcc agc acc aag ggc ccc agc gtg ttc ccc ctg gcc ccc agc
    G T T V T V S S A S T K G P S V F P L A P S
    >.....VHIZI06.1.....>> >>.....CH1.....>

463  agc aag agc acc tcc ggc ggc aca gcc gcc ctg ggc tgc ctg gtg aag gac tac ttc ccc gag ccc
    S K S T S G G T A A L G C L V K D Y F P E P
    >.....CH1.....>

529  gtg acc gtg tcc tgg aac agc gga gcc ctg acc agc ggc gtg cac acc ttc ccc gcc gtg ctg cag
    V T V S W N S G A L T S G V H T F P A V L Q
    >.....CH1.....>

595  agc agc ggc ctg tac agc ctg tcc agc gtg gtg acc gtg cca agc agc agc ctg gga acc cag acc
    S S G L Y S L S S V V T V P S S S L G T Q T
    >.....CH1.....>

661  tac atc tgc aac gtg aac cac aag ccc agc aac acc aag gtg gac aag aag gtg gga ggg agc ggc
    Y I C N V N H K P S N T K V D K K V G G S G
    >.....CH1.....>> >>..linker....>

      NheI
    +-----
727  ggt agc ggc gga gct agc acc aag ggc ccc agc gtg ttc ccc ctg gcc ccc agc agc aag agc acc
    G S G G A S T K G P S V F P L A P S S K S T
    >...linker...>> >>.....CH1.....>

793  tcc ggc ggc aca gcc gcc ctg ggc tgc ctg gtg aag gac tac ttc ccc gag ccc gtg acc gtg tcc
    S G G T A A L G C L V K D Y F P E P V T V S
    >.....CH1.....>

859  tgg aac agc gga gcc ctg acc agc ggc gtg cac acc ttc ccc gcc gtg ctg cag agc agc ggc ctg
    W N S G A L T S G V H T F P A V L Q S S G L
    >.....CH1.....>

925  tac agc ctg tcc agc gtg gtg acc gtg cca agc agc agc ctg gga acc cag acc tac atc tgc aac
    Y S L S S V V T V P S S S L G T Q T Y I C N
    >.....CH1.....>

991  gtg aac cac aag ccc agc aac acc aag gtg gac aag aag gtg gag ccc aag agc tgc gac aag acc
    V N H K P S N T K V D K K V E P K S C D K T
    >.....CH1.....>> >>.....Hinge.....>

1057  cac acc tgt cca cca tgc cca gcc ccc cca gtg gcc gga ccc tcc gtg ttc ctg ttc ccc ccc aag
    H T C P P C P A P P V A G P S V F L F P P K
    >.....Hinge.....>> >>.....CH2.....>

1123  ccc aag gac acc ctg atg atc agc agg acc ccc gag gtg acc tgc gtg gtg gtg gac gtg tcc cac
    P K D T L M I S R T P E V T C V V V D V S H
    >.....CH2.....>

1189  gag gac cca gag gtg aag ttc aat tgg tat gtg gac ggc gtg gag gtg cac aac gcc aag acc aag
    E D P E V K F N W Y V D G V E V H N A K T K
    >.....CH2.....>

```

```

1255 ccc aga gag gaa cag tac aac agc acc tac agg gtg gtg tcc gtg ctg acc gtg ctg cac cag gac
    P R E E Q Y N S T Y R V V S V L T V L H Q D
    >.....CH2.....>
1321 tgg ctg aac ggc aag gaa tac aag tgc aag gtc tcc aac aag ggc ctg ccc agc tcc atc gaa aag
    W L N G K E Y K C K V S N K G L P S S I E K
    >.....CH2.....>
1387 acc atc agc aag gcc aag ggc cag cca cgg gag ccc cag gtg tac acc ctg ccc ccc tcc cgg gac
    T I S K A K G Q P R E P Q V Y T L P P S R D
    >.....CH2.....>> >>.....CH3.....>
1453 gag ctg acc aag aac cag gtg tcc ctg acc tgt ctg gtg aag ggc ttc tac ccc agc gac atc gcc
    E L T K N Q V S L T C L V K G F Y P S D I A
    >.....CH3.....>
1519 gtg gag tgg gag agc aac ggc cag ccc gag aac aac tac aag acc acc ccc cct gtg ctg gac agc
    V E W E S N G Q P E N N Y K T T P P V L D S
    >.....CH3.....>
1585 gac ggc agc ttc ttc ctg tac agc aag ctg acc gtg gac aag agc agg tgg cag cag ggc aac gtg
    D G S F F L Y S K L T V D K S R W Q Q G N V
    >.....CH3.....>
1651 ttc tcc tgc agc gtg atg cac gag gcc ctg cac aac cac tac acc cag aag agc ctg agc ctg tcc
    F S C S V M H E A L H N H Y T Q K S L S L S
    >.....CH3.....>

                EcoRI
                +-+-----
1717 ccc ggc aaa taa gaa ttc att g
    P G K - E F I
    >...CH3...>>

```

7.7. FabATR Light Chain

```

HindIII
+-+-----
1 aag ctt gcc gcc acc atg gag aca gac aca ctc ctg cta tgg gta ctg ctg ctc tgg gtt cca ggt
    K L A A T M E T D T L L L W V L L L W V P G
                                Igk-Leader

                AgeI
                +-+-----
67 tcc acc ggt gat att gtg atg acc cag agc ccg ctg tct ctg ccg gtc acg ccg ggt gaa ccg gcg
    S T G D I V M T Q S P L S L P V T P G E P A
    >>.....VL-IZI06.1.....>

133 agc att agc tgc cgt agc agc cag agc ctg ctg cat agc aac ggc aac acc tat ctg cat tgg tat
    S I S C R S S Q S L L H S N G N T Y L H W Y
    >.....VL-IZI06.1.....>

199 ctg cag aaa ccg ggc cag agc ccg cag ctg ctg att tat acc gtg agc aac cgt ttt agc ggc gtg
    L Q K P G Q S P Q L L I Y T V S N R F S G V
    >.....VL-IZI06.1.....>

265 ccg gat cgc ttt agc ggc agc ggt agc ggc acc gat ttt acc ctg aaa att agc cgt gtg gaa gcg
    P D R F S G S G S G T D F T L K I S R V E A
    >.....VL-IZI06.1.....>

331 gaa gat gtg ggc gtg tat tat tgc agc cag agc acc cat gtg ccg tat acc ttt ggc ggt ggc acc
    E D V G V Y Y C S Q S T H V P Y T F G G G T
    >.....VL-IZI06.1.....>

                RsrII
                +-+-----
397 aaa gtg gaa att aaa cgg acc gtt gct gcg cca tct gtc ttc atc ttc ccg cca tct gat gag cag
    K V E I K R T V A A P S V F I F P P S D E Q
    >.....VL-IZI06.1.....>> >>.....CLk.....>

463 ttg aaa tct gga act gcc tct gtt gtg tgc ctg ctg aat aac ttc tat ccc aga gag gcc aaa gta
    L K S G T A S V V C L L N N F Y P R E A K V
    >.....CLk.....>

```

```

529  cag tgg aag gtg gat aac gcc ctc caa tcg ggt aac tcc cag gag agt gtc aca gag cag gac agc
      Q  W  K  V  D  N  A  L  Q  S  G  N  S  Q  E  S  V  T  E  Q  D  S
      >.....CLk.....>
595  aag gac agc acc tac agc ctc agc agc acc ctg acg ctg agc aaa gca gac tac gag aaa cac aaa
      K  D  S  T  Y  S  L  S  S  T  L  T  L  S  K  A  D  Y  E  K  H  K
      >.....CLk.....>
661  gtc tac gcc tgc gaa gtc acc cat cag ggc ctg agc tcg ccc gtc aca aag agc ttc aac agg gga
      V  Y  A  C  E  V  T  H  Q  G  L  S  S  P  V  T  K  S  F  N  R  G
      >.....CLk.....>

      EcoRI
      -+-----
727  gag tgt taa gaa ttc
      E  C  -  E  F
      >.....>>

```

7.8. FabATR Heavy Chain

```

HindIII
-+-----
1  aag ctt gcc gcc acc atg gag aca gac aca ctc ctg cta tgg gta ctg ctg ctc tgg gtt cca ggt
   K  L  A  A  T  M  E  T  D  T  L  L  L  W  V  L  L  L  W  V  P  G
                                     Igk-Leader

      AgeI
      -+-----
67  tcc acc ggt cag gtg cag ctg gtg cag agc gga gcc gag gtg aag aag ccc ggc agc tcc gtc aag
   S  T  G  Q  V  Q  L  V  Q  S  G  A  E  V  K  K  P  G  S  S  V  K
      >>.....VH-IZI06.1.....>

133  gtg tcc tgc aag gcc agc ggc tac acc ttc acc gac ttc tac atc aac tgg gtg cgc cag gtg cca
   V  S  C  K  A  S  G  Y  T  F  T  D  F  Y  I  N  W  V  R  Q  V  P
      >.....VH-IZI06.1.....>

199  gga cag gga ctg gag tgg atc ggc gag atc tac ccc tac agc ggc cac gcc tac tac aac gag aag
   G  Q  G  L  E  W  I  G  E  I  Y  P  Y  S  G  H  A  Y  Y  N  E  K
      >.....VH-IZI06.1.....>

265  ttc aag gcc aga gtg acc atc acc gcc gac aag agc acc agc acc gcc tac atg gaa ctg tcc agc
   F  K  A  R  V  T  I  T  A  D  K  S  T  S  T  A  Y  M  E  L  S  S
      >.....VH-IZI06.1.....>

331  ctg aga agc gag gac acc gcc gtg tac tac tgc gcc aga tgg gac ttc ctg gac tac tgg gga cag
   L  R  S  E  D  T  A  V  Y  Y  C  A  R  W  D  F  L  D  Y  W  G  Q
      >.....VH-IZI06.1.....>

397  ggc acc acc gtg aca gtc tcg agc gcc agc acc aag ggc ccc agc gtg ttc ccc ctg gcc ccc agc
   G  T  T  V  T  V  S  S  A  S  T  K  G  P  S  V  F  P  L  A  P  S
      >.....VH-IZI06.1.....>>>.....CH1-IZI06.1.....>

463  agc aag agc acc tcc ggc ggc aca gcc gcc ctg ggc tgc ctg gtg aag gac tac ttc ccc gag ccc
   S  K  S  T  S  G  G  T  A  A  L  G  C  L  V  K  D  Y  F  P  E  P
      >.....CH1-IZI06.1.....>

529  gtg acc gtg tcc tgg aac agc gga gcc ctg acc agc ggc gtg cac acc ttc ccc gcc gtg ctg cag
   V  T  V  S  W  N  S  G  A  L  T  S  G  V  H  T  F  P  A  V  L  Q
      >.....CH1-IZI06.1.....>

595  agc agc ggc ctg tac agc ctg tcc agc gtg gtg acc gtg cca agc agc agc ctg gga acc cag acc
   S  S  G  L  Y  S  L  S  S  V  V  T  V  P  S  S  S  L  G  T  Q  T
      >.....CH1-IZI06.1.....>

661  tac atc tgc aac gtg aac cac aag ccc agc aac acc aag gtg gac aag aag gtg gag ccc aag agc
   Y  I  C  N  V  N  H  K  P  S  N  T  K  V  D  K  K  V  E  P  K  S
      >.....CH1-IZI06.1.....>

      EcoRI
      -+-----
727  tgc taa gaa ttc
      C  -  E  F
      >>>

```

7.9. 2scFv-HSA

```

                                Igk-leader
                                -+-----
                                AgeI
                                -+-----
1  atg gag aca gac aca ctc ctg cta tgg gta ctg ctg ctc tgg gtt cca ggt tcc acc ggt cag gtt
   M E T D T L L L W V L L L W V P G S T G Q V
   >>.....>

67  cag ctg gtt cag agc ggt gcg gaa gtg aaa aaa ccg ggc agc agc gtg aaa gtg agc tgc aaa gct
   Q L V Q S G A E V K K P G S S V K V S C K A
   >.....scFvIZI06.1.....>

133 agc ggc tat acc ttt acc gat ttc tac att aac tgg gtg cgt cag gca ccc ggg cag ggc ctg gaa
   S G Y T F T D F Y I N W V R Q A P G Q G L E
   >.....scFvIZI06.1.....>

199 tgg att ggc gaa att tat ccg tat agc ggc cat gca tat tac aac gaa aaa ttc aaa gcg cgt gtg
   W I G E I Y P Y S G H A Y Y N E K F K A R V
   >.....scFvIZI06.1.....>

265 acc att acc gcg gat aaa agc acc agc acc gcg tat atg gaa ctg agc agc ctg cgt agc gaa gat
   T I T A D K S T S T A Y M E L S S L R S E D
   >.....scFvIZI06.1.....>

331 acc gcg gtg tat tat tgc gcg cgt tgg gat ttt ctg gat tat tgg ggc cag ggc acc acc gtt acg
   T A V Y Y C A R W D F L D Y W G Q G T T V T
   >.....scFvIZI06.1.....>

397 gtc tcg agt ggt gga ggc ggt tca ggc gga ggt ggc tct ggc ggt agt gca caa gat att gtg atg
   V S S G G G S G G G G S G G S A Q D I V M
   >.....scFvIZI06.1.....>

463 acc cag agc ccg ctg tct ctg ccg gtc acg ccg ggt gaa ccg gcg agc att agc tgc cgt agc agc
   T Q S P L S L P V T P G E P A S I S C R S S
   >.....scFvIZI06.1.....>

529 cag agc ctg ctg cat agc aac ggc aac acc tat ctg cat tgg tat ctg cag aaa ccg ggc cag agc
   Q S L L H S N G N T Y L H W Y L Q K P G Q S
   >.....scFvIZI06.1.....>

595 ccg cag ctg ctg att tat acc gtg agc aac cgt ttt agc ggc gtg ccg gat cgc ttt agc gga tcc
   P Q L L I Y T V S N R F S G V P D R F S G S
   >.....scFvIZI06.1.....>

661 ggt agc ggc acc gat ttt acc ctg aaa att agc cgt gtg gaa gcg gaa gat gtg ggc gtg tat tat
   G S G T D F T L K I S R V E A E D V G V Y Y
   >.....scFvIZI06.1.....>

                                                SalI*
                                                -+----
                                                XhoI*
                                                -+----
727 tgc agc cag agc acc cat gtg ccg tat acc ttt ggc ggt ggc acc aaa gtg gaa att aaa cgg tcg
   C S Q S T H V P Y T F G G G T K V E I K R S
   >.....scFvIZI06.1.....>>>

--
--
793 agt ggt gga tca ggc ggt gat gca cac aag agt gag gtt gct cat cgg ttt aaa gat ttg gga gaa
   S G G S G G D A H K S E V A H R F K D L G E
   >.....linker.....>>.....HSA.....>

859 gaa aat ttc aaa gcc ttg gtg ttg att gcc ttt gct cag tat ctt cag cag tgt cca ttt gaa gat
   E N F K A L V L I A F A Q Y L Q Q C P F E D
   >.....HSA.....>

925 cat gta aaa tta gtg aat gaa gta act gaa ttt gca aaa aca tgt gtt gct gat gag tca gct gaa
   H V K L V N E V T E F A K T C V A D E S A E
   >.....HSA.....>

991 aat tgt gac aaa tca ctt cat acc ctt ttt gga gac aaa tta tgc aca gtt gca act ctt cgt gaa
   N C D K S L H T L F G D K L C T V A T L R E
   >.....HSA.....>

```

```

1057 acc tat ggt gaa atg gct gac tgc tgt gca aaa caa gaa cct gag aga aat gaa tgc ttc ttg caa
    T Y G E M A D C C A K Q E P E R N E C F L Q
    >.....HSA.....>
1123 cac aaa gat gac aac cca aac ctc ccc cga ttg gtg aga cca gag gtt gat gtg atg tgc act gct
    H K D D N P N L P R L V R P E V D V M C T A
    >.....HSA.....>
1189 ttt cat gac aat gaa gag aca ttt ttg aaa aaa tac tta tat gaa att gcc aga aga cat cct tac
    F H D N E E T F L K K Y L Y E I A R R H P Y
    >.....HSA.....>
1255 ttt tat gcc ccg gaa ctc ctt ttc ttt gct aaa agg tat aaa gct gct ttt aca gaa tgt tgc caa
    F Y A P E L L F F A K R Y K A A F T E C C Q
    >.....HSA.....>
1321 gct gct gat aaa gct gcc tgc ctg ttg cca aag ctc gat gaa ctt cgg gat gaa ggg aag gct tcg
    A A D K A A C L L P K L D E L R D E G K A S
    >.....HSA.....>
1387 tct gcc aaa cag aga ctc aag tgt gcc agt ctc caa aaa ttt gga gaa aga gct ttc aaa gca tgg
    S A K Q R L K C A S L Q K F G E R A F K A W
    >.....HSA.....>
1453 gca gta gct cgc ctg agc cag aga ttt ccc aaa gct gag ttt gca gaa gtt tcc aag tta gtg aca
    A V A R L S Q R F P K A E F A E V S K L V T
    >.....HSA.....>
1519 gat ctt acc aaa gtc cac acg gaa tgc tgc cat gga gat ctg ctt gaa tgt gct gat gac agg gcg
    D L T K V H T E C C H G D L L E C A D D R A
    >.....HSA.....>
1585 gac ctt gcc aag tat atc tgt gaa aat caa gat tcg atc tcc agt aaa ctg aag gaa tgc tgt gaa
    D L A K Y I C E N Q D S I S S K L K E C C E
    >.....HSA.....>
1651 aaa cct ctg ttg gaa aaa tcc cac tgc att gcc gaa gtg gaa aat gat gag atg cct gct gac ttg
    K P L L E K S H C I A E V E N D E M P A D L
    >.....HSA.....>
1717 cct tca tta gct gct gat ttt gtt gaa agt aag gat gtt tgc aaa aac tat gct gag gca aag gat
    P S L A A D F V E S K D V C K N Y A E A K D
    >.....HSA.....>
1783 gtc ttc ctg ggc atg ttt ttg tat gaa tat gca aga agg cat cct gat tac tct gtc gtg ctg ctg
    V F L G M F L Y E Y A R R H P D Y S V V L L
    >.....HSA.....>
1849 ctg aga ctt gcc aag aca tat gaa acc act cta gag aag tgc tgt gcc gct gca gat cct cat gaa
    L R L A K T Y E T T L E K C C A A A D P H E
    >.....HSA.....>
1915 tgc tat gcc aaa gtg ttc gat gaa ttt aaa cct ctt gtg gaa gag cct cag aat tta atc aaa caa
    C Y A K V F D E F K P L V E E P Q N L I K Q
    >.....HSA.....>
1981 aat tgt gag ctt ttt gag cag ctt gga gag tac aaa ttc cag aat gcg cta tta gtt cgt tac acc
    N C E L F E Q L G E Y K F Q N A L L V R Y T
    >.....HSA.....>
2047 aag aaa gta ccc caa gtg tca act cca act ctt gta gag gtc tca aga aac cta gga aaa gtg ggc
    K K V P Q V S T P T L V E V S R N L G K V G
    >.....HSA.....>
2113 agc aaa tgt tgt aaa cat cct gaa gca aaa aga atg ccc tgt gca gaa gac tat cta tcc gtg gtc
    S K C C K H P E A K R M P C A E D Y L S V V
    >.....HSA.....>
2179 ctg aac cag tta tgt gtg ttg cat gag aaa acg cca gta agt gac aga gtc acc aaa tgc tgc aca
    L N Q L C V L H E K T P V S D R V T K C C T
    >.....HSA.....>
2245 gaa tcc ttg gtg aac agg cga cca tgc ttt tca gct ctg gaa gtc gat gaa aca tac gtt ccc aaa
    E S L V N R R P C F S A L E V D E T Y V P K
    >.....HSA.....>

```



```

2311 gag ttt aat gct gaa aca ttc acc ttc cat gca gat ata tgc aca ctt tct gag aag gag aga caa
    E F N A E T F T F H A D I C T L S E K E R Q
    >.....HSA.....>
2377 atc aag aaa caa act gca ctt gtt gag ctt gtg aaa cac aag ccc aag gca aca aaa gag caa ctg
    I K K Q T A L V E L V K H K P K A T K E Q L
    >.....HSA.....>
2443 aaa gct gtt atg gat gat ttc gca gct ttt gta gag aag tgc tgc aag gct gac gat aag gag acc
    K A V M D D F A A F V E K C C K A D D K E T
    >.....HSA.....>
                                           BspEI
                                           -+-
2509 tgc ttt gcc gag gag ggt aaa aaa ctt gtt gct gca agt caa gct gcc ggt ggc agc ggt ggg tcc
    C F A E E G K K L V A A S Q A A G G S G G S
    >.....HSA.....>> >>.....linker.....>
    ---
2575 gga cag gtt cag ctg gtt cag agc ggt gcg gaa gtg aaa aaa ccg gcc agc agc gtg aaa gtg agc
    G Q V Q L V Q S G A E V K K P G S S V K V S
    >>> >>.....scFvIZI06.1.....>
2641 tgc aaa gct agc gcc tat acc ttt acc gat ttc tac att aac tgg gtg cgt cag gca ccc ggg cag
    C K A S G Y T F T D F Y I N W V R Q A P G Q
    >.....scFvIZI06.1.....>
2707 ggc ctg gaa tgg att ggc gaa att tat ccg tat agc ggc cat gca tat tac aac gaa aaa ttc aaa
    G L E W I G E I Y P Y S G H A Y Y N E K F K
    >.....scFvIZI06.1.....>
2773 gcg cgt gtg acc att acc gcg gat aaa agc acc agc acc gcg tat atg gaa ctg agc agc ctg cgt
    A R V T I T A D K S T S T A Y M E L S S L R
    >.....scFvIZI06.1.....>
2839 agc gaa gat acc gcg gtg tat tat tgc gcg cgt tgg gat ttt ctg gat tat tgg gcc cag gcc acc
    S E D T A V Y Y C A R W D F L D Y W G Q G T
    >.....scFvIZI06.1.....>
2905 acc gtt acg gtc tcg agt ggt gga gcc ggt tca gcc gga ggt gcc tct gcc ggt agt gca caa gat
    T V T V S S G G G G S G G G G S G G S A Q D
    >.....scFvIZI06.1.....>
2971 att gtg atg acc cag agc ccg ctg tct ctg ccg gtc acg ccg ggt gaa ccg gcg agc att agc tgc
    I V M T Q S P L S L P V T P G E P A S I S C
    >.....scFvIZI06.1.....>
3037 cgt agc agc cag agc ctg ctg cat agc aac gcc aac acc tat ctg cat tgg tat ctg cag aaa ccg
    R S S Q S L L H S N G N T Y L H W Y L Q K P
    >.....scFvIZI06.1.....>
3103 ggc cag agc ccg cag ctg ctg att tat acc gtg agc aac cgt ttt agc gcc gtg ccg gat cgc ttt
    G Q S P Q L L I Y T V S N R F S G V P D R F
    >.....scFvIZI06.1.....>
3169 agc gga tcc ggt agc gcc acc gat ttt acc ctg aaa att agc cgt gtg gaa gcg gaa gat gtg gcc
    S G S G S G T D F T L K I S R V E A E D V G
    >.....scFvIZI06.1.....>
3235 gtg tat tat tgc agc cag agc acc cat gtg ccg tat acc ttt gcc ggt gcc acc aaa gtg gaa att
    V Y Y C S Q S T H V P Y T F G G G T K V E I
    >.....scFvIZI06.1.....>
                                           NotI
                                           -+-----
3301 aaa cgt gcg gcc gcc cac cat cat cac cat cac taa
    K R A A A H H H H H H -
    >.....>> >>.....His-Tag.....>>

```

7.10. scFvIG11

```

                                           pelB Leader
                                           -+-----
1 atg aaa tac cta ttg cct acg gca gcc gct gga ttg tta tta ctc gcg gcc cag ccg gcc atg gcc
  m k y l l p t a a a g l l l l a a q p a m a

```

```

67  cag gtt cag ctg gtt cag agc ggt gcg gaa gtg aaa aaa ccg ggc agc agc gtg aaa gtg agc tgc
    q v q l v q s g a e v k k p g s s v k v s c
    >>.....VH-IG11.....>

                                CDR H1
133  aaa gct agc ggc tat acc ttt acc gat ttc tac att aac tgg gtg cgt cag gca ccc ggg cag ggc
    k a s g y t f t d f y i n w v r q a p g q g
    >.....VH-IG11.....>

                                CDR H2
199  ctg gaa tgg att ggc gag att gtg ccg acg cag ggc gag gca aag tac aac gat aaa ttc aaa gcg
    l e w i g e i v p t q g e a k y n d k f k a
    >.....VH-IG11.....>

265  cgt gtg acc att acc gcg gat aaa agc acc agc acc gcg tat atg gaa ctg agc agc ctg cgt agc
    r v t i t a d k s t s t a y m e l s s l r s
    >.....VH-IG11.....>

                                CDR H3
331  gaa gat acc gcg gtg tat tat tgc gcg cgt tgg gat ttt ctg gat tat tgg ggc cag ggc acc acc
    e d t a v y y c a r w d f l d y w g q g t t
    >.....VH-IG11.....>

397  gtt acg gtc tcg agt ggt gga ggc ggt tca ggc gga ggt ggc tct ggc ggt agt gca caa gat att
    v t v s s g g g g s g g g s g g s a q d i
    >.....VH-IG11.....>>>.....Linker.....>>>

463  gtg atg acc cag agc ccg ctg tct ctg ccg gtc acg ccg ggt gaa ccg gcg agc att agc tgc cgt
    v m t q s p l s l p v t p g e p a s i s c r
    >.....VL-IG11.....>

                                CDR L1
529  agc agc cag agc ctg ctg cat agc aac ggc aac acc tat ctg cat tgg tat ctg cag aaa ccg ggc
    s s q s l l h s n g n t y l h w y l q k p g
    >.....VL-IG11.....>

                                CDR L2
595  cag agc ccg cag ctg ctg att tat acc gtg agc aac cgt ttt agc ggc gtg ccg gat cgc ttt agc
    q s p q l l i y t v s n r f s g v p d r f s
    >.....VL-IG11.....>

661  gga tcc ggt agc ggc acc gat ttt acc ctg aaa att agc cgt gtg gaa gcg gaa gat gtg ggc gtg
    g s g s g t d f t l k i s r v e a e d v g v
    >.....VL-IG11.....>

                                CDR L3
727  tat tat tgc agc cag agc acc cat gtg ccg tat acc ttt ggc ggt ggc acc aaa gtg gaa att aaa
    y y c s q s t h v p y t f g g g t k v e i k
    >.....VL-IG11.....>

                                NotI
                                ---+-----
793  cgt gcg gcc gca gaa caa aaa ctc atc tca gaa gag gat ctg aat ggg gcc gca cat cac cat cat
    r a a a e q k l i s e e d l n g a a h h h h
    >>>.....myc tag.....>>>.....His tag...>

                                EcoRI
                                ---+-----
859  cac cat taa taa gaa ttc
    h h - -
    >.....>>

```

7.11. scFvIG11-fsSTOP

```

                                pelB Leader
                                ---+-----
1   atg aaa tac cta ttg cct acg gca gcc gct gga ttg tta tta ctc gcg gcc cag ccg gcc atg gcc
    M K Y L L P T A A A G L L L L A A Q P A M A

                                NcoI
                                ---+-----
67  cag gtt cag ctg gtt cag agc ggt gcg gaa gtg aaa aaa ccg ggc agc agc gtg aaa gtg agc tgc
    Q V Q L V Q S G A E V K K P G S S V K V S C
    >>.....VH-IG11.....>

```

```

133 aaa gct agc ggc tat acc ttt acc gat ttc tac att aac tgg gtg cgt cag gca ccc ggg cag ggc
    K A S G Y T F T D F Y I N W V R Q A P G Q G
    >.....VH-IG11.....>

199 ctg gaa tgg att ggc gag att gtg ccg acg cag ggc gag gca aag tac aac gat aaa ttc aaa gcg
    L E W I G E I V P T Q G E A K Y N D K F K A
    >.....VH-IG11.....>

265 cgt gtg acc att acc gcg gat aaa agc acc agc acc gcg tat atg gaa ctg agc agc ctg cgt agc
    R V T I T A D K S T S T A Y M E L S S L R S
    >.....VH-IG11.....>

                                          BstZ17I
                                          ----+----

331 gaa gat acc gcg gtg tat tat tgc gcg cgt tgg gat ttt ctg gat taa gg gtg ccg tat acc ttt
    E D T A V Y Y C A R W D F L D - V P Y T F
    >.....VH-IG11.....>> >>...VL-IG11.....>

                                          NotI
                                          ---+-----

396 ggc ggt ggc acc aaa gtg gaa att aaa cgt gcg gcc gca cat cat cat cac cat cac ggg gcc gca
    G G G T K V E I K R A A A H H H H H H G A A
    >.....VL-IG11.....>> >>.....His-tag.....>>

                                          Amber STOP

462 gaa caa aaa ctc atc tca gaa gag gat ctg aat ggg gcc gca tag act gtt gaa agt tgt tta gca
    E Q K L I S E E D L N G A A - T V E S C L A
    >>.....myc-tag.....>> >>...Phage Protein g3...>

```

7.12. scFvT12B

```

                                          pelB Leader
                                          -+-----
1 atg aaa tac cta ttg cct acg gca gcc gct gga ttg tta tta ctc gcg gcc cag ccg gcc atg gcc
    M K Y L L P T A A A G L L L L A A Q P A M A

67 cat gtt cag ctg gtt cag agc ggt gcg gaa gtg aaa aaa ccg gcc agc agc gtg aaa gtg agc tgc
    H V Q L V Q S G A E V K K P G S S V K V S C
    >>.....VH-T12B.....>>

                                          CDR H1
133 aaa gct agc ggc tat acc ttt acc gat ttc tac att aac tgg gtg cgt cag gca ccc ggg cag ggc
    K A S G Y T F T D F Y I N W V R Q A P G Q G
    >.....VH-T12B.....>>

                                          CDR H2
199 ctg gaa tgg att ggc gag att gtg ccg tcg cag ggc gag gca aag tac aac gat aaa ttc aaa gcg
    L E W I G E I V P S Q G E A K Y N D K F K A
    >.....VH-T12B.....>>

265 cgt gtg acc att acc gcg gat aaa agc acc agc acc gcg tat atg gaa ctg agc agc ctg cgt agc
    R V T I T A D K S T S T A Y M E L S S L R S
    >.....VH-T12B.....>>

                                          CDR H3
331 gaa gat acc gcg gtg tat tat tgc gcg cgt tgg gat ttt ctg gat tat tgg ggc cag ggc acc acc
    E D T A V Y Y C A R W D F L D Y W G Q G T T
    >.....VH-T12B.....>>

XhoI
---+-----

397 gtt acg gtc tcg agt ggt gga ggc ggt tca ggc gga ggt ggc tct ggc ggt agt gca caa gat att
    V T V S S G G G S G G G S G G S G G S A Q D I
    >.....VH-T12B.....>> >>.....Linker.....>> >>.....

463 gtg atg acc cag agc ccg ctg tct ctg ccg gtc acg ccg ggt gaa ccg gcg agc att agc tgc cgt
    V M T Q S P L S L P V T P G E P A S I S C R
    >.....VL-T12B.....>>

                                          CDR L1
529 agc agc cag agc ctg ctg cat agc aac ggc aac acc tat ctg cat tgg tat ctg cag aaa ccg ggc
    S S Q S L L H S N G N T Y L H W Y L Q K P G
    >.....VL-T12B.....>>

```

```

                                CDR L2
595  cag agc ccg cag ctg ctg att tat acc gtg agc aac cgt ttt agc ggc gtg ccg gat cgc ttt agc
      Q  S  P  Q  L  L  I  Y  T  V  S  N  R  F  S  G  V  P  D  R  F  S
      >.....VL-T12B.....>

661  gga tcc ggt agc ggc acc gat ttt acc ctg aaa att agc cgt gtg gaa gcg gaa gat gtg ggc gtg
      G  S  G  S  G  T  D  F  T  L  K  I  S  R  V  E  A  E  D  V  G  V
      >.....VL-T12B.....>

                                CDR L3
727  tat tat tgc agc cag ggc acc cat gtg ccg tat acc ttt ggc ggt ggc acc aaa gtg gaa att aaa
      Y  Y  C  S  Q  G  T  H  V  P  Y  T  F  G  G  G  T  K  V  E  I  K
      >.....VL-T12B.....>

                                NotI
      -+-----
893  cgt gcg gcc gca gaa caa aaa ctc atc tca gaa gag gat ctg aat ggg gcc gca cat cac cat cat
      R  A  A  A  E  Q  K  L  I  S  E  E  D  L  N  G  A  A  H  H  H  H
      >>> >>.....myc tag.....>>> >>..His tag...>

859  cac cat taa
      H  H  -
      >.....>>

```

7.13. scFvFRK13.1

```

                                                                NcoI
                                                                -+-----
1   atg aaa tac cta ttg cct acg gca gcc gct gga ttg tta tta ctc gcg gcc cag ccg gcc atg gcc
      M  K  Y  L  L  P  T  A  A  A  G  L  L  L  L  A  A  Q  P  A  M  A

67  cag gtg cag ctg gtg gaa tct ggc ggc gga ctc gtg aag cct ggc ggc tct ctg aga ctg tct tgt
      Q  V  Q  L  V  E  S  G  G  G  L  V  K  P  G  G  S  L  R  L  S  C
      >>.....VH-FRK13.1.....>>

                                CDR H1
133  gcc gcc tcc gga ttc acc ttc agc gac ttc tac atc aac tgg att aga cag gcc ccc ggg aag ggc
      A  A  S  G  F  T  F  S  D  F  Y  I  N  W  I  R  Q  A  P  G  K  G
      >.....VH-FRK13.1.....>

                                CRD H2
199  cta gag tgg gtg tcc gaa atc tac ccc tac agc ggc cac gcc tac tac aac gag aag ttc aag gcc
      L  E  W  V  S  E  I  Y  P  Y  S  G  H  A  Y  Y  N  E  K  F  K  A
      >.....VH-FRK13.1.....>

265  cgg ttc acc atc agc cgg gac aac gcc aag aac agc ctg tac ctg cag atg aac tcc ctg cgg gcc
      R  F  T  I  S  R  D  N  A  K  N  S  L  Y  L  Q  M  N  S  L  R  A
      >.....VH-FRK13.1.....>

                                CDR H3
331  gag gac acc gcc gtg tac tat tgt gca cgc tgg gac ttt ctg gac tac tgg ggc cag ggc acc acc
      E  D  T  A  V  Y  Y  C  A  R  W  D  F  L  D  Y  W  G  Q  G  T  T
      >.....VH-FRK13.1.....>

                                XhoI
      -+-----
397  gtg aca gtc tcg agc gga ggc gga gga tca ggc ggc gga gga agt ggc gga ggg ggc agc gat att
      V  T  V  S  S  S  G  G  G  S  G  G  G  S  G  G  S  G  G  G  G  S  D  I
      >...VH-FRK13.1...>> >>.....Linker.....>> >>.....>

463  cag atg acc cag agc ccc agc agc ctg agc gcc tct gtg ggc gac aga gtg acc atc acc tgt cgg
      Q  M  T  Q  S  P  S  S  L  S  A  S  V  G  D  R  V  T  I  T  C  R
      >.....VL-FRK13.1.....>

                                CDR L1
529  agc agc cag agc ctg ctg cac agc aac ggc aac acc tac ctg cat tgg tac cag cag aag ccc ggc
      S  S  Q  S  L  L  H  S  N  G  N  T  Y  L  H  W  Y  Q  Q  K  P  G
      >.....VL-FRK13.1.....>

                                CDR L2
595  aag gcc ccc aag ctg ctg atc tac acc gtg tcc aac aga ttc agc ggc gtg ccc tct aga ttc tcc
      K  A  P  K  L  L  I  Y  T  V  S  N  R  F  S  G  V  P  S  R  F  S
      >.....VL-FRK13.1.....>

```

```

661 ggc tct ggc agc ggc acc gac ttc acc ctg acc atc tct agc ctg cag ccc gag gac ttc gcc acc
    G S G S G T D F T L T I S S L Q P E D F A T
    >.....VL-FRK13.1.....>

                                CDR L3
727 tac tac tgc agc cag tcc acc cac gtg ccg tat acc ttt ggc gga ggc acc aag gtg gaa atc aaa
    Y Y C S Q S T H V P Y T F G G G T K V E I K
    >.....VL-FRK13.1.....>>

NotI
---+-----
793 gcg gcc gca gaa caa aaa ctc atc tca gaa gag gat ctg aat ggg gcc gca cat cac cat cat cac
    A A A E Q K L I S E E D L N G A A H H H H H
    >>.....myc tag.....>>                >>....His tag.....>

859 cat taa
    H -
    >>>

```

7.14. scFvFRK13.2

```

                                pelB Leader                                NcoI
                                ---+-----
1  atg aaa tac cta ttg cct acg gca gcc gct gga ttg tta tta ctc gcg gcc cag ccg gcc atg gcc
    M K Y L L P T A A A G L L L L A A Q P A M A

67  cag gtg cag ctg gtg gaa tct ggc ggc gga ctc gtg aag cct ggc ggc tct ctg aga ctg tct tgt
    Q V Q L V E S G G G L V K P G G S L R L S C
    >>.....VH-FRK13.2.....>

                                CDR H1
133 gcc gcc tcc gga ttc acc ttc agc gac ttc tac atc aac tgg atc aga cag gcc ccc ggg aag ggc
    A A S G F T F S D F Y I N W I R Q A P G K G
    >.....VH-FRK13.2.....>

                                CDR H2
199 cta gag tgg gtg tcc gaa atc tac ccc tac agc ggc cac gcc tac tac aac gag aag ttc aag gcc
    L E W V S E I Y P Y S G H A Y Y N E K F K A
    >.....VH-FRK13.2.....>

265 cgg ttc acc atc tcc gcc gac aac gcc aag aac agc ctg tac ctg cag atg aac tcc ctg cgg gcc
    R F T I S A D N A K N S L Y L Q M N S L R A
    >.....VH-FRK13.2.....>

                                CDR H3
331 gag gac acc gcc gtg tac tat tgt gca cgc tgg gac ttt ctg gac tac tgg ggc cag ggc acc acc
    E D T A V Y Y C A R W D F L D Y W G Q G T T
    >.....VH-FRK13.2.....>

XhoI
---+-----
397 gtg aca gtc tcg agc gga ggc gga gga tca ggc ggc gga gga agt ggc gga ggg gga tct gat gtg
    V T V S S G G G G S G G G G S G G G S D V
    >...VH-FRK13.2...>> >>.....Linker.....>> >>...>

463 cag atg acc cag agc ccc agc agc ctg tct gcc agc gtg ggc gac aga gtg acc atc acc tgt cgg
    Q M T Q S P S S L S A S V G D R V T I T C R
    >.....VL-FRK13.2.....>

                                CDR L1
529 agc agc cag agc ctg ctg cac agc aac ggc aac acc tac ctg cat tgg tac cag cag aag ccc ggc
    S S Q S L L H S N G N T Y L H W Y Q Q K P G
    >.....VL-FRK13.2.....>

                                CDR L2
595 aag gcc ccc aag ctg ctg atc tac acc gtg tcc aac aga ttc agc ggc gtg ccc tct aga ttc tcc
    K A P K L L I Y T V S N R F S G V P S R F S
    >.....VL-FRK13.2.....>

661 ggc tct ggc agc ggc acc gac ttc acc ctg acc atc tct agc ctg cag ccc gag gac ttc gcc acc
    G S G S G T D F T L T I S S L Q P E D F A T
    >.....VL-FRK13.2.....>

```

```

                                CDR L3
727 tac tac tgc agc cag tcc acc cac gtg ccg tat acc ttt ggc gga ggc acc aag gtg gaa atc aaa
    Y Y C S Q S T H V P Y T F G G G T K V E I K
    >.....VL-FRK13.2.....>>

    NotI
    -+-----
793 gcg gcc gca gaa caa aaa ctc atc tca gaa gag gat ctg aat ggg gcc gca cat cac cat cat cac
    A A A E Q K L I S E E D L N G A A H H H H H
    >>.....myc tag.....>>                >>....His tag.....>

859 cat taa
    H -
    >>>

```

7.15. scFvFRK13.7

```

                                                                NcoI
                                                                -+-----
                                pelB Leader
1   atg aaa tac cta ttg cct acg gca gcc gct gga ttg tta tta ctc gcg gcc cag ccg gcc atg gcc
    M K Y L L P T A A A G L L L L A A Q P A M A

67  cat gtt cag ctg gtt cag agc ggt gcg gaa gtg aaa aaa ccg gcc agc agc gtg aaa gtg agc tgc
    H V Q L V Q S G A E V K K P G S S V K V S C
    >>.....VH-T12B.....>

                                CDR H1
133 aaa gct agc ggc tat acc ttt acc gat ttc tac att aac tgg gtg cgt cag gca ccc ggg cag ggc
    K A S G Y T F T D F Y I N W V R Q A P G Q G
    >.....VH-T12B.....>

                                CDR H2
199 ctg gaa tgg att ggc gag att gtg ccg tcg cag gcc gag gca aag tac aac gat aaa ttc aaa gcg
    L E W I G E I V P S Q G E A K Y N D K F K A
    >.....VH-T12B.....>

265 cgt gtg acc att acc gcg gat aaa agc acc agc acc gcg tat atg gaa ctg agc agc ctg cgt agc
    R V T I T A D K S T S T A Y M E L S S L R S
    >.....VH-T12B.....>

                                CDR H3
331 gaa gat acc gcg gtg tat tat tgc gcg cgt tgg gat ttt ctg gat tat tgg gcc cag gcc acc acc
    E D T A V Y Y C A R W D F L D Y W G Q G T T
    >.....VH-T12B.....>

    XhoI
    -+-----
397 gtt acg gtc tcg agc gga gcc gga gga tca gcc gcc gga gga agt gcc gga ggg gga tct gat gtg
    V T V S S G G G G S G G G S G G G S D V
    >.....VH-T12B.....>> >>.....Linker.....>> >>.....>

463 cag atg acc cag agc ccc agc agc ctg tct gcc agc gtg gcc gac aga gtg acc atc acc tgt ccg
    Q M T Q S P S S L S A S V G D R V T I T C R
    >.....VL-FRK13.2.....>

                                CDR L1
529 agc agc cag agc ctg ctg cac agc aac gcc aac acc tac ctg cat tgg tac cag cag aag ccc gcc
    S S Q S L L H S N G N T Y L H W Y Q Q K P G
    >.....VL-FRK13.2.....>

                                CDR L2
595 aag gcc ccc aag ctg ctg atc tac acc gtg tcc aac aga ttc agc gcc gtg ccc tct aga ttc tcc
    K A P K L L I Y T V S N R F S G V P S R F S
    >.....VL-FRK13.2.....>

661 ggc tct ggc agc gcc acc gac ttc acc ctg acc atc tct agc ctg cag ccc gag gac ttc gcc acc
    G S G S G T D F T L T I S S L Q P E D F A T
    >.....VL-FRK13.2.....>

                                CDR L3
727 tac tac tgc agc cag tcc acc cac gtg ccg tat acc ttt ggc gga ggc acc aag gtg gaa atc aaa
    Y Y C S Q S T H V P Y T F G G G T K V E I K
    >.....VL-FRK13.2.....>>

```

```

NotI
--+-----
793 gcg gcc gca gaa caa aaa ctc atc tca gaa gag gat ctg aat ggg gcc gca cat cac cat cat cac
    A  A  A  E  Q  K  L  I  S  E  E  D  L  N  G  A  A  H  H  H  H  H
    >>.....myc tag.....>>                >>....His tag.....>

859 cat taa
    H  -
    >>>

```

7.16. pAB1-L1-EMP1-CLk-Li1

```

HindIII
--+-----
1  aag ctt gcc gcc acc atg gag aca gac aca ctc ctg cta tgg gta ctg ctg ctc tgg gtt cca ggt
    K  L  A  A  T  M  E  T  D  T  L  L  L  W  V  L  L  L  W  V  P  G
                                Igk-Leader

AgeI
--+-----
67  tcc acc ggt ggc ggt acc tac agc tgc cac ttc ggc ccc ctg acc tgg gtg tgc aag ccc cag ggg
    S  T  G  G  G  T  Y  S  C  H  F  G  P  L  T  W  V  C  K  P  Q  G
    >>.....EMP1.....>>

133 gga ggc ggg tcc gga gga ggc ggg agc ggc ggc tcc acc gac ggc aac acc ggc ggg agc ggc gga
    G  G  G  S  G  G  G  G  S  G  G  S  T  D  G  N  T  G  G  S  G  G
    >>> >>.....Linker1.....>>>

RsrII
--+-----
199 cgg acc gtt gct gcg cca tct gtc ttc atc ttc cgg cca tct gat gag cag ttg aaa tct gga act
    R  T  V  A  A  P  S  V  F  I  F  P  P  S  D  E  Q  L  K  S  G  T
    >>.....CLk.....>>

265 gcc tct gtt gtg tgc ctg ctg aat aac ttc tat ccc aga gag gcc aaa gta cag tgg aag gtg gat
    A  S  V  V  C  L  L  N  N  F  Y  P  R  E  A  K  V  Q  W  K  V  D
    >.....CLk.....>

331 aac gcc ctc caa tcg ggt aac tcc cag gag agt gtc aca gag cag gac agc aag gac agc acc tac
    N  A  L  Q  S  G  N  S  Q  E  S  V  T  E  Q  D  S  K  D  S  T  Y
    >.....CLk.....>

397 agc ctc agc agc acc ctg acg ctg agc aaa gca gac tac gag aaa cac aaa gtc tac gcc tgc gaa
    S  L  S  S  T  L  T  L  S  K  A  D  Y  E  K  H  K  V  Y  A  C  E
    >.....CLk.....>

EcoRI
--+-----
463 gtc acc cat cag ggc ctg agc tcg ccc gtc aca aag agc ttc aac agg gga gag tgt taa gaa ttc
    V  T  H  Q  G  L  S  S  P  V  T  K  S  F  N  R  G  E  C  -  E  F
    >.....CLk.....>>

```

7.17. pAB1-L1-EMP1-hg1e3-Li1

```

HindIII
--+-----
1  aag ctt gcc gcc acc atg gag aca gac aca ctc ctg cta tgg gta ctg ctg ctc tgg gtt cca ggt
    K  L  A  A  T  M  E  T  D  T  L  L  L  W  V  L  L  L  W  V  P  G
                                Igk-Leader

AgeI
--+-----
67  tcc acc ggt ggc ggt acc tac agc tgc cac ttc ggc ccc ctg acc tgg gtg tgc aag ccc cag ggg
    S  T  G  G  G  T  Y  S  C  H  F  G  P  L  T  W  V  C  K  P  Q  G
    >>.....EMP1.....>>

133 gga ggc ggg tcc gga gga ggc ggg agc ggc ggc tcc acc gac ggc aac acc ggc ggg agc ggc gga
    G  G  G  S  G  G  G  G  S  G  G  S  T  D  G  N  T  G  G  S  G  G
    >>> >>.....Linker1.....>>>

```

```

NheI
--+-----
199 gct agc acc aag ggc ccc agc gtg ttc ccc ctg gcc ccc agc agc aag agc acc tcc ggc ggc aca
   A S T K G P S V F P L A P S S K S T S G G T
   >>.....CH1.....>

265 gcc gcc ctg ggc tgc ctg gtg aag gac tac ttc ccc gag ccc gtg acc gtg tcc tgg aac agc gga
   A A L G C L V K D Y F P E P V T V S W N S G
   >.....CH1.....>

331 gcc ctg acc agc ggc gtg cac acc ttc ccc gcc gtg ctg cag agc agc ggc ctg tac agc ctg tcc
   A L T S G V H T F P A V L Q S S G L Y S L S
   >.....CH1.....>

397 agc gtg gtg acc gtg cca agc agc agc ctg gga acc cag acc tac atc tgc aac gtg aac cac aag
   S V V T V P S S S L G T Q T Y I C N V N H K
   >.....CH1.....>

463 ccc agc aac acc aag gtg gac aag aag gtg gag ccc aag agc tgc gac aag acc cac acc tgt cca
   P S N T K V D K K V E P K S C D K T H T C P
   >.....CH1.....>>>.....Hinge.....>

529 cca tgc cca gcc ccc cca gtg gcc gga ccc tcc gtg ttc ctg ttc ccc ccc aag ccc aag gac acc
   P C P A P P V A G P S V F L F P P K P K D T
   >..Hinge.>>>.....CH2.....>

595 ctg atg atc agc agg acc ccc gag gtg acc tgc gtg gtg gtg gac gtg tcc cac gag gac cca gag
   L M I S R T P E V T C V V V D V S H E D P E
   >.....CH2.....>

661 gtg aag ttc aat tgg tat gtg gac ggc gtg gag gtg cac aac gcc aag acc aag ccc aga gag gaa
   V K F N W Y V D G V E V H N A K T K P R E E
   >.....CH2.....>

727 cag tac aac agc acc tac agg gtg gtg tcc gtg ctg acc gtg ctg cac cag gac tgg ctg aac ggc
   Q Y N S T Y R V V S V L T V L H Q D W L N G
   >.....CH2.....>

793 aag gaa tac aag tgc aag gtc tcc aac aag ggc ctg ccc agc tcc atc gaa aag acc atc agc aag
   K E Y K C K V S N K G L P S S I E K T I S K
   >.....CH2.....>

859 gcc aag ggc cag cca cgg gag ccc cag gtg tac acc ctg ccc ccc tcc cgg gac gag ctg acc aag
   A K G Q P R E P Q V Y T L P P S R D E L T K
   >.CH2>>>.....CH3.....>

925 aac cag gtg tcc ctg acc tgt ctg gtg aag ggc ttc tac ccc agc gac atc gcc gtg gag tgg gag
   N Q V S L T C L V K G F Y P S D I A V E W E
   >.....CH3.....>

991 agc aac ggc cag ccc gag aac aac tac aag acc acc ccc cct gtg ctg gac agc gac ggc agc ttc
   S N G Q P E N N Y K T T P P V L D S D G S F
   >.....CH3.....>

1057 ttc ctg tac agc aag ctg acc gtg gac aag agc agg tgg cag cag ggc aac gtg ttc tcc tgc agc
   F L Y S K L T V D K S R W Q Q G N V F S C S
   >.....CH3.....>

1123 gtg atg cac gag gcc ctg cac aac cac tac acc cag aag agc ctg agc ctg tcc ccc ggc aaa taa
   V M H E A L H N H Y T Q K S L S L S P G K -
   >.....CH3.....>>

EcoRI
--+-----
1189 gaa ttc
     E F

```

7.18. pAB1-L1-EMP1-CH1only

```

HindIII
--+-----
1 aag ctt gcc gcc acc atg gag aca gac aca ctc ctg cta tgg gta ctg ctg ctc tgg gtt cca ggt
   K L A A T M E T D T L L L W V L L L W V P G

```

Igk-Leader


```

      AgeI
    -+-----
67  tcc acc ggt ggc ggt acc tac agc tgc cac ttc ggc ccc ctg acc tgg gtg tgc aag ccc cag ggg
    S T G G G T Y S C H F G P L T W V C K P Q G
    >>.....EMP1.....>

133  gga ggc ggg tcc gga gga ggc ggg agc ggc ggc tcc acc gac ggc aac acc ggc ggg agc ggc gga
    G G G S G G G G S G G S T D G N T G G S G G
    >>> >>.....Linker1.....>

      NheI
    -+-----
199  gct agc acc aag ggc cca tcg gtc ttc ccc ctg gcc ccc agc agc aag agc acc tcc ggc ggc aca
    A S T K G P S V F P L A P S S K S T S G G T
    >>.....CH1.....>

265  gcc gcc ctg ggc tgc ctg gtg aag gac tac ttc ccc gag ccc gtg acc gtg tcc tgg aac agc gga
    A A L G C L V K D Y F P E P V T V S W N S G
    >.....CH1.....>

331  gcc ctg acc agc ggc gtg cac acc ttc ccc gcc gtg ctg cag agc agc ggc ctg tac agc ctg tcc
    A L T S G V H T F P A V L Q S S G L Y S L S
    >.....CH1.....>

397  agc gtg gtg acc gtg cca agc agc agc ctg gga acc cag acc tac atc tgc aac gtg aac cac aag
    S V V T V P S S S L G T Q T Y I C N V N H K
    >.....CH1.....>

                                           EcoRI
                                           -+-----
463  ccc agc aac acc aag gtg gac aag aag gtg gag ccc aag agc tgc taa gaa ttc
    P S N T K V D K K V E P K S C - E F
    >.....CH1.....>

```

7.19. pAB1-L1-EMP1-2CLk

```

      HindIII
    -+-----
1  aag ctt gcc gcc acc atg gag aca gac aca ctc ctg cta tgg gta ctg ctg ctc tgg gtt cca ggt
    K L A A T M E T D T L L L W V L L L W V P G
                                Igk-Leader

67  tcc acc ggt ggc ggt acc tac agc tgc cac ttc ggc ccc ctg acc tgg gtg tgc aag ccc cag ggg
    S T G G G T Y S C H F G P L T W V C K P Q G
    >>.....EMP1.....>

133  gga ggc ggg tcc gga gga ggc ggg agc ggc ggc tcc acc gac ggc aac acc ggc ggg agc ggc gga
    G G G S G G G G S G G S T D G N T G G S G G
    >>> >>.....Linker1.....>

      RsrII
    -+-----
199  cgg acc gtt gct gcg cca tct gtc ttc atc ttc ccg cca tct gat gag cag ttg aaa tct gga act
    R T V A A P S V F I F P P S D E Q L K S G T
    >>.....CLk.....>

265  gcc tct gtt gtg tgc ctg ctg aat aac ttc tat ccc aga gag gcc aaa gta cag tgg aag gtg gat
    A S V V C L L N N F Y P R E A K V Q W K V D
    >.....CLk.....>

331  aac gcc ctc caa tcg ggt aac tcc cag gag agt gtc aca gag cag gac agc aag gac agc acc tac
    N A L Q S G N S Q E S V T E Q D S K D S T Y
    >.....CLk.....>

397  agc ctc agc agc acc ctg acg ctg agc aaa gca gac tac gag aaa cac aaa gtc tac gcc tgc gaa
    S L S S T L T L S K A D Y E K H K V Y A C E
    >.....CLk.....>

463  gtc acc cat cag ggc ctg agc tcg ccc gtc aca aag agc ttc aac agg ggt ggg agc gga ggg agc
    V T H Q G L S S P V T K S F N R G G S G G S
    >.....CLk.....>>>.....Linker8.....>

```

```

529  ggc gga cgt acc gtt gct gcg cca tct gtc ttc atc ttc ccg cca tct gat gag cag ttg aaa tct
      G  G  R  T  V  A  A  P  S  V  F  I  F  P  P  S  D  E  Q  L  K  S
      >.....>> >>.....CLk.....>

595  gga act gcc tct gtt gtg tgc ctg ctg aat aac ttc tat ccc aga gag gcc aaa gta cag tgg aag
      G  T  A  S  V  V  C  L  L  N  N  F  Y  P  R  E  A  K  V  Q  W  K
      >.....CLk.....>

661  gtg gat aac gcc ctc caa tcg ggt aac tcc cag gag agt gtc aca gag cag gac agc aag gac agc
      V  D  N  A  L  Q  S  G  N  S  Q  E  S  V  T  E  Q  D  S  K  D  S
      >.....CLk.....>

727  acc tac agc ctc agc agc acc ctg acg ctg agc aaa gca gac tac gag aaa cac aaa gtc tac gcc
      T  Y  S  L  S  S  T  L  T  L  S  K  A  D  Y  E  K  H  K  V  Y  A
      >.....CLk.....>

793  tgc gaa gtc acc cat cag ggc ctg agc tcg ccc gtc aca aag agc ttc aac agg gga gag tgt taa
      C  E  V  T  H  Q  G  L  S  S  P  V  T  K  S  F  N  R  G  E  C  -
      >.....CLk.....>>

EcoRI
-+-----
859  gaa ttc
      E  F

```

7.20. pAB1-L1-EMP1-2CH1

```

HindIII
-+-----
1   aag ctt gcc gcc acc atg gag aca gac aca ctc ctg cta tgg gta ctg ctg ctc tgg gtt cca ggt
      K  L  A  A  T  M  E  T  D  T  L  L  L  W  V  L  L  L  W  V  P  G
      Igk-Leader

AgeI
-+-----
67  tcc acc ggt ggc ggt acc tac agc tgc cac ttc ggc ccc ctg acc tgg gtg tgc aag ccc cag ggg
      S  T  G  G  G  T  Y  S  C  H  F  G  P  L  T  W  V  C  K  P  Q  G
      >>.....EMP1.....>

133  gga ggc ggg tcc gga gga ggc ggg agc ggc ggc tcc acc gac ggc aac acc ggc ggg agc ggc gga
      G  G  G  S  G  G  G  G  S  G  G  S  T  D  G  N  T  G  G  S  G  G
      >>> >>.....Linker1.....>>>

NheI
-+-----
199  gct agc acc aag ggc ccc agc gtg ttc ccc ctg gcc ccc agc agc aag agc acc tcc ggc ggc aca
      A  S  T  K  G  P  S  V  F  P  L  A  P  S  S  K  S  T  S  G  G  T
      >>.....CH1.....>

265  gcc gcc ctg ggc tgc ctg gtg aag gac tac ttc ccc gag ccc gtg acc gtg tcc tgg aac agc gga
      A  A  L  G  C  L  V  K  D  Y  F  P  E  P  V  T  V  S  W  N  S  G
      >.....CH1.....>

331  gcc ctg acc agc ggc gtg cac acc ttc ccc gcc gtg ctg cag agc agc ggc ctg tac agc ctg tcc
      A  L  T  S  G  V  H  T  F  P  A  V  L  Q  S  S  G  L  Y  S  L  S
      >.....CH1.....>

397  agc gtg gtg acc gtg cca agc agc agc ctg gga acc cag acc tac atc tgc aac gtg aac cac aag
      S  V  V  T  V  P  S  S  S  L  G  T  Q  T  Y  I  C  N  V  N  H  K
      >.....CH1.....>

463  ccc agc aac acc aag gtg gac aag aag gtg gga ggg agc ggc ggt agc ggc gga gcc agc acc aag
      P  S  N  T  K  V  D  K  K  V  G  G  S  G  G  S  G  G  A  S  T  K
      >.....CH1.....>> >>.....Linker8.....>> >>.....CH1.....>

529  ggc ccc agc gtg ttc ccc ctg gcc ccc agc agc aag agc acc tcc ggc ggc aca gcc gcc ctg ggc
      G  P  S  V  F  P  L  A  P  S  S  K  S  T  S  G  G  T  A  A  L  G
      >.....CH1.....>

595  tgc ctg gtg aag gac tac ttc ccc gag ccc gtg acc gtg tcc tgg aac agc gga gcc ctg acc agc
      C  L  V  K  D  Y  F  P  E  P  V  T  V  S  W  N  S  G  A  L  T  S
      >.....CH1.....>

```

```

661 ggc gtg cac acc ttc ccc gcc gtg ctg cag agc agc ggc ctg tac agc ctg tcc agc gtg gtg acc
    G V H T F P A V L Q S S G L Y S L S S V V T
    >.....CH1.....>

727 gtg cca agc agc agc ctg gga acc cag acc tac atc tgc aac gtg aac cac aag ccc agc aac acc
    V P S S S L G T Q T Y I C N V N H K P S N T
    >.....CH1.....>

                                EcoRI
                                --+----
793 aag gtg gac aag aag gtg gag ccc aag agc tgc taa gaa ttc
    K V D K K V E P K S C - E F
    >.....CH1.....>>

```

7.21. pAB1-L1-EMP1-CLk-CH3

```

HindIII
--+----
1 aag ctt gcc gcc acc atg gag aca gac aca ctc ctg cta tgg gta ctg ctg ctc tgg gtt cca ggt
  K L A A T M E T D T L L L W V L L L W V P G
                                Igk-Leader

AgeI
--+----
67 tcc acc ggt ggc ggt acc tac agc tgc cac ttc ggc ccc ctg acc tgg gtg tgc aag ccc cag ggg
  S T G G G T Y S C H F G P L T W V C K P Q G
    >>.....EMP1.....>>

133 gga ggc ggg tcc gga gga ggc ggg agc ggc ggc tcc acc gac ggc aac acc ggc ggg agc ggc gga
    G G G S G G G G S G G S T D G N T G G S G G
    >>> >>.....Linker1.....>>>

RsrII
--+----
199 cgg acc gtt gct gcg cca tct gtc ttc atc ttc cgg cca tct gat gag cag ttg aaa tct gga act
    R T V A A P S V F I F P P S D E Q L K S G T
    >>.....CLk.....>>

265 gcc tct gtt gtg tgc ctg ctg aat aac ttc tat ccc aga gag gcc aaa gta cag tgg aag gtg gat
    A S V V C L L N N F Y P R E A K V Q W K V D
    >.....CLk.....>

331 aac gcc ctc caa tcg ggt aac tcc cag gag agt gtc aca gag cag gac agc aag gac agc acc tac
    N A L Q S G N S Q E S V T E Q D S K D S T Y
    >.....CLk.....>

397 agc ctc agc agc acc ctg acg ctg agc aaa gca gac tac gag aaa cac aaa gtc tac gcc tgc gaa
    S L S S T L T L S K A D Y E K H K V Y A C E
    >.....CLk.....>

                                                                Sali
                                                                --+----
463 gtc acc cat cag ggc ctg agc tcg ccc gtc aca aag agc ttc aac agg gga gag tgt ggg tcg acg
    V T H Q G L S S P V T K S F N R G E C G S T
    >.....CLk.....>>

529 ggt gga ggc ggt tca ggc gga ggt ggc tct ggc cag cca cgg gag ccc cag gtg tac acc ctg ccc
    G G G G S G G G S G Q P R E P Q V Y T L P
    >>.....Linker10.....>> >>.....CH3.....>>

XmaI
--+----
595 ccc tcc cgg gac gag ctg acc aag aac cag gtg tcc ctg acc tgt ctg gtg aag ggc ttc tac ccc
    P S R D E L T K N Q V S L T C L V K G F Y P
    >.....CH3.....>

661 agc gac atc gcc gtg gag tgg gag agc aac ggc cag ccc gag aac aac tac aag acc acc ccc cct
    S D I A V E W E S N G Q P E N N Y K T T P P
    >.....CH3.....>

```

```

727  gtg ctg gac agc gac ggc agc ttc ttc ctg tac agc aag ctg acc gtg gac aag agc agg tgg cag
      V  L  D  S  D  G  S  F  F  L  Y  S  K  L  T  V  D  K  S  R  W  Q
      >.....CH3.....>

793  cag ggc aac gtg ttc tcc tgc agc gtg atg cac gag gcc ctg cac aac cac tac acc cag aag agc
      Q  G  N  V  F  S  C  S  V  M  H  E  A  L  H  N  H  Y  T  Q  K  S
      >.....CH3.....>

                                EcoRI
                                -+-----
859  ctg agc ctg tcc ccc ggc aaa taa gaa ttc
      L  S  L  S  P  G  K  -  E  F
      >.....CH3.....>>

```

7.22. pAB1-L1-EMP1-CH1-CH3

```

HindIII
-+-----
1  aag ctt gcc gcc acc atg gag aca gac aca ctc ctg cta tgg gta ctg ctg ctc tgg gtt cca ggt
   K  L  A  A  T  M  E  T  D  T  L  L  L  W  V  L  L  L  W  V  P  G
                                Igk-Leader

AgeI
-+-----
67  tcc acc ggt ggc ggt acc tac agc tgc cac ttc ggc ccc ctg acc tgg gtg tgc aag ccc cag ggg
   S  T  G  G  G  T  Y  S  C  H  F  G  P  L  T  W  V  C  K  P  Q  G
   >>.....EMP1.....>>

133  gga ggc ggg tcc gga gga ggc ggg agc ggc ggc tcc acc gac ggc aac acc ggc ggg agc ggc gga
   G  G  G  S  G  G  G  S  G  G  S  G  S  T  D  G  N  T  G  G  S  G  G
   >>> >>.....Linker1.....>>>

NheI
-+-----
199  gct agc acc aag ggc cca tgc gtc ttc ccc ctg gca ccc tcc tcc aag agc acc tct ggg ggc aca
   A  S  T  K  G  P  S  V  F  P  L  A  P  S  S  K  S  T  S  G  G  T
   >>.....CH1.....>>

                                AgeI
                                -+-----
265  gcg gcc ctg ggc tgc ctg gtc aag gac tac ttc ccc gaa ccg gtg acg gtg tgc tgg aac tca ggc
   A  A  L  G  C  L  V  K  D  Y  F  P  E  P  V  T  V  S  W  N  S  G
   >.....CH1.....>

331  gcc ctg acc agc ggc gtg cac acc ttc ccg gct gtc cta cag tcc tca gga ctc tac tcc ctc agc
   A  L  T  S  G  V  H  T  F  P  A  V  L  Q  S  S  G  L  Y  S  L  S
   >.....CH1.....>

397  agc gtg gtg acc gtg ccc tcc agc agc ttg ggc acc cag acc tac atc tgc aac gtg aat cac aag
   S  V  V  T  V  P  S  S  S  L  G  T  Q  T  Y  I  C  N  V  N  H  K
   >.....CH1.....>

                                Sali
                                --+-----
463  ccc agc aac acc aag gtg gac aag aga gtt gag ccc aaa tct tgt ggg tgc acg ggt gga ggc ggt
   P  S  N  T  K  V  D  K  R  V  E  P  K  S  C  G  S  T  G  G  G  G
   >.....CH1.....>>>.....Linker10....>>>

                                XmaI
                                -+-----
529  tca ggc gga ggt ggc tct ggc cag cca cgg gag ccc cag gtg tac acc ctg ccc ccc tcc cgg gac
   S  G  G  G  G  S  G  Q  P  R  E  P  Q  V  Y  T  L  P  P  S  R  D
   >.....Linker10.....>>>.....CH3.....>>>

595  gag ctg acc aag aac cag gtg tcc ctg acc tgt ctg gtg aag ggc ttc tac ccc agc gac atc gcc
   e  l  t  k  n  q  v  s  l  t  c  l  v  k  g  f  y  p  s  d  i  a
   >.....CH3.....>

661  gtg gag tgg gag agc aac ggc cag ccc gag aac aac tac aag acc acc ccc cct gtg ctg gac agc
   v  e  w  e  s  n  g  q  p  e  n  n  y  k  t  t  p  p  v  l  d  s
   >.....CH3.....>

```

```

727 gac ggc agc ttc ttc ctg tac agc aag ctg acc gtg gac aag agc agg tgg cag cag ggc aac gtg
    d g s f f l y s k l t v d k s r w q q g n v
    >.....CH3.....>

793 ttc tcc tgc agc gtg atg cac gag gcc ctg cac aac cac tac acc cag aag agc ctg agc ctg tcc
    f s c s v m h e a l h n h y t q k s l s l s
    >.....CH3.....>

          EcoRI
          +-+----
859 ccc ggc aaa taa gaa ttc
    p g k - e f
    >...CH3...>

```

7.23. Light Chain Variable Domain of IgG13.7, Fab13.7, Fab13.7L and Fab13.7CH3

```

                                Igk-Leader
                                +-+-----
                                AgeI
                                -+-----
1  atg gag aca gac aca ctc ctg cta tgg gta ctg ctg ctc tgg gtt cca ggt tcc acc ggt gat gtg
    M E T D T L L L W V L L L W V P G S T G D V
    >>.....>

67  cag atg acc cag agc ccc agc agc ctg tct gcc agc gtg ggc gac aga gtg acc atc acc tgt cgg
    Q M T Q S P S S L S A S V G D R V T I T C R
    >.....VL-FRK13.7.....>

133 agc agc cag agc ctg ctg cac agc aac ggc aac acc tac ctg cat tgg tac cag cag aag ccc ggc
    S S Q S L L H S N G N T Y L H W Y Q Q K P G
    >.....VL-FRK13.7.....>

199 aag gcc ccc aag ctg ctg atc tac acc gtg tcc aac aga ttc agc ggc gtg ccc tct aga ttc tcc
    K A P K L L I Y T V S N R F S G V P S R F S
    >.....VL-FRK13.7.....>

265 ggc tct ggc agc ggc acc gac ttc acc ctg acc atc tct agc ctg cag ccc gag gac ttc gcc acc
    G S G S G T D F T L T I S S L Q P E D F A T
    >.....VL-FRK13.7.....>

331 tac tac tgc agc cag tcc acc cac gtg ccg tat acc ttt ggc gga ggc acc aag gtg gaa atc aaa
    Y Y C S Q S T H V P Y T F G G G T K V E I K
    >.....VL-FRK13.7.....>

          RsrII
          -+-----
397 cgg acc gtt
    R T V

```

7.24. Heavy Chain Variable Domain of IgG13.7, Fab13.7, Fab13.7L and Fab13.7CH3

```

                                Igk-Leader
                                +-+-----
                                AgeI
                                -+-----
1  atg gag aca gac aca ctc ctg cta tgg gta ctg ctg ctc tgg gtt cca ggt tcc acc ggt cat gtt
    M E T D T L L L W V L L L W V P G S T G H V
    >>.....>

                                NheI
                                +---
67  cag ctg gtt cag agc ggt gcg gaa gtg aaa aaa ccg ggc agc agc gtg aaa gtg agc tgc aaa gct
    Q L V Q S G A E V K K P G S S V K V S C K A
    >.....VH-FRK13.7.....>

---
133 agc ggc tat acc ttt acc gat ttc tac att aac tgg gtg cgt cag gca ccc ggg cag ggc ctg gaa
    S G Y T F T D F Y I N W V R Q A P G Q G L E
    >.....VH-FRK13.7.....>

199 tgg att ggc gag att gtg ccg tcg cag ggc gag gca aag tac aac gat aaa ttc aaa gcg cgt gtg
    W I G E I V P S Q G E A K Y N D K F K A R V
    >.....VH-FRK13.7.....>

```

```
265 acc att acc gcg gat aaa agc acc agc acc gcg tat atg gaa ctg agc agc ctg cgt agc gaa gat
    T I T A D K S T S T A Y M E L S S L R S E D
    >.....VH-FRK13.7.....>

331 acc gcg gtg tat tat tgc gcg cgt tgg gat ttt ctg gat tat tgg ggc cag ggc acc acc gtt acg
    T A V Y Y C A R W D F L D Y W G Q G T T V T
    >.....VH-FRK13.7.....>

                NheI
                +-+-----
397 gtc tcg agc gct agc
    V S S A S
    >.....>> VH-FRK13.7
```

8. Acknowledgements

Above all, I would like to express my deep gratitude to my supervisor Roland Kontermann, thank you for five and hopefully a lot more great years in your group, for helpful discussions of results, manuscripts and surely, of this thesis. Your support and understanding of me and my (sometimes odd) ideas were absolutely essential for me to be able to finish this dissertation. It was and is a pleasure to work for you and with you.

I also want express my appreciation to Peter Scheurich, for never being tired to answer my TNF questions with all his precious experience in the field. I am also very thankful for revising this thesis and especially for hiring me as PhD-less Post-Doc in the last year. Moreover, I am very grateful to Klaus Pfizenmaier for the collaboration and suggestions on the SELECT project. A very special thank is also due to Andreas Herrmann, Eric Günzi, Timo Liebig and Verena Berger from Celonic/Baliopharm, for great cooperation, very interesting meetings, and especially Timo for performing the ADCC/CDC experiments. I am also very thankful to Teodor Aastrup and his employees at Attana for being always there with support on the biosensor experiments as well as for financial support of my conference visit in Boston. I want to express my gratitude to Baliopharm for funding the first 1.5 years of my time at the IZI. This work further supported by a BMBF grant (SELECT).

I am deeply grateful to all members of the Kontermann/Müller group for an amazing time in the lab and during our leisure activities. I have met you as colleagues and I am happy to call you friends by now. Dear Oliver, I sincerely appreciate your contribution to my dissertation in terms of the PK experiments and I am really fortunate to have your company since the 5th semester. You have the gift to make good days out of bad ones. Another special thank is due to the members of the AG-Scheurich/AG-Nadine for the warm welcome and the wonderful time in my new lab.

Finally, I also want to thank Stefan Trepel, my high school biology teacher, to set fire in my passion for biology, this thesis is where it led to. Last but not least, I would like to thank my family for the support, not only during the past years of my dissertation. But most of all, I would like to express my endless gratitude to my wife Rebekka, thank you for your support, your understanding and motivation, especially during the tough times. The completion of this thesis in the present form would not have been possible without you.

9. Curriculum Vitae - Fabian Richter

Personal Details

Date of birth: 12 January 1984

City of birth: Filderstadt

Address: Ulrichstr. 42, 73230 Kirchheim unter Teck

e-m@il: fabian.richter@izi.uni-stuttgart.de

Working Experience

Since September 2014

Research Associate, AG Scheurich, Institute of Cell Biology and Immunology, University of Stuttgart, Germany

September 2010 - August 2014

PhD Student, AG Kontermann, Institute of Cell Biology and Immunology, University of Stuttgart, Germany, Thesis title: " Evolution of the Antagonistic Tumor Necrosis Factor One-Specific Antibody ATROSAB " - Date of Defense: June 2015

April 2008 - September 2008

Research Associate, Hochstrasser Lab, Dept. Molecular Biophysics and Biochemistry, Yale University, New Haven, CT, USA

Education

July 2009 - August 2010

Diploma thesis, AG-Kontermann, Institute of Cell Biology and Immunology, University of Stuttgart, Germany, Thesis title: "Beneficial Multivalency!? Evaluation of tetravalent EMP1 Peptide Antibody Fusion Proteins"; Grade: excellent (1.0)

October 2004 - August 2010

Diploma Program "Technische Biologie", University of Stuttgart, Germany; Degree: Diplom-Biologe (technisch orientiert); Grade: excellent (1.0)

September 2006

Intermediate Degree: "Diplomvorprüfung"; Grade: excellent (1.2)

June 2013

Abitur (High School Degree), Grade: excellent (1.4)

September 1998 - June 2003

High School, Rudolf Steiner Schule Nürtingen, Germany

September 1990 - August 1998

Elementary School and Middle School, Freie Waldorfschule Kirchheim, Germany

Further Education

June 2012

Certified course: "Basic laboratory animal science and experimental methods", Interfakultäre Biomedizinische Forschungseinrichtung, University of Heidelberg, Germany

Publications

Richter F, Seifert O, Zettlitz K, Scheurich P, Pfizenmaier K, Kontermann RE. Evolution of ATROSAB by affinity maturation and framework exchange - *in preparation*

Richter F, Berger V, Guenzi E, Herrmann A, Scheurich P, Pfizenmaier K, Kontermann RE. ATROSAB Derivatives Substantiate its Unique Antagonistic Potential - *in preparation*

Richter F, Liebig T, Guenzi E, Herrmann A, Scheurich P, Pfizenmaier K, Kontermann RE. Antagonistic TNF receptor one-specific antibody (ATROSAB): receptor binding and in vitro bioactivity. PLoS One. 2013

Berger V, **Richter F**, Zettlitz K, Unverdorben F, Scheurich P, Herrmann A, Pfizenmaier K, Kontermann RE. An anti-TNFR1 scFv-HSA fusion protein as selective antagonist of TNF action. Protein Eng Des Sel. 2013

Siegemund M, **Richter F**, Seifert O, Unverdorben F, Kontermann RE. Expression and purification of recombinant antibody formats and antibody fusion proteins. Methods Mol Biol. 2014

Unverdorben F, Färber-Schwarz A, **Richter F**, Hutt M, Kontermann RE. Half-life extension of a single-chain diabody by fusion to domain B of staphylococcal protein A. Protein Eng Des Sel. 2012

Hutt M, Färber-Schwarz A, Unverdorben F, **Richter F**, Kontermann RE. Plasma half-life extension of small recombinant antibodies by fusion to immunoglobulin-binding domains. J Biol Chem. 2012

Seifert O, Plappert A, Heidel N, Fellermeier S, Messerschmidt SK, **Richter F**, Kontermann RE. The IgM CH2 domain as covalently linked homodimerization module for the generation of fusion proteins with dual specificity. Protein Eng Des Sel. 2012

Patent

Affinity maturated and framework optimized monovalent TNFR1 antagonists. **Richter F**, Kontermann RE, Pfizenmaier K, Zettlitz K, Scheurich P. - *in preparation*

Conference Contributions

PEGS, Protein Engineering Summit, Boston, USA; Poster presentation (May 2014)

ECI, European Congress of Immunology, Glasgow, Scotland; Short talk (September 2012)